

A STUDY OF RHODIUM CATALYZED HYDROBORATIONS AND
SULFUR YLIDE EPOXIDATIONS

by

DAVID RYAN EDWARDS

A thesis submitted to the Department of Chemistry
In conformity with the requirements for
The degree of Doctor of Philosophy

Queen's University
Kingston, Ontario, Canada
August, 2007

Copyright © David Ryan Edwards, 2007

Abstract

A rhodium-catalyzed process has been developed in which mixtures of internal and terminal olefins are isomerized and hydroborated in one step yielding the corresponding terminal pinacolboronates. Homologation and subsequent oxidation regioselectively affords the terminal aldehyde in what amounts to a one-pot CO free hydroformylation. Good overall yields are obtained in all substrates examined. In a related study, mechanistic aspects of the rhodium catalyzed hydroboration of vinyl arenes have been probed. A combination of substituent effects (Hammett study), deuterium labeling studies and heavy atom isotope effects has demonstrated mechanistic differences in the hydroboration of electron rich and electron poor substrates. The results of the study further demonstrate the differences in reaction mechanism for hydroborations mediated with catecholborane versus pinacolborane.

The Corey-Chaykovsky reaction, in which an aldehyde and a sulfur ylide are coupled to yield an epoxide has proven to be a versatile and valuable method for the production of epoxides. The reaction between benzaldehyde and benzyldimethylsulfonium tetrafluoroborate has been subjected to a kinetic analysis. Activation parameters were determined for the reaction and a large negative ΔS^\ddagger of $-35 \text{ cal/mol}\cdot\text{K}^{-1}$ was calculated for the epoxidation of benzaldehyde. A large carbon kinetic isotope effect of 1.026 and an inverse deuterium isotope effect of 0.93 were determined for the reaction. A large positive Hammett ρ of +2.50 was found for the epoxidation of various substituted benzaldehydes by competition experiments. These results aided in the

identification of the rate limiting step as addition of the ylide species to benzaldehyde. In a separate, although related study, the mechanism of the collapse of hydroxysulfonium salts has been examined with regard for implications in the epoxidation of aldehydes. The *anti*-diastereomer reacted with complete retention of stereochemistry and no crossover, while the *syn*-diastereomer gave crossover products along with *cis* and *trans* epoxides. Deprotonation and re-protonation on the carbon of the alpha-hydroxy sulfonium ylide was responsible for production of the *trans* epoxide as demonstrated by deuterium labeling.

Preface

Part A of this thesis is a summary of our forays into the rhodium catalyzed hydroboration reaction. The first chapter presents a broad overview of the field and attempts to place the experimental work of latter chapters into the appropriate context. Chapter 2 reveals a devised synthetic methodology amenable to the procurement of linear aldehydes in high yield and complete regioselectivity, in which a metal-catalyzed hydroboration is the key step. A highlight of the reported method is that it accomplishes the conversion of crude olefinic mixtures into highly desirable products in a single pot without the need for toxic gases such as carbon monoxide. Chapter 3 delves into a mechanistic study of the rhodium catalyzed hydroboration reaction employed in the previous chapter. In Chapter 3, aryl substituted alkenes are examined in detail as these substrates are important in the preparation of pharmaceutical compounds. This study was undertaken in order to elucidate reaction features responsible for the unique regioselectivity obtained in the reaction of this substrate class. A combination of substituent effects, labeling studies and kinetic isotope effects were used to as mechanistic probes.

These same tools were employed in the study of a key reaction used for the preparation of epoxides via sulfur ylides called the Corey-Chaykovsky reaction. This reaction is the subject of Part B of this thesis. Remarkably, despite the importance of this reaction in the preparation of epoxides, which are key intermediates in synthesis, a detailed study of its mechanism was lacking in the literature at the time we began our study. A broad overview of the Corey-Chaykovsky reaction is presented in Chapter 4. Chapter 5 discloses the results of a mechanistic study of the titled reaction in acetonitrile.

Results and conclusions from this study are then compared and contrasted to those obtained in a mixed solvent system of acetonitrile/water. The results of this latter study are presented in full in Chapter 6.

Acknowledgements

During the course of graduate studies I have had the distinct pleasure of being taught by the more experienced members of the Crudden research group. To those individuals I owe a great debt and I thank-you one and all. In particular I would like to acknowledge the near Herculean efforts made by one Dr. Pedro Montoya-Pelaez. The chastisement I received from you on a daily basis undoubtedly improved me both as a chemist as well as a person.

I would also like to thank-you Dr. Cathleen Crudden. It has been a long and eventful road from second year undergraduate organic chemistry. You helped get me my first job in a lab and later hired me as a summer student in your own labs. Of course you have also been my diligent supervisor throughout graduate studies. I have always enjoyed our conversations on chemistry and they have certainly help shape my views on the subject matter. As my understanding of the molecular world continues to grow over time, I will often be reminded of the lessons I learned so early on and at your hand.

One of the greatest benefits of attending an institution such as Queen's University is the caliber of fellow graduate students, research assistants and faculty members with whom one has contact over the course of a graduate degree. You have all enriched me as a chemist in one aspect or another. In particular I would like to thank Dr. Francoise Sauriol for so graciously lending her expertise in the field of NMR whenever called upon to do so, which incidentally was a whole lot. I would also like to extend my appreciation to Dr. Stan Brown and Dr. Alexei Neverov. These two individuals have always been receptive to questions and patient with their answers pertaining to the finer points of physical organic chemistry.

Last but certainly not least I need to thank every single member of my family for the support both emotional and financial received over the course of my graduate studies. To my father, whose passion for science in all its forms is a constant inspiration to us all, I thank you for your unwavering encouragement. To my lovely wife Jessica, who hasn't seen nearly enough of me of late, you pretty much ROCK.

Statement of Originality

I, David Ryan Edwards, state that I am the sole author of this thesis.

I, David Ryan Edwards, state that the following known compounds were prepared by me using novel methodology: (1-heptanal), (1-octanal), (1-nonanal), (1-decanal), (**3-12**).

I, David Ryan Edwards, state that the following previously unknown compounds were prepared by me for the first time: (*anti*-**6-6**), (*syn*-**6-6**).

Table of Contents

Abstract	ii
Preface	iv
Acknowledgements	vi
Statement of Originality	viii
Table of Contents	ix
List of Figures and Schemes	xiii
List of Tables	xvii
List of Abbreviations	xix
Part A: Rhodium Catalyzed Hydroborations	
Chapter 1: Introduction to Rhodium Catalyzed Hydroborations	
1.1 Introduction	1
1.2 Mechanistic Studies	3
1.3 Oxidation of Catalyst	8
1.4 Hydroborating Reagents	12
1.5 Substrate Scope	15
1.6 Enantioselective Hydroborations	23
1.7 Functionalization of Carbon-Boron Bonds	28
1.8 Conclusions	32
1.9 References	32
Chapter 2: One-Pot Carbon Monoxide Free Hydroformylation of Internal Olefins to Terminal Aldehydes	
2.1 Introduction	36

2.2	Isomerization and Hydroboration	41
2.3	Homologation	43
2.4	Oxidation	45
2.5	Hydroformylation of Alkene Mixtures	46
2.6	Conclusions	48
2.7	Experimental Section	48
2.8	References	49

Chapter 3: Electronic Effects in the Rh catalyzed Hydroboration of Vinyl Arenes

3.1	Introduction	52
3.2	Hydroboration of 1-naphthyl-2-phenylethene	53
3.3	Hydroboration of Unsymmetrical Stilbenes	57
3.4	Relative Reactivity of Simple Vinyl Arenes	61
3.5	Labeling Study	62
3.6	¹³ C Carbon Isotope Effects	70
3.7	Paramagnetic Relaxation Agents	74
3.8	Conclusions	76
3.9	Experimental Section	77
3.10	References	96

Part B: Sulfur Ylide Epoxidations

Chapter 4: Introduction to Sulfur Ylide Epoxidations

4.1	General Introduction	100
4.2	Generation of Sulfur Ylides	103
4.3	Sulfonium Salt and Ylide Decomposition	106

4.4	Reaction Mechanism	108
4.5	Forays into Asymmetry	115
4.6	Conclusions	123
4.7	Research Objectives	124
4.8	References	126
Chapter 5: Epoxidation Mechanism Explored		
5.1	Research Objectives	129
5.2	Rate Studies	130
5.3	Activation Parameters	133
5.4	Cross-Over Experiments	136
5.5	¹³ C Carbon Isotope Effects	137
5.6	² H-Isotope Effects	140
5.7	Hammett Study	141
5.8	<i>ortho</i> -Substituted Benzaldehydes	144
5.9	SET Versus PL Mechanisms	145
5.10	Discussion	147
5.11	Conclusion	150
5.12	Experimental Section	151
5.13	References	164
Chapter 6: Epoxidations in an Aqueous System		
6.1	Introduction	167
6.2	Hammett Study	168
6.3	Deuterium Labeling Study	170

6.4	Cross-over experiments with <i>anti-1</i>	171
6.5	Cross-Over Experiments with <i>syn-6-1</i>	175
6.6	Studies of other sulfonium reagents	180
6.7	Conclusions	185
6.8	Experimental Section	186
6.9	References	193
Chapter 7: Conclusions and Future Work		194

List of Figures and Schemes

Chapter 1: Introduction to Rhodium Catalyzed Hydroborations

Figure 1-1: Resonance Structures of Catecholborane	1
Figure 1-2: Deuterium Labeling Experiment (DBcat)	10
Figure 1-3: Deuterioboration of 1-25	12
Figure 1-4: Hydroborating reagents	13
Figure 1-5: Relative Reactivities of Various Olefines	16
Figure 1-6: Hydroboration of <i>exo</i> -Cyclic Alkenes	22
Scheme 1-1: Hydroboration Mechanism with Wilkinson's Catalyst	4
Scheme 1-2: Boryl Insertion Pathway	6
Scheme 1-3: Hydroboration and Hydrogenation of Vinylboronate Esters	6
Scheme 1-4: Phosphine Free Catalytic Cycle	7
Scheme 1-5: Proposed Diastereoselective <i>beta</i> -Hydride Elimination from 1-24	11
Scheme 1-6: Pinacol Quench	14
Scheme 1-7: Hydroboration of Internal Alkenes	17
Scheme 1-8: Production of <i>cis</i> -Vinylboronates	19
Scheme 1-9: Hydroboration of Protected Cyclohexeneol	22
Scheme 1-10: Enantioselective Hydroboration of Substituted Cyclopropenes	25
Scheme 1-11: Homologation/Substitution Sequence	29
Scheme 1-12: Oxidation of <i>alpha</i> -Halo-Boronates	30
Scheme 1-13: Amination Strategy	31
Chart 1-1: Catalyzed Versus Uncatalyzed Reaction Selectivity	2
Chart 1-2: Common Chiral Ligands	24

Chart 1-3: Transformation of Carbon-Boron Bonds	29
Chapter 2: One-Pot Carbon Monoxide Free Hydroformylation of Internal Olefins to Terminal Aldehydes	
Figure 2-1: Isomerization/Hydroformylation Process	38
Scheme 2-1: Synthetic Strategy	41
Chapter 3: Electronic Effects in the Rh catalyzed Hydroboration of Vinyl Arenes	
Figure 3-1: Stilbene Hammett Plot	60
Figure 3-2: Styrene Hammett Plot	62
Figure 3-3: ¹³ C Carbon Kinetic Isotope Effect (¹³ C-KIE)	72
Figure 3-4: Quantitative ¹³ C-NMR spectrum of <i>p</i> -chlorophenethanol	73
Scheme 3-1: First Synthesis of Deuterated Substrate	65
Scheme 3-2: Hydride Insertion Process	69
Chart 3-1: Hydroboration of <i>trans</i> -Stilbene	54
Chart 3-2: Hydroboration of <i>cis</i> -Stilbenes (3-8a-g)	59
Chapter 4: Introduction to Sulfur Ylide Epoxidations	
Figure 4-1: Structure of Fluorenylide 4-2	102
Figure 4-2: <i>Cisoid</i> and <i>Transoid</i> Addition Geometries	115
Scheme 4-1: Reactions of Carvone with Sulfur Ylides	101
Scheme 4-2: Forbes Decarboxylation Strategy	104
Scheme 4-3: Sulfur Ylides from N-Tosylhydrazone Salts	105
Scheme 4-4: Sommelet-Hauser Rearrangement	107
Scheme 4-5: Initial Mechanistic Proposal of Johnson	108
Scheme 4-6: The Cross-Over Experiment	109

Scheme 4-7: Cross-Over Experiments in DMSO and DCM	113
Scheme 4-8: Configurational Stability	117
Scheme 4-9: Stereochemical Model for Ylide Epoxidation	123
Chart 4-1: Acidities of Various Sulfonium Salts	103
Chapter 5: Epoxidation Mechanism Explored	
Figure 5-1: Plot of k_{obs} Versus [DBU]	131
Figure 5-2: Plot of k_{obs} Versus [benzaldehyde]	132
Figure 5-3: Reciprocal Plot of $1/k_{\text{obs}}$ Versus [benzaldehyde]	133
Figure 5-4: Eyring Plot	135
Figure 5.5: ^{13}C Carbon Kinetic Isotope Effect (^{13}C -KIE)	139
Figure 5-6: Secondary Deuterium Kinetic Isotope Effect (SDKIE)	141
Figure 5-7: Hammett Plot	143
Figure 5-8: Determination of k_{obs} dependence on [benzaldehyde], (expt #1)	153
Figure 5-9: Determination of k_{obs} dependence on [benzaldehyde], (expt #2)	153
Figure 5-10: Determination of k_{obs} dependence on [benzaldehyde], (expt #3)	154
Figure 5-11: Determination of k_{obs} dependence on [benzaldehyde], (expt #4)	154
Figure 5-12: Determination of k_{obs} dependence on [benzaldehyde], (expt #5)	155
Figure 5-13: Determination of k_{obs} dependence on [benzaldehyde], (expt #6)	155
Figure 5-14: Determination of k_{obs} dependence on [DBU], experiment #1	156
Figure 5-15: Determination of k_{obs} dependence on [DBU], experiment #2	156
Figure 5-16: Determination of k_{obs} dependence on [DBU], experiment #3	157
Figure 5-17: Plot of $\text{Ln}[k_{\text{obs}}]$ versus $\text{Ln}[\text{DBU}]$	157
Figure 5-18: Temperature Studies, experiment #1	158

Figure 5-19: Temperature Studies, experiment #2	158
Figure 5-20: Temperature Studies, experiment #3	159
Figure 5-21: ^{13}C -NMR spectra of benzaldehyde	162
Scheme 5-1: Epoxidation Mechanism	132
Scheme 5-2: Polar Addition and Single Electron Transfer Processes	145
Chapter 6: Epoxidations in an Aqueous System	
Figure 6-1: Hammett Plot (<i>trans</i> -stilbene oxide)	169
Figure 6-2: Hammett Plot (<i>cis</i> -stilbene oxide)	169
Figure 6-3: Hammett Plot for Sulfonium Salt 6-5 (<i>trans</i> -epoxide)	181
Figure 6-4: Hammett Plot for Sulfonium Salt 6-5 (<i>cis</i> -epoxide)	182
Scheme 6-1: Epoxidation Mechanism	171
Scheme 6-2: Possible invertive process yielding <i>trans</i> - 6-2 from <i>syn</i> - 6-1	177
Scheme 6-3: Base Catalyzed Isomerization	178

List of Tables

Chapter 1: Introduction to Rhodium Catalyzed Hydroborations

Table 1-1: Effect of Catalyst Purity on Regioselectivity	9
Table 1-2: Directed Hydroborations	21

Chapter 2: One-Pot Carbon Monoxide Free Hydroformylation of Internal Olefins to Terminal Aldehydes

Table 2-1: Hydroboration Reaction Conditions	42
Table 2-2: Homologation Reaction Conditions	43
Table 2-3: One-Pot Preparation of Homologated Aldehyde	46
Table 2-4: Hydroformylation of Various Internal Olefins	47

Chapter 3: Electronic Effects in the Rh catalyzed Hydroboration of Vinyl Arenes

Table 3-1: Hydroboration of 1-Naphthyl-2-Phenylethene	56
Table 3-2: Labeling Results	68
Table 3-3: Results of Styrene Competition Experiment	83
Table 3-4: Integration values for standard reaction of <i>p</i> -methoxystyrene taken to 100% conversion	88
Table 3-5: Integration values for KIE determination reaction of <i>p</i> -methoxystyrene taken to 20% conversion (reaction #1)	89
Table 3-6: Integration values for KIE determination reaction of <i>p</i> -methoxystyrene taken to 20% conversion (reaction #2)	90
Table 3-7: Isotope effects and associated errors for hydroboration of <i>p</i> -methoxystyrene	91

Table 3-8: Integration values for standard reaction of <i>p</i> -chlorostyrene taken to 100% conversion	93
Table 3-9: Integration values for KIE determination reaction of <i>p</i> -chlorostyrene taken to 17% conversion (reaction #1)	94
Table 3-10: Integration values for KIE determination reaction of <i>p</i> -chlorostyrene taken to 17% conversion (reaction #2)	95
Table 3-11: Isotope effects and associated errors for hydroboration of <i>p</i> -chlorostyrene	96
Chapter 5: Epoxidation Mechanism Explored	
Table 5-1: Rate Constants k_{obs} and k_{app} as a Function of Temperature	136
Table 5-2: Various Carbon Isotope Effects for Arylcarbonyl Additions	140
Table 5-3: Relative Rate Data for Benzaldehyde Competition Experiments	143
Table 5-4: ^{13}C -NMR Data for KIE Determination	161
Table 5-5: Calculated ^{13}C -KIE Data and Errors	161
Table 5-6: ^1H -NMR Data for SDKIE Determination	163
Chapter 6: Epoxidations in an Aqueous System	
Table 6-1: Competition Experiments	173
Table 6-2. Cross-Over Studies with <i>syn-6-1</i>	176
Table 6-3: Cross-Over Studies with <i>syn-6-6</i>	184

List Of Abbreviations

acac	acetylacetonate
Ac	acetyl
app.	apparent
Ar	aryl
9-BBN	9-borabicyclo[3.3.1]nonane
BDPP	2,4-bis(diphenylphosphino)pentane
BINAP	2,2'-bis(diphenylphosphino)-1,1'-binaphthyl
B:L	branched-to-linear
Bu	butyl
°C	Celsius
cat	catalyst
COD	1,5-cyclooctadiene
Cy	cyclohexyl
D	deuterium
DBP	dibenzylphosphorane
DBU	1,5-diazabicyclo[4.3.0]non-5-ene
DCE	dichloroethane
DCM	dichloromethane
DFT	density functional theory
DIOP	2,3- <i>O</i> -isopropylidene-2,3-dihydroxy-1,4-bis(diphenylphosphino)butane
DPPB	1,2-bis(diphenylphosphino)butane
DPPF	(diphenylphosphino)ferrocene

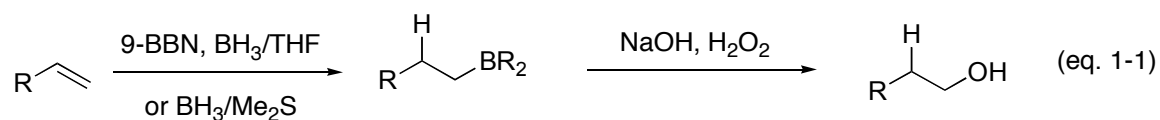
ee	enantiomeric excess
eq.	equation
equiv.	equivalents
Et	ethyl
F	fractional conversion
FID	free induction decay
GC	gas chromatography
HBpin	pinacolborane
HBcat	catecholborane
HRMS	high-resolution mass spectrometry
hrs	hours
Hz	hertz
<i>J</i>	coupling constant
K	kelvin
KIE	kinetic isotope effect
L	ligand
LAH	lithium aluminum hydride
LDA	lithium diisopropylamide
Me	methyl
MeOH	methanol
Min	minute
NAPHOS	2,2'-(CH ₂ -PPh ₂) ₂ -1,1'-binaphthene
NBD	2,5-norbornadiene

NMO	N-methyl-morpholine-N-oxide
NMR	nuclear magnetic resonance
[O]	oxidation
Ph	phenyl
ppm	parts per million
Pr	propyl
QUINAP	1-(2-diphenylphosphino-1-naphthyl)isoquinoline
R	integration ratio
RDS	rate determining step
SBH	sodium borohydride
SDKIE	secondary deuterium isotope effect
sec	second
SNR	signal to noise ratio
T	temperature
TBDMS	<i>tert</i> -butyldimethylsilyl
THF	tetrahydrofuran
TLC	thin layer chromatography
TMANO	trimethylamine-N-oxide
TOF	turn over frequency
Tol	toluene

Chapter 1: Introduction to Rhodium Catalyzed Hydroborations

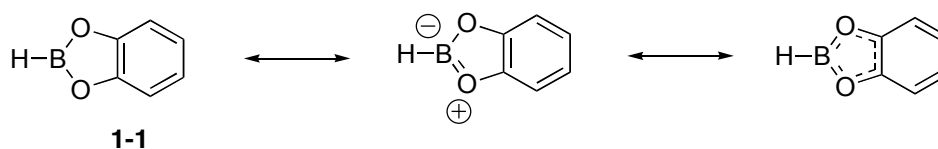
1.1: Introduction

The hydroboration of carbon-carbon multiple bonds with reagents such as 9-BBN or BH_3 adducts is a well-established methodology.¹ Generally, the resulting alkylborane is oxidized with alkaline hydrogen peroxide to afford alcohols with overall anti-Markovnikov selectivity, equation 1-1.



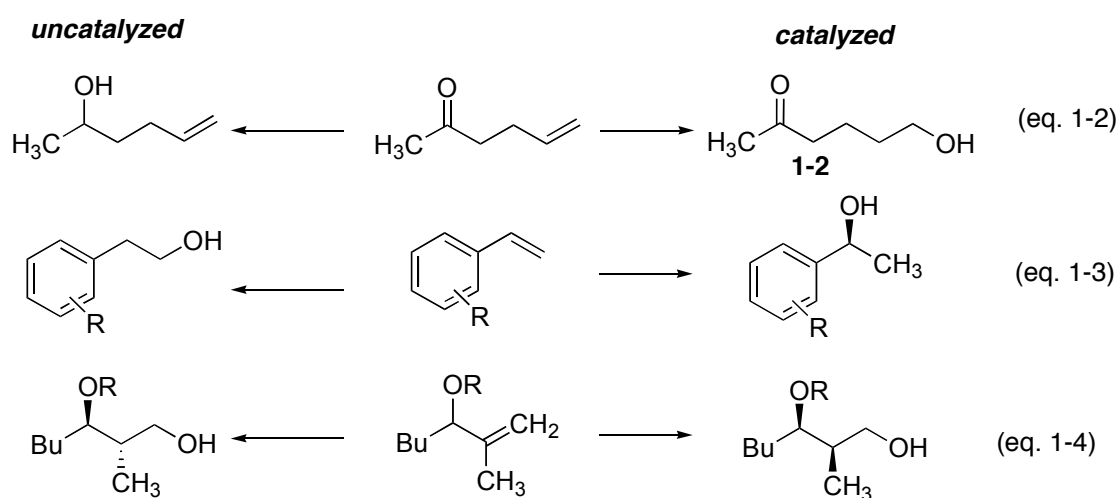
In a seminal publication, Mannig and Noth demonstrated that hydroborations of alkenes with catecholborane **1-1** could be catalyzed by rhodium in a synthetically useful manner.² Reagent **1-1** had previously been shown to require elevated temperatures and extended reaction times to effect hydroboration of alkenes and alkynes in the absence of a catalyst.³ This lack of reactivity, as compared to typical boranes such as 9-BBN, has been attributed to the decreased Lewis basicity of the vacant p-orbital on boron. The nature of the decreased Lewis basicity of **1-1** is made clear upon examination of the resonance structures of **1-1** in Figure 1-1. The use of heteroatom substituted hydroborating reagents has proven key in the development of transition metal catalyzed B-H additions as these reagents preclude the uncatalyzed background reaction from competing.

Figure 1-1: Resonance Structures of Catecholborane



It was further shown that in the presence of Wilkinson's catalyst, $\text{RhCl}(\text{PPh}_3)_3$, 5-hexen-2-one underwent hydroboration/oxidation to afford **1-2** in which the olefin has undergone H-B addition in preference to the ordinarily more reactive ketone, equation 1-2.² It has subsequently been shown that transition metal catalyzed hydroborations often alter the selectivity relative to typical uncatalyzed reactions affording products that are of complementary chemo-, regio- and even stereoselectivity, Chart 1-1.⁴ To date a number of transition metals have been employed to catalyze the B-H addition to multiple bonds including Zr,⁵ Sm,⁶ Ru,⁷ Ti⁸ and Ir.⁹ However, it is neutral and cationic complexes of Rh that have ultimately proven the most effective catalysts for transition metal catalyzed hydroborations.¹⁰ The advantages of catalyzed hydroborations over their uncatalyzed counterparts include mild reaction conditions, improved or even altered reaction selectivity and perhaps most importantly, the ability to affect chiral amplification through the use of catalytic quantities of optically active ligands on the metal leading to highly enantioenriched products.

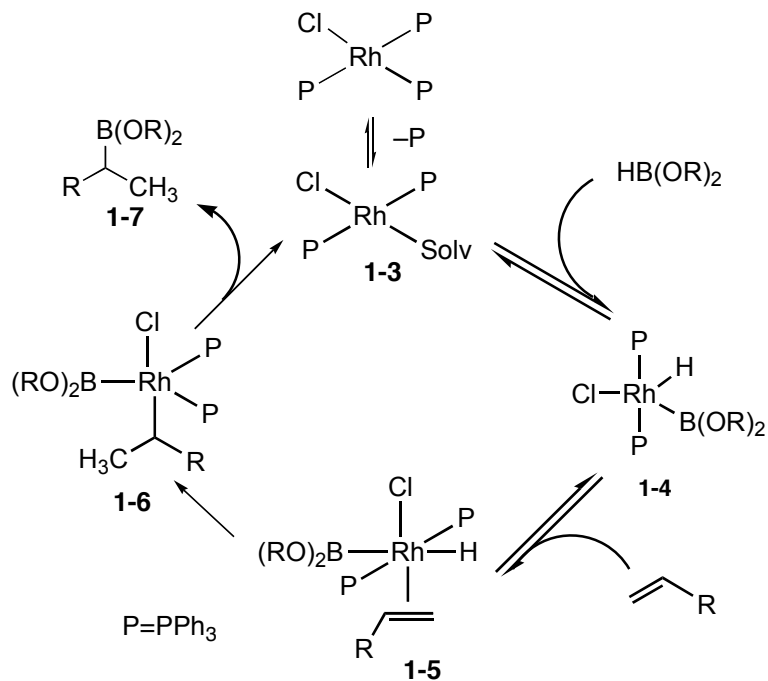
Chart 1-1: Catalyzed Versus Uncatalyzed Reaction Selectivity



1.2: Mechanistic Studies

It was determined in the seminal publication of Mannig and Noth that Wilkinson's catalyst was the most active of a large number of metal species examined in the hydroboration reaction.² Hydroborations carried out in the presence of this catalyst and other similar rhodium analogues remain today one of the most thoroughly studied class of metal catalyzed hydroborations. At present, a detailed kinetic study on this reaction is still lacking, however, a mechanism consistent with Scheme 1-1 has been proposed.^{2,11} The precatalyst $\text{ClRh}(\text{PPh}_3)_3$ enters the catalytic cycle following disassociation of one phosphine ligand and subsequently undergoes oxidative addition with catecholborane to generate **1-4**. An analogue of this species where $\text{P} = \text{P}(\text{iPr})_3$ has been isolated and its structure characterized by X-ray crystallography.¹² Complexation of olefin generates the six coordinate intermediate **1-5** where it is predicted by theoretical calculations that the hydride and boryl ligands are trans in the reactive species.¹³ Insertion of the complexed olefin into the rhodium hydride bond affords **1-6**, which then reductively eliminates the alkyl boronate product **1-7**. Precedent for reductive elimination of the alkyl boronate from **1-6** can be found in stoichiometric studies on osmium boryl compounds.¹⁴

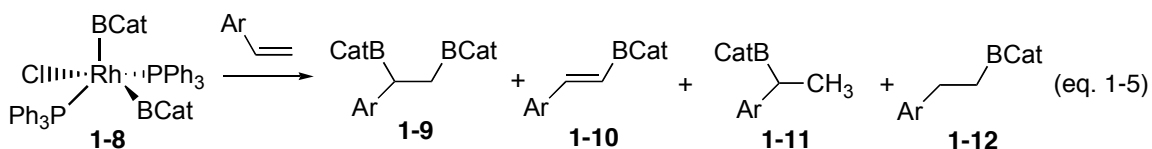
Scheme 1-1: Hydroboration Mechanism with Wilkinson's Catalyst



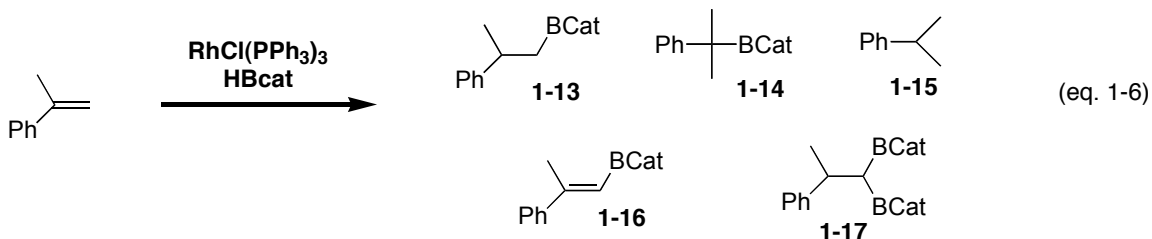
There certainly is adequate precedent for olefin insertions into metal-hydride bonds as well as for the subsequent reductive elimination of the alkyl and boryl substituents to substantiate the mechanism in Scheme 1.¹⁵ Nonetheless, there exists substantial experimental evidence that under certain reaction conditions the catalytic cycle may actually diverge at intermediate **1-5** and proceed via an alkyl insertion into the rhodium boryl bond. The evidence for this alternate pathway is best delineated with vinylarenes and as such the ensuing discussion will focus on these substrates for rhodium catalyzed hydroborations.

The bis(boryl) rhodium complex **1-8** has been isolated and when reacted in the presence of vinylanisole, a mixture of products is obtained, equation 1-5.¹⁶ The formation of carbon-boron bonds in these species evidences the potential for alkyl insertions to

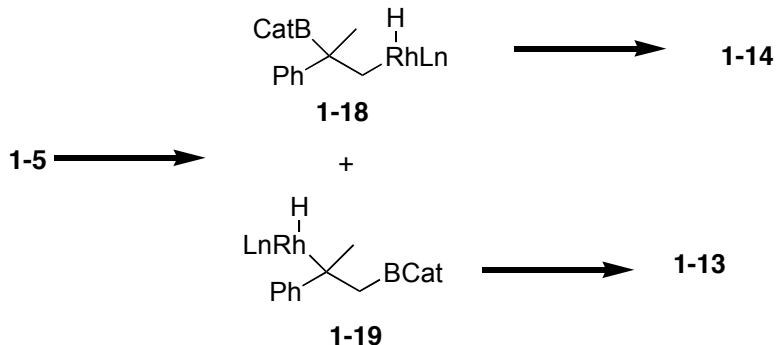
occur into rhodium boron bonds.¹⁷ Perhaps more convincingly, vinylboronate esters have also been observed as products of typical hydroboration reactions.



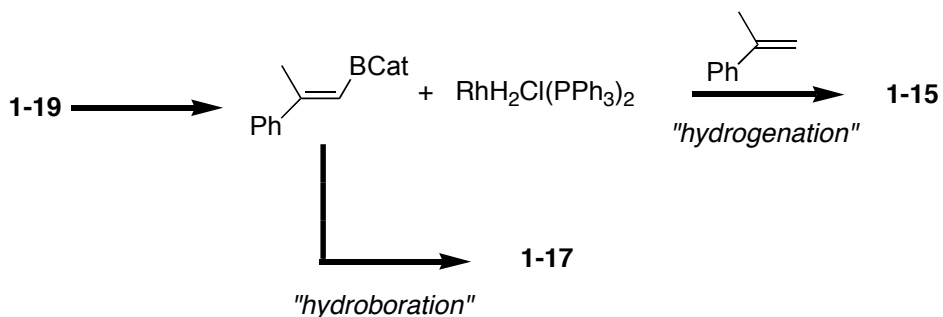
Subjecting 2-phenylpropene to rhodium-catalyzed hydroboration affords several products as shown in equation 1-6.¹⁸ In addition to the expected linear and branched boronate products **1-13** and **1-14**, 2-phenylpropane **1-15**, vinylboronate ester **1-16** and bis(boronate)ester **1-17** are all produced in varying amounts depending on the exact reaction conditions employed. It is proposed that the catalytic cycle of Scheme 1-1 diverges at intermediate **1-5** and proceeds via an insertion into the rhodium-boron bond to generate intermediates **1-18** and **1-19** depending on the regioselectivity of the process, Scheme 1-2. Subsequent reductive elimination generates either the linear or branched boronate ester **1-13** or **1-14**. To account for products **1-15**, **1-16** and **1-17** it is proposed that *beta*-hydride elimination from **1-19** competes with reductive elimination thus directly producing vinylboronate ester **1-16** and an active hydrogenation catalyst $\text{RhH}_2\text{Cl}(\text{PPh}_3)_2$, Scheme 1-3. Hydrogenation of 2-phenylpropene leads to the formation of reduced product **1-15**. Vinylboronate ester **1-16** can conceivably furnish bis(boryl) ester **1-17** following standard hydroboration and may even undergo hydrogenation thus presenting a second pathway for the generation of **1-13**.



Scheme 1-2: Boryl Insertion Pathway

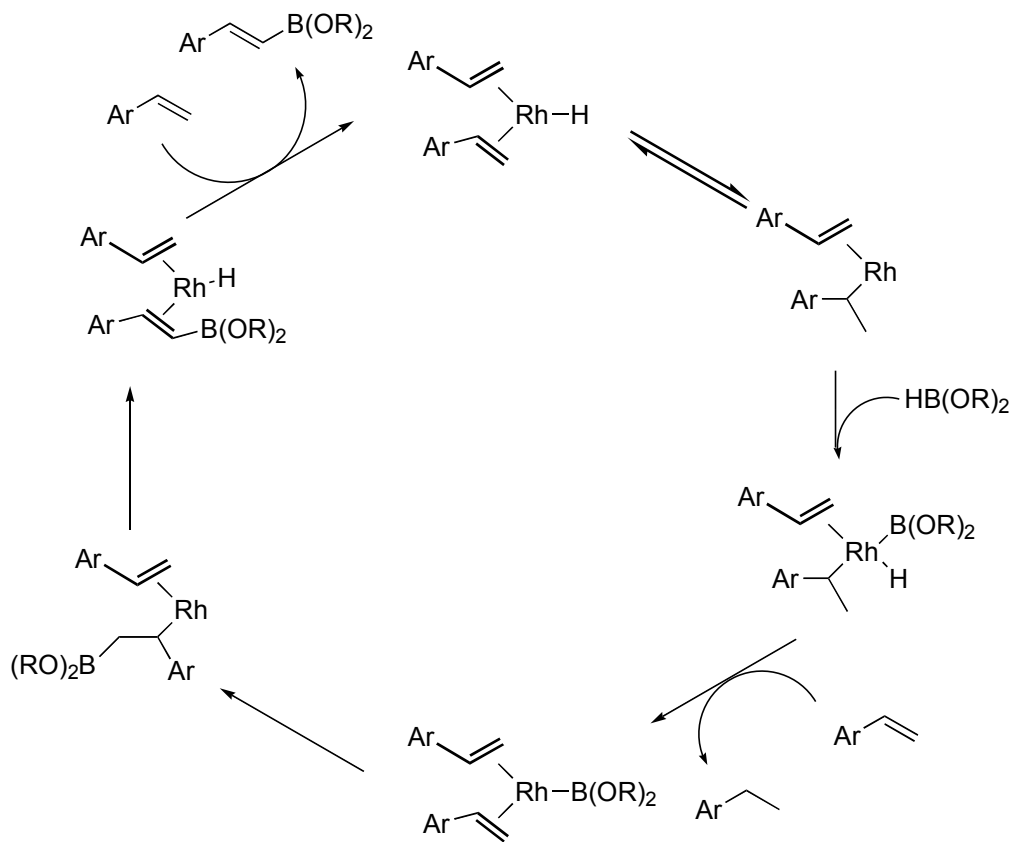


Scheme 1-3: Hydroboration and Hydrogenation of Vinylboronate Esters



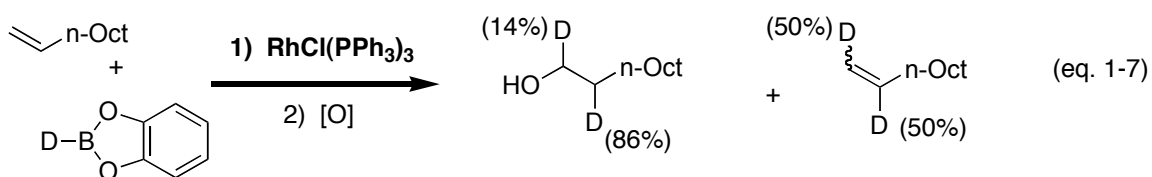
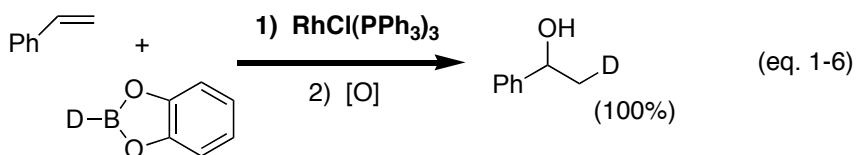
An additional mechanism has been proposed for the production of vinylboronate esters and reduced alkanes with a phosphine free catalyst under otherwise typical hydroboration conditions. Under these reaction conditions, alkane and vinylboronate ester are produced in approximately equal amounts suggesting that their production may be linked in the catalytic cycle. The reaction was found to be first order in borane and rhodium (half order in rhodium dimer) but inverse order in alkene. Subjecting deuterated styrene to the reaction led to extensive scrambling of the label in both starting material and products. The authors proposed the mechanism depicted in Scheme 1-4 as consistent with these findings.¹⁹ The key features being the presence of both a hydride and a boryl insertion as part of the catalytic cycle.

Scheme 1-4: Phosphine Free Catalytic Cycle



The use of deuterium labeling has been employed to identify the presence and extent of reversibility in olefin complexation as well as hydride insertion steps in the catalytic cycle. For example hydroboration of styrene with d^1 -catecholborane leads to quantitative incorporation of the label into the methyl substituent of 1-phenylethanol, equation 1-6.²⁰ This result is contrasted with that obtained for deuterioboration of 1-decene, equation 1-7. In this instance, deuterium is incorporated into both the terminal and internal carbons of the unreacted olefin as well as into both positions of the resulting alcohol product with a preference for label placement at the 2-position. Both of these results were interpreted in terms of a mechanism consisting of initial hydride transfer followed by reductive carbon-boron bond formation as in Scheme 1-1. The key

difference being that olefin complexation and hydride insertion were reversible for 1-decene but either or both steps were irreversible for styrene. In all fairness, however, the results obtained for styrene are also consistent with an initial and irreversible transfer of boron followed by fast reductive elimination. Nonetheless, these results are compelling evidence that the reaction mechanism for rhodium catalyzed hydroborations is highly substrate dependent.

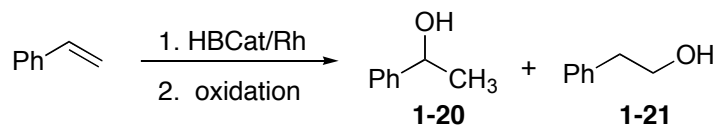


1.3: Oxidation of Catalyst

Severely complicating the issue of reaction mechanism in early reports of rhodium catalyzed hydroborations was that seemingly small quantities of oxygen impurities were found to have a profound impact on product distributions and accordingly the mechanism by which these species were produced. For example in two separate publications by different groups it was reported that styrene undergoes hydroboration to afford a mixture of alcohols **1-20** and **1-21** following oxidation, Table 1-1 entry 1.²¹ In a separate publication, styrene was reported to undergo clean conversion to alcohol **1-20**, Table 1-1 entry 2.²⁰ The disparity in product distribution in these studies

was ultimately attributed to incidental oxidation of the Wilkinson's catalyst employed in the studies depicted by entry 1, Table 1-1.

Table 1-1: Effect of Catalyst Purity on Regioselectivity



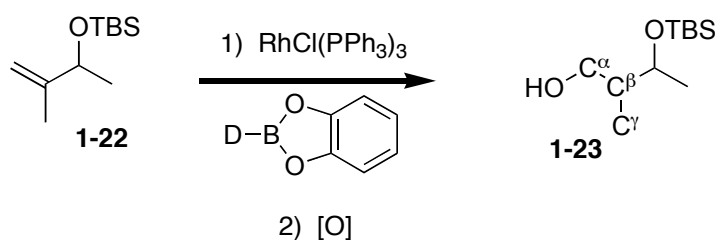
Entry	Catalyst	Purity	1-20	1-21	Ref.
1	RhCl(PPh ₃) ₃	O ₂ treated	60	40	21
2	RhCl(PPh ₃) ₃	Fresh	99	<1	20
3	RhCl(PPh ₃) ₃	O ₂ treated, then add 2 PPh ₃	99	<1	20,21

In solution, Wilkinson's catalyst is oxidized to RhCl(O₂)(PPh₃)₃ which then further decomposes to [Rh(μ-Cl)(PPh₃)₂]₂ and [RhCl(O₂)(PPh₃)₂]₂ producing triphenylphosphine oxide.²² It is thought that the production of triphenylphosphine oxide produces a phosphine deficient and yet still competent catalytic rhodium species responsible for the anomalous results reported in the literature. Consistent with this statement is the finding that the excellent selectivity observed in entry 2 of Table 1-1 can be regained simply by adding exogenous triphenylphosphine to oxygen treated Wilkinson's catalyst, entry 3.^{20,21}

In the last example, the effects of oxygen on the reaction were immediately apparent simply by comparing the product distribution obtained with different batches of Wilkinson's catalyst. This need not always be the case as is exemplified by the hydroboration of allyl silyl ether **1-22**. It has been reported that deuterioboration of **1-22** followed by oxidation affords the primary alcohol **1-23** containing the deuterium label

almost exclusively positioned at C^β as shown in the first entry of Figure 1-2.²³ This would certainly imply an irreversible transfer of hydride during the catalytic cycle. On the other hand, it has also been reported that under similar reaction conditions the deuterium label is incorporated into both the C^β and C^α sites as is shown in a ratio of 83:17 (C^β: C^α).²⁰ This result coupled with the finding that negligible deuterium was found in the olefinic positions of the unreacted starting material led the authors of this second study to conclude that while hydride transfer is indeed reversible, complexation of olefin to rhodium apparently is not.

Figure 1-2 Deuterium Labeling Experiment (DBcat)

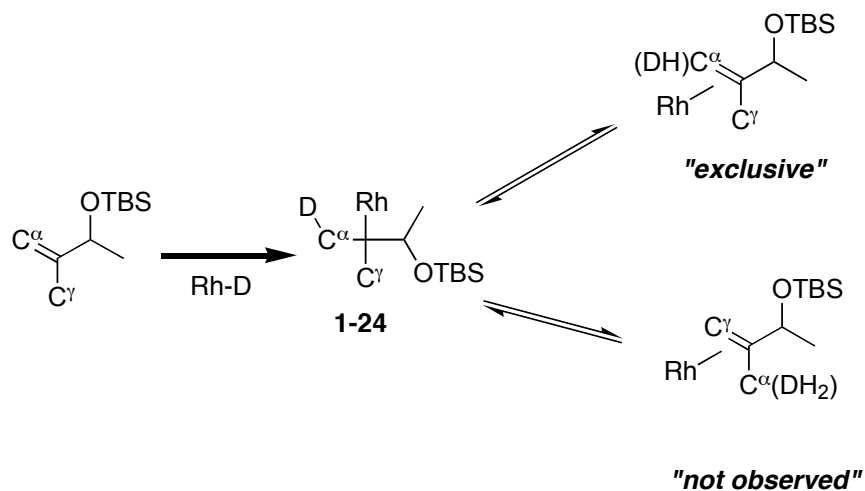


	C ^α	C ^β	C ^γ	Ref.
% deuterium	0	100	0	23
% deuterium	17	83	0	20

A follow up study was conducted in order to reconcile the disparate results obtained in the first two studies.²¹ It was indeed determined that the results depicted in entry 1 were a result of oxidized catalyst and that entry 2 represented a more accurate depiction of the expected label distribution in the hydroboration of **1-22**. However, more perplexing was the observation that 17% of the label was incorporated into the α-position and none into the γ-position. This result was initially explained based on a preferential β-

hydride elimination from one of the two diastereotopic methyl substituents of proposed intermediate **1-24**, Scheme 1-5.²⁰

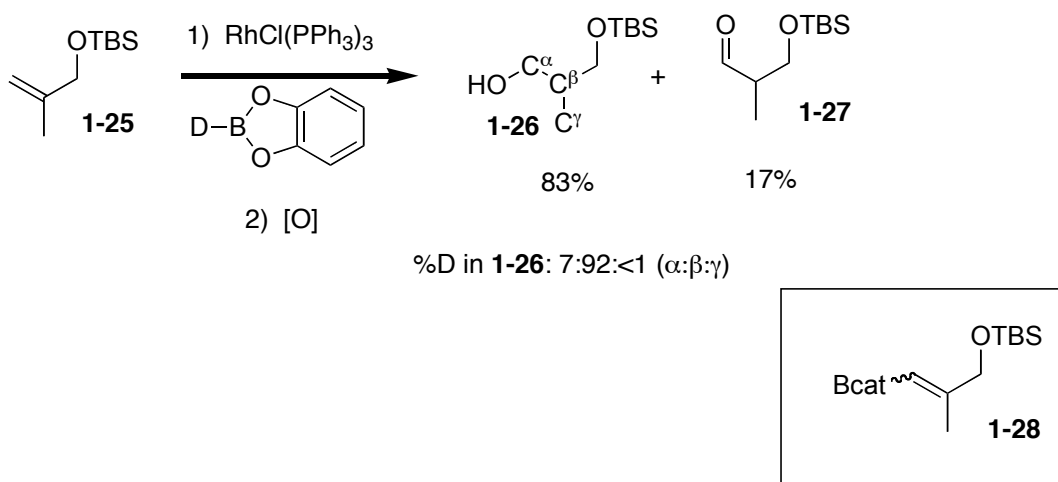
Scheme 1-5: Proposed Diastereoselective β -Hydride Elimination from **1-24**



To test this hypothesis unsaturated silyl ether **1-25** was deuterioborated under typical conditions to obtain alcohol **1-26**.²¹ In **1-25** the methyl substituents are rendered enantiotopic upon initial hydride insertion and as such there ought to be no preference for deuterium incorporation into the α - and γ -carbons. Despite this fact, there still remains a strong preference for deuterium incorporation into the alpha over the gamma carbon, Figure 1-3. Furthermore, unlabelled aldehyde **1-27** was also formed and subsequently demonstrated to have been produced following oxidation of vinylboronate **1-28**. It was thus concluded that deuterium label incorporation into the alpha carbon of **1-26** did not arise from reversible hydride insertion but rather as a result of hydrogenation of the vinylboronate ester formed in the reaction. The label incorporation into the β -carbon was presumed to result from typical hydroboration of the allyl silyl ether. In addition to demonstrating the complexity inherent to the hydroboration mechanism, this study

demonstrates that identical products may actually be produced in the same reaction but by different mechanisms.

Figure 1-3 Deuterioboration of **1-25**



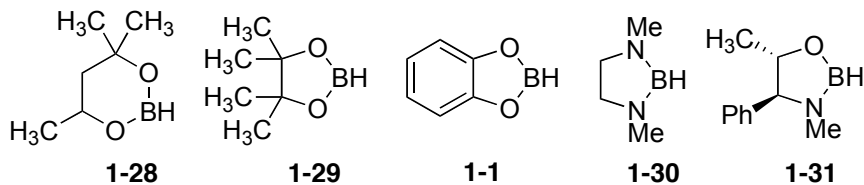
As described above, it is generally accepted that rhodium catalyzed hydroborations may proceed via different mechanisms depending on the reaction conditions and catalyst employed. Certainly the product distributions obtained in these reactions appears to be highly tunable depending on such reaction parameters as choice of substrate, borane, rhodium source and ligand as well as phosphine to rhodium ratio, solvent and even the presence of trace oxygen impurities.

1.4: Hydroborating Reagents

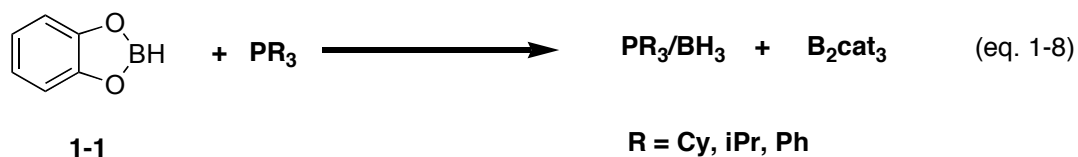
To date a number of boranes have successfully been employed in rhodium catalyzed hydroborations. Several are shown in Figure 1-4. Each of these reagents contains boron substituted by heteroatoms in line with the previous discussion on the

need to limit background uncatalyzed hydroborations by attenuating the Lewis acidity of the reagent.

Figure 1-4 Hydroborating reagents

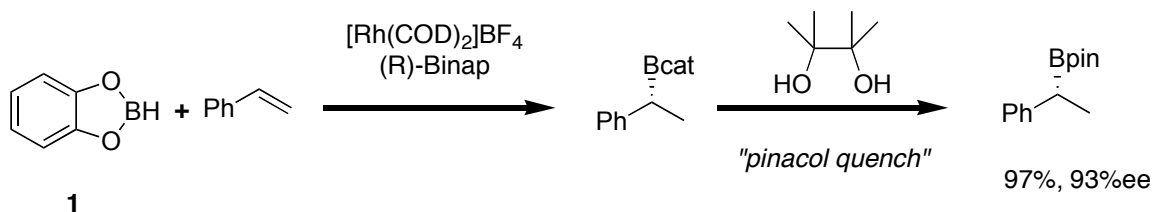


Boranes **1-1** and **1-28** were both featured in the original report of Mannig and Noth and it was reported that catecholborane **1-1** was deemed superior in terms of activity.² In fact, catecholborane **1-1** remains today the most widely used borane for rhodium catalyzed hydroborations. Despite catecholborane's wide use in synthesis it is prone to decomposition under typical hydroborating reaction conditions. For example, in the presence of nucleophiles such as phosphines, catecholborane decomposes to B_2cat_3 and phosphine borane adducts (PR_3/BH_3), equation 1-8.²⁴ Given the ease with which BH_3 adds to olefins this process represents a deleterious side reaction capable of altering the product distribution of the reaction. Additionally, due to the propensity for degradation, hydroborations carried out with borane **1-1** generally require an excess of the reagent. Another drawback to the use of **1-1** is that the alkylboronates produced in the reaction generally require immediate oxidation prior to isolation due to their inherent instability. This obviously precludes further transformation on the newly installed carbon-boron bond and limits the synthetic utility of this reagent.

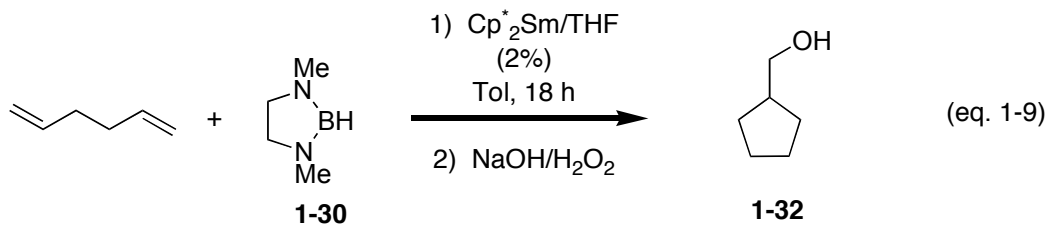


Sterically hindered pinacolborane **1-29** has proven a more robust reagent than **1-1**.^{5,25} It may be used in equimolar concentrations with the alkene substrate and isolation of the resulting alkylboronate product is easily performed by flash chromatography. In fact, if isolation of alkylboronates derived from catecholborane is desirable, then a pinacol quench which exchanges the dialkoxy ligands on boron can be performed prior work-up, Scheme 1-6.²⁶ In this example, not only could the pinacolboronate be isolated by flash chromatography in high yield, 97%, but no erosion of enantioselectivity was apparent during the pinacol quench. The resulting alkyl substituted pinacolboranes are not only amenable to direct isolation but they may also be subjected to further carbon-carbon bond forming reactions. This topic will be discussed fully in a latter section.

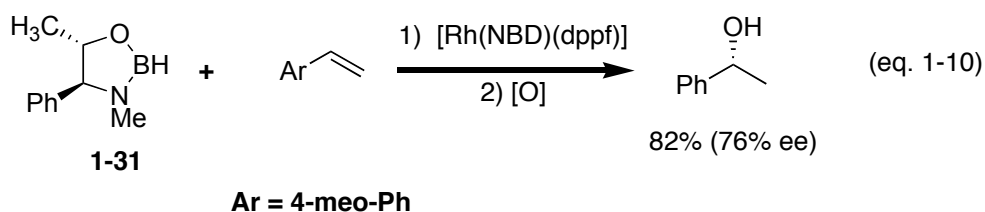
Scheme 1-6: Pinacol Quench



Borane **1-30** has seen limited use and then only when a relatively unreactive hydroborating reagent was required.²⁷ Carrying out the Sm catalyzed tandem hydroboration/cyclization reaction of equation 1-9 with either **1-1** or **1-29** led to extensive decomposition of the borane and lower yields of alcohol **1-32**. Switching to the even less Lewis acidic borane **1-30** led to the isolation of **1-32** in an 86% yield.



Borane **1-31** derived from pseudoephedrine has been employed in an attempt to effect transfer of chirality from the hydroborating reagent itself to a prochiral olefin. Moderate levels of asymmetric induction were obtained in the case of vinyl anisole, equation 1-10.²⁸ Ultimately, it is **1-1** and ever more so **1-29** that are typically used as standard hydroborating reagents in the rhodium catalyzed addition of B-H to olefins.



1-5: Substrate Scope

Simple alkyl substituted alkenes undergo efficient hydroboration. The rate at which these species react is a function of the substitution pattern. Generally, the higher the degree of substitution the less reactive the alkene and the following trend is generally observed: monosubstituted alkenes > 1,1-disubstituted alkenes > 1,2-disubstituted alkenes >> tri- and tetrasubstituted alkenes.²⁹ Figure 1-5 shows approximate reaction times for these general classes of alkenes to go to completion under typical reaction conditions.³⁰ Based on the relative reactivity of the alkene substituents in Limonene **1-33**, a selective hydroboration/oxidation sequence was performed to afford product **1-34** in 80% yield, equation 1-11.³⁰

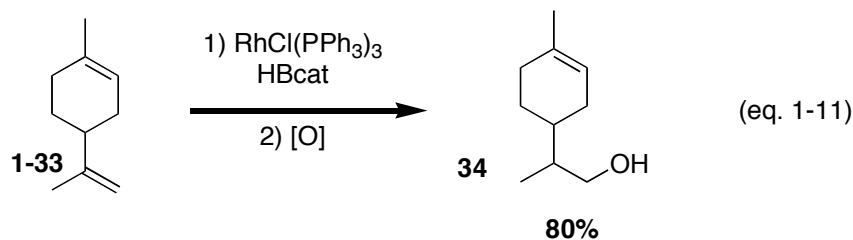
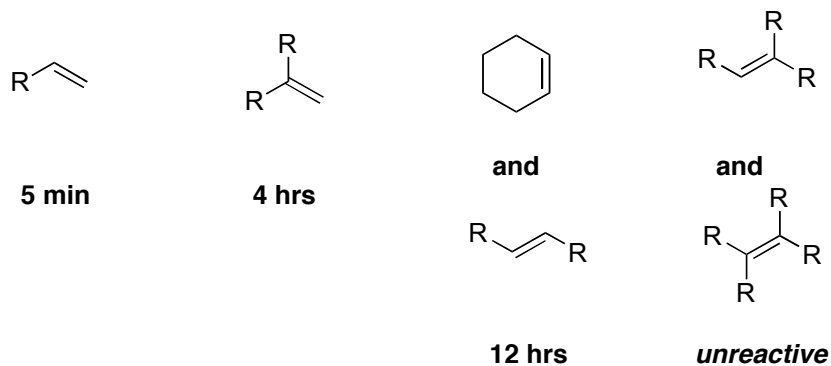
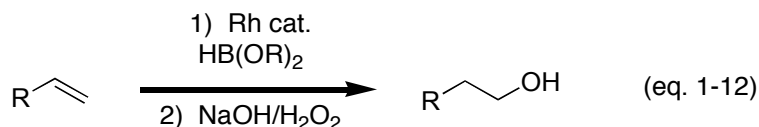


Figure 1-5: Relative Reactivities of Various Olefines^a



^a Reaction conditions: Wilkinson's catalyst, catecholborane (2 equiv.), THF, 20 °C.

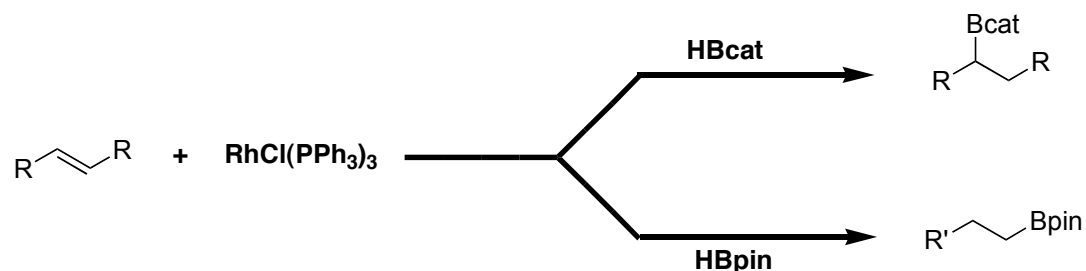
Generally terminal olefins are hydroborated to provide anti-Markovnikov alcohols following oxidation, equation 1-12.



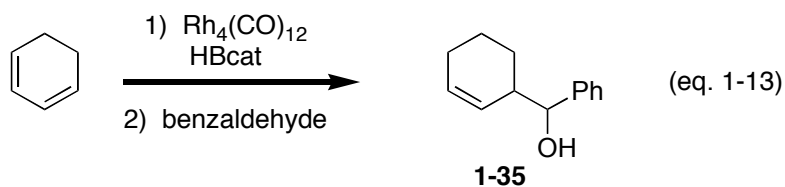
Internal olefins, on the other hand, may be hydroborated to provide either branched boronates^{20b} or alternatively linear boronates^{5c} depending on choice of hydroborating reagent, Scheme 1-7. The different regioselectivities obtained simply by switching the borane reagent has been attributed to the increased steric bulk of pinacolborane **1-29** as compared to catecholborane **1-1**. It was further speculated that hydroborations performed with **1-29** lead to fast *beta*-hydride eliminations isomerizing the double bond to the

terminal position whereupon a boryl insertion step occurs to produce the linear boronate isomer.^{5c}

Scheme 1-7: Hydroboration of Internal Alkenes

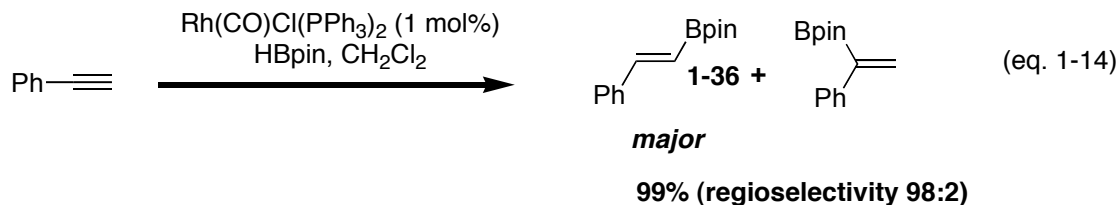


Cyclohexa-1,3-diene is efficiently hydroborated in a 1,4-fashion with $Rh_4(CO)_{12}$ and catecholborane **1-1**.³¹ The resulting allylic boronate is not isolated but rather immediately treated with benzaldehyde to produce **1-35** in an overall yield of 92%, equation 1-13. Acyclic dienes are less effective substrates with rhodium catalysts, however, employing $Pd(PPh_3)_3$ as catalyst leads to the efficient 1,4-hydroboration of these substrates.³¹ Simple *alpha*-haloalkenes are hydroborated to yield *alpha*-haloboronates.³²

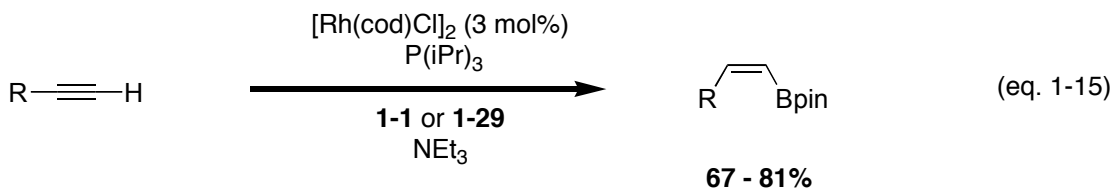


Hydroboration of alkynes to generate vinylboronate esters is a synthetically useful strategy and has been investigated in an effort to obtain substrates for coupling chemistry.³³ Subjecting phenylacetylene to Wilkinson's catalyzed hydroboration with catecholborane **1-1** results in a mixture of products.³⁴ Switching the hydroborating reagent to pinacolborane and the rhodium source to the commercially available

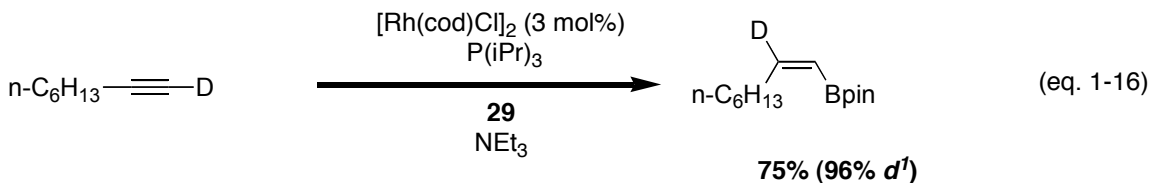
$\text{Rh}(\text{CO})\text{Cl}(\text{PPh}_3)_2$ results in the near quantitative formation of anti-Markovnikov product **1-36**, equation 1-14.^{5b} The substituents on the resulting double bond are preferentially positioned *trans* indicating an overall *cis*-addition of the B-H bond across the triple bond. A large number of terminal alkynes have been subjected to the reaction with similarly good results.



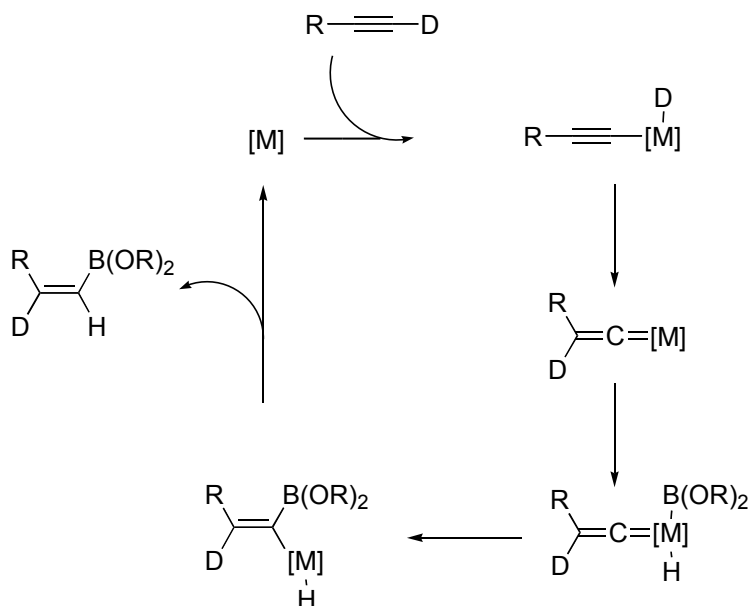
A relatively recent report describes a methodology amenable to the production of the isomeric *cis*-vinylboronates from the corresponding terminal alkyne, equation 1-15.³⁵



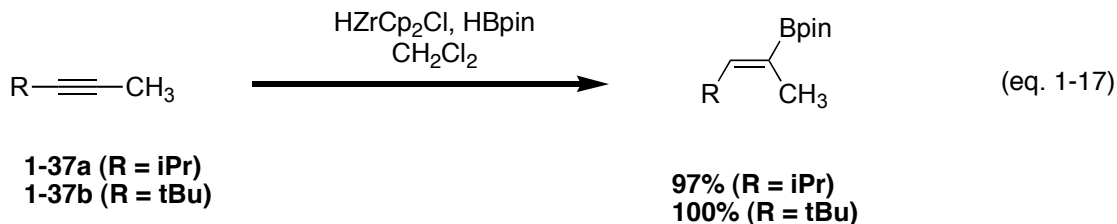
Under optimized conditions, including the addition of up to 2.5 equivalents of NEt_3 , the *cis*-vinylboronates are obtained in good yield and with excellent selectivity. Carrying out the reaction on *d*¹-octyne led to migration of the label from the acetylenic carbon to the β -carbon, equation 1-16. The authors propose the mechanism shown in Scheme 1-8 proceeding through a vinylidene intermediate to account for this unusual *trans*-addition of B-H across the alkyne.



Scheme 1-8: Production of *cis*-Vinylboronates

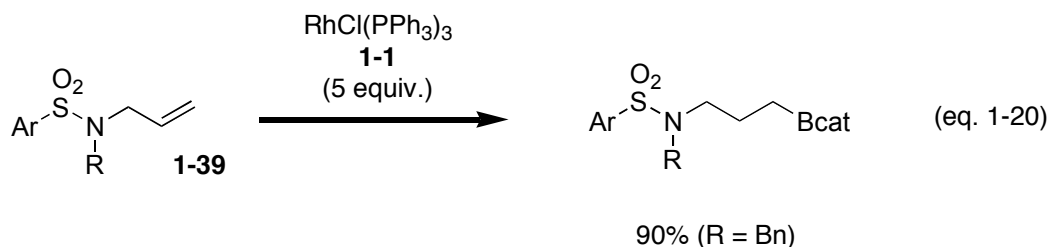
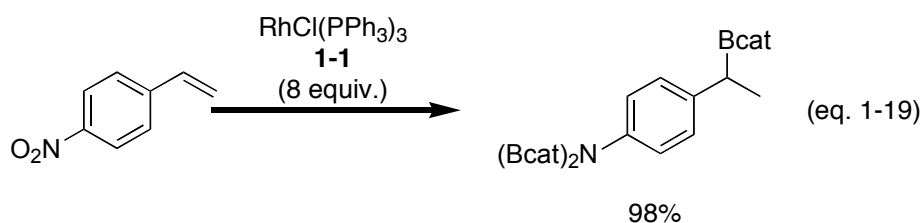
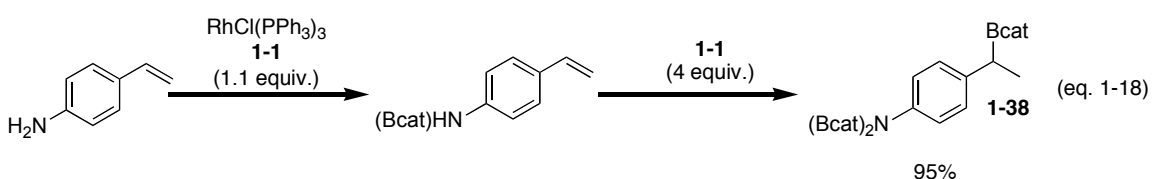


Hydroboration of internal alkynes with rhodium catalysts has not been extensively studied, however, it does appear that if the two carbons of the triple bond are sufficiently differentiated based on steric bulk then highly regioselective transformations are possible employing HZrCp_2Cl .^{5a} For example, the hydroboration of internal alkynes **1-37a** and **1-37b** preferentially positions boron proximal to the least hindered methyl substituted carbon, equation 1-17.



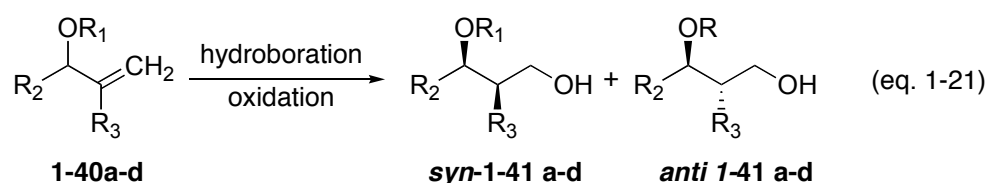
Heteroatom substituted alkenes present an additional complication in the case of metal catalyzed hydroborations. It is often seen that the heteroatoms complex to or even directly react with the metal and/or hydroborating reagent. In particular, nitrogen

containing substrates tend to give complicated product mixtures derived from nitrogen-mediated degradation of the hydroborating reagent. For example, hydroboration of 4-vinylaniline leads to the initial borylation of the amine substituent.³⁶ However, if an excess of **1-1** is employed then product **1-38** is obtained in a 95% yield, equation 1-18. Interestingly, changing the oxidation state of nitrogen from a primary amine to a nitro functionality does not preclude borylation of nitrogen, equation 1-19.³⁶ On the other hand, the nitrogen of sulfonamide **1-39** is tolerated in the hydroboration reaction provided that it is protected with R= Ph or Bn.³⁷ If R = H a complex mixture of products is obtained consistent with hydroboration, isomerization of the olefin and hydrogenation all occurring concurrently during the reaction. Degradation products and side reactions were reported to accompany each of the reactions in equations 1-18 through 1-20 and it was only through careful screening of catalyst choice and reaction conditions that useful syntheses were ultimately accomplished.



Despite the obvious difficulties associated with rhodium catalyzed hydroborations of functionalized substrates, these procedures significantly broaden the scope of the reaction and allow for the introduction of increased complexity in the synthesized molecules. Furthermore, heteroatoms have also successfully been used to direct hydroborations in an effort to alter and often improve upon the selectivity obtained in the hydroboration reaction. Chiral centers composed of protected ethers allylic to 1,1-disubstituted olefins have been used to direct hydroborations stereospecifically to one face of the alkene, Table 1-2. Both uncatalyzed reactions with 9-BBN and Rh catalyzed hydroborations are stereoselective, however, these examples illustrate stereocomplementry routes to both the *syn*- and *anti*-isomers of **1-41**.^{30,38,39} Allylic amines have been used in a similar fashion to direct facial selectivity in hydroborations of these substrates.⁴⁰

Table 1-2: Directed Hydroborations



Substrate	R ₁	R ₂	R ₃	Conditions	<i>syn</i> - 1-41	<i>anti</i> - 1-41
1-40a^a	H	Me	<i>n</i> -Pr	9-BBN	8	92
				Rh/HBcat	75	25
1-40b^a	Si ^t BuMe ₂	Me	<i>n</i> -Pr	9-BBN	11	89
				Rh/HBcat	96	4
1-40c^b	COCF ₃	<i>n</i> -Bu	Me	9-BBN	7	93
				Rh/HBcat	88	12
1-40d^b	CO ^t Bu	<i>n</i> -Bu	Me	9-BBN	4	96
				Rh/HBcat	87	13

^aTaken from reference 30. ^bTaken from reference 39.

A comparison of the major products formed upon hydroboration of silyl protected cyclohexenol in the presence and absence of rhodium gives another example of complementary selectivity between the catalyzed and uncatalyzed reactions.

Hydroboration with Wilkinson's catalyst preferentially affords the *anti* 1,3-diol following oxidation whereas the uncatalyzed reaction with 9-BBN generates the *anti* 1,2-diol as the major product, albeit with lower overall yield, Scheme 1-9. While not an example of complementary selectivity, the reaction depicted in Figure 1-6 demonstrates how the incorporation of a directing group affords much higher levels of selectivity in the catalyzed versus uncatalyzed hydroboration of **1-42**.³⁰ Phosphinates have also been explored as directing groups for hydroborations and although selectivities were determined to be high the reaction is of little synthetic importance due to the requirement for stoichiometric quantities of expensive rhodium.³⁰

Scheme 1-9: Hydroboration of Protected Cyclohexeneol

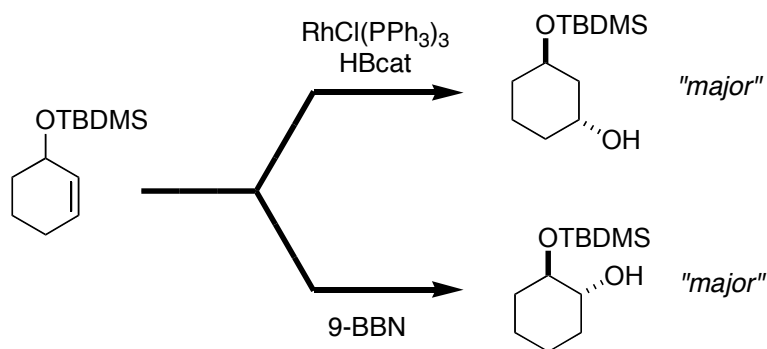
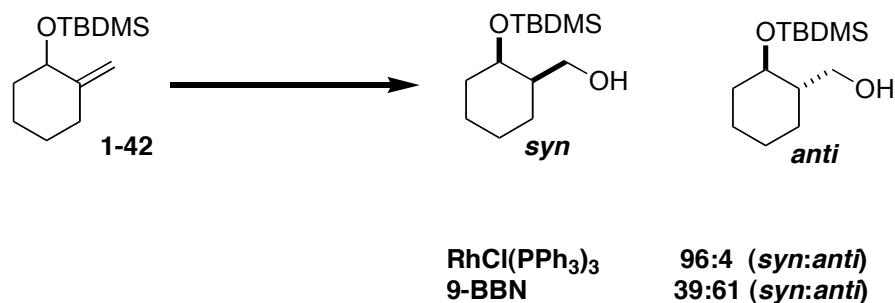


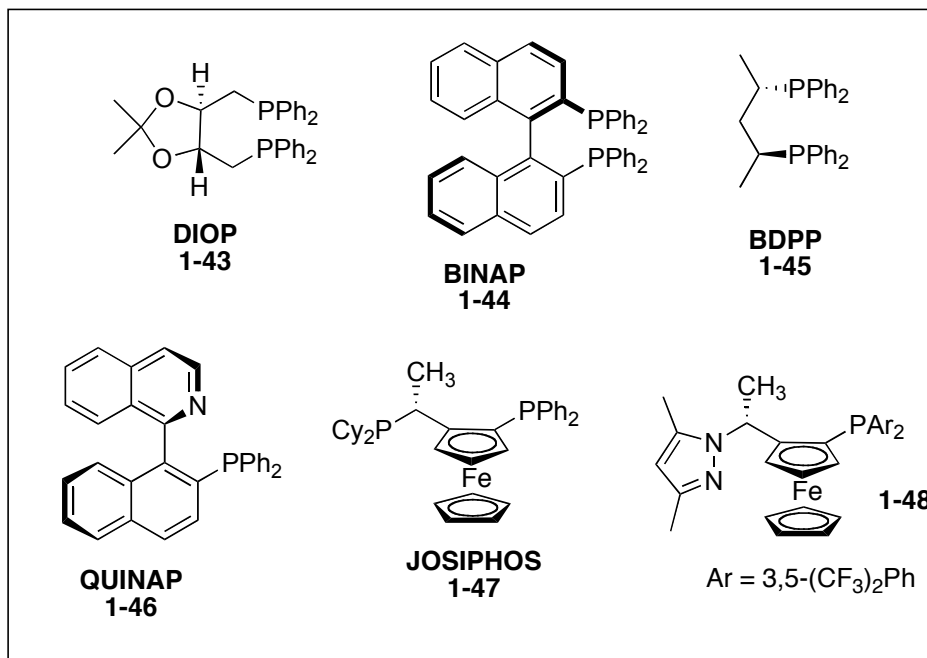
Figure 1-6: Hydroboration of *exo*-Cyclic Alkenes



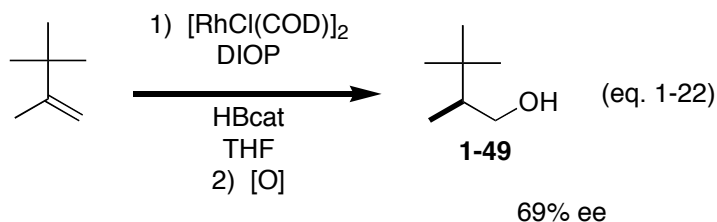
1.6: Enantioselective Hydroborations

The pinnacle achievement in terms of reaction selectivity is certainly the attainment of enantioselective variants. Two main strategies have been explored to affect asymmetric H-B additions to prochiral alkenes. The first has already been discussed and makes use of chiral hydroborating reagents such as **1-31**. Synthetically useful levels of chiral induction were indeed obtained, however, the main drawback is the requirement for stoichiometric amounts of chiral borane. Furthermore, since the installed carbon-boron bond is rarely the ultimate goal in hydroborations this represents a wasteful use of precious optically enriched material unless the borane can be effectively recycled. The second strategy makes use of chiral ligands employed in sub-stoichiometric amounts to affect chiral amplification in the reaction. A large number of chiral ligands and metal complexes have been investigated and high levels of enantioselectivity are obtainable albeit for a limited number of substrates. Contained in Chart 1-2 are several of the chiral ligands commonly employed for rhodium catalyzed asymmetric hydroborations.

Chart 1-2: Common Chiral Ligands



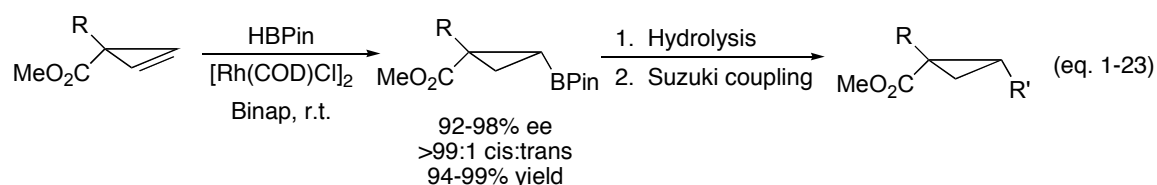
In order for rhodium catalyzed hydroborations to be rendered enantioselective, the products of the reaction must necessarily be chiral. Due to the regioselectivity of the reaction with simple terminal alkenes these substrates are not ideal candidates for asymmetric induction. Nonetheless, some examples exist where significant levels of ee are obtained in the reaction. Alcohol **1-49** is obtained with an ee of 69% following a hydroboration/oxidation sequence with Rh/DIOP, equation 1-22.⁴¹



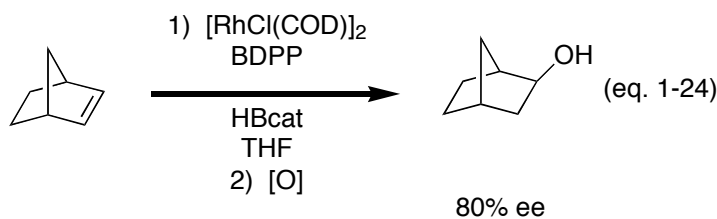
Asymmetric hydroboration of internal olefins would seem an important extension to the reaction. However, the level of asymmetric induction with these substrates is generally

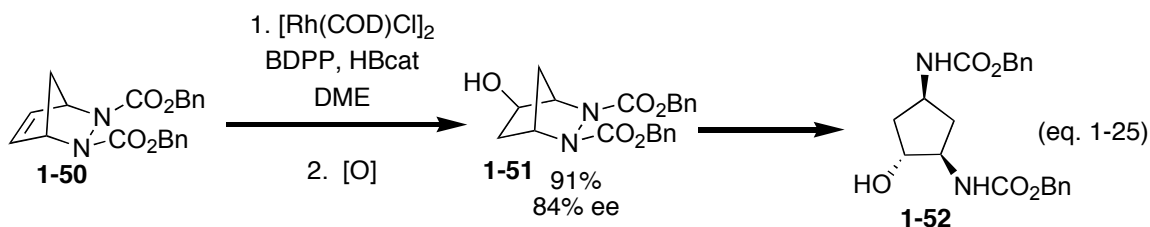
marginal. Hydroboration of 3,3-disubstituted cyclopropenes containing an ester as one substituent are efficiently hydroborated in excellent chemical and optical yield, Scheme 1-10.⁴² Pinacolborane is found to be a superior reagent in this reaction as compared to catecholborane. Hydrolysis of the pinacol substituent on boron permits further functionalization of the cyclopropylboronic acid via Suzuki coupling without loss of chirality.

Scheme 1-10: Enantioselective Hydroboration of Substituted Cyclopropenes

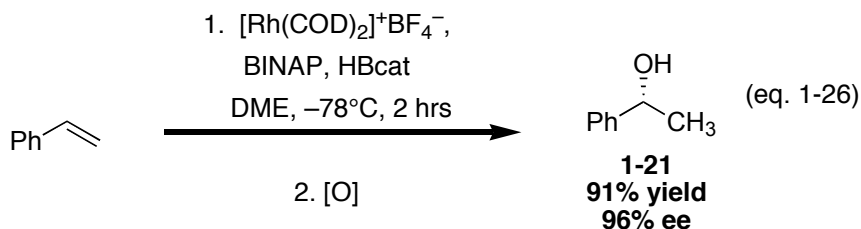


Norbornene undergoes regioselective hydroboration to afford the *exo*-isomer preferentially. Performing the reaction with Rh/BDPP affords *exo*-alcohol with an ee of 80%, equation 1-24.⁴³ Subjecting the diazonorbornene derivative **1-50** to the reaction with BDPP as ligand affords *exo*-alcohol **1-51** in a 91% yield and with an ee of 84%. **1-51** can be further reacted to obtain optically enriched polysubstituted diaminocyclopentane **1-52**, equation 1-25.



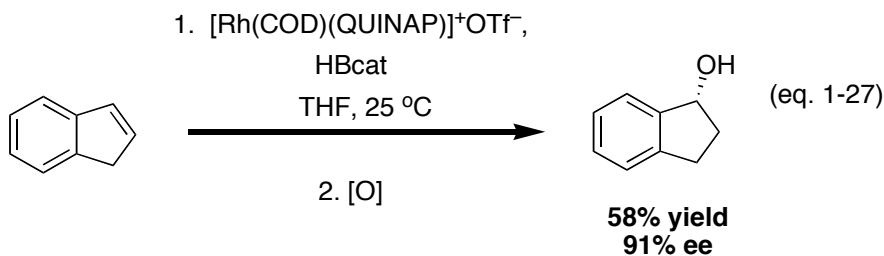


The highly regioselective placement of boron at the benzylic carbon of vinylarenes renders these substrates ideal candidates for the development of asymmetric rhodium catalyzed hydroborations. Indeed this class of olefin is the subject of a large number of studies and there are currently several highly active and selective catalytic systems that may be employed for the transformation. Cationic rhodium complexes of BINAP catalyze the hydroboration of styrene in a yield of 91% and with excellent enantioselectivity, 96% ee, equation 1-26.⁴⁴ Lower levels of asymmetric induction are obtained for electron deficient vinylarenes. Optimally the hydroboration is carried out at -78 °C to maximize ee. Accordingly, sluggish substrates such as indene, which require reaction at ambient temperature, undergo lower levels of asymmetric induction in the reaction, 13% ee.

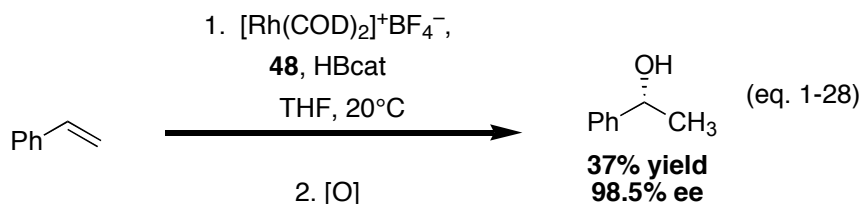


Ligands containing chelating P,N-substituents have also been explored and shown to catalyze the reaction with high optical purity. Employing Rh⁺/QUINAP, styrene is hydroborated and subsequently oxidized to obtain almost exclusively the 2-phenethanol product with a yield of 61% and an ee of 88%.⁴⁵ Most importantly hydroborations carried out with QUINAP as a ligand do not require cryogenic temperatures to effect high

levels of asymmetric induction. In fact, no improvements in this regard were observed when reaction temperature was reduced, although regioselectivity in the hydroboration underwent erosion. Hydroboration of the sluggish substrate indene was accomplished with a yield of 58% and an ee of 91%, equation 1-27.⁴⁵ This is a significant improvement over the room temperature hydroboration employing BINAP as ligand.

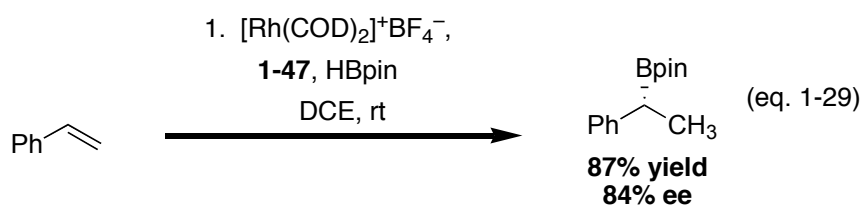


Ferrocene derivatives containing chelating P,P- or P,N-substituents have proven valuable additions to the list of highly selective ligands used in asymmetric hydroborations. Reactions of vinylarenes performed in the presence of Rh/JOSIPHOS are on par with reports using BINAP.⁴⁶ However substituting the benzylic phosphine of JOSIPHOS with a pyrazole moiety substantially increases the level of asymmetric induction obtained in the reaction.⁴⁷ To date the highest reported level of enantioselectivity obtained in the hydroboration of styrene is 98.5% ee and this was obtained using ligand **1-48**, equation 1-28. However it should be noted that significant amounts of the linear isomer are also produced in the reaction.



Recently the enantioselective hydroboration of vinylarenes has been extended to reactions carried out with pinacolborane **1-29**.²⁵ High levels of chiral induction were

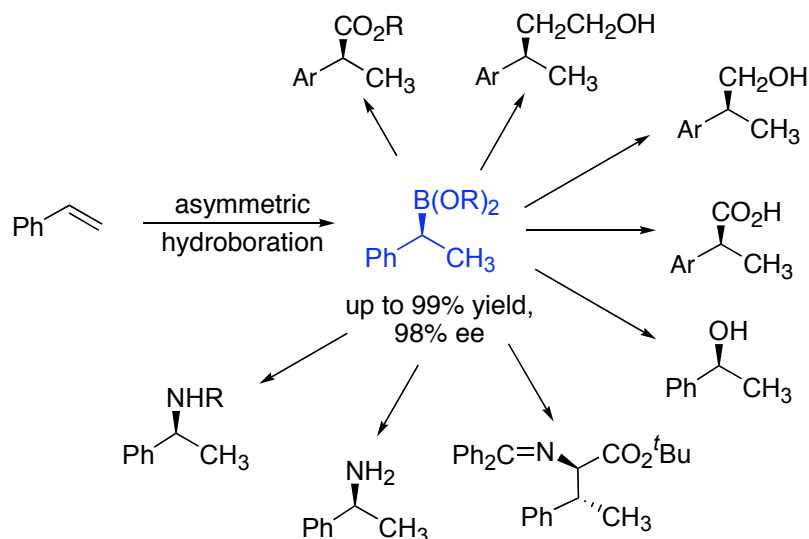
obtained in the reaction using several different ligands. It was determined that a combination of cationic rhodium and JOSIPHOS **1-47** was optimal providing 1-phenethanol with an 84% ee, equation 1-29. This new entry into asymmetric hydroboration increases the scope of the reaction by directly producing the more stable and therefore isolable pinacolboronate in high optical purity. Interestingly, carrying out the reaction with catecholborane **1-1** under otherwise similar conditions generates 1-phenethanol of opposite absolute configuration.



1.7: Functionalization of Carbon-Boron Bonds

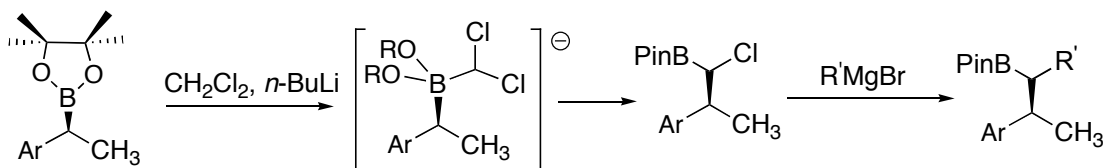
It has already been stated that the carbon-boron bond installed via hydroboration of olefins is generally not the ultimate goal in the transformation. Indeed, hydroborations are quite often terminated by the addition of alkaline hydroperoxide to afford the oxidized alcohol product. However, in recent years there have been efforts made to increase the scope of transformations that are capable of being carried out on alkylboronates derived from catalyzed hydroboration reactions, for representative examples see Chart 1-3.

Chart 1-3: Transformation of Carbon-Boron Bonds



Treating boronates with LiCHCl₂ generated by the slow addition of organolithiums reagents to dichloromethane at low temperature leads to the extension of the alkyl chain by one carbon, Scheme 1-11.⁴⁸ The *alpha*-chloro-boronates produced in this first step may subsequently be treated with nucleophiles resulting in halogen displacement and a further increase in molecular complexity. Each step in the sequence has been shown to be stereospecific and if a chiral diol is present as a ligand on boron then the sequence can actually be rendered stereoselective.

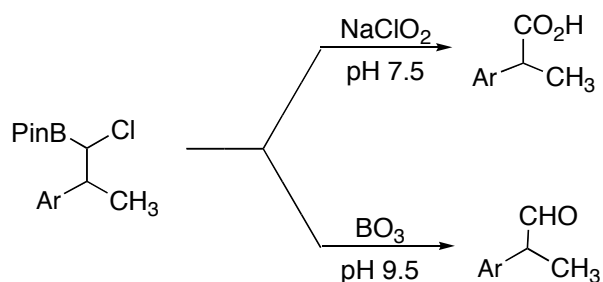
Scheme 1-11: Homologation/Substitution Sequence



The *alpha*-chloro-boronate obtained in the first step of the sequence may also be oxidized with a number of reagents to obtain either aldehyde or carboxylic acid

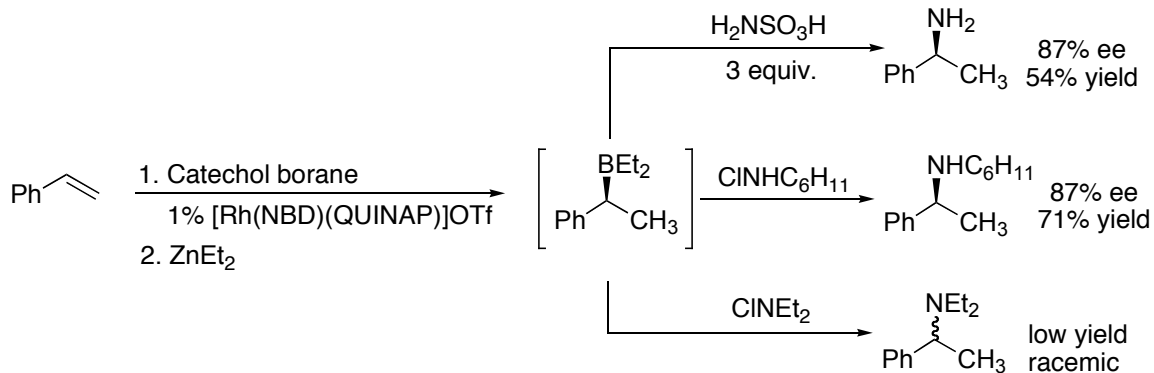
functional groups depending on reagent choice, Scheme 1-12.^{25,26} The general homologation methodology is not compatible with catecholboronates and as such if the carbon-carbon bond formation strategy is to be implemented either the hydroboration to install the alkylboronate group needs to be performed directly with pinacolborane **1-29** or alternatively a pinacol quench can be carried out at the end of the hydroboration itself. Both strategies have successfully been employed.^{25,26} In addition to LiCHCl_2 , other lithiohalomethanes,⁴⁹ sulfur ylides⁵⁰ and TMSCHN_2 ⁵¹ have all been used to homologate alkylboronates.

Scheme 1-12: Oxidation of *alpha*-Halo-Boronates

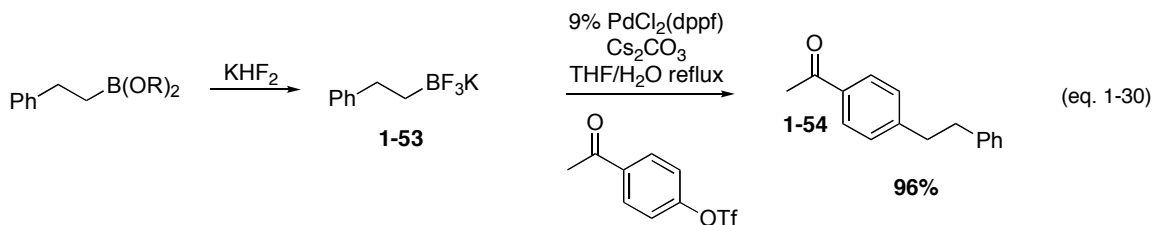


Following hydroboration, conversion of the carbon-boron bond to an amine may be accomplished provided that the boronate is first converted to a borane with either Grignard reagents or dialkyl zincs, Scheme 1-13.⁵² Employing suitable reagents, primary and secondary amines can be obtained with satisfactory yields and with retention of stereochemical purity. Similar attempts to convert enantioenriched boranes to tertiary amines resulted in low yields of racemic product.

Scheme 1-13: Amination Strategy



The anti-Markovnikov hydroboration of terminal alkenes provides access to important substrates for Pd catalyzed Suzuki coupling reactions.⁵³ Generally the primary alkylboronate is first converted into an organotrifluoroborate, equation 1-30. Unlike boronic acids and esters these species are indefinitely stable to air and moisture. Subjecting **1-53** to Pd catalyzed cross coupling with an aryltriflate generates the corresponding **1-54** in excellent yields, equation 1-31. The reaction is only compatible with primary boronates or alternatively with sp²-hybridized alkenyl- and arylboronates. There are examples of cyclopropylboronates undergoing the reaction however this likely is a result of the increased s-character of the exocyclic bonds of these substrates.



1.8: Conclusion

The synthetic utility and mechanistic understanding of rhodium catalyzed hydroborations has progressed significantly since the seminal publication of Mannig and Noth. A number of efficient catalytic systems have been reported and generally high levels of predictable selectivity are obtainable in the reaction. Synthetically useful levels of enantioselection have been obtained for a limited number of substrates. Broadening the scope of the asymmetric reaction to include substrates such as linear internal olefins would be a major advance in the field. A number of transformations have been devised to further functionalize the primary products of hydroborations. Alcohols, amines and even new carbon-carbon bonds may all be obtained following installment of the carbon-boron moiety through hydroboration.

1.9: References

- 1) Smith, M.B.; March, J. *March's Advanced Organic Chemistry: Reactions, Mechanisms, and Structure* 5th Edition, **2001**, Wiley-Interscience.
- 2) Männig, D.; Nöth, H. *Angew. Chem. Int. Ed.* **1985**, *24*, 878.
- 3) Brown, H.C.; Gupta, S.K. *J. Am. Chem. Soc.* **1975**, *97*, 5249.
- 4) Burgess, K.; Ohlmeyer, M.J. *Chem. Rev.* **1991**, *91*, 1179.
- 5) a) Pereira, S.; Srebnik, M. *Organometallics* **1995**, *14*, 3127. b) Pereira, S.; Srebnik, M. *Tetrahedron Lett.* **1996**, *37*, 3283. c) Pereira, S.; Srebnik, M. *J. Am. Chem. Soc.* **1996**, *118*, 909.
- 6) a) Harrison, K.N.; Marks, T.J. *J. Am. Chem. Soc.* **1992**, *114*, 9220. b) Molander, G.A.; Pfeiffer, D. *Org. Lett.* **2001**, *3*, 361.

- 7) Burgess, K.; S.; Jaspers, M. *Organometallics* **1993**, *12*, 4197.
- 8) He, X.; Hartwig, J.F. *J. Am. Chem. Soc.* **1996**, *118*, 1696.
- 9) a) Mirabelli, M.G.L.; Sneddon, L.G. *J. Am. Chem. Soc.* **1988**, *110*, 449. b) Knorr, J.R.; Merola, J.S. *Organometallics* **1990**, *9*, 3008.
- 10) Beletskaya, I.; Pelter, A. *Tetrahedron* **1997**, *53*, 4957.
- 11) Hewes, J.D.; Kreimendahl, C.W.; Marder, T.B.; Hawthorne, M.F. *J. Am. Chem. Soc.* **1984**, *106*, 5757.
- 12) Westcott, S.A.; Taylor, N.J.; Marder, T.B.; Baker, R.T.; Jones, N.J.; Calabrese, J.C. *J. Chem. Soc., Chem. Commun.* **1991**, 304.
- 13) Widauer, C.; Grützmacher, H.; Ziegler, T. *Organometallics* **2000**, *19*, 2097.
- 14) Rickard, C.E.F.; Roper, W.R.; Williamson, A.; Wright, L.J. *Angew. Chem. Int. Ed.* **1999**, *38*, 1110.
- 15) Collman, J.P.; Hegedus, L.S.; Norton, J.; Finke, R. *Principles and Applications of Organotransition Metal Chemistry* **1987**, 2nd Edition, University Science Press: Mill Valley, California.
- 16) Baker, R.T.; Calabrese, J.C.; Westcott, S.A.; Nguyen, P.; Marder, T.B. *J. Am. Chem. Soc.* **1993**, *115*, 4367.
- 17) It should be noted that during the course of the reaction rhodium hydrides might be produced via *beta*-hydride eliminations. Their involvement is evidenced by the formation of linear boronate **12** presumably following hydrogenation of VBE **1-10**.
- 18) Westcott, S.A.; Marder, T.B.; Baker, R.T. *Organometallics* **1993**, *12*, 975.
- 19) Brown, J.M.; Lloyd-Jones, G.C. *J. Am. Chem. Soc.* **1994**, *116*, 866.
- 20) a) Evans, D.A.; Fu, G.C. *J. Org. Chem.* **1990**, *55*, 2280. b) Evans, D.A.; Fu, G.C.; Anderson, B.A. *J. Am. Chem. Soc.* **1992**, *114*, 6679.
- 21) Burgess, K.; Van der Donk, W.A.; Westcott, S.A.; Marder, T.B.; Baker, R.T.; Calabrese, J.C. *J. Am. Chem. Soc.* **1992**, *114*, 9350.
- 22) Bennett, M.J.; Donaldson, P.B., K. *Inorg. Chem.* **1977**, *16*, 1581.
- 23) Burgess, K.; van der Donk, W.A.; Kook, A.M. *J. Org. Chem.* **1991**, *56*, 2949.

- 24) Westcott, S.A.; Blom, H.P.; Marder, T.B.; Baker, R.T.; Calabrese, J.C. *Inorg. Chem.* **1993**, *32*, 2175.
- 25) Crudden, C.M.; Hleba, Y.B.; Chen, A.C. *J. Am. Chem. Soc.* **2004**, *126*, 9200.
- 26) Chen, A.C.; Ren, L.; Crudden, C.M. *J. Org. Chem.* **1999**, *64*, 9704.
- 27) Molander, G.A.; Pfeiffer, D. *Org. Lett.* **2001**, *3*, 361.
- 28) a) Brown, J.M.; Lloyd-Jones, G.C. *J. Am. Chem. Soc.* **1994**, *116*, 866. b) Brown, J.M.; Lloyd-Jones, G.C. *J. Chem. Soc. Chem., Commun.* **1992**, 710. c) Brown, J.M.; Lloyd-Jones, G.C. *Tetrahedron: Asymmetry*. **1990**, *1*, 869.
- 29) Beletskaya, I.; Pelter, A. *Tetrahedron* **1997**, *14*, 4957.
- 30) Evans, D.A.; Fu, G.C.; Hoveyda, A.H. *J. Am. Chem. Soc.* **1992**, *114*, 6671.
- 31) Sato, M.; Nomoto, Y.; Miyaura, N.; Suzuki, A. *Tetrahedron Lett.* **1989**, *30*, 3789.
- 32) a) Elgendy, S.; Patel, G.; Kakkar, V.V.; Claeson, G.; Green, D.; Skordalakes, E.; Baban, J.A.; Deadman, J. *Tetrahedron Lett.* **1994**, *35*, 2435. b) Elgendy, S.; Patel, G.; Green, D.; Kakkar, V.V.; Baban, J.A.; Claeson, G.; Deadman, J. *Tetrahedron* **1994**, *50*, 3803.
- 33) Miyaura, N.; Suzuki, A. *Chem. Rev.* **1995**, *95*, 2457.
- 34) Zhang, J.; Lou, B.; Guo, G.; Dai, L. *J. Org. Chem.* **1991**, *56*, 1670.
- 35) Ohmura, T.; Yamamoto, Y.; Miyaura, N. *J. Am. Chem. Soc.* **2000**, *122*, 4990.
- 36) Vogels, C.M.; Decken, A.; Westcott, S.A. *Tetrahedron Lett.* **2006**, *47*, 2419.
- 37) Hamilton, M.G.; Hughes, C.E.; Irving, A.M.; Vogels, C.M.; Westcott, S.A. *J. Organomet. Chem.* **2003**, *680*, 143.
- 38) Still, W.C.; Barrish, J.C. *J. Am. Chem. Soc.* **1983**, *105*, 2487.
- 39) Burgess, K.; van der Donk, W.A.; Jarstfer, M.B.; Ohlmeyer, M.J. *J. Am. Chem. Soc.* **1991**, *113*, 6139.
- 40) Burgess, K.; Ohlmeyer, M.J. *J. Org. Chem.* **1991**, *56*, 1027.
- 41) Burgess, K.; Ohlmeyer, M.J. *J. Org. Chem.* **1988**, *53*, 5178.
- 42) Rubina, M.; Rubin, M.; Gevorgyan, V. *J. Am. Chem. Soc.* **2003**, *125*, 7189.

- 43) Luna, A.P.; Bonin, M.; Micouin, L.; Husson, H.P. *J. Am. Chem. Soc.* **2002**, *12*, 12098.
- 44) Hayashi, T.; Matsumoto, Y., C.M. *Tetrahedron: Asymmetry* **1991**, *7*, 601.
- 45) Brown, J.M.; Hulmes, D.I.; Layzell, L.P. *J. Chem. Soc., Chem. Commun.* **1993**, 1673.
- 46) Togni, A.; Breutel, C.; Schnyder, A.; Spindler, F.; Landert, H.; Tijani, A. *J. Am. Chem. Soc.* **1994**, *116*, 4062.
- 47) Schnyder, A.; Hintermann, L.; Togni, A. *Angew. Chem. Int. Ed.* **1995**, *34*, 931.
Burckhardt, U.; Hintermann, L.; Schnyder, A.; Togni, A. *Organometallics* **1995**, *14*, 5415.
- 48) Matteson, D.S.; *Synthesis*, **1986**, 973.
- 49) Ren, L.; Crudden, C.M. *Chem. Commun.* **2000**, 721.
- 50) Aggarwal, V.K.; Fang, G.Y.; Schmidt, A. *J. Am. Chem. Soc.* **2005**, *127*, 1642.
- 51) Goddard, J.-P.; Le Gall, T.; Mioskowski, C. *Org. Lett.* **2000**, *2*, 1455.
- 52) Meda, K.; Brown, J.M. *Chem. Commun.* **2002**, 310.
- 53) Molander, G.A.; Ellis, N. *Acc. Chem. Res.* **2007**, *40*, 275.

Chapter 2: One-Pot Carbon Monoxide Free Hydroformylation of Internal Olefins to Terminal Aldehydes

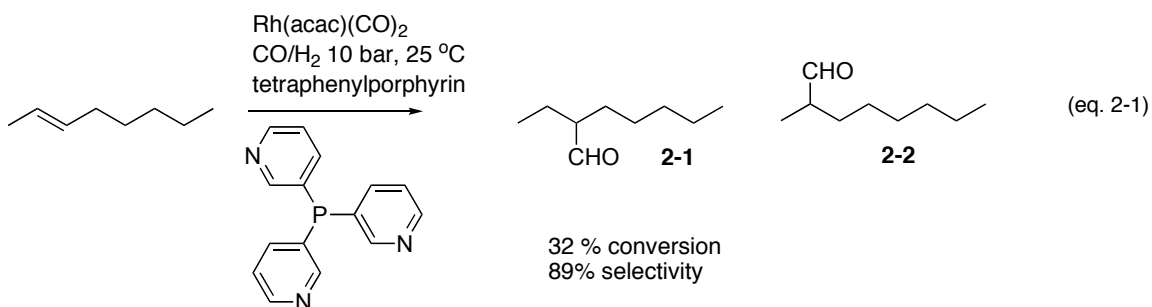
2.1: Introduction

The hydroformylation of olefins is the oldest and largest chemical process currently in use employing homogenous transition metal catalysts.¹ Estimates place the total amount of aldehyde and alcohol products produced by this method somewhere between 600 and 800 million tonnes per annum.² A major limitation of this process is the requirement for terminal olefin feedstocks in order to access the terminal aldehyde, which is desired for most applications.² Innovations geared towards the use of economically more feasible olefin mixtures, such as raffinate II containing a mixture of butene isomers, are highly desirable. Cobalt based catalytic systems have the dual problem of high temperature and pressure requirements as well as low regioselectivity towards terminal aldehydes.^{2,3} Cobalt has similar activity towards internal and terminal carbon-carbon double bonds yielding a complex mixture of aldehydes when olefin mixtures such as raffinate II are employed.

Rhodium based catalytic systems have received a surge in academic interest over the last decade with the goal of selectively hydroformylating internal alkenes.⁴ Encapsulation of rhodium within a zinc(II) tetraphenylporphyrin leads to a remarkably selective catalyst for the hydroformylation of *trans*-2-octene, equation 2-1.⁵ Branched isomer **2-1** is obtained with a selectivity of 89% over **2-2** despite the apparent similarities in steric and electronic properties of the 2- and 3-positions of the alkene. The catalyst

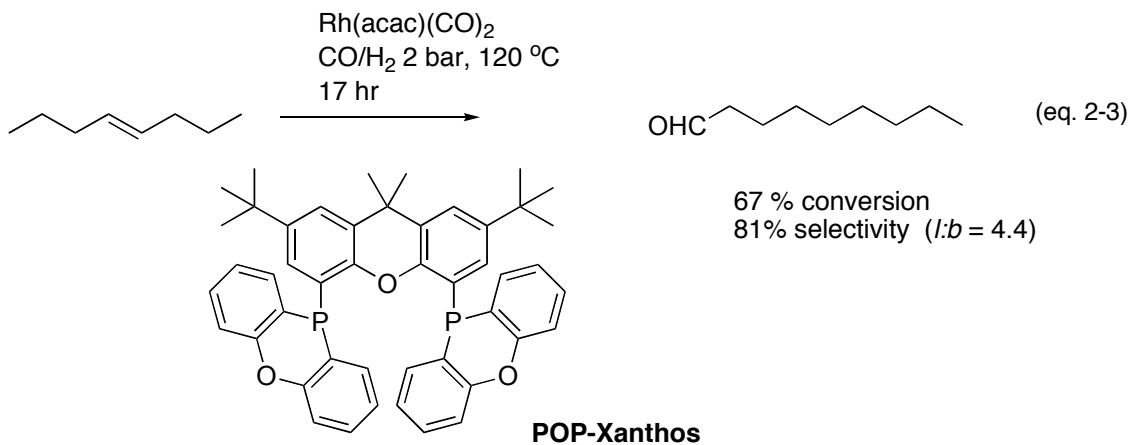
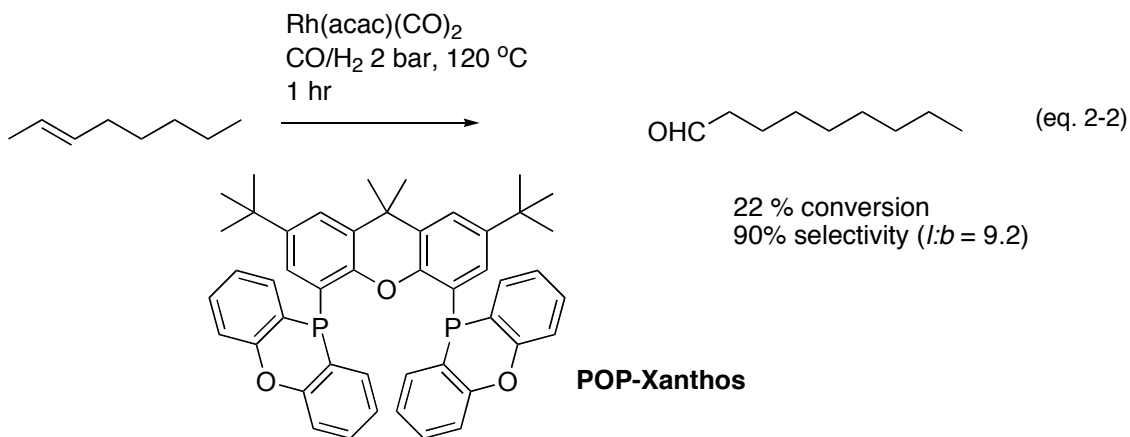
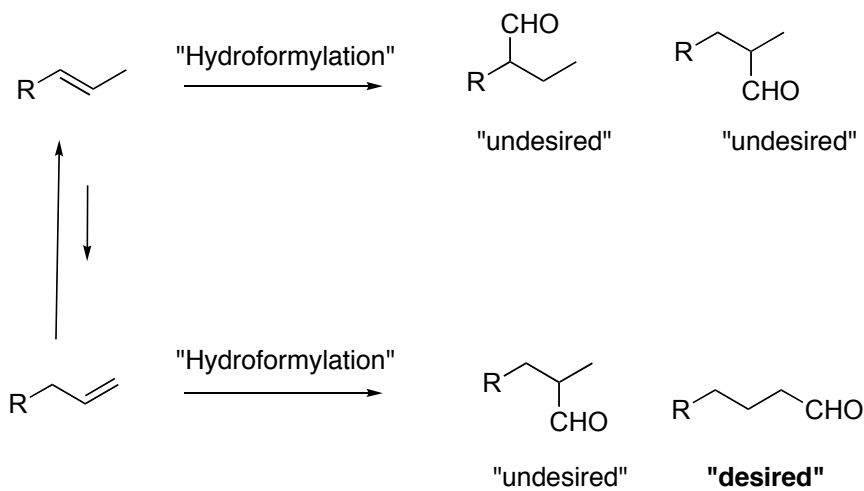
suffers from low activity and only a 32% conversion was obtained after 73 hours.

Selectivity was reported to be significantly lower for the hydroformylation of *trans*-3-octene.

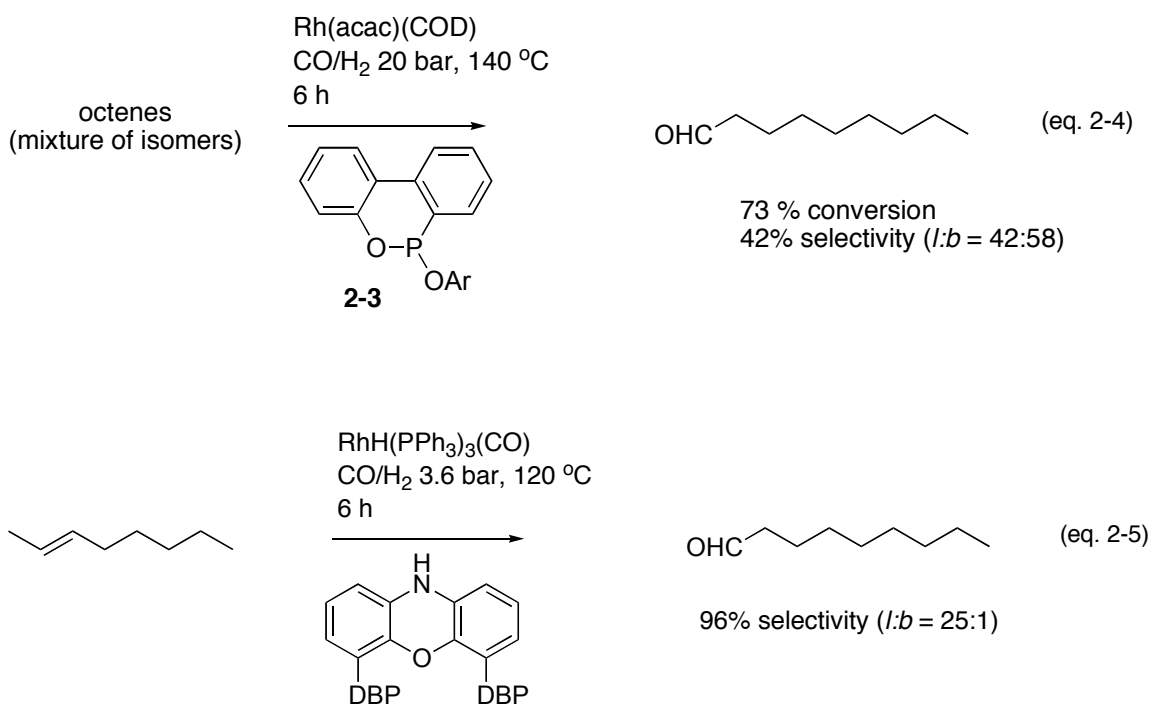


More promising are strategies geared toward the development of catalysts capable of converting internal olefins into terminal aldehydes. These systems generally rely on a fast olefin isomerization within the catalytic cycle to continuously produce terminal olefin substrate, Figure 2-1. Inherent to this strategy is the requirement for a fast hydroformylation of terminal olefins relative to internal isomers. Several examples have been reported to date. Hydroformylation of *trans*-2- or *trans*-4-octene with Rh/POP-Xanthos preferentially produces the linear nonanal with linear to branched isomer ratios (*l:b*) of up to 9.2:1, equations 2-2 and 2-3.⁶ Unfortunately catalyst activity is low and turn-over-frequencies (TOF) were determined to be on the order of 100. Similar results are obtained with Beller's system employing a NAPHOS derivative.⁷

Figure 2-1: Isomerization/Hydroformylation Process

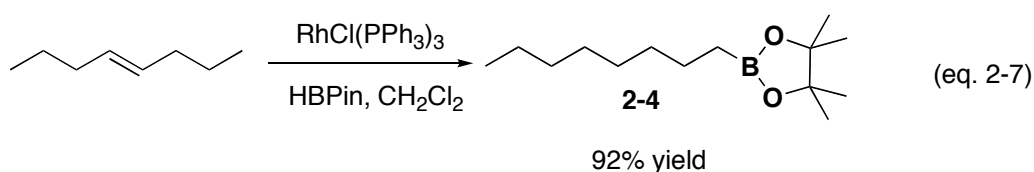
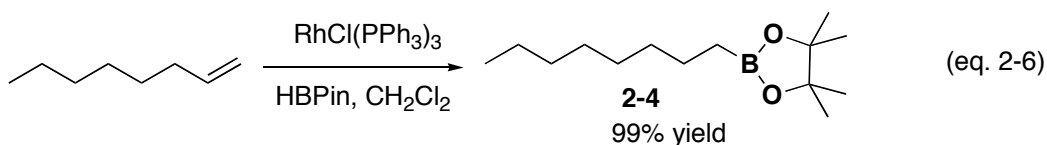


High catalyst activity generally correlates to a decrease in the regioselectivity obtained in the hydroformylation. For example Borner's system with ligand **2-3** produces hydroformylated products in good yield and with a reported TOF of over 18000, equation 2-4.⁸ However, selectivity for terminal nonanal was marginal (*b:l* = 58:42) and the reaction required 50 equivalents of phosphine per rhodium atom. The highest reported selectivities to date are for van Leeuwen's system employing a DBP derivative as ligand. In this case selectivities for terminal nonanal were as high as 96%, (*l:b* = 25:1), equation 2-5, although as might be expected the TOF was decidedly low at 60.⁹



New methods to generate linear aldehydes from olefin mixtures containing both terminal and internal isomers are highly desirable. For this reason, we were intrigued by a report of Srebnik *et al.*, in which 1-octene and *trans*-4-octene were both hydroborated

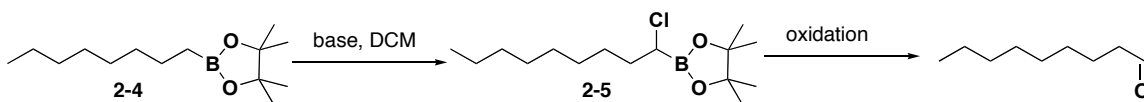
with complete regioselectivity to the linear boronate **2-4** using pinacolborane, equation 2-6 and 2-7.¹⁰ Combined with our recently reported homologation chemistry,¹¹ we felt this would provide an interesting possibility of performing a CO free hydroformylation in which internal olefins were converted into terminal aldehydes.



The proposed synthetic strategy is outlined in Scheme 2-1. Hydroboration of octenes, employing the Srebnik protocol, would generate the key intermediate **2-4**. Alkylboronates can be converted to *alpha*-chloroboronates such as **2-5** by a homologation strategy consisting of LiCHCl₂ addition. This reagent is usually generated by the addition of strong base to dichloromethane.¹² Since the first transformation, namely the hydroboration of octene, reportedly proceeds smoothly in dichloromethane as solvent, it was proposed that a one-pot procedure be developed with the solvent of the first transformation functioning as reagent in the following homologation step. After homologation, oxidation would give the product of hydroformylation without the need for carbon monoxide. The homologation has precedent in the work of Matteson¹² on boronic esters in general and by us specifically with the homologation of substituted phen-1-ethylpinacolboronate¹¹ during the asymmetric synthesis of Ibuprofen and Naproxen. Thus, we set out to develop a one-pot carbon monoxide free

hydroformylation procedure for mixtures of olefins, which produces linear aldehydes in high yields.

Scheme 2-1: Synthetic Strategy



2.2: Isomerization and Hydroboration

Our initial efforts focused on hydroborating 1-octene with Wilkinson's catalyst according to the reported procedure of Srebnik *et al.*¹⁰ The reaction was found to be quite sluggish.¹³ Even after 120 minutes, conversion to **2-4** was only 6%. Freshly prepared and recrystallized catalyst gave identical results. Quite surprisingly, catalyst that had been stored outside the glove box and showed signs of phosphine oxide in its ³¹P-NMR gave significantly better results. In fact, GC yields of up to 92% could be obtained by passing a stream of air through a solution of RhCl(PPh₃)₃ in dichloromethane prior to reaction. Ultimately this method gave variable yields of **2-4** and thus a more dependable procedure was sought.

The dual observation that catalyst exposure to oxygen and the presence of phosphine oxide in the pre-catalyst both correlate to increased yields of **2-4** is significant. It would appear that catalyst exposure to oxygen generates phosphine oxides, which ultimately leads to a phosphine deficient rhodium species capable of hydroborating 1-octene efficiently. Accordingly, [RhCl(PPh₃)₂]₂ was examined as a catalyst precursor since it contains a latent free coordination site and a decreased phosphine to Rh ratio compared to Wilkinson's catalyst. Gratifyingly, hydroboration of 1-octene proceeded

with a 90% conversion to **2-4** after 3 hours reaction time, Table 2-1, entry 3. In an effort to further optimize the Rh:phosphine ratio, $[\text{RhCl}(\text{C}_2\text{H}_2)_2]_2/\text{PPh}_3$ combinations were examined, see Table 2-1. It was determined that a ratio of 1.25 phosphine to 1 Rh was optimal, entry 5. Use of 1 mole percent of catalyst precursor resulted in near quantitative isolated and GC yields of linearboronate **2-4**. Attempts to decrease catalyst loading below 1 % resulted in increased production of the isomerization product 2-octene and the reduced product octane. Results are summarized in Table 2-1.

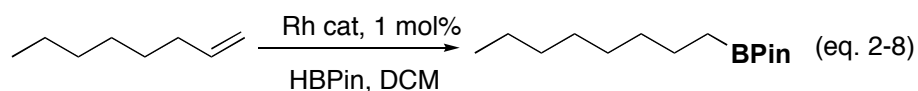


Table 2-1: Hydroboration Reaction Conditions

Entry	Catalyst	Additive (equivs.) ^[a]	Time (hrs)	Yield (%) ^[b]
1	$\text{RhCl}(\text{PPh}_3)_3$	-	2	6
2	$\text{RhCl}(\text{PPh}_3)_3$	Air ^[c]	2	31-92
3	$[\text{RhCl}(\text{PPh}_3)_2]_2$	-	3	88 ^[d]
4	$[\text{RhCl}(\text{C}_2\text{H}_2)_2]_2$	PPh_3 (1)	0.5	71
5	$[\text{RhCl}(\text{C}_2\text{H}_2)_2]_2$	PPh_3 (1.25)	0.5	98
6	$[\text{RhCl}(\text{C}_2\text{H}_2)_2]_2$	PPh_3 (1.5)	0.5	83
7	$[\text{RhCl}(\text{C}_2\text{H}_2)_2]_2$	PPh_3 (2)	0.5	79

^[a] Equivalents of PPh_3 : Rhodium monomer. ^[b] GC Yield of **1**. ^[c] Air was bubbled through the reaction mixture until the colour changed from pale yellow to black.

^[d] Isolated yield.

2.3: Homologation

Having established a suitable protocol for the regioselective and nearly quantitative conversion of 1-octene to the corresponding linear pinacolboronates, our attention next turned to the task of converting **2-4** to the *alpha*-chloropinacolboronate **2-5**, equation 2-9. Invariably, the crude reaction mixture resulting from the first transformation was diluted to a 0.1 M concentration in dry THF. The reaction flask was then cooled to the desired temperature and base was added slowly according to the Matteson protocol.¹⁴ The resulting homologated product was then worked up and examined for conversion of **2-4** to **2-5** by ¹H NMR, see Table 2-2.

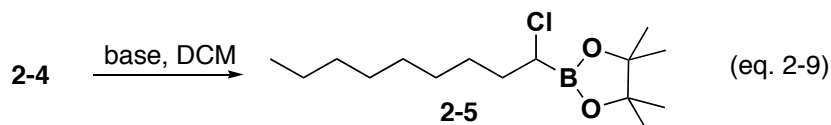


Table 2-2: Homologation Reaction Conditions^a

Entry	Base	Amount	Temperature (°C)	Additive	Conversion (%)
1	<i>n</i> -BuLi	2 eq	-100	ZnCl ₂	82
2	<i>n</i> -BuLi	3 eq	- 100	ZnCl ₂	89
3	<i>n</i> -BuLi	3 eq	- 100	-	89
4	<i>n</i> -BuLi	3 eq	- 78	-	88
5	LDA	2 eq	- 40	-	100

^[a] Reactions were worked up and conversion to the *alpha*-chloropinacolboronate was determined by the ¹H-NMR integration ratio corresponding to resonances *alpha* to boron.

Matteson has demonstrated that the addition of ZnCl_2 aids in the breakdown of the borate complex and permits the reaction to take place with high diastereoselectivity when the boronate ester is derived from a chiral diol.¹⁵ Since our reaction employs an achiral boronate ester and is not diastereoselective, ZnCl_2 was unnecessary. Entries two and three reveal that omission of the zinc additive made no difference to the reaction.

Generally, base is added to dichloromethane at $-100\text{ }^\circ\text{C}$ to generate LiCHCl_2 and subsequently the boronate substrate is transferred to the reaction flask as a THF solution. The extremely low temperature of $-100\text{ }^\circ\text{C}$ is required to prevent decomposition of LiCHCl_2 and the formation of reactive carbene species in the absence of a suitable electrophile. In order to affect the desired one-pot procedure using the solvent from the hydroboration step as reagent during the homologation step, LiCHCl_2 needed to be generated in-situ in the presence of the boronate substrate.¹⁶ Fortuitously this in situ homologation procedure permitted the slightly milder temperature of $-78\text{ }^\circ\text{C}$ to be employed, entry 4.

For completeness, it should be noted that LDA was able to affect this transformation with quantitative conversion of **2-4** to **2-5** at the more desirable temperature of $-40\text{ }^\circ\text{C}$, entry 5. Nonetheless, all attempts to oxidize **2-5** in the presence of the resulting two equivalents of diisopropyl amine failed. Carrying out a simple extractive workup procedure to remove the amine allowed the oxidation to proceed, however, this did not fit with our initial goal of developing a one-pot procedure so the protocol described in entry 4 was employed.

2.4: Oxidation

The crude reaction mixture containing **2-5** was treated with various oxidizing reagents to complete the sequence outlined in Scheme 2-1. Reactions were monitored by GC and the *overall yield* of aldehyde from 1-octene was calculated.¹⁷ Amine oxides have previously been employed for oxidation in organoborane chemistry and we tested three such reagents, trimethylamine-N-oxide (TMAO), N-methyl-morpholine-N-oxide (NMO), N,N-dimethylundecylamine N-oxide, entries 1,2,3 of Table 3.¹⁸ Unfortunately none of these reagents was soluble in THF. TMAO could only be employed following a solvent switch, in which THF was partially removed and benzene subsequently added to the crude reaction flask. Reflux for 9 hrs furnished nonyl aldehyde in an overall yield of 74-76% over the three steps. Other amine oxides tested showed no conversion to the aldehyde. Hydroperoxides in various forms have often been employed to carry out the oxidation of carbon-boron bonds; however, neither Kabalka's perborate¹⁹ nor basic hydroperoxide²⁰ led to sufficient levels of aldehyde formation, entries 4 and 5. We were delighted to see, however, that sodium percarbonate, a very inexpensive oxidant, cleanly furnished nonyl aldehyde in good overall yield, entry 6.²¹ The reaction proceeded faster and with better conversion in the presence of two equivalents of the reagent, entry 7.

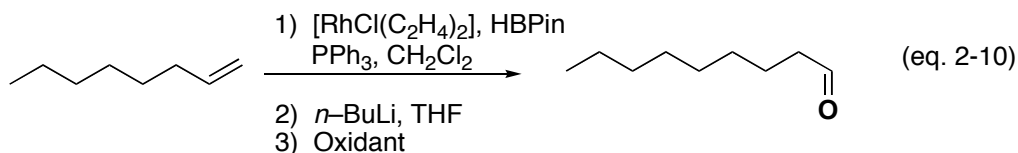


Table 2-3: One-Pot Preparation of Homologated Aldehyde: Optimization of the Final Step

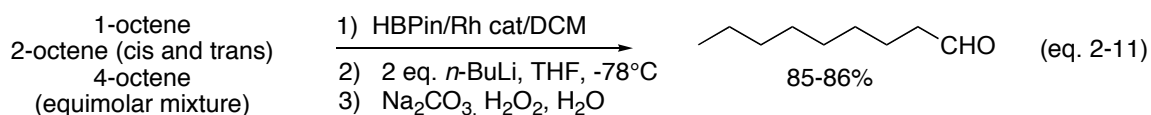
Entry	Oxidant	Amount (equivs)	Conditions	Overall Yield ^[a] (%)
1	TMANO ^[b]	3.0	PhH, 60°C, 9 h	74-76
2	NMO ^[c]	3.0	PhH, 60°C, 24 h	0
3	ONMe ₂ C ₁₁ H ₂₄	3.0	PhH, 60°C, 9 h	0
4	NaBO ₃	1.2	H ₂ O ^[d] , 25°C, 2h	42
5	H ₂ O ₂ /NaOH	1.2	H ₂ O ^[d] , 25°C, 2h	<20
6	Na ₂ CO ₃ /1.5H ₂ O ₂	1.2	H ₂ O ^[d] , 25°C, 2 h	65
7	Na ₂ CO ₃ /1.5H ₂ O ₂	2.0	H ₂ O ^[d] , 25°C, 2 h	80

^[a]Yields of nonyl aldehyde over the three step one-pot synthesis were obtained by GC referenced to authentic sample. ^[b]Trimethyl-amine-N-oxide (TMANO). ^[c]N-methyl-morpholine-N-oxide. ^[d]Crude reaction mixture was further diluted to a 0.2 M concentration in water.

2.5: Hydroformylation of Alkene Mixtures

Having identified a suitable protocol for the conversion of 1-octene, a linear olefin, to nonyl aldehyde, it remained to be shown that the same procedure could be applied to mixtures of octene isomers. A stock solution consisting of equimolar amounts of 1-, *cis*-2-, *trans*-2- and *trans*-4-octene was subjected the one-pot hydroboration/homologation/oxidation reaction, equation 2-11. In order to further

optimize the procedure, we carried out the hydroboration with a slight increase in dichloromethane (0.5 M instead of 1.0 M in DCM). This simple switch allowed us to decrease the amount of base in the following homologation step, and did not adversely affect the hydroboration reaction itself. Presumably the addition of extra DCM was sufficient to drive the homologation reaction to high conversion without the requirement for three equivalents of base. Employing the new protocol, the overall yield of the reaction was 85-86%, employing a mixture of several isomers of octene, equation 2-11.



To further probe the scope of the reaction and demonstrate its validity as a viable option for the production of aldehydes from a variety of olefin mixtures, a series of internal olefins of varying carbon length were next subjected to the optimized protocol, Table 2-4. In all substrates examined, good overall yields of the linear aldehyde were obtained. Most gratifying were the results obtained for 2-hexene, in which an excellent yield of 90-95 % was observed over the three steps.

Table 2-4: Hydroformylation of Various Internal Olefins

Olefin	Yield of Aldehyde (%) ^[a]
2-hexene	90-95
2-heptene	79-83
octenes ^[b]	85-86
3-nonene	60-64

^[a] GC yield. ^[b] equimolar mixture of 1-octene, 2-octene and *trans*-4-octene.

2.6: Conclusions

A one-pot protocol for the conversion of olefins to linear aldehydes without the need for carbon monoxide has been developed. A highlight of the devised methodology is the ability to convert mixtures of olefins to the more desirable linear aldehyde in up to 95% yield. This represents a significant step towards the development of hydroformylation procedures capable of functioning on cheaper feedstocks comprised of internal as well as terminal carbon-carbon double bonds. While our procedure eliminates the need for carbon monoxide, it does require a stoichiometric amount of pinacolborane at an increased cost over the standard H₂/CO synthesis gas mixture used in commercial hydroformylations. Current efforts in our lab are directed towards developing a procedure that is catalytic in borane, which would eliminate the costs associated with this reagent.

2.7: Experimental Section

General Remarks: [RhCl(C₂H₂)₂]₂ was prepared from commercial rhodium chloride trihydrate by the reported procedure.²² *n*-BuLi was freshly titrated against *N*-benzylbenzamide to the deep blue endpoint. All other reagents were commercially available and were purified according to Perrin and Perrin techniques prior to use.²³ Hydroborations took place in the oxygen free environment of a glove box. Yields of all aldehydes were obtained via an Agilent 6850 GC referenced to a commercially available authentic sample. Calibration curves were constructed by running a series of samples

containing the aldehyde and internal standard, decane, at four different concentrations. All attempts to obtain isolated yields of **2** led to partial decomposition of the *alpha*-chloropinacolboronates. Conversion of **1** to **2** was calculated based on crude ¹H-NMR integration ratios for proton signals *alpha* to boron.

Nonyl Aldehyde: [RhCl(C₂H₂)₂]₂ (0.1 mol %, 3.9 mg) was weighed into a 50 ml two necked RBF inside a glove box. To this PPh₃ (0.25 mol %, 6.6 mg) was added followed by 2 ml deoxygenated and dry DCM. The reddish-yellow solution stirred for five minutes and then 1-octene (1.02 mmol, 0.16 mL) was added by syringe followed immediately by pinacolborane (1.2 mmol, 0.18 mL). The clear reddish-yellow solution went dark within five minutes and reactions were left in the glove box for a further 30 minutes. The reaction flask was then removed from the glove box diluted with 10 ml dry THF and cooled to -78 °C. Freshly titrated *n*-BuLi (2 eq) was then added slowly down the side of the flask. Reactions were then left to slowly warm to room temperature overnight. The following morning the reaction mixture was further diluted with 5 mL distilled water and 2 eq sodium percarbonate (2.04 mmol, 320 mg) were added at 0 °C and the reaction was left to warm to room temperature over 2 hours. Decane was added as internal standard and a small aliquot was removed for yield determination by GC.

2.8: References

- 1) Spessard, G.O.; Miessler, G.L. *Organometallic Chemistry*, John Prentice Hall, New Jersey **1996**, 255-264.
- 2) Bhaduri, S.; Mukesh, D. *Homogeneous Catalysis Mechanisms and Industrial Applications*, Wiley-Interscience, New York, **2000**, 1-13.

- 3) Trzeciak, A.M.; Ziolkowski, J.J. *Coord. Chem. Rev.* **1999**, 883-900.
- 4) Kamer, P.C.; Van Leeuwen, P.W.N.M.; Reek, J.N.H. *Acc. Chem. Res.* **2001**, 34, 895.
- 5) Kuil, M.; Soltner, T.; Van Leeuwen, P.W.N.M.; Reek, J.N.H. *J. Am. Chem. Soc.* **2006**, 128, 11344.
- 6) van der Veen, L.A.; Kamer, P.C.J.; Van Leeuwen, P.W.N.M. *Organometallics* **1999**, 18, 4765.
- 7) Klein, H.; Jackstell, R.; Wiese, K.D.; Borgmann, C.; Beller, M. *Angew. Chem. Int. Ed.* **2001**, 40, 3408.
- 8) Selent, D.; Wiese, K.D.; Rottger, D.; Borner, A. *Angew. Chem. Int. Ed.* **2000**, 39, 1639.
- 9) Bronger, R.P.J.; Kamer, P.C.J.; Van Leeuwen, P.W.N.M. *Organometallics* **2003**, 22, 5358.
- 10) Pereira, S.; Srebnik, M. *J. Am. Chem. Soc.* **1996**, 118, 909.
- 11) Crudden, C.M.; Hleba, Y.B.; Chen, A.C. *J. Am. Chem. Soc.* **2004**, 126, 9200. b) Chen, A.C.; Ren, L.; Crudden, C.M. *J. Org. Chem.* **1999**, 64, 9704.
- 12) Matteson, D.S.; *Synthesis* **1986**, 973.
- 13) Similar difficulties with the Schrebnik procedure have been reported by other groups: Yamamoto, Y.; Fujikawa, R.; Umemoto, T.; Miyaura, N. *Tetrahedron* **2004**, 60, 10695.
- 14) Matteson, D.S.; Majumdar, D.J. *Organometallics* **1983**, 2, 1529-1535
- 15) Matteson, D.S.; Majumdar, D.J. *J. Am. Chem. Soc.* **1980**, 102, 7588-7590.
- 16) Rangaishenvi, M.V.; Singaram, B.; Brown, H.C. *J. Org. Chem.* **1991**, 56, 3286.
- 17) Initial attempts to determine yields of the oxidation step alone, following isolation of **2-5**, were abandoned early on as it was observed that by-products from previous transformations could greatly influence the results once the optimized protocol was attempted as a one-pot procedure.

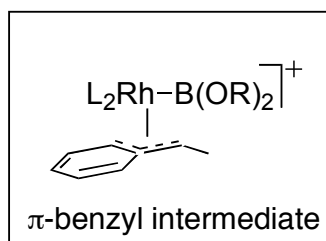
- 18) Soderquist, J.; Najafi, M.R. *J. Am. Chem. Soc.* **1986**, *51*, 1330-1336.
- 19) Kabalka, G.; Shoup, T.; Goudgaon, N. *J. Am. Chem. Soc.* **1989**, *54*, 5930-5933.
- 20) Kabalka, G.; Hedgecock, H.C. *J. Org. Chem.* **1975**, *40*, 1776-1779.
- 21) Kabalka, G.; Wadgaonkar, P.; Shoup, T. *Organometallics* **1990**, *9*, 1316-1320.
- 22) Cramer, R. *Inorganic Syntheses* **1974**, *15*, 14.
- 23) Armarego, W.L.F.; Perrin, D.P. *Purification of Laboratory Chemicals*, Butterworth-Heinemann, Oxford, 2000.

Chapter 3: Electronic Effects in the Rh catalyzed Hydroboration of Vinyl Arenes

3.1: Introduction

A major advantage of the use of metal catalysts to promote the hydroboration of olefinic substrates, as compared to uncatalyzed variants, lies in the ability of the metal catalyst to alter or even improve upon reaction selectivity. For example, the rhodium catalyzed hydroboration of vinyl arenes by-and-large leads to the Markovnikov or branched boronate product.¹ The large number of reports purporting to carry out the transformation asymmetrically illustrates the utility of these species in synthesis.² Less

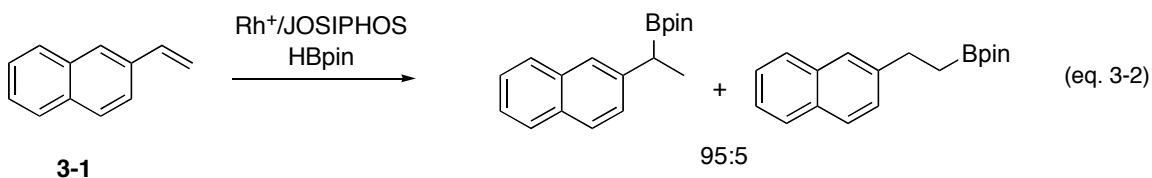
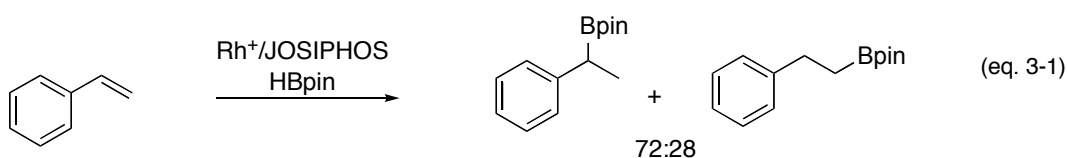
clearly defined in the literature are the underlying causes or interactions responsible for the unique regioselectivity of the rhodium catalyzed hydroboration of vinylarenes. It has often been stated



that hydroboration regioselectivity of these substrates may result from a stabilizing π -benzyl interaction following hydride insertion, see inset.³ However no clear evidence for how such an interaction might govern reaction selectivity has at present been reported. The current study was undertaken in an effort to better understand the effects of aryl substituents on the olefinic substrate and to decipher what role they might play in controlling the regioselectivity.

3.2: Hydroboration of 1-naphthyl-2-phenylethene

Hydroboration of a standard vinylarene, such as styrene, under the conditions shown in equation 3-1 affords a mixture of regioisomers in a ratio of 72:28 with the expected branched product predominating.⁴ Carrying out the reaction on the naphthyl derivative **3-1** under otherwise identical conditions affords the product distribution shown in equation 3-2. It is clearly seen that by simply switching the aryl substituent from phenyl to naphthyl leads to a marked increase in the preference for benzylic borylation in the reaction. It might be speculated that this results from a stronger directing effect of the naphthyl versus the phenyl substituent. The effect of the aryl substituent on reaction selectivity might be probed by carrying out a hydroboration on a 1,2-disubstituted-ethene. Given the results depicted in equations 3-1 and 3-2 it would appear that substituting ethene with one phenyl and one naphthyl substituent would allow for a comparison of the respective directing effects of the two groups to be made by pitting them against one another in an intramolecular competition.



Test substrate **3-2** was prepared by Wittig olefination of 2-naphthaldehyde with triphenylphosphonium benzylide, equation 3-3. Not surprisingly, for a reaction

employing a semi-stabilized ylide, a mixture of *cis*- and *trans*-olefins was produced.⁵ Importantly for our purposes, separation of the geometric isomers was easily performed by repeated column chromatography. Prior to hydroborating substrate **3-2** reaction conditions were first partially optimized on the commercially available *trans*-stilbene, Chart 3-1. In the presence of Wilkinson's catalyst no hydroboration was observed after reaction at room temperature for 52 hours. On the other hand heating the reaction to 80 °C in a sealed tube for 24 hrs led to approximately 50% conversion. Pinacolborane has been reported to hydroborate alkenes and alkynes at elevated temperatures in the absence of catalyst.⁶ To ensure that no uncatalyzed reaction was in fact contributing to the 50% conversion obtained with Wilkinson's catalyst at 80 °C, the reaction was repeated in the absence of a rhodium source under otherwise identical conditions. No conversion was evident even after 48 hours reaction time.

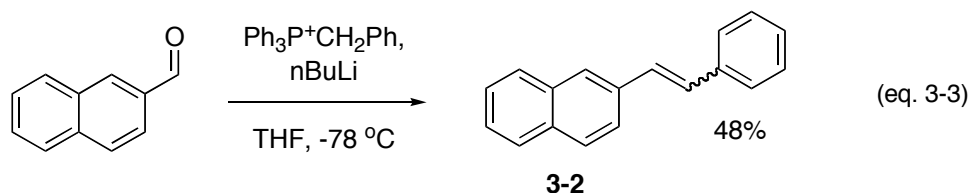
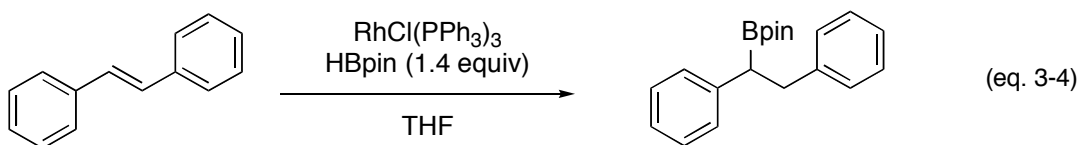


Chart 3-1: Hydroboration of *trans*-Stilbene



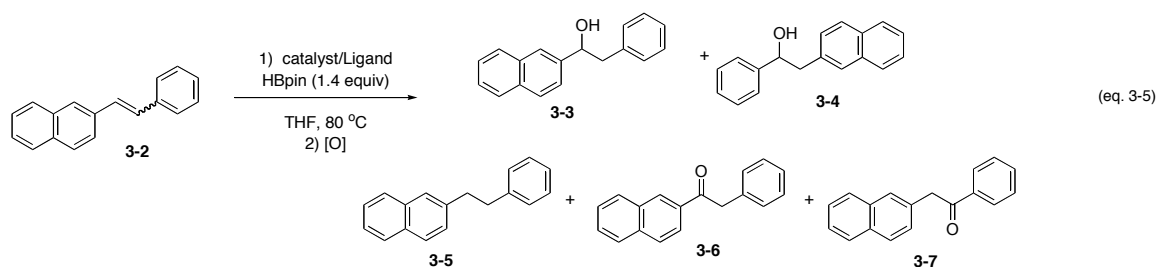
RhCl(PPh ₃) ₃	Temperature	Time	Conversion
5%	r.t.	52 hrs	0%
5%	80 °C	16 hrs	50%
0%	80 °C	48 hrs	0%

In the next part of the study, substrates *cis*- and *trans*-**3-2** were separately subjected to hydroboration with pinacolborane in the presence of Wilkinson's catalyst. A mixture of all possible products was obtained in each of the reactions, Table 3-1, entries 1 and 2. From the product distribution it was determined that there was essentially no selectivity in the reaction for the production of alcohols **3-3** and **3-4**. Furthermore significant amounts of hydrogenated **3-5** and ketones **3-6** and **3-7** were also isolated. The presence of these products has typically been attributed to a boryl insertion/ β -hydride elimination sequence ultimately leading to the production of vinylboronates and rhodium hydride species.⁷ One should also consider that the vinylboronate produced in the reaction may undergo partial hydrogenation in-situ to ultimately furnish alcohols **3-3** and **3-4** following oxidation.⁷ Small amounts of starting material were also isolated following both reactions. Interestingly, no *cis*-**3-2** was ever detected in the crude following either reaction and it was only the *trans*-isomer of **3-2** that was ever recovered. This result was interpreted as consistent with a fast and reversible hydride insertion/ β -hydride elimination sequence capable of isomerizing the *cis*-olefin to the more thermodynamically stable *trans*-isomer.

Higher levels of selectivity, *circa* 5:1, for alcohol **3-3** over alcohol **3-4** were obtained when the hydroboration was catalyzed with [Ir(COD)Cl]₂.⁸ Once again, all recovered starting material was completely devoid of the *cis*-isomer, regardless of which isomer of **3-2** was employed. A small amount of hydrogenated product was also isolated following reaction. The highest level of activity and selectivity for the production of alcohol **3-3** was obtained using a cationic rhodium source and chelating bis-phosphine ligand such as DPPB, Table 3-1, entry 5. Under these conditions alcohols **3-3** and **3-4**

were isolated in an 84% combined yield and with a selectivity of 7:1 in favor of isomer **3-3** where borylation was seen to occur proximal to the naphthyl substituent. Small amounts of hydrogenated alkane and *trans*-olefin were also isolated. The ketone product resulting from dehydrogenative borylation was not observed. It would thus appear from this study, at least for Ir and cationic Rh catalysts, that naphthyl is a stronger directing substituent than phenyl.

Table 3-1: Hydroboration of 1-Naphthyl-2-Phenylethene



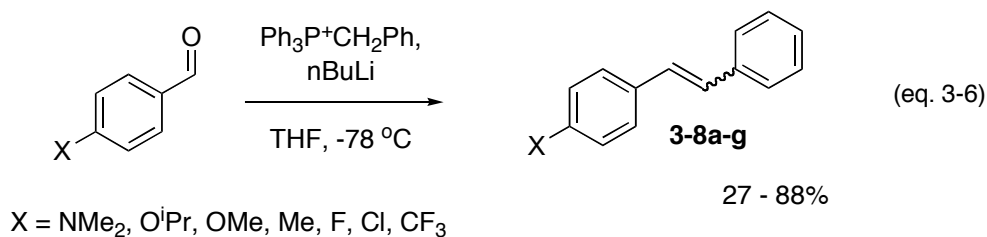
Entry	Catalyst	Ligand	Substrate	3-3/3-4 (%yield)	Ratio 3-3:3-4	3-5^a (%yield)	3-6/3-7 ^{a,b} (%yield)	3-2^{a,c} (%yield)
1	RhCl(PPh ₃) ₃	NA	<i>trans</i> - 3-2	23	1:1	32	21	< 5
2	RhCl(PPh ₃) ₃	NA	<i>cis</i> - 3-2	34	1:1	38	8	< 5
3	[Ir(COD)Cl] ₂	PPh ₃	<i>trans</i> - 3-2	42	5:1	< 5	< 5	40
4	[Ir(COD)Cl] ₂	PPh ₃	<i>cis</i> - 3-2	34	5:1	< 5	< 5	59
5	[Rh(COD) ₂]BF ₄	DPPB	<i>cis</i> - 3-2	84	7:1	< 5	< 5	12

^a A value of < 5 % refers to trace amounts to none detected. ^b Isomeric ratio of **3-6** and **3-7** not determined

^c Recovered starting material **3-2** was always devoid of the *cis*-isomer and therefore values in the Table refer to % isolated *trans*-**3-2**.

3.3: Hydroboration of Unsymmetrical Stilbenes

The results obtained for the Rh⁺/DPPB system prompted a further study of simple unsymmetrical stilbenes, in which, one of the two arenes contains a *para*-substituent capable of electronically differentiating the two olefinic sites of the molecule. Once again, the substrates were prepared by Wittig olefination, only in this instance the reaction was carried out with triphenylphosphonium benzylide and different commercially available *para*-substituted benzaldehydes, equation 3-6. A mixture of *cis*- and *trans*-stilbenes were once again produced in the reaction and gratifyingly could generally be separated by repeated column chromatography. Despite several lower yielding reactions, a sufficient number of substrates could indeed be prepared by this route and in sufficient quantities for the purposes at hand.



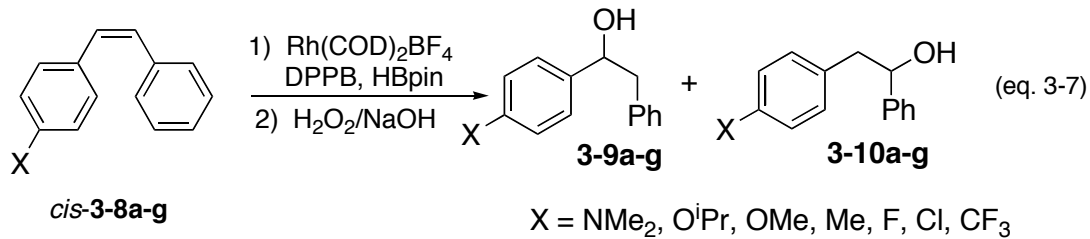
With the desired substrates in hand, the hydroboration reaction was carried out on mono-*para*-substituted *Z*-stilbenes **3-8a-g**, equation 3-7. Following oxidation with basic hydrogen peroxide, the resulting alcohols were isolated by column chromatography as a mixture of isomers. The identities of the individual regioisomers were verified by comparison to authentic samples prepared by Grignard addition to the corresponding aldehydes. With the one exception of *p*-dimethylaminostilbene, the reactions were quite clean with mass balances generally exceeding 90%. Recovered starting material was

always devoid of the *cis*-isomer, apparently due to a concurrent isomerization to the more stable *trans*-isomer. The results of this study are shown in Chart 3-2.

The major isomer always corresponded to borylation proximal to the substituted aromatic ring, irrespective of the electronic influence of the *para*-substituent. The greatest selectivities were observed for the most electron donating, NMe₂, and the most electron withdrawing, CF₃, *para*-substituents. A graph of log(isomer ratio) versus σ revealed a linear free energy relationship with a minimum centered approximately at the origin, Figure 3-1. Hammett plots such as this, which feature a minimum are usually interpreted as resulting from a competition between two mechanisms, one favored by electron donating, and the other by electron withdrawing substituents.¹⁰ Interestingly, it would appear that if two mechanisms are in fact operating, then each leads to the preferential formation of the same regioisomer.

The results of our study on the hydroboration of 1,2-diarylstilbenes are contrasted by a recent report by Brown.¹¹ In this report it is stated that the hydroboration of unsymmetrical 1,2-diarylstilbenes with Rh⁺/QUINAP employing catecholborane proceeds with excellent regioselectivity in favor of borylation proximal to the more electron deficient arene. Switching the ligand from QUINAP to DPPB had the effect of significantly lowering reaction regioselectivity to approximately a 60:40 mixture of products, however, the preference for borylation proximal to the electron deficient arene remained. Taken together with our results, it is evident that both the nature of the ligand on Rh⁺ and the source of hydroborating reagent in the reaction can have a dramatic impact on regioselectivity.

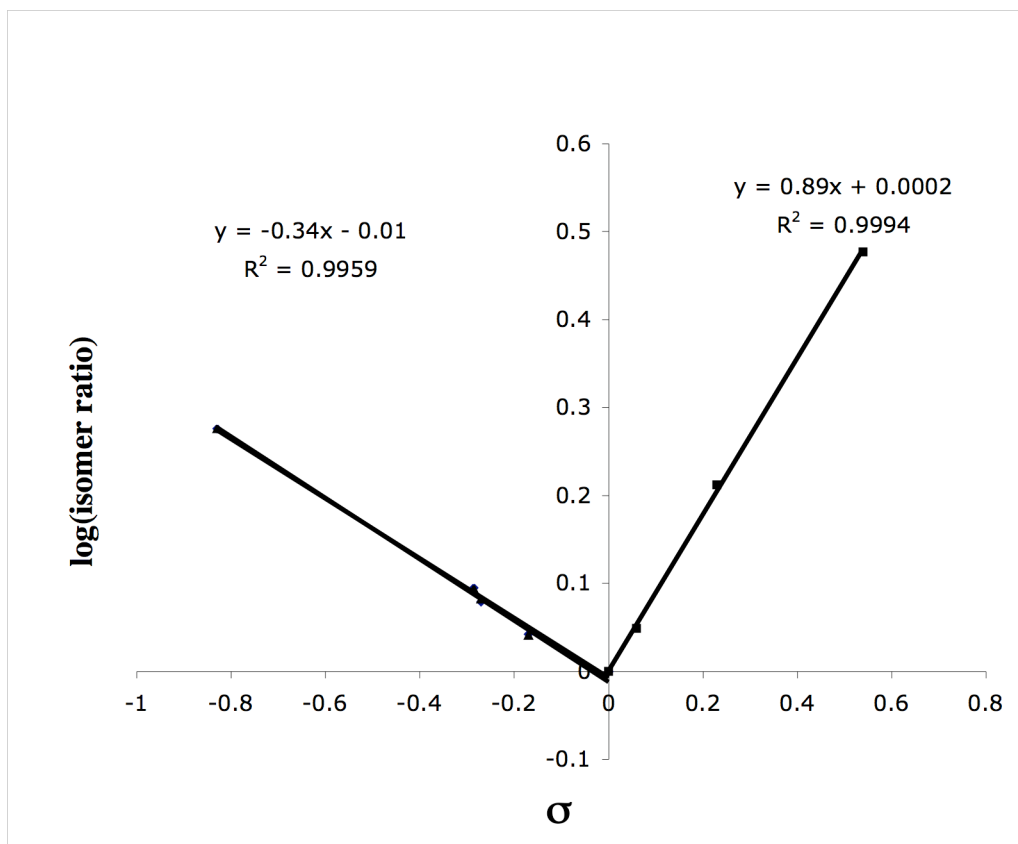
Chart 3-2: Hydroboration of *cis*-Stilbenes (**3-8a-g**)



Substrate, X	Substituent Constant (σ)	Isomer Ratio 3-9:3-10	Yield ^a (%)	Mass Balance ^a (%)
CF ₃	0.54	3.00:1	67(63)	93(87)
Cl	0.23	1.63:1	43(43)	87(97)
F	0.06	1.12:1	78(86)	99(94)
Me	-0.17	1.10:1	49(49)	91(96)
OMe	-0.27	1.20:1	81(78)	90(95)
O ⁱ Pr	-0.29	1.25:1	61(59)	98(91)
NMe ₂	-0.83	1.89:1	18	50

^a Yields determined by ¹H-NMR integrated relative to internal standard, isolated yields in parentheses.

Figure 3-1: Stilbene Hammett Plot



The shape of the Hammett plot in Figure 3-1 is indicative of the changing nature of the charge development experienced by the different stilbene substrates up to and including the mechanistic step ultimately responsible for the regioselectivity in the reaction. However, the question remains if the same phenomenon is also expressed in terms of reactivity in the hydroboration reaction. One may envision a mechanism in which the rate determining step occurs prior to a branching point in the mechanism. Should this branching point, leading to parallel reaction paths, be responsible for the regioselectivity obtained in the reaction then in fact, one would not expect to see a similar appearance in a Hammett plot constructed based on relative reactivities.

3.4: Relative Reactivity of Simple Vinyl Arenes

The relative reactivities of simple vinyl arenes can be ascertained by employing an *intermolecular* competition experiment as in equation 3-8.¹² A series of competition experiments were carried out in which equimolar amounts of *para*-substituted styrene derivatives and styrene itself were exposed to a limiting amount of hydroborating reagent. The relative conversion of each competing substrate was determined by GC analysis and from this data the k_X/k_H ratio was calculated. A graph of $\log(k_X/k_H)$ vs σ is shown in Figure 3-2. The appearance of Figure 3-2, constructed based on the relative reactivity of a series of substituted styrene derivative, is strikingly similar to that shown in Figure 3-1, constructed based on the regioselectivity of the hydroboration of stilbene substrates. A simple interpretation of these results would be that both the rate and the regioselectivity of the reaction are determined at the same point in the multi-step reaction and that both are influenced by the ability of aryl-substituents to dissipate charge.

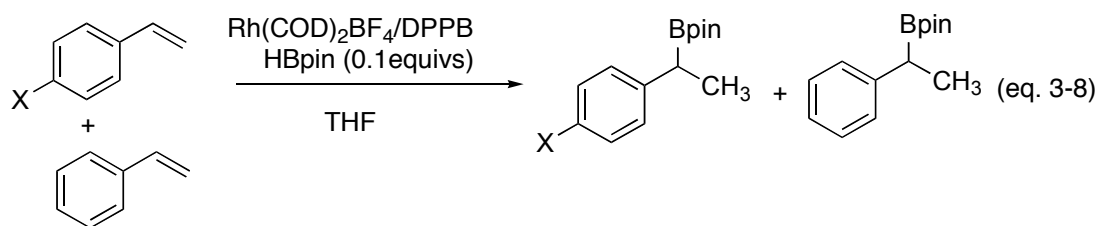
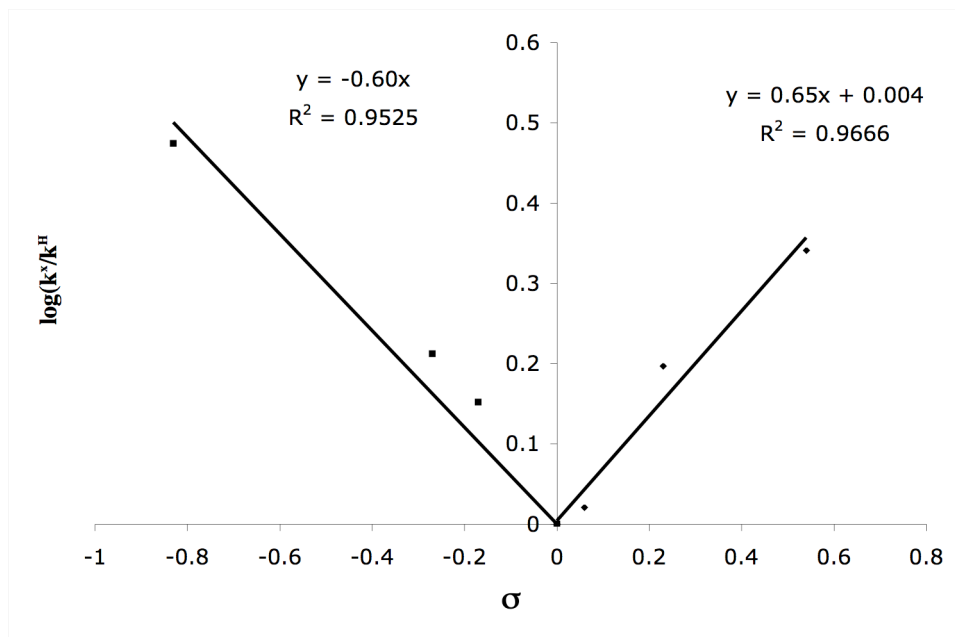


Figure 3-2: Styrene Hammett Plot



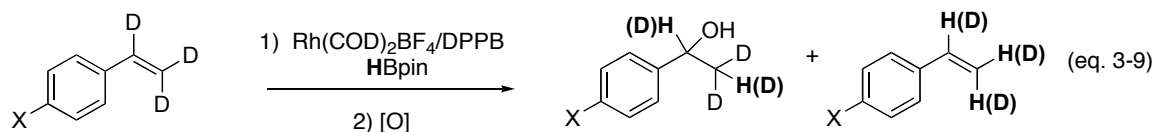
3.5: Labeling Study

The fact that purely the *trans*-stilbene starting material was recovered following hydroborations taken to less than complete conversion is a fair indication that a reversible hydride insertion/ β -hydride elimination manifold is in operation during these transformations. That *cis*-stilbene substrates are quantitatively converted to *trans*-stilbenes and not only partially so is furthermore a good indication that this process is *fast* relative to product formation. Styrene derivatives on the other hand do not possess the requisite geometrical features upon which to base a similar finding. For this reason a labeling study was embarked upon in an effort to quantify the existence and extent of reversible hydride transfer during the hydroboration of these simpler substrates.

Deuterated borane analogues, including d_1 -catecholborane, have previously been prepared.¹³ Carrying out hydroborations (deuterioborations) with these reagents allows

one to determine where in the product and starting material hydride transfer has occurred during the reaction and to what extent this transfer is reversible. Analysis of the experiment generally relies on a combination of ^1H - and ^2H -NMR to identify labeled sites and determine the quantity of label residing at each of the labeled positions. Deuterated pinacolborane, DBpin, has been prepared in our labs and employed in labeling experiments on various substrates including styrene. Unfortunately, the results of these studies were difficult to interpret owing to a combination of low (and overly high) deuterium mass balances, as well as the appearance of spurious peaks of unknown origin in the ^2H -NMR spectrum.¹⁴ For this reason, an alternate labeling strategy was ultimately sought, the results of which are presented here.

It was envisioned that a labeling experiment employing deuterated substrate subjected to typical hydroboration with HBpin, as in equation 3-9, could reveal information concerning reversibility in the hydride transfer step of the reaction. The results of such an experiment are completely analogous to those that might be obtained from deuterioboration of a protiated substrate with two key exceptions.¹⁵ The first being that DBpin need not be prepared for use in the reaction, which is important because it was theorized that the anomalies in the previous study might be a result of trace impurities carried through during the synthesis of the labeled borane reagent. Secondly, analysis of the experimental results relies heavily on observation of the proton label by quantitative ^1H -NMR as opposed to ^2H -NMR. The former is generally regarded as a superior technique in many respects. The difficulties with this approach therefore reside mainly in the procurement of deuterated styrene substrate on which to carry out the study.¹⁶



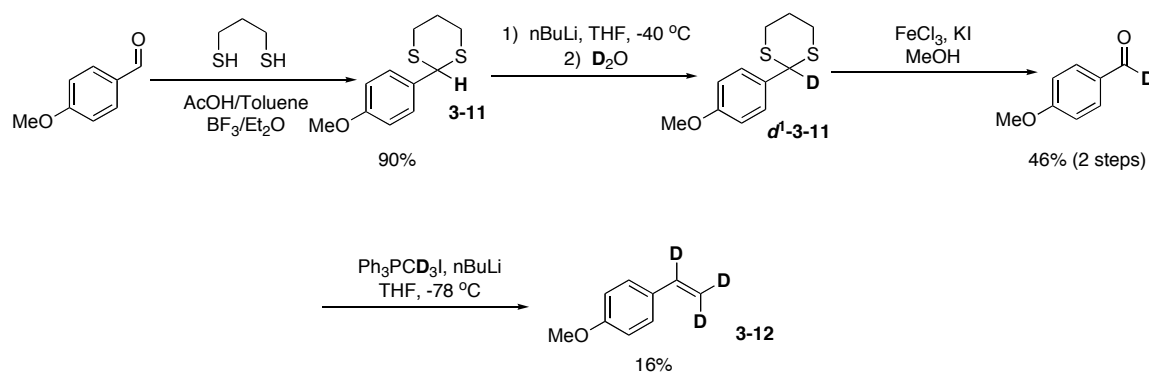
In designing a synthetic strategy for deuterated styrene derivatives, two criteria needed to be satisfied. Firstly, the deuterium source needs to be readily available and preferably at a relatively low cost for an isotopic species. Secondly, the introduction of deuterium atoms needed to be quantitative or nearly so and not subject to exchange with proton sources during work-up and isolation or even during latter synthetic steps. The first synthetic plan implemented for the synthesis of d_3 -vinyl-anisole is outlined in Scheme 3-1.

Deuteration of *p*-anisaldehyde was accomplished in three chemical steps via an umpolung strategy. Protection of the aldehyde as a dithiane proceeded smoothly under typically reported procedures.¹⁷ Recrystallization of **3-11** from refluxing hexanes furnished pure product in a yield of 90%. The key feature in this transformation was the conversion of the electrophilic aldehyde into a dithiane containing a pseudo-acidic hydrogen atom. The pK_{aDMSO} of this hydrogen atom, shown in bold, can be estimated at 39 and is certainly capable of being abstracted by strong bases such as organolithium species.¹⁸ Treatment of **3-11** with *n*BuLi in the next synthetic step was followed by a D_2O quench. This led to the quantitative incorporation of deuterium into the requisite site and did so using one of the cheapest sources of deuterium available.¹⁹

Several strategies were sought to affect deprotection of the dithiane to furnish d_1 -*p*-anisaldehyde. All strategies had in common that the reagents required for the transformation were already present within our labs and this necessarily precluded the use of mercury containing reagents. Strategies calling for the use of SelectfluorTM and

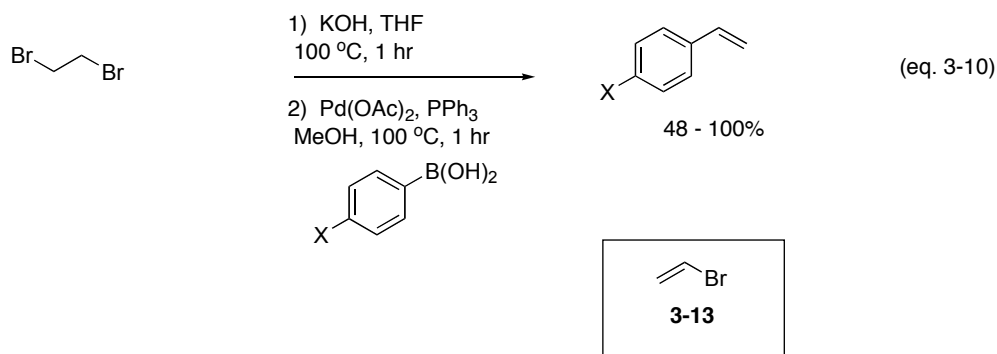
AgBF₄/I₂ ultimately proved largely ineffective.²⁰ The use of FeCl₃/KI in refluxing methanol, on the other hand, proved sufficiently effective providing *d*₁-*p*-anisaldehyde in a 46% yield over two steps.²¹ The next step in the synthetic plan called for Wittig coupling of *d*₁-*p*-anisaldehyde with a *d*₃-methyl(triphenyl)phosphonium halide. The phosphonium reagent was prepared in quantitative yield from triphenylphosphine and *d*₃-iodomethane.²² Once again a cheap source of deuterium was employed and this time at a cost as low as \$6 per gram.²³ The Wittig olefination of *d*₁-*p*-anisaldehyde to generate the target molecule **3-12** was accomplished with a yield of 16%. This low yielding step, especially in the last transformation of the sequence, significantly lowered the overall efficiency of the synthetic strategy. However, this certainly was not an unexpected outcome based on similar reports of Wittig olefinations between electron rich arylaldehydes and unstabilized Wittig reagents.²⁴

Scheme 3-1: First Synthesis of Deuterated Substrate



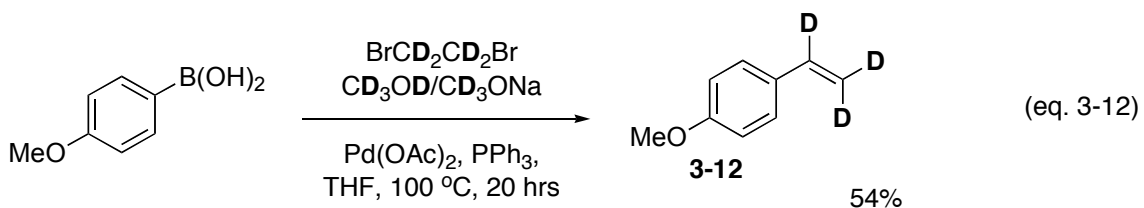
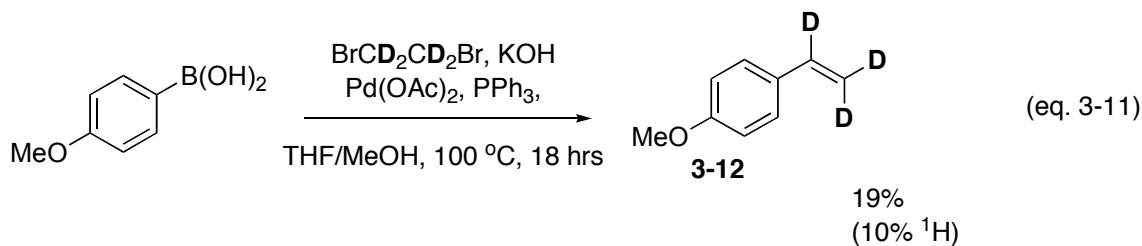
Prior to completing the hydroboration labeling study we became aware of a recent report employing Pd catalyzed coupling chemistry in the synthesis of substituted vinyl arenes, equation 3-10.²⁵ The procedure called for the in-situ generation of **3-13** by base mediated elimination from BrCH₂CH₂Br. Generally high yields were reported and importantly electron rich boronic acids were reported to be more active than electron

poor substrates. It was theorized that this route might possibly circumvent the poor efficiency of the Wittig olefination outlined in Scheme 3-1. For our purposes, the deuterated analogue $\text{BrCD}_2\text{CD}_2\text{Br}$ was to be employed as a coupling partner in the transformation. This reagent was commercially available at a cost of \$10 per gram and therefore once again fit with our stated goal of employing only relatively cheap deuterium sources.²⁶



A modified procedure related to that depicted in equation 3-10 was also reported in the communication, which called for the one-step-one-pot conversion of arylboronic acid to vinyl arene. Longer reaction times and marginally lower yields were reported employing this procedure. However, considering the potential for a slower generation of the deuterated analogue of **3-13** owing to isotope effects, this alternate procedure was deemed potentially more viable for our purposes. Adding all reagents into an autoclave and heating at 100 °C for 18 hours led to an isolated yield of 19%, equation 3-11. Despite the initial low yield of this reaction the new procedure already presented significant improvements over the previously employed four-step procedure of Scheme 3-1. Unfortunately, it was also determined by $^1\text{H-NMR}$ that the terminal methyl carbon had undergone partial loss of deuterium label and contained approximately 10% ^1H content at each site. It was unclear by what means proton had been incorporated into **3-**

12 and certainly this substrate was not thought to be an ideal candidate for an E1_{CB} type elimination with reversible loss of proton. Nonetheless, employing deuterated analogues of all reagent and solvents capable of undergoing proton transfer completely suppressed the undesired loss of deuterium label into **3-12**. The optimized procedure led to isolation of quantitatively deuterated **3-12** and in an isolated yield of 54%, equation 3-12. The newer procedure of equation 3-12 displayed several distinct advantages over that depicted in Scheme 3-1; including fewer overall reaction steps (1 vs 4), higher overall yield (54% vs 7%) and a significantly decreased time to procure the material (20 hours vs 72 hours). Furthermore, the procedure has also been employed in the preparation of *d*₃-chlorostyrene.

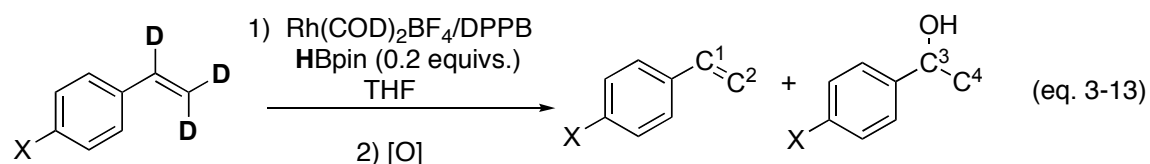


Having obtained the requisite labeled styrene substrates, the next goal was to carry out the actual labeling experiments in the hydroboration reaction. An adapted Evans protocol was employed in the experiments consisting of carrying the reactions out with an excess of styrene.²⁷ This prevented the reactions from proceeding to quantitative conversion and allowed for the recovery of unreacted starting material. This strategy

permitted the analysis of label content incorporated into styrene and made possible the assessment of the extent of hydride insertion reversibility.

A five-fold excess of styrene was subjected to hydroboration with HBpin and following the reaction, an oxidative work-up was carried out to convert the alkylboronate into a phenethanol derivative, equation 3-13. At this point, a crude $^1\text{H-NMR}$ was run and an intermolecular comparison of label content was made between the terminal carbon of unreacted styrene and the benzylic carbon of phenethanol.²⁸ Isolation of product and starting material was subsequently carried out by column chromatography. At this point, an intramolecular comparison of label content was possible by comparing $^1\text{H-NMR}$ integrals for the benzylic and terminal carbons of phenethanol and unreacted starting material respectively. The results of the labeling experiments are shown in Table 3-2 for all three substrates subjected to the study, namely *p*-vinylanisole, styrene and *p*-chlorostyrene.

Table 3-2: Labeling Results

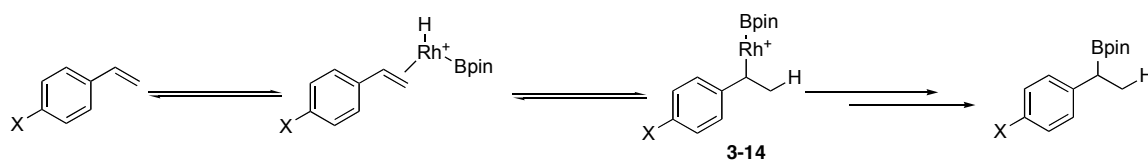


X	% Label (C1)	% Label (C2)	% Recovery	% Label (C3)	% Label (C4)	% Yield	Mass Balance (%)
OMe	8.3	14.2	65	3.3	74.3	19	84
H	11.4	18.6	35	5.6	64.4	16	51
Cl	4.2	27.7	75	6.3	61.8	19	94

The most striking feature of the labeling study is that proton is incorporated into both the terminal and benzylic sites of product and starting material alike. The presence of label into starting material indicates that both the steps of olefin complexation to Rh *and* hydride transfer are reversible. However, the percent of label determined to reside in the starting material is far from what might reasonably be expected should these two steps combined represent a fast pre-equilibrium preceding product formation. If a fast pre-equilibrium were in existence then it is predicted that 20% of the label would be found in product while 80% would be retained in the starting material. This ratio corresponds to the ratio of olefinic substrate and hydroborating reagent employed in the reactions. Interestingly, there does not seem to be a correlation between the electronics of the arene and the selectivity for label placement at the benzylic and terminal carbons.

Analysis of the data in Table 3-2 further reveals that the percent label incorporation into the terminal methyl carbon of the product (C4) increases with the electron donating ability of the *para*-substituents, OMe > H > Cl. Conversely, the percent label incorporation into the terminal methyl carbon of the starting material (C2) decreases with the electron donating ability of the *para*-substituents, OMe < H < Cl. The combination of these two results indicates that once hydride insertion intermediate **3-14** of Scheme 3-2 is formed, the level of commitment to product formation is highest for X= OMe and lowest for X= Cl.²⁹ This may imply that reductive elimination is faster for X = OMe and slower for X = Cl.

Scheme 3-2: Hydride Insertion Process



3.6: ^{13}C Carbon Isotope Effects

Kinetic isotope effects, defined as the ratio of rate constants between isotopomers, are probes of tremendous utility in elucidating reaction mechanisms.³⁰ In their most basic form they are employed to identify atoms undergoing bond change in steps up to and including the rate-determining step of multi-step reactions. However, more sophisticated techniques allow for the identification of atom rehybridization,³¹ transition state position along the reaction coordinate³² and with the aid of DFT calculations the precise geometry of the activated complex³³. The most common techniques are those employing the isotopes of hydrogen, because the magnitudes of the isotope effects tend to be comparatively large and experimental analysis straightforward. For a catalytic reaction, such as hydroboration, the reversible transfer of hydrogen atom might be expected to complicate analysis of the deuterium isotope experiment. Alternatively, it might appear that carbon isotope effects would not be subject to the same difficulties as those associated with hydrogen and in fact ^{13}C carbon kinetic isotope effects (^{13}C -KIEs) are becoming routine mechanistic probes.³⁴ ^{13}C -KIEs were obtained for the hydroboration *p*-methoxystyrene and *p*-chlorostyrene with the stated goal of obtaining further information on the nature of the reaction mechanism for electron rich and electron poor substrates.

^{13}C -KIEs were determined by the Singleton protocol³⁵ in which unlabelled, natural abundance ^{13}C containing styrene derivatives were subjected to a large-scale hydroboration and taken to low conversion. During a reaction taken to low conversion the product becomes enriched in the faster reacting isotope. The isotopic enrichment of which can be gauged by comparison to a standard reaction taken to quantitative

conversion and consequently not subjected to isotopic fractionation. Following reaction, the phenethanol products were isolated and the isotopic enrichment was determined via quantitative ^{13}C -NMR. The *para*-carbons of the styrene derivatives were assumed to undergo a negligible KIE during the reaction, and as such serve as a reference for the depletion of ^{13}C at the remaining carbon centers in the molecule. From this data, a ^{13}C -KIE can be calculated in accordance with standard theory using equation 3-14.³⁶

$$\text{KIE} = \frac{\text{Ln}(1-F)}{\text{Ln}[(1-FR_p/R)]} \quad (\text{eq. 3-14})$$

where; F = fractional conversion and R_p/R = ratio of ^{13}C in the phenethanol derivatives isolated following reaction to low conversion as compared to a reaction taken to quantitative conversion.

The reactions were carried out on large scale (100 mmol) and a deficiency of the borane reagent was employed to ensure low conversion of styrene substrate. The resulting alkylboranes were oxidized by standard means in a procedure known to be quantitative. The phenethanol products were then isolated by column chromatography and subsequently subjected to quantitative ^{13}C -NMR analysis.³⁷ In preparing the samples for analysis, the NMR tube was charged with the phenethanol derivative (70% by volume) and for the purposes of obtaining a lock and preventing field drift CD_3CN (30% by volume) was also added.³⁸ A T_1 determination was carried out by the inversion recovery method and delays between successive pulses were set greater than ten times T_1 . This corresponded to delays of 40 and 62 seconds between pulses for the *p*-methoxy and *p*-chloro derivatives, respectively. The long delays employed are necessary to prevent saturation effects. The combination of highly concentrated NMR samples and 128 scans

led to sufficient signal to noise ratios in the carbon spectrum to allow accurate integrations to be made.³⁹ In order to prevent truncation of the FID, the acquisition time was set manually to 4 seconds to acquire 256k points. All spectra were recorded at a constant temperature of 298 K.⁴⁰

The spectra were processed without applying a line broadening function and the integral regions were set so as to encompass the entire peak region spanning 0.10 ppm or greater than 10 times the half height peak width. Multiple spectra (between six and ten) were obtained following each experiment and the average integrations from these were then used to calculate the isotope effect using equation 3-14. The ¹³C-KIEs determined for hydroboration of *p*-chlorostyrene and *p*-methoxystyrene are shown in Figure 3-3 along with the standard deviations (shown in parentheses) calculated by propagation of errors. A representative ¹³C-NMR spectrum is shown in Figure 3-4.

Figure 3-3: ¹³Carbon Kinetic Isotope Effect (¹³C-KIE)

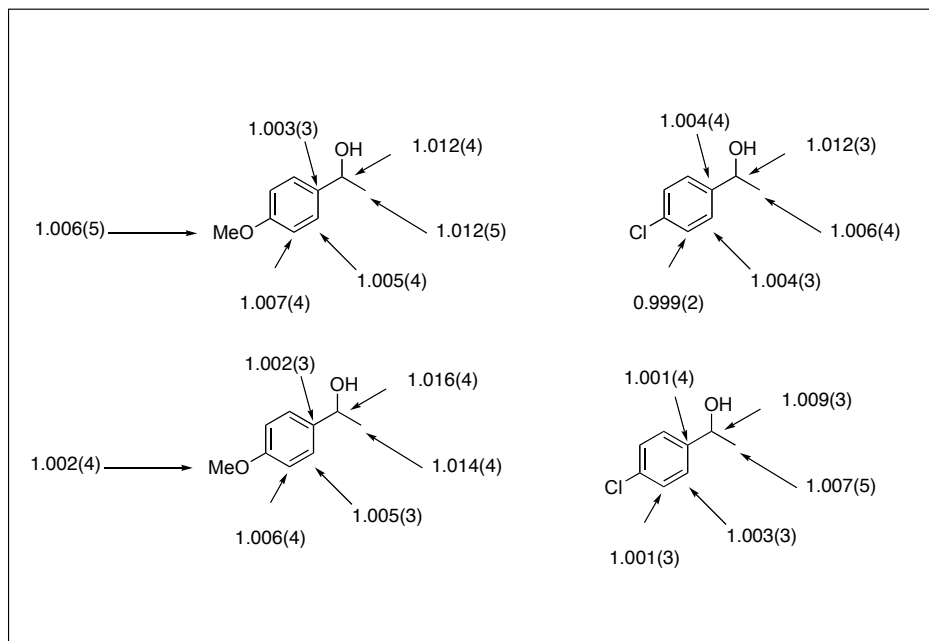
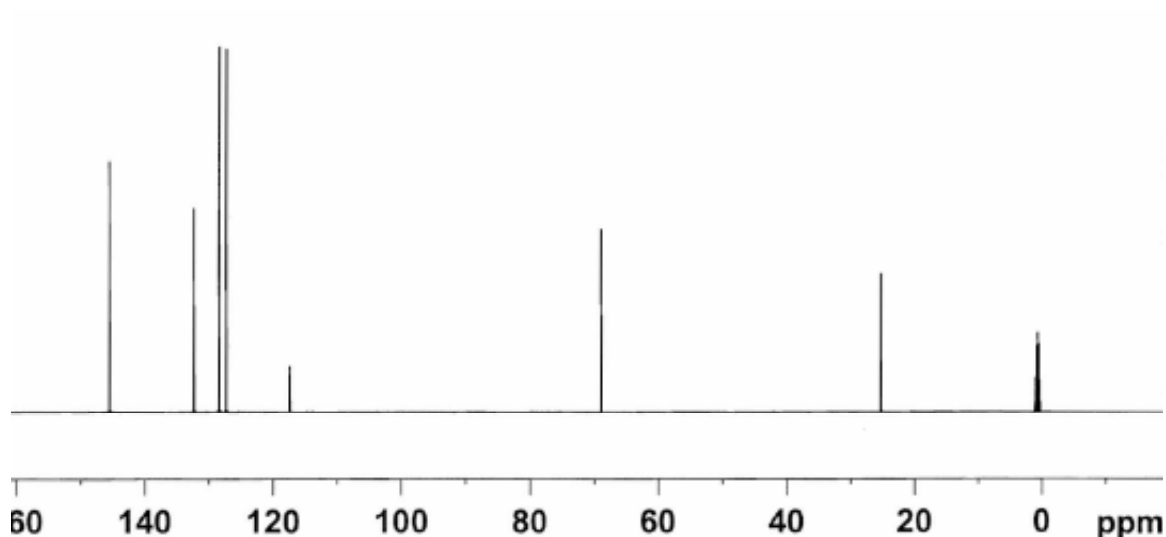


Figure 3-4: Quantitative ^{13}C -NMR spectrum of *p*-chlorophenethanol (SNR >1000:1)



It can clearly be seen from the results of Figure 3-3 that small isotope effects are observed throughout both aryl rings. *p*-Chlorostyrene displays a non-negligible isotope effect at both the *ipso* and *ortho*-carbons.⁴¹ *p*-Methoxystyrene displays small isotope effects extensively throughout its aryl backbone. In fact a small isotope effect is observed at the *meta*-carbon in contrast to the results for *p*-chlorostyrene. Additionally, a small isotope effect is also seen at the methoxy carbon. This result is unusual considering the distance between this substituent and the reaction center.

The isotope effects displayed by the benzylic and terminal carbons, both of which undergo direct bond change during the transformation, are small in magnitude for primary effects, but significantly greater than zero considering the errors involved. The benzylic carbon of *p*-chloro and *p*-methoxystyrene both display isotope effects of slightly greater than 1%. It can be seen, however, that there is a significant difference in the magnitudes of the terminal isotope effects displayed by these two substrates. The isotope effect of 1.2–1.4% for *p*-methoxystyrene is approximately twice as large as that observed for *p*-chlorostyrene at 0.6–0.7%.

Interpretation of the results for the isotope effect study are complicated by several issues. Firstly, it is unclear what the nature of the rate determining step is for either substrate. The observation of a reversible hydride insertion for both substrates, as determined by the labeling study, certainly points to a rate limiting reductive elimination. However, it remains to be determined whether or not the reversible hydride insertion actually constitutes a productive step in the catalytic cycle and is not merely a side reaction. Furthermore, if the reversible hydride insertion does in fact represent a productive step in the hydroboration then to what extent this step and the previous complexation step are reversible can significantly impact the outcome of the observed ^{13}C -KIEs. It is clear from the labeling studies that a fast pre-equilibrium between free substrate and **3-14** does *not* exist. This means that the observed isotope effects determined in this study will necessarily be a composite function of all isotope effects for chemical steps preceding and including the rate determining step. Carbon isotope effects are currently being sought in our labs on a more clearly defined system in which hydride insertion is thought to be rate limiting. This avenue of research may very well aid in the interpretation of the current study's results by demonstrating the expected magnitudes for isotope effects associated with this simpler two-step mechanism.

3.7: Paramagnetic Relaxation Agents

The two major drawbacks to determining isotope effects by the natural abundance NMR methodology are the need to carry out the chemical reactions on large scale and the almost prohibitive amount of spectrometer time required. The spectrometer time required

for analysis of the experiments is largely a result of the long delays employed between successive pulses during acquisition of the NMR spectra. In acquiring the quantitative ^{13}C -NMR data discussed in the last section delays of 40 and 62 seconds were employed for the *p*-methoxy and *p*-chloro derivatives, respectively. These long delays prevent saturation effects and permit accurate integrations to be made. Carrying the reactions out on large scale ensures that sufficient material is obtained to permit NMR analysis in an acceptable time frame, while still allowing for the long delays required in between successive pulses. If the T_1 relaxation times for the atoms of interest could be artificially reduced, then this could potentially eliminate the need for large scale reactions, as well as, reduce the required spectrometer time.

It was theorized that this might be accomplished with the use of a paramagnetic relaxation agent such as $\text{Cr}(\text{acac})_3$. Such strategies have previously been employed in quantitative ^{13}C -NMR analysis of polymers.⁴² What remained to be determined was whether such a strategy could be employed with sufficient precision for our purposes. Addition of $\text{Cr}(\text{acac})_3$ to the samples submitted to NMR analysis did in fact drastically reduce the T_1 relaxation and allowed for repetitive scans to be made with 9 second delays. Excellent reproducibility in the NMR integrations was obtained when the sample was subjected to the acquisition of multiple spectra. However, comparison between different samples treated with the paramagnetic relaxation agent showed wide variability in the NMR integrations. It was theorized the difficulties encountered resulted from small differences in the quantity of $\text{Cr}(\text{acac})_3$ added to each sample.

The linewidths in the carbon spectrum are related to the T_1 relaxation times, with shorter relaxation corresponding to broader peaks.⁴³ This ultimately results in the

broadening of peaks whenever a paramagnetic relaxation agent is introduced into the spectrometer. Small differences in the amount of $\text{Cr}(\text{acac})_3$ added to the different samples subjected to NMR analysis resulted in significant differences in linewidths and precluded accurate comparisons to be made from sample to sample.⁴⁴ This result is not altogether unexpected based on past literature precedent. Singleton, who is singly responsible for the development of the technique for determining isotope effects at natural abundance employing NMR, strongly cautions against the use paramagnetic species in the analysis.³⁴ Any samples displaying variations in T_1 are discarded based on the presumption that they contain trace paramagnetic impurities. A recent report by Gable highlights the need to rigorously exclude paramagnetic species from NMR samples subjected to quantitative integration.⁴⁵

3.8: Conclusion

The effects of aryl substitution on the regioselectivity of the hydroboration reaction have been studied. It was found that for cationic rhodium and iridium catalysts that the naphthyl substituent possesses a higher directing effect in the reaction for proximal borylation than does the phenyl substituent. A series of unsymmetrical 1,2-diarylethenes were subjected to hydroboration and interestingly the regioselectivity in the reaction increased with both electron rich and poor substituents. This same phenomenon was displayed in terms of relative reactivity when substituted styrene derivatives were subjected to an intermolecular competition. A labeling study has revealed the reversibility of both olefin complexation to rhodium and hydride insertion steps.

Differences in the extent of reversibility of these steps, for electron rich and electron poor systems were highlighted by the labeling study. Heavy atom isotope effects were determined for the reaction of both an electron rich and poor substrate. Analysis of the observed isotope effects were complicated by several issues, however, differences in reactivity between these two classes of substrate was once again illustrated.

3.9: Experimental Section

General experimental considerations: All manipulations were carried out under an inert atmosphere of nitrogen. THF was distilled from sodium/benzophenone prior to use. All liquid reagents and solvents used in the glovebox were subjected to three freeze-pump-thaw cycles for the purposes of degassing. Styrene substrates were purchased at the highest level of purity available, passed through an alumina plug, distilled and degassed prior to use. Neat pinacolborane was purchased from Aldrich and was distilled and degassed prior to use. DPPB was recrystallized from hot isopropanol prior to use and stored in a glove box. nBuLi was titrated against N-benzylbenzamide to the deep blue end point. $[\text{Rh}(\text{COD})_2]\text{BF}_4$,^{46a} $\text{RhCl}(\text{PPh}_3)_3$ ^{46b} and $[\text{Ir}(\text{COD})\text{Cl}]_2$ ^{46c} were all prepared by previously reported means. 1-(4-trifluoromethyl-phenyl)-2-phenylethanol was prepared by the previously reported procedure.⁴⁷ 1-(4-methoxy-phenyl)-2-phenylethanol was purchased from Aldrich. Identification of compounds **3-2** to **3-7** inclusive was made by comparison to reported spectral data.⁴⁸

General procedure for the synthesis of stilbenes (3-8a-g): Into a flame dried reaction flask equipped with a stir bar was added benzyltriphenylphosphonium bromide (3.81g, 8.80 mmol) and this was taken up in 50 mL THF. The reaction flask was immersed in an ice bath and to this was added nBuLi (1.1 eq) and allowed to stir 30 min. A deep red colour evolved during this period. Next was added 4-methylbenzaldehyde (1.35 mL, 11.44 mmol, 1.3 eq). The deep red colour immediately dissipated and a white precipitate formed. Reaction was left to stir overnight and then quenched with distilled water and extracted with diethyl ether. Concentration of the organic fraction afforded a yellow oil with a small amount of solid. The crude reaction mixture was purified by flash chromatography eluting with hexanes. Yield 78% (mixture of *cis/trans* isomers). Repeating the same chromatography procedure afforded the *cis* isomer in a 20% yield.

Cis-4-trifluoromethylstilbene: ¹H-NMR (500 MHz, CDCl₃) δ 7.49 (d, 8.1 Hz, 2H), 7.36 (d, 8.0 Hz, 2H), 7.25 (m, 5H), 6.74 (d, 12.2 Hz, 1H), 6.05 (d, 12.3 Hz, 1H); ¹⁹F-NMR (400 MHz, CDCl₃) δ -63.43 (s); HRMS (TOF MS EI+) calcd. 248.0813, found 248.0814 (C₁₅H₁₁F₃); Yield 68% (mixture of isomers), 30% (*cis*-isomer).

Cis-4-chloro-stilbene: ¹H-NMR (500 MHz, CDCl₃) δ 7.20 (m, 9H), 6.62 (d, 12.2 Hz, 1H), 6.53 (d, 12.2 Hz, 1H); ¹³C-NMR (125 MHz, CDCl₃) δ 136.89, 135.67, 132.77, 130.97, 130.33, 130.13, 128.94, 128.74, 128.53, 128.33; HRMS (TOF MS EI+) calcd. 214.0549, found 214.0557 (C₁₄H₁₁Cl); Yield 88% (mixture of isomers), 21% (*cis*-isomer).

Cis-4-fluoro-stilbene: $^1\text{H-NMR}$ (500 MHz, CDCl_3) δ 7.23 (m, 7H), 6.30 (app. t, 2H), 6.59 (app. dd, 2H); $^{13}\text{C-NMR}$ (125 MHz, CDCl_3) δ 163.44, 160.99, 137.42, 133.58, 130.90 (d, 7.59 Hz), 130.65, 129.44, 129.20, 129.22, 128.68, 127.57, 115.51 (d, 21.22 Hz); $^{19}\text{F-NMR}$ (400 MHz, CDCl_3) δ -115.46; HRMS (TOF MS EI+) calcd. 198.0845, found 198.0846 ($\text{C}_{14}\text{H}_{11}\text{F}$); Yield 34% (mixture of isomers), 29% (*cis*-isomer).

Cis-4-methyl-stilbene: $^1\text{H-NMR}$ (500 MHz, CDCl_3) δ 7.2 (m, 7H), 7.05 (app. d, 2H), 6.58 (app. s, 2H), 2.34 (s, 3H); $^{13}\text{C-NMR}$ (125 MHz, CDCl_3) δ 137.92, 137.26, 134.68, 130.61, 129.96, 129.30, 129.24, 129.19, 128.58, 127.36, 21.62; HRMS (TOF MS EI+) calcd. 194.1096, found 194.1097 ($\text{C}_{15}\text{H}_{14}$); Yield 78% (mixture of isomers), 20% (*cis*-isomer).

Cis-4-methoxy-stilbene: $^1\text{H-NMR}$ (500 MHz, CDCl_3) δ 7.26 (m, 7H), 6.79 (d, 8.8 Hz, 2H), 6.6 (app. d, 2H), 3.81 (s, 3H); $^{13}\text{C-NMR}$ (125 MHz, CDCl_3) δ 159.11, 138.05, 130.55, 130.18, 130.10, 129.22, 129.18, 128.62, 127.29, 114.01, 55.59; HRMS (TOF MS EI+) calcd. 210.1045, found 210.1052 ($\text{C}_{15}\text{H}_{14}\text{O}$); Yield 78% (mixture of isomers), 20% (*cis*-isomer).

Cis-4-isopropoxy-stilbene: $^1\text{H-NMR}$ (500 MHz, CDCl_3) δ 7.26 (m, 7H), 6.77 (d, 8.5 Hz, 2H), 6.6 (app. s, 2H), 4.55 (m, 1H) 1.36 (d, 6.0 Hz, 6H); $^{13}\text{C-NMR}$ (125 MHz, CDCl_3) δ 157.45, 138.10, 130.58, 130.25, 129.82, 129.24, 128.99, 128.63, 127.28, 115.82, 70.16, 22.48; HRMS (TOF MS EI+) calcd. 194.1096, found 194.1097 ($\text{C}_{15}\text{H}_{14}$); Yield 78% (mixture of isomers), 20% (*cis*-isomer).

Cis-4-dimethylamino-stilbene: $^1\text{H-NMR}$ (500 MHz, CDCl_3) δ 7.25 (m, 7H), 6.58 (app. d, 2H), 6.46 (app. q, 2H), 2.95 (s, 3H), 2.94 (s, 3H); $^{13}\text{C-NMR}$ (125 MHz, CDCl_3) δ 149.85, 138.59, 130.57, 130.24, 129.09, 128.47, 127.18, 126.87, 125.48, 112.17, 40.68; HRMS (TOF MS EI+) calcd. 223.1361, found 223.1365 ($\text{C}_{16}\text{H}_{17}\text{N}$); Yield 97% (mixture of isomers), 12% (*cis*-isomer).

General procedure for hydroboration of cis-stilbenes (3-8a-g): All reactions were set up inside a glove box. To a sealed tube was added $\text{Rh}(\text{COD})_2\text{BF}_4$ (10.15mg, 5 mol%), and DPPB (10.7mg, 5 mol%). This was dissolved in 4 mL THF and stirred for 5 min. To the stirring suspension was successively added *cis*-4-fluoro-stilbene (99.1 mg, 0.50mmol) and pinacolborane (0.09 mL, 0.60 mmol). The reaction tube was sealed within a glove box and removed to a fume hood. Reactions were then heated in an oil bath set at 80 °C for 3 days. The reaction flask was cooled to ambient temperature and 2 mL 30% H_2O_2 and 2 mL 2 M NaOH were then added. The reaction was left under vigorous stirring for 2 hrs. The crude reaction was then subjected to an aqueous work-up and extracted with diethyl ether. The crude material was purified by flash chromatography using a gradient elution of 1-20% EtOAc in hexanes. $^1\text{H-NMR}$ spectra were taken on 500 or 600 MHz spectrometers to determine the isomer ratio. The isomeric identity was confirmed by doping the NMR sample with authentic **3-9a-g**.

General procedure for synthesis of authentic alcohols (3-9a-g): Into a flame dried 50 mL reaction flask, immersed in an ice bath, was added 2 M benzylmagnesium chloride (1.0 mL, 2 mmol) to 10 mL THF. To this was added 4-fluorobenzaldehyde (0.14 mL, 2

mmol) in 5 mL THF via cannula. The reaction was left to stir and warm to room temperature overnight. The reaction was quenched with $\text{NH}_4\text{Cl}_{\text{sat}}$ and extracted with ether. Column chromatography was performed using a gradient elution of 10-20% EtOAc in hexanes.

1-(4-chloro-phenyl)-2-phenylethanol: $^1\text{H-NMR}$ (500 MHz, CDCl_3) δ 7.31 (m, 7H), 7.19 (d, 7.1 Hz, 2H), 4.90 (dd, 5.1 Hz, 8.2 Hz, 1H), 3.01 (m, 2H); $^{13}\text{C-NMR}$ (125 MHz, CDCl_3) δ 142.64, 137.93, 133.64, 129.91, 128.99, 128.92, 127.70, 127.18, 75.04, 46.50; HRMS (TOF MS Cl^+) calcd. 231.0577, found 231.0578 ($\text{C}_{14}\text{H}_{12}\text{OCl}$) $[\text{M}-2\text{H}+\text{H}]^+$; Yield 32%.

1-(4-fluoro-phenyl)-2-phenylethanol: $^1\text{H-NMR}$ (500 MHz, CDCl_3) δ 7.33 (m, 4H), 7.27 (m, 1H), 7.19 (app. d, 2H), 7.05 (m, 2H), 4.90 (dd, 5.3 Hz, 13.4 Hz, 1H), 3.02 (m, 2H); $^{13}\text{C-NMR}$ (125 MHz, CDCl_3) δ 162.62 (d, 245.7 Hz), 139.89 (d, 3.0 Hz), 138.10, 129.91, 128.96, 127.95 (d, 8.0 Hz), 127.12, 115.59 (d, 21.32 Hz), 75.10, 46.59; $^{19}\text{F-NMR}$ (400 MHz, CDCl_3) δ -116.03; HRMS (TOF MS EI^+) calcd. 216.0950, found 216.0961 ($\text{C}_{14}\text{H}_{13}\text{OF}$); Yield 55%.

1-(4-methyl-phenyl)-2-phenylethanol: $^1\text{H-NMR}$ (500 MHz, CDCl_3) δ 7.33 (m, 2H), 7.25 (m, 5H), 7.19 (m, 2H), 4.88 (dd, 5.6 Hz, 7.7 Hz, 1H), 3.04 (m, 2H), 2.39 (s, 3H); $^{13}\text{C-NMR}$ (125 MHz, CDCl_3) δ 147.45, 138.73, 137.57, 129.94, 129.46, 128.84, 126.90, 126.30, 75.58, 46.47, 21.54; HRMS (TOF MS Cl^+) calcd. 211.1123, found 211.1115 ($\text{C}_{15}\text{H}_{15}\text{O}$); Yield 81%.

1-(4-isopropoxy-phenyl)-2-phenylethanol: $^1\text{H-NMR}$ (500 MHz, CDCl_3) δ 7.26 (m, 7H), 6.90 (d, 8.6 Hz, 2H), 4.87 (t, 6.6 Hz, 1H), 4.58 (m, 1H), 3.03 (d, 6.7 Hz, 2H); $^{13}\text{C-NMR}$ (125 MHz, CDCl_3) δ 158.07, 138.95, 136.54, 130.21, 129.15, 127.87, 127.21, 116.49, 75.70, 70.62, 46.67, 22.75; HRMS (TOF MS EI+) calcd. 256.1463, found 256.1465 ($\text{C}_{17}\text{H}_{20}\text{O}_2$); Yield 18%.

1-(4-dimethylamino-phenyl)-2-phenylethanol: $^1\text{H-NMR}$ (500 MHz, CDCl_3) δ 7.33 (m, 7H), 6.78 (d, 8.7 Hz, 2H), 4.85 (t, 6.5 Hz, 1H), 3.08 (m, 2H), 3.00 (s, 6H); $^{13}\text{C-NMR}$ (125 MHz, CDCl_3) δ 150.70, 139.15, 132.48, 129.99, 128.79, 127.38, 126.77, 113.04, 75.60, 46.24, 41.13; HRMS (TOF MS CI+) calcd. 241.1467, found 241.1464 ($\text{C}_{16}\text{H}_{19}\text{NO}$); Yield 59%.

General procedure for styrene competition experiments: All reactions were set up in a glove box. Into a flask were combined $\text{Rh}(\text{COD})_2\text{BF}_4$ (10.15 mg, 5 mol%), and DPPB (10.7 mg, 5 mol%) and 2 mL THF. This was allowed to stir for 5 minutes. To this was added simultaneously styrene (0.50 mmol) and *para*-substituted-styrene (0.50 mmol) in 2 mL THF. Lastly was added pinacolborane (15 μL , 0.10 mmol) to commence the reaction. Reaction was allowed to stir in glove box for 24 h. Upon removal of flask from glove box the reaction was immediately quenched with wet ether and 0.08 mL of decane was added as a GC internal standard. The relative conversion of each substrate was determined by GC. Results shown in Table 3-3 are averages of 2 runs.

Table 3-3: Results of Styrene Competition Experiment

Substrate, X	σ	k_{rel} (k_X/k_H)
CF ₃	0.54	2.41
Cl	0.23	1.53
F	0.06	1.06
Me	-0.17	1.42
OMe	-0.27	1.63
NMe ₂	-0.83	2.98

General procedure for preparation of deuterated styrene substrates: Into a sealed tube was added d₄-dibromoethane (430 μ l, 5.0 mmol, Aldrich), *p*-methoxy-phenyl boronic acid (1.14 g, 7.5 mmol), palladium acetate (56 mg, 0.24 mmol), triphenylphosphine (130 mg, 0.50 mmol), 10 mL THF and CD₃ONa/CD₃OD (10 mL, 2M). Note: CD₃ONa was prepared prior to use via the slow addition of CD₃OD to sodium lump. The reaction vessel was affixed with a screw-on top and then placed into oil bath at 100 °C for 20 hrs. The sealed vessel was cooled to 0 °C prior to opening stopper. The crude reaction mixture was subjected to an aqueous work-up with distilled water and ether. The organic fraction was dried with MgSO₄ and filtered. The deuterated vinyl arene was isolated by column chromatography (gradient elution 1-4% EtOAc in hexanes). Isolate 362 mg (54% yield) of d₃-*p*-methoxy styrene. No vinylic proton peaks observed by high field ¹H-NMR.

Labelling study with d₃-styrene and HBpin: All reactions were set up in a glove box. Into a 15 mL flask was added Rh(COD)₂BF₄ (5 mg, 0.0125 mmol), and DPPB (6 mg, 0.014 mmol) and the solids were taken up in 2 mL THF. The suspension was allowed to stir for 15 minutes. To the stirring reaction flask was added styrene (467 mg, 4.36 mmol) in 2 mL THF. Lastly, pinacolborane (125 µL, 0.87 mmol) was added. The reaction was allowed to stir in a glove box for 24 h. At this time the reaction vessel was removed to a fume hood and placed in an ice bath. To the reaction flask was added 2 mL 2M NaOH and 2 mL 30% H₂O₂. After 2 hours the reaction was subjected to an aqueous work-up with NH₄Cl and DCM. The unreacted alkene and alcohol product were isolated by column chromatography with gradient elution 10-27% EtOAc in hexanes. The mass recovery of styrene was 35% (volatile compound) and the yield of the alcohol was 16% (from theoretical max of 20%). Proton label incorporation was determined by high field (600 MHz) ¹H-NMR of crude material prior to column chromatography and compared to ratios determined in the purified material.

Labelling study with d₃-p-methoxystyrene and HBpin: All reactions were set up in a glove box. Into a 15 mL flask was added Rh(COD)₂BF₄ (5 mg, 0.0125 mmol), and DPPB (6 mg, 0.014 mmol) and the solids were taken up in 2 mL THF. The suspension was allowed to stir for 15 minutes. To the stirring reaction flask was added d₃-methoxystyrene (216 mg, 1.58 mmol) in 2 mL THF. Lastly, pinacolborane (46 µL, 0.32 mmol) was added. The reaction was allowed to stir in a glove box for 24 h. At this time the reaction vessel was removed to a fume hood and placed in an ice bath. To the reaction flask was added 2 mL 2M NaOH and 2 mL 30% H₂O₂. After 2 hours the

reaction was subjected to an aqueous work-up with NH_4Cl and DCM. The unreacted alkene and alcohol product were isolated by column chromatography with gradient elution 10-40% EtOAc in hexanes. The mass recovery of *p*-methoxystyrene was 65% and the yield of the alcohol was 19% for a mass balance of 84%. Proton label incorporation was determined by high field (600 MHz) ^1H -NMR of crude material prior to column chromatography and compared to ratios determined in the purified material.

*Labelling study with d_3 -*p*-chlorostyrene and HBpin:* All reactions were set up in a glove box. Into a 15 mL flask was added $\text{Rh}(\text{COD})_2\text{BF}_4$ (5 mg, 0.0125 mmol), and DPPB (6 mg, 0.014 mmol) and the solids were taken up in 2 mL THF. The suspension was allowed to stir for 15 minutes. To the stirring reaction flask was added d_3 -chlorostyrene (701 mg, 4.95 mmol) in 2 mL THF. Lastly, pinacolborane (150 μl , 1.0 mmol) was added. The reaction was allowed to stir in a glove box for 24 h. At this time the reaction vessel was removed to a fume hood and placed in an ice bath. To the reaction flask was added 2 mL 2M NaOH and 2 mL 30% H_2O_2 . After 2 hours the reaction was subjected to an aqueous work-up with NH_4Cl and DCM. The unreacted alkene and alcohol product were isolated by column chromatography with gradient elution 10-35% EtOAc in hexanes. The mass recovery of *p*-chlorostyrene was 75% and the yield of the alcohol was 19% for a mass balance of 94%. Proton label incorporation was determined by high field (600 MHz) ^1H -NMR of crude material prior to column chromatography and compared to ratios determined in the purified material.

Experimental procedure for isotope effect determination (p-methoxy-styrene): Into a 1000 mL flask equipped with a stir bar was added RhCOD₂BF₄ (390 mg, 0.96 mmol), DPPB (498 mg, 1.17 mmol) and this was taken up in approximately 100 mL THF. Stirring was affected for 15 minutes at which time *p*-methoxystyrene (13.44 g, 100 mmol) was added dropwise followed by 300 ml THF and finally pinacolborane (2.65 g, 20.7 mmol) was added dropwise to commence the reaction. After stirring in the glovebox for 16 hrs an aliquot was removed, volatiles concentrated off at reduced pressure and a ¹H-NMR spectrum was obtained. The reaction was deemed complete and was removed to a fumehood, placed in an ice bath under nitrogen and 2M NaOH (50 mL, 100 mmol) and 30% H₂O₂ (50mL) were sequentially added to the reaction flask. The reaction was left to slowly warm to room temperature and at 2 hours subjected to an aqueous extraction with diethyl ether, dried with MgSO₄, filtered and concentrated under reduced pressure. The crude reaction mixture containing both unreacted *p*-methoxystyrene and the *p*-methoxyphenethanol product was subjected to ¹H-NMR analysis from which the percent conversion of the reaction was determined to be 20%. The crude reaction mixture was then purified by flash column chromatography employing 1 L silica and 35% ethyl acetate in hexanes as eluent to yield 2.496 g of product (79% yield based on amount of limiting reagent pinacoborane). In preparing the sample for NMR analysis the NMR tube was charged with 70% by volume phenethanol derivative and 30% by volume CD₃CN. Quantitative ¹³C-NMR spectra were taken at 150.93 MHz using a 600 MHz Bruker spectrometer with inverse gated decoupling. All spectra were recorded at 298 K. The T₁ values were determined by the inversion recovery method and delays greater than 10 times T₁ were used in between successive

pulses (40 seconds). The acquisition time was set manually to 3.999 seconds to collect 287764 points. The spectra were processed manually without applying an exponential decay (line broadening function) or performing any zero filling. A zero order base line correction was applied to all spectra. Integration ranges for all peaks of interest were set to a constant value of 0.10 ppm and this value was kept constant from one experiment to the next. The integral for the peak corresponding to the *para*-carbon was manually set to 1000 and acted as internal reference. Two KIE determinations were performed. Isotopic depletion in each KIE determination was performed by comparison to a reaction taken to quantitative conversion. This reaction was performed on a 20 mmol scale but all other reaction parameters are completely analogous to those depicted above.

Table 3-4: Integration values for standard reaction of *p*-methoxystyrene taken to 100% conversion

	C _{para}	C _{ipso}	C _{ortho}	C _{meta}	C _{benzylic}	C _{methoxy}	C _{methyl}
Spectra #1	1000	1018.64	2033.07	2037.47	1020.57	978.08	981.61
Spectra #2	1000	1013.97	2023.51	2034.47	1017.92	974.86	971.91
Spectra #3	1000	1011.17	2028.98	2038.05	1020.08	977.54	975.55
Spectra #4	1000	1016.1	2035.37	2047.77	1026.64	982.08	983.2
Spectra #5	1000	1017.5	2033.51	2044.36	1019.19	978.35	979.08
Spectra #6	1000	1014.61	2033.85	2046.01	1022.74	982.83	978.18
Spectra #7	1000	1013.98	2025.46	2037.99	1021.4	978.96	975.19
Spectra #8	1000	1013.21	2024.58	2042.71	1018.67	975.5	976.72
Spectra #9	1000	1014.2	2034.19	2041.37	1025.73	976.2	978.46
Ave. Int.	1000	1014.82	2030.28	2041.13	1021.44	978.27	977.77
Std. dev. (ΔInt)	NA	2.27	4.68	4.44	3.06	2.74	3.42

Table 3-5: Integration values for KIE determination reaction of *p*-methoxystyrene taken to 20% conversion (reaction #1)

	C _{para}	C _{ipso}	C _{ortho}	C _{meta}	C _{benzylic}	C _{methoxy}	C _{methyl}
Spectra #1	1000	1011.78	2025.03	2033.18	1010.98	976.94	970.97
Spectra #2	1000	1012.43	2015.54	2024.63	1008.89	974.83	968.52
Spectra #3	1000	1011.98	2015.91	2025.08	1011.03	970.95	965.64
Spectra #4	1000	1012.45	2017.64	2023.77	1009.48	967.79	964.67
Spectra #5	1000	1014.01	2023.61	2024.63	1010.55	974.76	963.93
Spectra #6	1000	1011.62	2021	2028.71	1009.02	971.36	970.26
Spectra #7	1000	1012.43	2026.42	2040.05	1012.36	974.89	966.79
Ave. Int.	1000	1012.39	2020.74	2028.58	1010.33	973.07	967.25
Std. dev. (ΔInt)	NA	0.79	4.45	6.05	1.26	3.15	2.74

Table 3-6: Integration values for KIE determination reaction of *p*-methoxystyrene taken to 20% conversion (reaction #2)

	C _{para}	C _{ipso}	C _{ortho}	C _{meta}	C _{benzylic}	C _{methoxy}	C _{methyl}
Spectra #1	1000	1012.3	2021.75	2028.92	1006.41	977.3	967.97
Spectra #2	1000	1009.98	2023.81	2029.87	1006.77	975.34	966.05
Spectra #3	1000	1012.68	2020.86	2031.24	1007.15	973.27	966.88
Spectra #4	1000	1013.89	2021.86	2035.29	1006.32	976.08	964.98
Spectra #5	1000	1012.16	2019.97	2031.46	1007.33	976.21	966.49
Spectra #6	1000	1016.41	2020.66	2027.72	1008.06	977.24	965.98
Spectra #7	1000	1015.27	2024.91	2029.71	1008.75	979.16	964.32
Ave. Int.	1000	1013.24	2021.97	2030.60	1007.26	976.37	966.10
Std. dev. (ΔInt)	NA	2.14	1.78	2.44	0.89	1.83	1.20

$$\text{KIE} = \frac{\ln(1-F)}{\ln(1-F(R_p/R))} \quad (\text{eq. 3-14})$$

$$\Delta R_p/R = \sqrt{((\Delta \text{Int}_{\text{std}}/\text{Ave. Int.}_{\text{std}})^2 + (\Delta \text{Int}_{\text{Rx}}/\text{Ave. Int.}_{\text{Rx}})^2)} \quad (\text{eq. 3-15})$$

$$\Delta \text{KIE} = \frac{(\Delta R_p/R)(-F)\ln(1-F)}{(1-F(R_p/R)\ln^2(1-F(R_p/R)))} \quad (\text{eq. 3-16})$$

These equations are taken from reference 49.

Table 3-7: Isotope effects and associated errors for hydroboration of *p*-methoxystyrene

	C _{para}	C _{ipso}	C _{ortho}	C _{meta}	C _{benzylic}	C _{methoxy}	C _{methyl}
Expt. #1							
R _p /R	1	0.9976	0.9953	0.9938	0.9891	0.9947	0.9892
ΔR _p /R	NA	0.0024	0.0032	0.0037	0.0032	0.0043	0.0045
¹³ C-KIE	1	1.0027	1.0053	1.0069	1.0123	1.0060	1.0122
ΔKIE	NA	0.0027	0.0036	0.0042	0.0037	0.0048	0.0052
Expt. #2							
R _p /R	1	0.9984	0.9959	0.9948	0.9861	0.9981	0.9881
ΔR _p /R		0.0031	0.0024	0.0025	0.0031	0.0034	0.0037
¹³ C-KIE	1	1.0017	1.0046	1.0058	1.0158	1.0022	1.0135
ΔKIE	NA	0.0034	0.0028	0.0028	0.0035	0.0039	0.0042

Experimental procedure for isotope effect determination (p-chlorostyrene): Into a 1000 mL flask equipped with a stir bar was added RhCOD₂BF₄ (409 mg, 1.01 mmol), DPPB (517 mg, 1.21 mmol) and this was taken up in approximately 100 mL THF. Stirring was affected for 15 minutes at which time *p*-chlorostyrene (14.07 g, 102 mmol) was added dropwise followed by 300 mL THF and finally pinacolborane (2.61 g, 20.4 mmol) was added dropwise to commence the reaction. After stirring in the glovebox for 16 hrs an aliquot was removed, the volatiles were concentrated off at reduced pressure and a ¹H-NMR spectrum was obtained. The reaction was deemed complete and the flask was removed to a fumehood, placed in an ice bath under nitrogen and 2M NaOH (50 mL, 100 mmol) and 30% H₂O₂ (50mL) were sequentially added to the reaction flask. The reaction was left to slowly warm to room temperature and at 2 hours was subjected to an aqueous extraction with diethyl ether, dried with MgSO₄, filtered and concentrated under reduced pressure. The crude reaction mixture containing both unreacted *p*-chlorostyrene and the

p-chlorophenethanol product was subjected to ^1H -NMR analysis from which the percent conversion of the reaction was determined to be 17%. The crude reaction mixture was then purified by flash column chromatography employing 1 L silica and 30% ethyl acetate in hexanes as eluent to yield 1.91 g of product (60% yield based on amount of limiting reagent pinacborane). In preparing the sample for NMR analysis the NMR tube was charged with 70% by volume phenethanol derivative and 30% by volume CD_3CN . Quantitative ^{13}C -NMR spectra were taken at 150.93 MHz using a 600 MHz Bruker spectrometer with inverse gated decoupling. All spectra were recorded at 298 K. The T_1 values were determined by the inversion recovery method and delays greater than 10 times T_1 were used in between successive pulses (62 seconds). The acquisition time was set manually to 3.999 seconds to collect 287764 points. The spectra were processed manually without applying an exponential decay (line broadening function) or performing any zero filling. A zero order base line correction was applied to all spectra. Integration ranges for all peaks of interest were set to a constant value of 0.10 ppm and this value was kept constant from one experiment to the next. The integral for the peak corresponding to the *para*-carbon was manually set to 1000. Two KIE determinations were performed. Isotopic depletion in each KIE determination was performed by comparison to a reaction taken to quantitative conversion. This reaction was performed on a 20 mmol scale but all other reaction parameters are completely analogous to those depicted above.

Table 3-8: Integration values for standard reaction of *p*-chlorostyrene taken to 100% conversion

	C _{ipso}	C _{para}	C _{meta}	C _{ortho}	C _{benzylic}	C _{methyl}
Spectra #1	955.73	1000	1968.31	1966.90	957.29	955.73
Spectra #2	954.53	1000	1962.30	1963.52	954.64	954.53
Spectra #3	950.98	1000	1969.70	1960.35	955.65	950.98
Spectra #4	950.06	1000	1967.70	1953.76	953.17	950.06
Spectra #5	948.22	1000	1965.96	1959.67	957.12	948.22
Spectra #6	950.10	1000	1964.43	1963.71	957.16	950.10
Ave. Int.	951.60	1000	1966.40	1961.32	955.84	951.60
Std. dev. (ΔInt)	2.90	NA	2.73	4.53	1.68	2.90

Table 3-9: Integration values for KIE determination reaction of *p*-chlorostyrene taken to 17% conversion (reaction #1)

	C _{ipso}	C _{para}	C _{meta}	C _{ortho}	C _{benzylic}	C _{methyl}
Spectra #1	947.82	1000	1968.34	1952.27	944.06	965.88
Spectra #2	948.34	1000	1973.58	1957.91	945.35	968.68
Spectra #3	947.45	1000	1961.37	1952.68	942.94	967.88
Spectra #4	950.42	1000	1969.04	1953.75	945.94	965.63
Spectra #5	947.96	1000	1970.97	1956.95	948.46	971.06
Spectra #6	946.39	1000	1966.63	1947.68	945.83	962.79
Ave. Int.	948.06	1000	1968.32	1953.54	945.43	966.99
Std. dev. (ΔInt)	1.33	NA	4.16	3.67	1.88	2.86

Table 3-10: Integration values for KIE determination reaction of *p*-chlorostyrene taken to 17% conversion (reaction #2)

	C _{ipso}	C _{para}	C _{meta}	C _{ortho}	C _{benzylic}	C _{methyl}
Spectra #1	950.4	1000	1962.45	1951.67	944.53	970.19
Spectra #2	951.06	1000	1966.52	1954.62	946.03	963.06
Spectra #3	949.82	1000	1963.79	1957.3	947.74	966.53
Spectra #4	949.55	1000	1966.03	1956.77	948.69	964.12
Spectra #5	951.32	1000	1966.07	1959.19	948.94	967.27
Spectra #6	951.75	1000	1964.55	1956.06	950.38	966.16
Ave. Int.	950.65	1000	1964.90	1955.94	947.72	966.22
Std. dev. (ΔInt)	0.87	NA	1.59	2.57	2.12	2.50

Table 3-11: Isotope effects and associated errors for hydroboration of *p*-chlorostyrene

	C _{ipso}	C _{para}	C _{meta}	C _{ortho}	C _{benzylic}	C _{methyl}
Expt. #1						
R _p /R	0.9963	1	1.0010	0.9960	0.9891	0.9945
ΔR _p /R	0.0032	NA	0.0016	0.0027	0.0028	0.0039
¹³ C-KIE	1.0041	1	0.9989	1.0044	1.0121	1.006
ΔKIE	0.0035	NA	0.0018	0.0029	0.0032	0.0044
Expt. #2						
R _p /R	1.0037	1	0.9990	1.0040	1.0110	1.0056
ΔR _p /R	0.0034	NA	0.0025	0.0030	0.0027	0.0042
¹³ C-KIE	1.0011	1	1.0008	1.0030	1.0094	1.0070
ΔKIE	0.0037	NA	0.0028	0.0033	0.0030	0.0047

3.10: References

- 1) a) Beletskaya, I.; Pelter, A. *Tetrahedron* **1997**, *53*, 4957. b) Crudden, C.M.; Edwards, D.R. *Eur. J. Org. Chem.* **2003**, 4695.
- 2) a) Brown, J.M.; Hulmes, D.I.; Layzell, L.P. *J.C.S., Chem. Commun.* **1993**, 1673. b) Togni, A.; Breutel, C.; Schnyder, A.; Spindler, F.; Landert, H.; Tijani, A. *J. Amer. Chem. Soc.* **1994**, *116*, 4062. c) Schnyder, A.; Hintermann, L.; Togni, A. *Angew. Chem. Int. Ed.* **1995**, *34*, 931. d) Burckhardt, U.; Hintermann, L.; Schnyder, A.; Togni, A. *Organometallics* **1995**, *14*, 5415.
- 3) a) Hayashi, T.; Matsumoto, Y. *Tetrahedron: Asymmetry.* **1991**, *2*, 601. b) Ramachandran, P.V.; Jennings, M.P.; Brown, H.C. *Org. Lett.* **1999**, *1*, 1399. c) Doucet, H.; Fernandez, E.; Layzell, T.P.; Brown, J.M. *Chem. Eur. J.* **1999**, *5*, 1320.
- 4) Crudden, C.M.; Hleba, Y.B.; Chen, A.C. *J. Am. Chem. Soc.* **2004**, *126*, 9200.
- 5) Wheeler, O.H.; Batlle de Pabon, H.N. *J. Org. Chem.* **1965**, *30*, 1473.
- 6) Tucker, C.E.; Davidson, J.; Knochel, P. *J. Org. Chem.* **1992**, *57*, 3482.
- 7) Burgess, K.; Van der Donk, W.A.; Westcott, S.A.; Marder, T.B.; Baker, R.T.; Calabrese, J.C. *J. Am. Chem. Soc.* **1992**, *114*, 9350.
- 8) Yamamoto, Y.; Fujikawa, R.; Umemoto, T.; Miyaura, N. *Tetrahedron*, **2004**, 10695.
- 9) Ho, T.,I.; Chang, C.M.; Wang, S.R.; Cheng, C.P. *J. Chem. Soc. Dalton Trans.* **1988**, 123.
- 10) Isaacs, N. *Physical Organic Chemistry*, Longman Group, London, **1998**. Chapter 4, pages 163-164.
- 11) Black, A.; Brown, J.M.; Pichon, C. *Chem. Commun.* **2005**, 5284.
- 12) a) Fristrup, P.; Le Quement, S.; Tanner, D.; Norrby, P.-O. *Organo. Met.* **2004**, *23*, 6160. b) Yamataka, H.; Nagareda, K.; Takai, Y.; Sawda, M.; Hanafusa, T. *J. Org. Chem.* **1988**, *53*, 3877.
- 13) Mannig, D.; Noth, H. *J. Chem. Soc. Dalton. Trans.* **1985**, 1689.
- 14) Unpublished work from our labs

- 15) Another potential difference between the two labeling strategies involves isotope effects, both primary and secondary, that might result in underestimation of the extent of β -hydride elimination.
- 16) Brown, J.M.; Lloyd-Jones, G.C. *J. Am. Chem. Soc.* **1994**, *116*, 866.
- 17) Roberts, C.F.; Hartley, R.C. *J. Org. Chem.* **2004**, *69*, 6145.
- 18) Bordwell, F.G.; Drucker, G.E.; Andersen, N.H.; Denniston, A.D. *J. Am. Chem. Soc.* **1986**, *108*, 7310.
- 19) Note that at the time of preparing this manuscript D₂O can be purchased from Aldrich at a cost of less than \$1 per gram.
- 20) a) Nishide, K.; Yokota, K.; Nakamura, D.; Sumiya, T.; Node, M. *Tetrahedron Lett.* **1993**, *34*, 3425. b) Liu, J.; Wong, C.-H. *Tetrahedron Lett.* **2002**, *43*, 4037.
- 21) Chavan, S.; Soni, P.; Kale, R.; Pasupathy, K. *Synth. Commun.* **2003**, *33*, 879.
- 22) Yamataka, H.; Nagareda, K.; Ando, K.; Hanafusa, T. *J. Org. Chem.* **1992**, *57*, 2865.
- 23) Note this cost refers to the catalogue price at the time of manuscript preparation and from Sigma-Aldrich.
- 24) Okuma, K.; Sakai, O.; Shioji, K. *Bull. Chem. Soc. Jpn.* **2003**, *76*, 1675.
- 25) Lando, V.R.; Monteiro, A.L. *Org. Lett.* **2003**, *5*, 2891.
- 26) Note this cost refers to the catalogue price at the time of manuscript preparation and from Sigma-Aldrich.
- 27) Evans, D.A.; Fu, G.C.; Anderson, B.A. *J. Am. Chem. Soc.* **1992**, *114*, 6679.
- 28) A ²H-NMR spectrum of the crude reaction mixture was also obtained and revealed peaks corresponding to only deuterated styrene and phenethanol products.
- 29) The potential exists for the olefin to undergo decomplexation containing the protium label and subsequently undergo either hydroboration or even deuterioboration. It might be envisioned that this occurrence will complicate analysis of the labeling experiment. However, owing to the five-fold excess of olefin employed in the reaction and the overall low levels of free olefin generated upon decomplexation, it is felt these considerations pose no significant concern.
- 30) Marlier, J.F. *Acc. Chem. Res.* **2001**, *34*, 283.

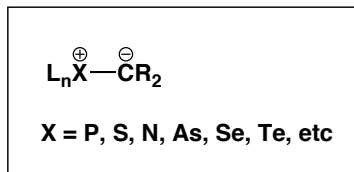
- 31) Gajewski, J.J.; Wojciech, B.; Harris, N.J.; Olson, L.P.; Gajewski, J.P. *J. Am. Chem. Soc.* **1999**, *121*, 326.
- 32) Yamataka, H.; Sasaki, D.; Kuwatani, Y.; Mishima, M.; Tsuno, Y. *J. Am. Chem. Soc.* **1997**, *119*, 9975.
- 33) Singleton, D.A.; Merrigan, S.R.; Liu, J.; Houk, K.N. *J. Am. Chem. Soc.* **1997**, *119*, 3385.
- 34) For representative examples see: a) Singleton, D.A.; Wang, Z. *J. Am. Chem. Soc.* **2005**, *127*, 6679. b) Meyer, M.P.; Delmonte, A.J.; Singleton, D.A. *J. Am. Chem. Soc.* **1999**, *121*, 10865. c) Merrigan, S.R.; Singleton, D.A. *Org. Lett.* **1999**, *1*, 327. d) Singleton, D.A.; Szymanski, M.J. *J. Am. Chem. Soc.* **1999**, *121*, 9455.
- 35) Singleton, D. A.; Thomas, A. A. *J. Am. Chem. Soc.* **1995**, *117*, 9357.
- 36) Melander, L.; Saunders, W.H. *Reaction Rates of Isotopic Molecules*, Wiley-Interscience Publication, New York, **1980**. Chapter 4, pages 95-102.
- 37) Crude reactions were checked by ¹H-NMR prior to isolation in order to determine percent conversion.
- 38) The use of CD₃CN also helped to break up aggregates that were identified from the apparent doubling of certain peaks in the spectrum when the NMR analysis was run in CDCl₃ as solvent. These presumably arose from π-stacking interactions in the highly concentrated NMR tube.
- 39) The SNR in the current study was determined to be greater than 500:1 in all cases.
- 40) Accurate temperature control during the acquisition is important to prevent shifting of peaks. Successive spectra obtained at ambient temperature displayed peak shifts of up to 0.5 ppm presumably arising from temperature changes in the building during the overnight acquisitions.
- 41) This result might be interpreted as consistent with the involvement of a p-benzyl interaction during the course of the reaction. However owing to the small size of the isotope effects, the associated errors with their determination, as well as, the inherent difficulty of interpreting carbon isotope effects without the aid of high level DFT calculations, an interpretation such as this is beyond our abilities to make at this time. For a discussion on the topic of p-benzyl interactions and the use of isotope effects to identify them see: Vo, L.K.; Singleton, D.A. *Org. Lett.* **2004**, *6*, 2469.
- 42) Rego, R.; Adriaensens, P.J.; Carleer, R.A.; Gelan, J.M. *Polymer* **2004**, *45*, 33.
- 43) Keeler, J. *Understanding NMR Spectroscopy*, Wiley, London, **2005**.

- 44) Isotope effects determined by this method were calculated to be as large as 1.25 and significantly larger than the theoretical maximum of 1.05.¹⁰
- 45) Gable, K.P.; Zhuravlev, F.A. *J. Am. Chem. Soc.* **2002**, *124*, 3970.
- 46) a) Schrock, R.R.; Osborn, J.A. *J. Am. Chem. Soc.* **1971**, *93*, 3089. b) Osborn, J.A.; Wilkinson, G. *Inorg. Synth.* **1967**, *10*, 67. c) Herde, J.L.; Lambert, J.C.; Senoff, C.V. *Inorg. Synth.* **1974**, *15*, 18.
- 47) Singh, R.P.; Twamley, B.; Fabry-Asztalos, L.; Matteson, D.S.; Schreeve, J.M. *J. Org. Chem.* **2000**, *65*, 8123.
- 48) a) Zhao, B.; Xiyang, L. *Org. Lett.* **2006**, *8*, 5987. b) Baumgartner, M.T.; Jimenez, L.B.; Pierini, A.B.; Rossi, R.A. *J. Chem. Soc. Perkin Trans. 2*, **2002**, 1092. c) Shao, P.; Gendron, R.L.; Berg, D.J.; Bushnell, G.W. *Organometallics* **2000**, *19*, 509. d) Balema, V.P.; Wiench, J.W.; Pruski, M.; Percharsky, V.K. *J. Am. Chem. Soc.* **2002**, *124*, 6244.
- 49) Melander, L.; Saunders, W.H. *Reaction Rates of Isotopic Molecules*, Wiley-Interscience Publication, New York, **1980**.

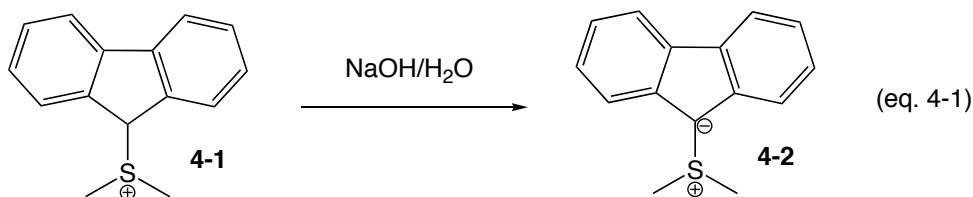
Chapter 4: Introduction to Sulfur Ylide Epoxidations

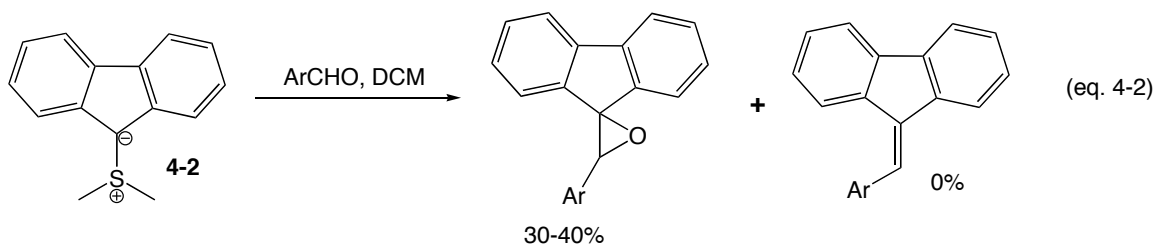
4.1: General Introduction

Ylides are a special class of zwitterionic compounds, which contain both a heteroatom bearing a formal positive charge and an anion at adjacent sites in the molecule, see inset. The most commonly used ylides in synthesis are the phosphorous derivatives of the Wittig olefination.¹ However numerous applications employing sulfur ylides have also been reported ranging from dearomatizations² and ring expansions³ to homologations of boranes⁴. The synthetic prowess of sulfur-based ylides nonetheless resides in their ability to convert the carbonyl functional group into that of an epoxide.⁵ Ylides of other heteroatoms have also been developed into synthetically useful procedures albeit to a lesser extent.^{5b}



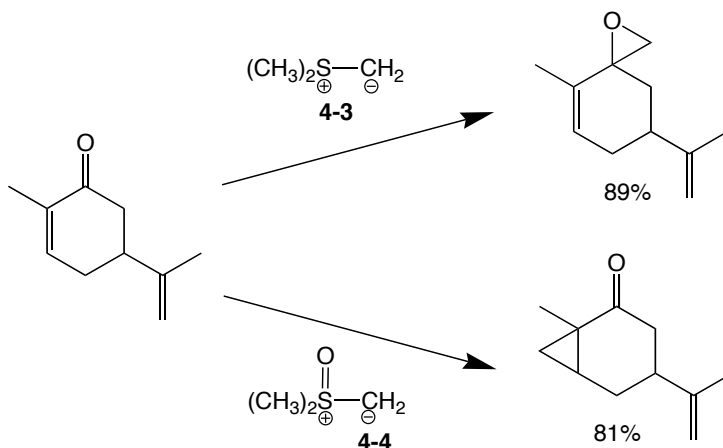
The first report of an isolable sulfur ylide came from Ingold in which **4-2** was precipitated following treatment of **4-1** with NaOH in water, equation 4-1.⁶ In a subsequent study by Johnson, **4-2** was reacted with arylcarbonyls in a failed attempt to affect Wittig olefinations with ylides derived from heteroatoms other than phosphorous, equation 4-2.⁷ To the surprise of the researchers, epoxides not alkenes were obtained as the major products of the reaction.





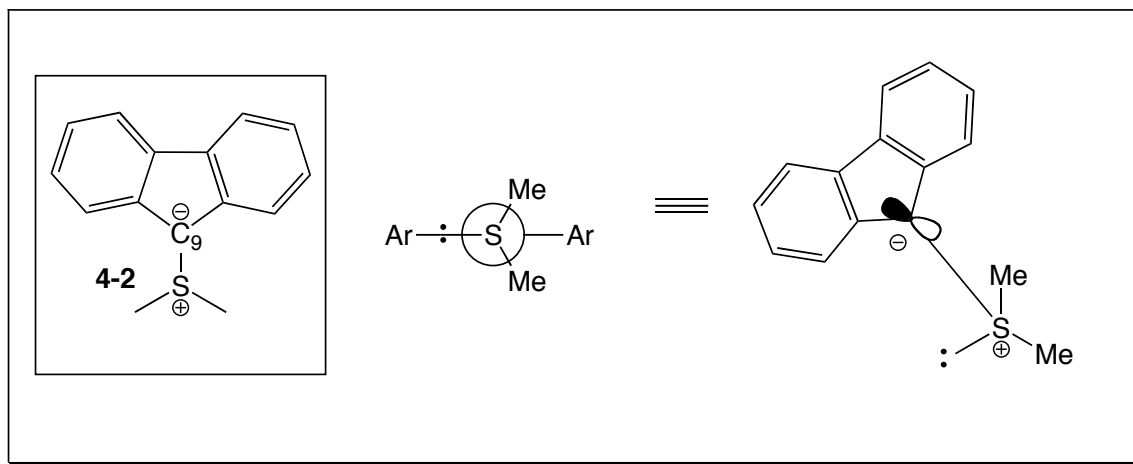
The work of Johnson was shortly thereafter overshadowed by Corey's disclosure of the use of trimethylsulfonium iodide **4-3** and trimethylsulfoxonium iodide **4-4** in the epoxidation of a wide variety of ketones and aldehydes in high yield.⁸ Highly valued, especially at the time, was that the chemoselectivity of these two reagents was of a complimentary nature. The dimethylsulfonium methylene of **4-3** underwent preferential 1,2-addition to carvone resulting in overall methylene transfer and epoxidation, Scheme 4-1. The softer nucleophile obtained from **4-4** led to cyclopropanation of carvone, presumably from a Micheal addition into the enone system. Furthermore, 4-tert-butyl-cyclohexanone undergoes preferential axial attack by **4-3** while reaction of **4-4** is observed to proceed via an equatorial attack of the nucleophile.

Scheme 4-1: Reactions of Carvone with Sulfur Ylides



Following the successful isolation of **4-2**, Ingold reported the first physical data on this new class of ylide.⁶ It was characterized as a semi-stable solid with mp = 120-122 °C. Its IR spectrum was nearly identical to other fluorenylides, however its dipole moment was significantly lower at 6.2 D. Structural characteristics in solution were determined much later in an NMR study of **4-2** by Aggarwal.⁹ It was determined that at low temperature (-83 °C), the methyl carbons but not the aromatic carbons displayed equivalency in both the ¹H- and the ¹³C-NMR spectra. These results are most consistent with fixed rotation about the C9-S bond of **4-2** as in the conformer shown in Figure 4-1. From these studies it was deduced that the carbon of the ylide was indeed sp² hybridized while sulfur retains sp³ hybridization. Furthermore the lone pairs on sulfur and carbon lie perpendicular to one another at a 90° degree angle. The ΔG[‡] to C-S bond rotation was found to be 42 KJ/mol from variable temperature NMR.

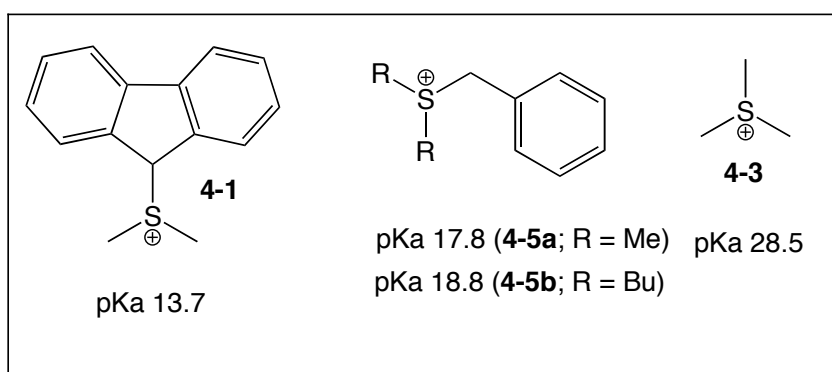
Figure 4-1: Structure of Fluorenylide **4-2**



4.2: Generation of Sulfur Ylides

Among the available methods for sulfur ylide generation, the simplest procedure is certainly the treatment of sulfonium salts with base. Generally a metal alkoxide is used, however, there are reports citing the use of strong alkylolithiums⁷ and NaH¹⁰ or alternatively weaker bases such as P(MeNCH₂CH₂CH₂)₃N¹¹ and DBU¹². The pK_a's of several sulfonium salts have been reported. These species are generally 2-3 pK_a units more acidic than the corresponding phosphonium salts both of which are significantly more acidic than ammonium salts. The pK_as of several common sulfonium salts are listed in Chart 1, the reported values for **4-5a** and **4-5b**¹³ are in DMSO while those of **4-1**¹⁴ and **4-3**¹⁵ are in water. In addition to thermodynamic acidities, the second order rate constants for proton abstraction have been determined for both **4-1**¹⁴ and **4-3**¹⁵. The second order rate constants for loss of a proton in **4-3** is reported to be $7.5 \times 10^{-4} \text{ M}^{-1}\text{sec}^{-1}$ while that of **4-1** is found to be several orders of magnitude larger at $5.9 \times 10^4 \text{ M}^{-1}\text{sec}^{-1}$.

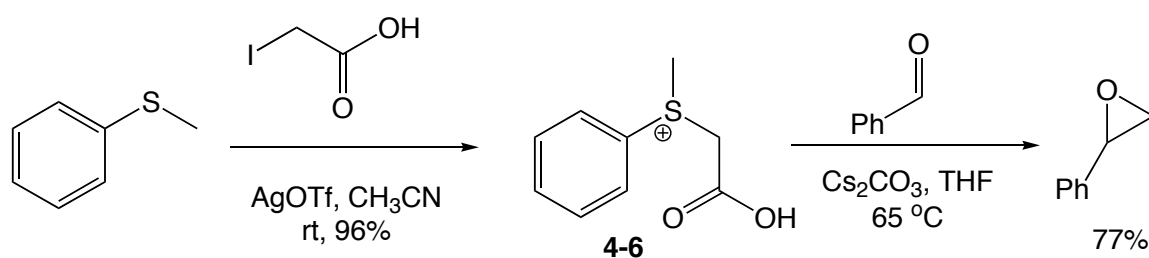
Chart 4-1: Acidities of Various Sulfonium Salts



Another strategy amenable to generation of sulfur ylides is the betaine decarboxylation strategy of Forbes, Scheme 4-2.¹⁶ Carboxymethylsulfonium betaine **4-6**

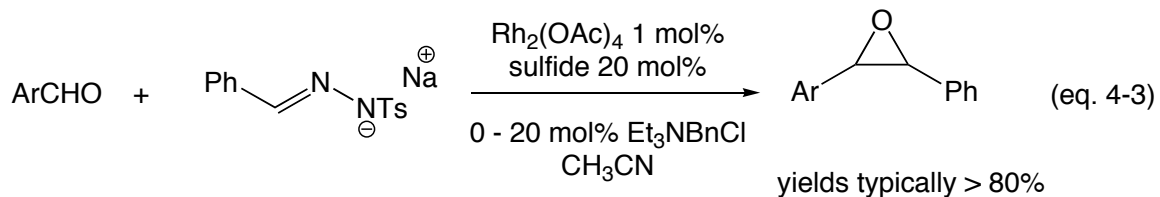
is prepared in one step from thioanisole and iodoacetic acid in a 96% yield. Heating of **4-6** in a THF solution containing Cs₂CO₃ leads to decarboxylation and generation of the sulfur ylide. This species generated in-situ can then undergo electrophilic trapping in the presence of arylaldehydes. Reaction efficiency is highly dependent on effective trapping of the ylide by a reactive aldehyde prior to decomposition at elevated temperatures. Accordingly, lower levels of conversion are obtained for electron rich aldehydes. The half-life for decarboxylation of **4-6** was determined to be 13.3 minutes.

Scheme 4-2: Forbes Decarboxylation Strategy

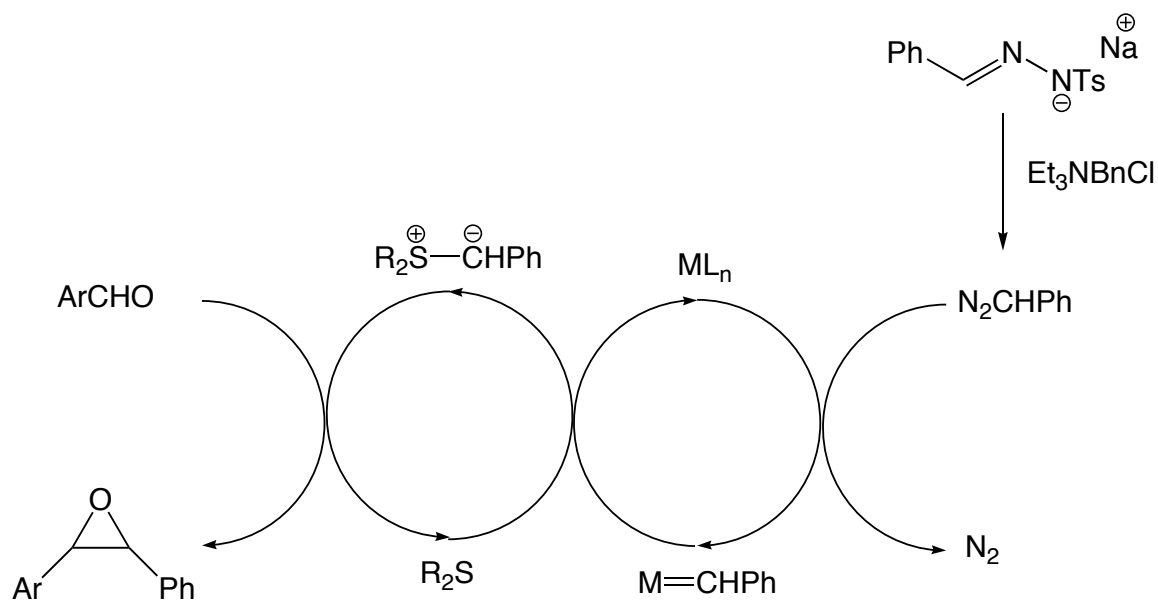


Another method of generating sulfur ylides is from the reaction of diazo compounds with Cu(acac)₂ in the presence of a sulfide.¹⁷ The advantage of this methodology is that no base is required. However, it does necessitate the use and handling of toxic and potentially explosive diazo compounds. Furthermore the diazo reagent needs to be added slowly over the course of the reaction to prevent formation of stilbene by-products resulting from dimerization of the resulting metal carbene. Aggarwal has reported a significantly improved method for generating the diazo compounds in-situ from their N-tosyl-hydrazone salts, Scheme 4-3.¹⁸ Generating these species in-situ ensures their low concentration over the course of the reaction and greatly reduces side reactions. The optimized conditions are shown in equation 4-3, where it is

seen that $\text{Rh}_2(\text{OAc})_4$ has replaced the earlier copper catalyst. It is also found that a quaternary ammonium salt is required as a phase transfer catalyst. Aryl substituted N-tosylhydrazones containing both electron rich and poor substituents are all amenable to the new methodology.



Scheme 4-3: Sulfur Ylides from N-Tosylhydrazone Salts

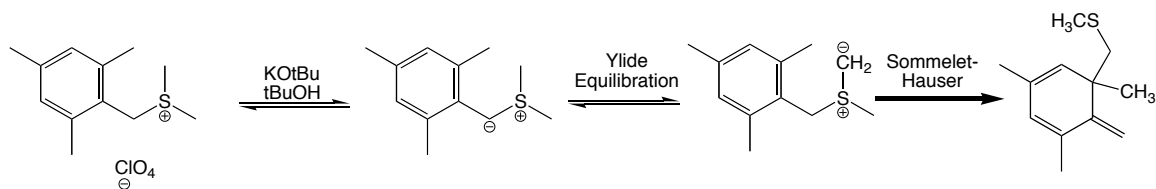


4.3: Sulfonium Salt and Ylide Decomposition

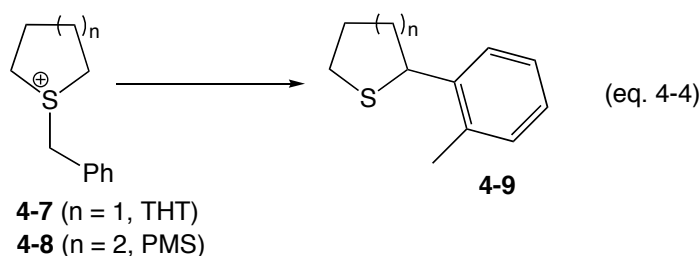
Sulfonium salts and their corresponding ylides both undergo decomposition by various means. The hydrolysis of benzylmethylphenylsulfonium tosylate with 0.1 M NaOH has been studied.¹⁹ Displacement of sulfur occurs almost exclusively at the benzyl carbon liberating thioanisole. The second order rate constant for the process is reported to be $2.2 \times 10^{-3} \text{ M}^{-1}\text{sec}^{-1}$. It was further shown that sulfonium halides undergo decomposition under neutral conditions in a second-order process consisting of displacement of the corresponding dialkylsulfide by the nucleophilic counter anion.²⁰ Furthermore, considering the relatively good leaving group ability of dialkylsulfides, it is not surprising to find that sulfonium salts possessing *beta*-hydrogen atoms may also undergo elimination.²¹

Degradation of sulfonium salts can largely be avoided if ylide generation is carried in the absence of base. Nonetheless, there still remains the potential for sulfur ylides themselves to undergo decomposition. Their primary means of decomposing is via an intramolecular reaction known as a Sommelet-Hauser rearrangement.^{2,22} Formally a 2,3- σ -sigmatropic rearrangement, it possesses sufficient driving force that dearomatizations have been reported, see Scheme 4-4.²³ The Sommelet-Hauser rearrangement has been adapted in some instances into a useful procedure for the synthesis of quaternary carbons. However, in terms of sulfur ylide epoxidations, it is in the least an unwanted side reaction that lowers reaction efficiency and at worst responsible for the destruction of precious chiral sulfides negating substoichiometric protocols.

Scheme 4-4: Sommelet-Hauser Rearrangement



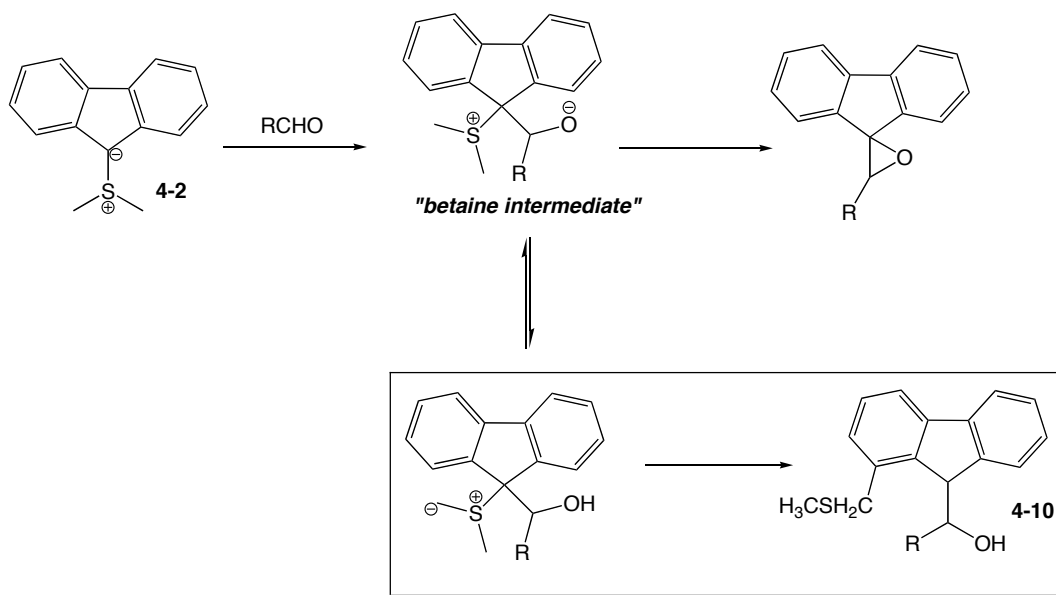
In order to limit the decomposition of sulfur ylides through Sommelet-Hauser rearrangements, one strategy that has been employed is to render the ylide equilibration of Scheme 4-4 less favorable. For example, epoxidations of ketones and other substrates possessing low reactivity with tetrahydrothiophene (THT) derivative **4-7** were seen to produce significant quantities of **4-9**, equation 4-4.¹⁸ This by-product presumably arises from a Sommelet-Hauser rearrangement. Carrying the reaction out with PMS derivative **4-8**, which positions the sulfur atom within a six membered ring leads to increased reaction efficiency with ketone substrates (yields 15 – 69%). The success of this strategy is rationalized based on a report by Fava²⁴ stating that the rate of proton abstraction in 6 membered rings was an order of magnitude lower than for the corresponding 5 membered rings.



4.4: Reaction Mechanism

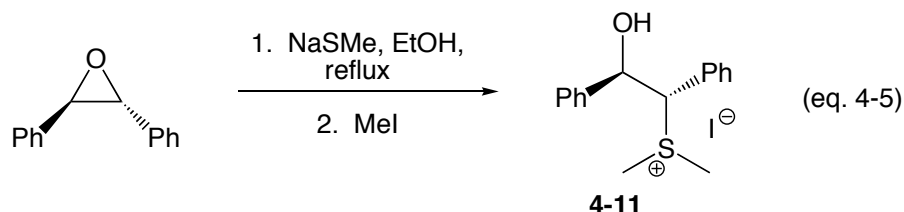
The first mechanistic proposal for sulfur ylide epoxidations appeared in the seminal report by Johnson.⁷ Two key findings needed to be accounted for, firstly the increased reactivity of electron deficient arylaldehydes over more electron rich substrates and secondly the production of an alcohol by-product **4-10**. The mechanism was proposed to proceed via a betaine intermediate in part owing to currently held theories on Wittig olefinations, Scheme 4-5. Incidentally, it would appear that alcohol **4-10** is produced via a Sommelet-Hauser rearrangement.

Scheme 4-5: Initial Mechanistic Proposal of Johnson



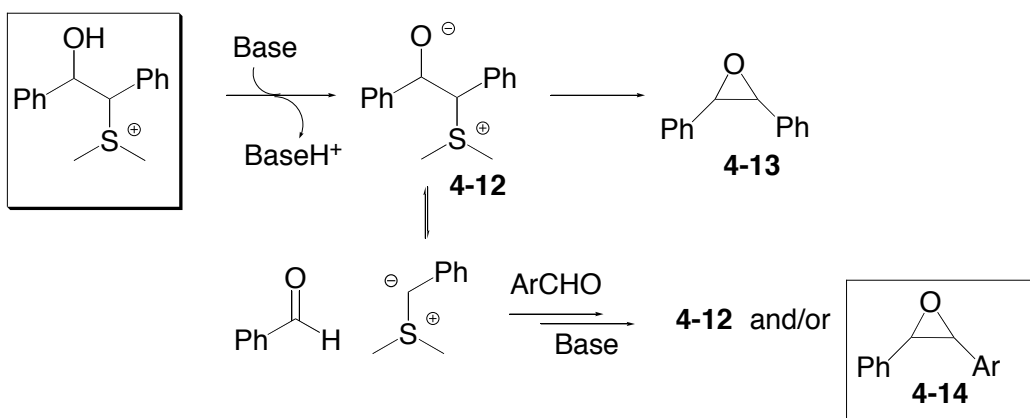
The proposal of Johnson has largely withstood the test of time and subsequent studies geared towards the epoxidation mechanism have largely focused on a better understanding the individual steps of ylide addition and betaine collapse. The single most pervasive tool employed to better elucidate these reaction features has been the use of cross-over experiments.²⁵ Species of type **4-11**, *alpha*-hydroxy-sulfonium salts, can be

viewed as betaine precursors. These species are readily available starting from the corresponding epoxides using the Aggarwal procedure, equation 4-5.^{25c} *trans*-Stilbene oxide is first treated with an excess of sodium thiomethoxide in ethanol. The ring-opened product is then methylated in the presence of methyl iodide.

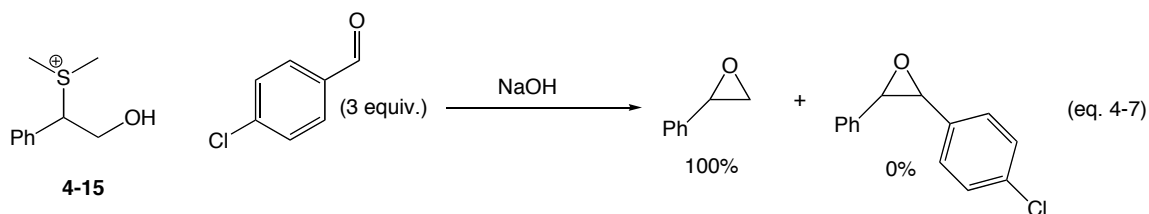
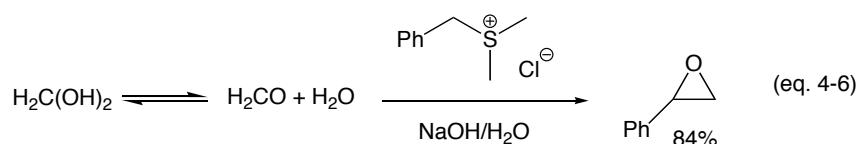


In a typical cross-over experiment, an *alpha*-hydroxy sulfonium salt is treated with base to generate a betaine **4-12**, Scheme 4-6. If this reaction is performed in the presence of a second aldehyde **ArCHO**, the collapse or reversion of betaine **4-12** can be explored. The reaction is biased by using an aldehyde that has significantly greater reactivity than benzaldehyde, such as *p*-nitrobenzaldehyde as the trapping agent. Accordingly, the observation of unsymmetrical arylepoxides such as **4-14** in the experiment is interpreted in terms of a reversible addition in the typical epoxidation reaction.

Scheme 4-6: The Cross-Over Experiment

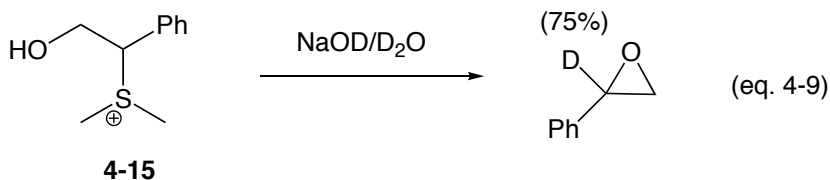
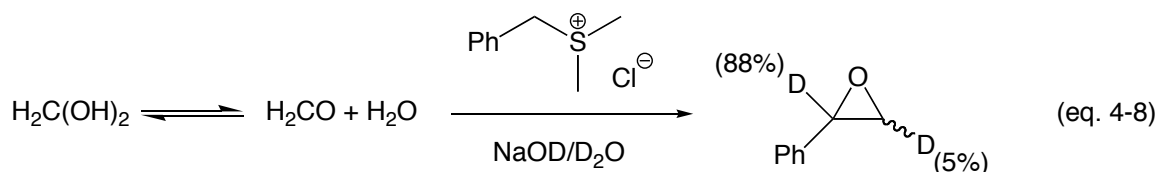


Hatch carried out a series of cross-over experiments in a study of sulfur ylide epoxidations in water.^{25e} The general reaction producing styrene oxide from formaldehyde is shown in equation 4-6. Hatch treated the *alpha*-hydroxy-sulfonium chloride **4-15** under the usual reaction conditions in the presence of a three-fold excess of the more reactive *para*-chlorobenzaldehyde. Cross-over products were not observed and accordingly it was proposed that addition of ylide to aldehyde was irreversible and therefore rate determining, equation 4-7.



To further confirm the rate determining nature of the addition step, an elegant competition experiment was devised. First the betaine precursor **4-15** was treated with aqueous sodium hydroxide and the reaction quenched at 2 minutes. The yield of styrene oxide in the reaction was determined to be 97%. Treating formaldehyde with benzyldimethylsulfonium chloride under similar conditions and once again quenching the reaction at 2 minutes led to less than 1% yield of styrene oxide. It was thus concluded that the betaine collapses to epoxide at a rate approximately 100 times faster than that of the reaction between formaldehyde and benzyldimethylsulfonium chloride.

Conducting the epoxidation reaction of equation 4-6 with NaOD/D₂O led to incorporation of deuterium label into both the *alpha* and *beta* positions of styrene oxide, equation 4-8. A standard interpretation of this result is that ylide generation from deprotonation of benzyldimethylsulfonium chloride is a reversible process. This was not a surprising result considering ylide addition to formaldehyde was thought to be rate determining from the competition experiments. Interestingly, treating *alpha*-hydroxysulfonium salt **4-15** to the labeling experiment also led to significant levels of deuterium incorporation into the benzylic position, equation 4-9.



The work of Hatch conducted in the late sixties demonstrates the utility of cross-over experiments particularly when employed in conjunction with competition experiments and labeling strategies. Unfortunately, Hatch failed to distinguish between reaction proceeding through formaldehyde and paraformaldehyde. This point is made clear upon comparing label incorporation into the *beta*-position of styrene oxide in the labeling experiments. *alpha*-Hydroxysulfonium salt **4-15** undergoes undetectable levels of label incorporation at the *beta* position in contrast to the results depicted in equation 4-8 for the typical epoxidation reaction between ylide and formaldehyde. This fact has led

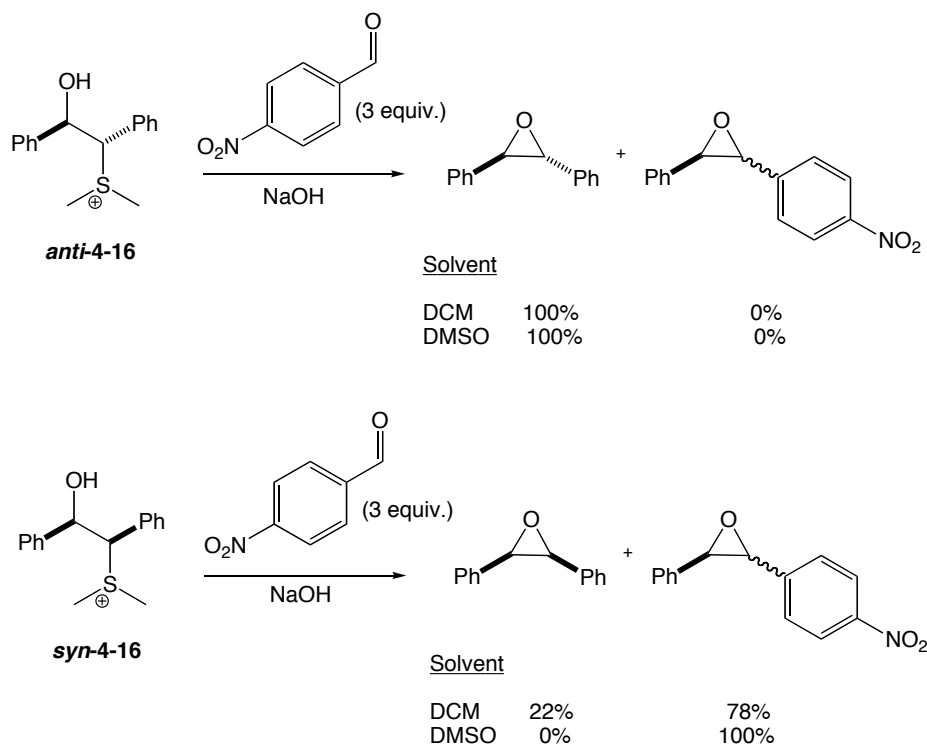
to criticism^{25c} of Hatch's results and potentially renders them completely invalid. The outcome is highly unfortunate although certainly not without cause. Owing to the perceived elegance of Hatch's methodology and its ability to enlighten various aspects of the reaction sequence, the method has been adapted to a more clearly defined system and these results will be fully disclosed in a later chapter.

Following an almost thirty year hiatus in the study of this reaction by cross-over experiments, a comprehensive study was disclosed by Aggarwal.^{25c} Five separate *alpha*-hydroxysulfonium salts were subjected to cross-over experiments. These experiments were conducted in both DMSO and dichloromethane in order to access the effect of solvent polarity on the reaction. In addition, the reactivity of *syn*- and *anti-alpha*-hydroxysulfonium salts was compared so as to probe isomeric pathways to epoxide formation. Subjecting *anti-4-16* to NaOH in the presence of *para*-nitrobenzaldehyde as trapping agent led to quantitative conversion to *trans*-stilbene oxide, Scheme 4-7. The complete absence of cross-over products in both DCM and DMSO indicates that formation of the *anti*-betaine is irreversible.

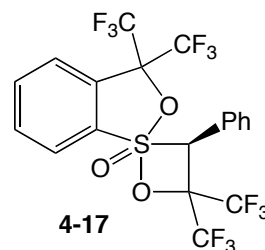
Treating *syn-4-16* to the cross over experiment led to the product distribution shown in Scheme 4-7. Significant amounts of cross-over products were obtained in both DCM and DMSO. It would thus appear that formation of *syn-4-16* is reversible in the typical epoxidation reaction between ylide and benzaldehyde. These results led Aggarwal to conclude that the high *trans*-selectivity obtained in the Corey-Chaykovsky epoxidation results from a combination of irreversible addition to produce *anti-4-16* and reversible formation of *syn-4-16* followed by slow collapse to *cis*-epoxide. Consistent with this statement is the finding that factors which increase the reversibility of *syn-4-16*

formation in cross-over experiments, such as the use of polar solvents, also tend to lead to increased levels of *trans*-epoxide selectivity in the typical reaction.

Scheme 4-7: Cross-Over Experiments in DMSO and DCM



Evidence for the role of betaines as intermediates in sulfur ylide epoxidations is first and foremost obtained from the observation that *alpha*-hydroxysulfonium salts produce epoxide products upon treatment with base.²⁵ Their role is further substantiated by theoretical calculations.²⁶ Nonetheless, an oxathietane **4-17** has been proposed by Okazaki as another possible intermediate in the reaction.²⁷ The proposal followed the observation that **4-17** underwent epoxide formation upon heating. However it should be noted that oxathietane **4-17** is a chemically distinct species from any intermediate that might reasonably be expected from the reaction of sulfur ylides with carbonyl compounds. It contains both an alkoxy and an oxo ligand not present in

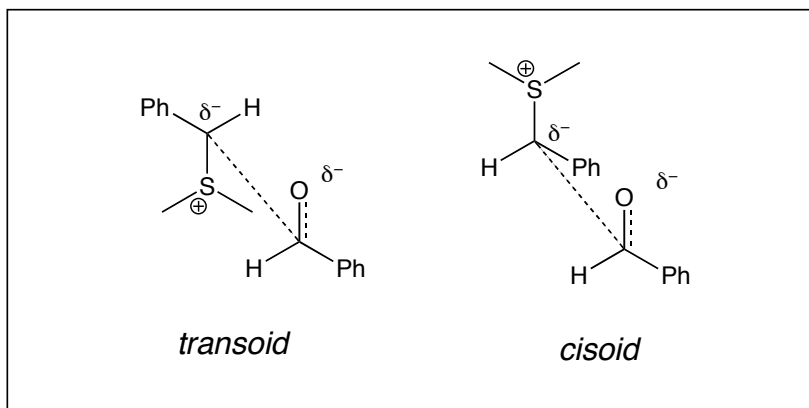


the typically proposed betaine intermediates. It is therefore not surprising that the proposal of oxathietanes as intermediates in the Corey-Chaykovsky epoxidation reaction does not feature prominently in the literature. It suffices to say that the debate concerning betaine intermediates in the Wittig olefination is not currently a topic of discussion concerning sulfur ylide epoxidations.²⁸

The epoxidation reaction has been subjected to DFT calculations and potential energy surfaces have been constructed for both a model system consisting of $\text{Me}_2\text{SCH}_2^-/\text{CH}_2\text{O}$ and the more synthetically relevant $\text{Me}_2\text{SCH}^-/\text{Ph}/\text{PhCHO}$ system.²⁶ In the latter system, the key features are that both the *syn*- and the *anti*-betaines are predicted to lie lower in energy than the free ylide and benzaldehyde starting materials. Addition of ylide to benzaldehyde is predicted to be rate determining for *anti*-betaine production. This is consistent with the findings of cross over experiments which indicated an irreversible formation of *anti*-betaine. The addition step is calculated to proceed with a relatively small activation energy of 4.5 kcal/mol.

The most striking feature of the report, however, is that both reaction manifolds are predicted to proceed via a cisoid or quasi 2 + 2 addition of the ylide to benzaldehyde. The respective *transoid* and *cisoid* transition state geometries are shown in Figure 4-2. This would initially seem counterintuitive owing to the obvious steric interactions between eclipsing substituents on both the ylide and aldehyde partners. However, it is predicted that an electrostatic interaction between the developing negative charge on oxygen and positive charge on sulfur more than compensates for any increased steric interactions incurred in the cisoid addition geometry.

Figure 4-2: *Cisoid* and *Transoid* Addition Geometries



Rotation about the newly formed carbon-carbon bond is considered to be hindered by the presence of the O-S electrostatic interaction. So much so that rotation of this bond to align the oxyanion antiperiplanar to the sulfonium leaving group is predicted to be rate determining for the *cis*-epoxide producing pathway. An E_a of 8.1 kcal/mol has been calculated for this process. It would therefore appear that the reversible nature of *syn*-betaine **4-16** formation, as revealed by cross over experiments, is a result not of slow ring closure to produce *cis*-stilbene oxide but rather a result of hindered bond rotation to properly align the oxyanion and sulfonium leaving groups for ring closure.

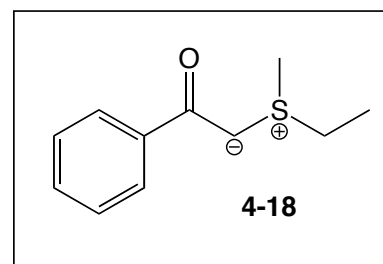
4.5: Forays into Asymmetry

The use of chiral epoxides in synthesis is widespread in part owing to the various stereospecific transformations that these functionalities may undergo. Chiral enantioenriched epoxides may be obtained in two steps from a carbonyl functional group by regioselective Wittig-type olefination followed by stereoselective epoxidation using, for example, Shi's dioxirane catalysts.²⁹ It was realized early on that if the one-step

Corey-Chaykovsky epoxidations could be rendered highly enantioselective then this would represent a significant improvement over the typical two-step procedure. In order for this strategy to be successful, a number of requirements need be satisfied. Sulfonium salts and their corresponding ylides need to be prepared in enantioenriched form and loss of optical purity must be slow relative to reaction with carbonyls. Furthermore an efficient transfer of chirality needs to be affected from the chiral sulfur ylide to the activated complex for betaine formation.

Sulfonium salts and their corresponding ylides are tetrahedral at sulfur and a number of optically active species have been prepared.^{5b} Sulfonium salts can racemize via typical pyramidal inversion or alternatively via

solvolysis and other means.³⁰ The enthalpic barrier for inversion appears to be rather high at 25-29 kcal for sulfonium salts and generally elevated

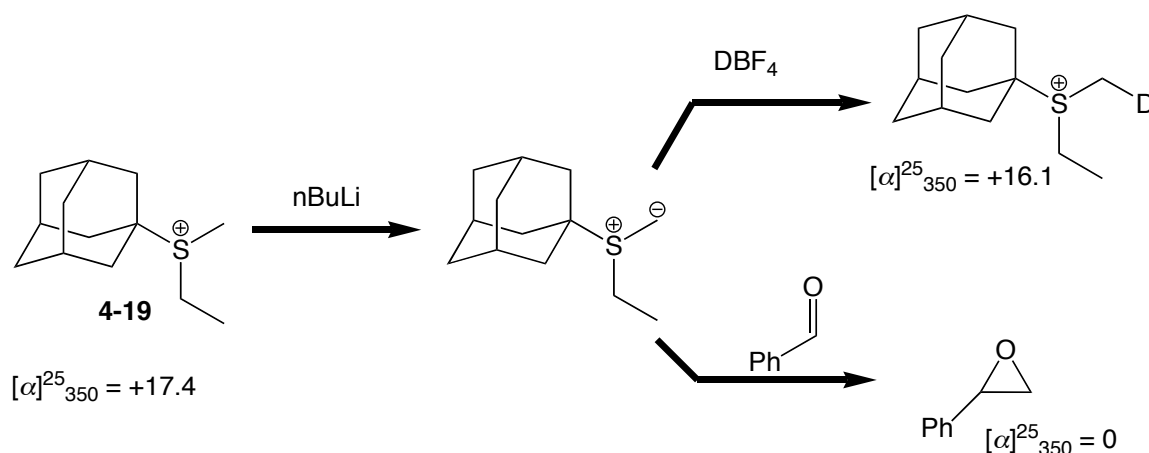


temperatures are required for racemization.³¹ Positioning the sulfur atom within a ring system and making the sp^2 transition state geometry more difficult to attain can be envisioned to further disfavor pyramidal inversion. In fact, it is telling that many successful chiral sulfur ylide catalysts do in fact position sulfur within a cyclic structure, although this may be seen so as to better differentiate the two lone pairs of sulfur as is discussed below. The sulfur ylide may also lose enantiopurity through pyramidal inversion, although once again this process is shown to proceed via a rather large enthalpic barrier. For example, the barrier to pyramidal inversion is reported to be 23.3 kcal for ylide **4-18**.³¹ In any event, these two processes involving loss of optical activity

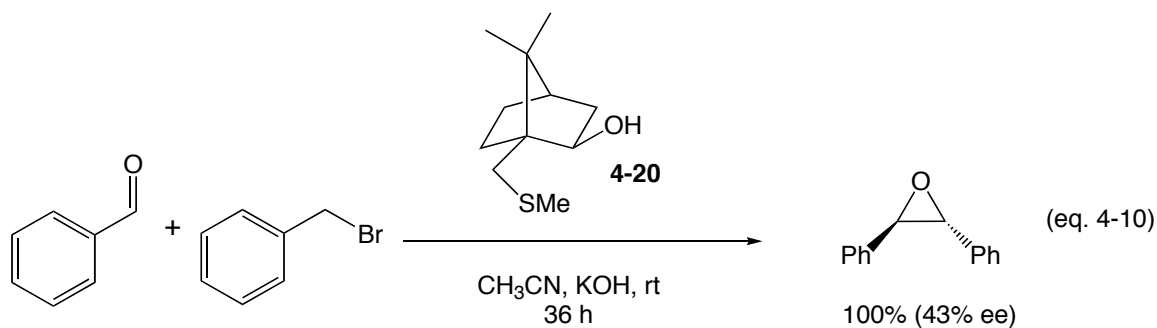
in the sulfonium salt and ylide appear to be relatively slow compared to the epoxidation reaction predicted to occur through an E_a of 4.5 kcal.

Trost has demonstrated that sulfonium salts and their corresponding ylides are indeed configurationally stable. Enantiomerically pure 1-adamantyethylmethylsulfonium salt **4-19** was treated with *n*-BuLi and the reaction was subsequently quenched with deuteriofluoroborate, Scheme 4-8.³² It was determined that deuterated-**4-19** had a near identical optical rotation, $[\alpha]_{350}^{25} = +16.1$, as the starting material, $[\alpha]_{350}^{25} = +17.4$. It was also determined that **4-19** had undergone almost exclusive deuteration at the methyl carbon. The first attempt at a stereoselective epoxidation with sulfur ylides was also described in the report. Quenching the ylide of **4-19** with benzaldehyde furnished styrene oxide in an unspecified yield but more importantly with the complete absence of optical activity. The lack of stereoselection in the transformation was likely a result of poor stereochemical communication between the methylene and benzaldehyde during betaine formation.

Scheme 4-8: Configurational Stability

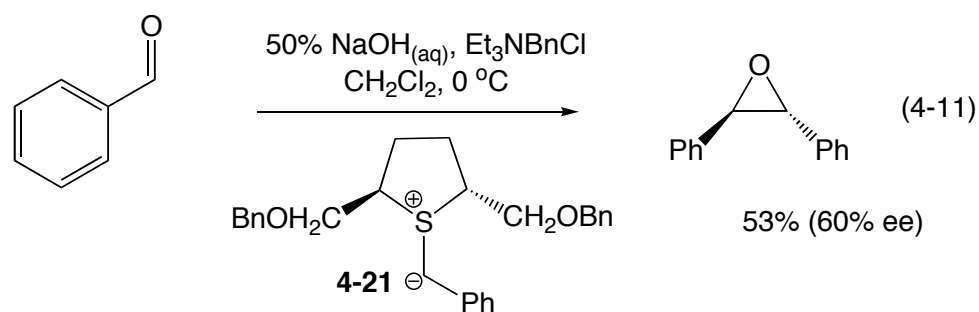


It was not until sixteen years later that Furukawa reported a successful attempt at an asymmetric sulfur ylide epoxidation.³³ Importantly, the disclosed procedure focused on benzylides, in which stereochemical communication between ylide and carbonyl has since been shown to be more efficient. Under Furukawa's conditions employing chiral sulfide **4-20**, *trans*-stilbene oxide was obtained in quantitative yield and with a reported 47% ee, equation 4-10. This report was of significant importance because it was the first asymmetric epoxidation reported for this system and because the sulfide was used in substoichiometric amounts. The sulfonium salt is generated in-situ from reaction of sulfide with benzyl bromide. Ylide generation was affected in the two-phase system with powdered KOH. This type of catalytic system, which employs substoichiometric amounts of sulfide in the presence of an alkylating agent, featured prominently until the Aggarwal protocol was disclosed.

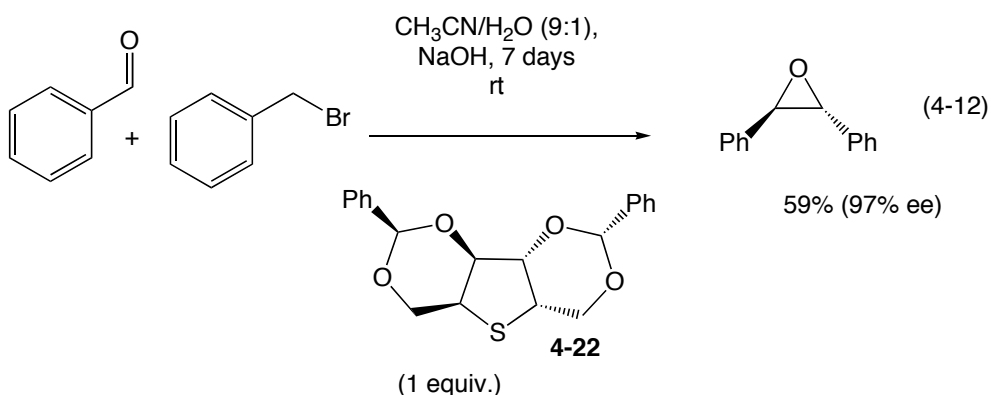


It was theorized that the moderately low levels of asymmetric induction obtained using Furukawa's sulfide **4-20** could be a result of poor selectivity obtained between the diastereotopic lone pairs on sulfur during the alkylation process. To overcome this issue, the next generation of chiral sulfides generally featured one of two strategies. The first strategy was to incorporate C_2 -symmetry into the sulfide to negate the issue of lone pair selectivity. Durst was the first to prepare a C_2 -symmetric sulfide **4-21** and test the theory, equation 4-11.³⁴ *trans*-Stilbene oxide was obtained in a 53% yield and with a modest ee

of 60%. Markedly better results were obtained for *p*-nitro-stilbene oxide for which an 83% ee was reported.

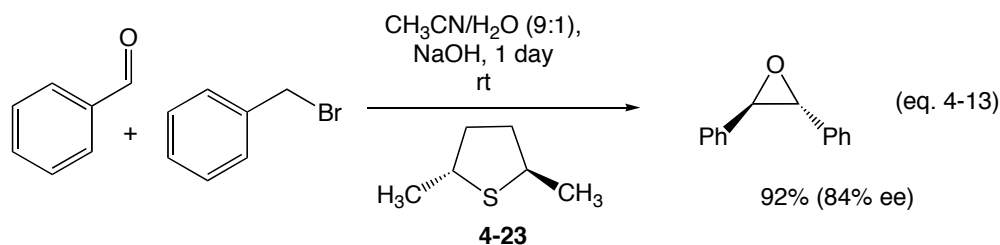


Higher levels of chiral induction were obtained for the C₂-symmetric sulfides **4-22**³⁵ and **4-23**³⁶ of Goodman and Metzner, equations 4-12 and 4-13. Goodman's sulfide **4-22** was converted to the active ylide in-situ employing a modified Furukawa procedure. *trans*-Stilbene oxide was obtained in a 59% yield and was contaminated by approximately 10% of the *cis*-isomer. An excellent 97% ee was achieved in the epoxidation, although the reaction was rather sluggish and required seven days to go to completion. It was also reported that the sulfide could be used in loadings as low as 10 mol% without adversely affecting the selectivity, however, the reaction was not surprisingly even slower.

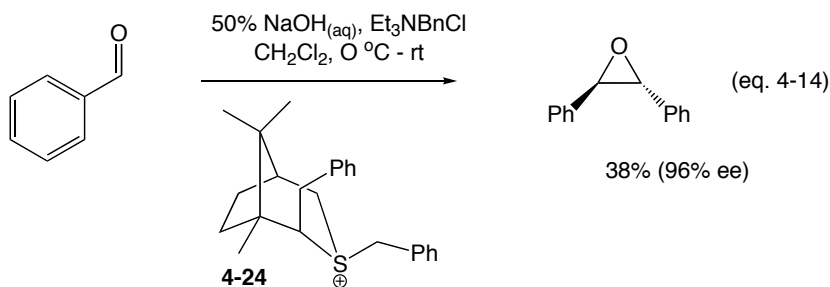


Metzner's thiophene derivative **4-23** is more reactive and only requires one-day to produce *trans*-stilbene oxide in a 92% yield, equation 4-13. The enantioselectivity

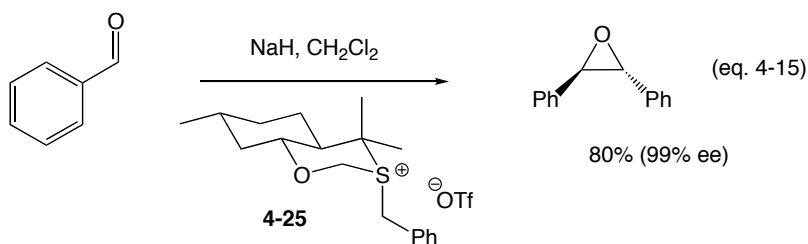
obtained with this sulfide is somewhat lower than Goodman's at 84% ee. It does however have the advantage that it can be easily prepared from (2*S*,5*S*)-hexanediol in two steps with an overall yield of 95%.



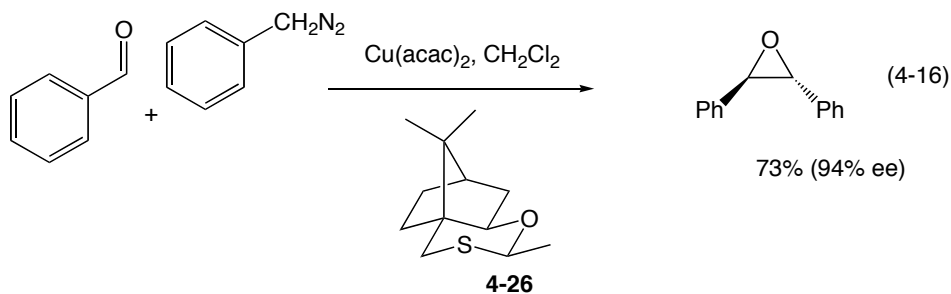
An alternative strategy to the use of C_2 -symmetric sulfides has been to incorporate the sulfur atom within a cyclic structure. This could conceivably render the diastereotopic lone pairs of sulfur sufficiently different in terms of reactivity that only one diastereomer of the sulfonium salt is produced. Durst reported on the use of (1*R*,3*S*)-(+)-camphoric acid derivative **4-24**.³⁷ The corresponding sulfide was shown to undergo alkylation to afford a single diastereomer of the sulfonium salt **4-24** thus validating the theory. Employing **4-24** in the epoxidation of benzaldehyde led to high levels of asymmetry, 96% ee, equation 4-14. However, a relatively low yield was obtained in the reaction possibly owing to degradation of the sulfonium salt **4-24** via *beta*-elimination.



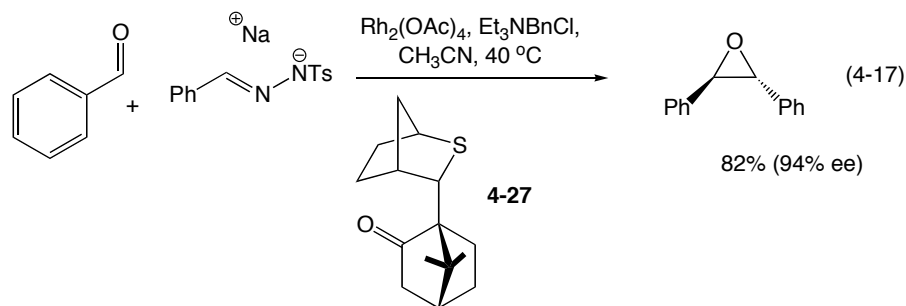
The *trans*-fused oxathiane system **4-25** of Solladie-Cavallo is an interesting example of serendipity.³⁸ Only one diastereomer of the sulfonium triflate is indeed produced upon alkylation of the sulfide. However, it is unexpectedly the axial lone pair on sulfur that is seen to react. This result was rationalized based on the 1,3-anomeric effect. It was proposed that the equatorial lone pair on sulfur was participating in $n_S-\sigma^*_{C-O}$ hyperconjugation. Employing **4-25** in the epoxidation of benzaldehyde resulted in *trans*-stilbene oxide production with a yield of 80% and with an excellent 99% ee, equation 4-15.



Sulfide **4-26** is readily available in two steps from camphorsulfonyl chloride and is a proficient catalyst for the epoxidation of a range of carbonyl substrates in good yields and generally high selectivities.³⁹ Employing sulfide **4-26** at loading of 20 mol% in Aggarwal's first generation catalytic procedure resulted in the production of *trans*-stilbene oxide in a yield of 73% and with an enantioselectivity of 94% ee, equation 4-16. The level of chiral induction for a broad range of substrates was generally high, featuring ee's > 90% with a few exceptions. However, attempts to apply sulfide **4-26** to Aggarwal's second-generation catalytic procedure with N-tosyl-hydrazones failed to produce epoxides in high yields.



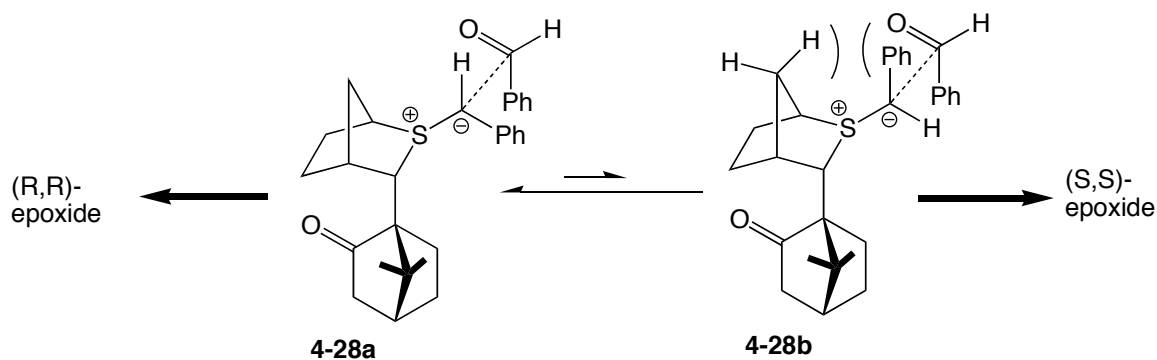
In order to achieve optimum reaction efficiency with Aggarwal's second-generation catalytic procedure, chiral sulfide **4-27** is employed.⁴⁰ Employing **4-27** in loadings as low as 5 mol%, epoxidations can be affected in high yields and enantioselectivities. For example, benzaldehyde undergoes reaction to afford *trans*-stilbene oxide in a yield of 82% and with an excellent enantioselectivity of 94% ee, equation 4-17. Furthermore the chiral sulfide can be re-isolated after reaction without loss of optical purity. The same reaction could be performed on a 50 mmol scale with just 0.5 mol% catalysts and the same excellent yields and enantioselectivities were obtained.



It has previously been determined by cross-over experiments that addition of a sulfur ylide to an arylaldehyde to produce the *anti*-betaine intermediate is an irreversible process.^{25c} It therefore follows that enantioselectivity in the reaction results from non-bonded interactions between the carbonyl and the chiral sulfur ylide in the transition state leading to betaine formation. Models to account for the high levels of selectivity have

been proposed, Scheme 4-9.⁵ Control of ylide facial selectivity hinges upon an inherent preference for an orthogonal orientation between the lone pair on sulfur and those of the carbanion. This leads to the prediction that conformers **4-28a** and **4-28b** are favored. Steric interactions between the phenyl substituent of the ylide and the one carbon bridge further differentiates between these species with the prediction that **4-28a** is the actual reactive conformer. It can be clearly seen that the camphor substituent would then block one face of the ylide and that the arylaldehyde would approach from the back face producing the (R,R)-epoxide isomer. While the correct stereoisomer is indeed predicted based on the model it should be stated that there is no clear indication that the reaction does in fact proceed through the more stable conformer of **4-28**.

Scheme 4-9: Stereochemical Model for Ylide Epoxidation



4.6: Conclusion

Reactions of sulfur ylides with carbonyl substrates have advanced significantly since the initial disclosure by Johnson that these species preferentially afford epoxides not olefins. There are currently several amenable means of generating the active sulfur ylide species either from sulfonium salts or alternatively directly from the sulfide. The

synthetic chemist seeking to affect epoxidations enantioselectively has a number of available options in terms of reagent choice and reaction conditions that should in most instances afford high levels of reaction efficiency and selectivity. The major drawback to the methodology is the near complete inability to procure epoxides containing a *cis*-geometry of substituents about the epoxide ring. Lastly, advances over the last decade have led to variants of this method in which high diastereo- and enantioselectivities are obtained for a broad range of products including cyclopropanes, aziridines, glycidic amides and acids.⁴¹

4.7: Research Objectives

The results of cross over experiments and DFT calculations have shed significant light on the reaction mechanism. It is now established that addition of dimethylsulfonium benzylide to benzaldehyde is rate determining. A theoretical potential energy surface has been constructed and from this the activation energy for the reaction calculated. Despite these advances in the understanding of reaction mechanism there are still a number of issues yet to be resolved.

The reaction between sulfur ylides and arylaldehydes involves a number of charge-separated species namely the zwitterionic ylide itself and also the betaine produced as an intermediate in the reaction. Considering the potential for highly polar solvent systems to stabilize the various intermediates and transition states in the reaction it is of interest to determine what effects incorporation of hydroxylic co-solvents in the reaction may have. In fact solely organic solvent systems were examined in both the

DFT calculations (CH_3CN) and cross over experiments (DMSO/DCM) reported by Aggarwal. However, a large number of reported sulfur ylide epoxidation protocols do in fact incorporate hydroxylic solvent systems.⁵

Furthermore, the interesting results of Hatch leads to speculation that betaine intermediates may be sufficiently persistent so as to allow proton transfer processes to occur. If the experimental protocol of Hatch could be carried out on a more clearly defined system then the putative proton transfer may be verified. This could be of potential interest as proton transfers on betaines could ultimately lead to geometrical isomerization. In fact, phosphonium betaines have been shown to undergo just such a process.⁴² Furthermore, a base catalyzed equilibration of betaines in cross-over experiments has been proposed previously but never experimentally verified.^{25b,c}

Lastly and most importantly, while the epoxidation reaction in CH_3CN has been studied by means of DFT calculations, there has been no corresponding experimental study incorporating the use of kinetic analysis. For this reason, we sought to carry out a kinetic study of the reaction in an effort to determine reaction order and ultimately to provide a rate expression for the epoxidation of benzaldehyde. In order to address these issues, a parallel study of sulfur ylide epoxidations has been performed. The first set of experiments was conducted in acetonitrile as solvent employing DBU as base. These reaction conditions were chosen so as to allow appropriate comparisons to be made to the DFT calculations performed by Aggarwal. The second set of experiments was carried out in a mixed solvent system of acetonitrile/water. It was predicted that incorporation of a hydroxylic co-solvent might reveal interesting reaction features when compared to the

results of the first study performed in a purely organic solvent system. The results of these studies are presented in the subsequent chapters.

4.8: References

- 1) a) Wittig, G.; Schollkopf, U. *Chem. Ber.*, **1954**, *87*, 1318. b) Vedejs, E.; Peterson, M.J. *Adv. Carbanion. Chem.* **1996**, *2*, 1.
- 2) Berger, R.; Ziller, J.W.; Van Vraken, D.L. *J. Am. Chem. Soc.* **1998**, *120*, 841.
- 3) Shoemaker, J.; Pulgam, V.R.; Borhan, B. *J. Am. Chem. Soc.* **2004**, *126*, 13600.
- 4) a) Aggarwal, V. K.; Fanf, G.Y.; Schmidt, A.T. *J. Am. Chem. Soc.* **2005**, *127*, 1642. b) Busch, B.B.; Paz, M.M.; Shea, K.J.; Staiger, C.L.; Stoddard, J.M.; Walker, J.R.; Zhou, X.Z.; Zhu, H. *J. Am. Chem. Soc.* **2002**, *124*, 3636.
- 5) a) Aggarwal, V. K.; Winn, C. L. *Acc. Chem. Res.* **2004**, *37*, 611; (b) Li, An-Hu; Dai, Li-Xin; Aggarwal, V. K. *Chem. Rev.* **1997**, *97*, 2341.
- 6) Ingold, C.K.; Jessop, J.A. *J. Chem. Soc.* **1930**, 713.
- 7) Johnson, A.W.; Lacount, R.B. *J. Am. Chem. Soc.* **1961**, *83*, 417.
- 8) a) Corey, E.J.; Chaykovsky, M. *J. Am. Chem. Soc.* **1962**, *84*, 3782.; b) Corey, E.J.; Chaykovsky, M. *J. Am. Chem. Soc.* **1965**, *87*, 1353.
- 9) Aggarwal, V.K.; Schade, S.; Taylor, B. *J. Chem. Soc. Perkin Trans. I* **1997**, 2811.
- 10) Trost, B.M.; Arndt, H.C. *J. Org. Chem.* **1973**, *38*, 3140.
- 11) Fei, X.S.; Verkade, J.G. *Heteroat. Chem.* **1999**, *10*, 538.
- 12) Vedejs, E. *J. Org. Chem.* **2004**, *69*, 5159.
- 13) Cheng, J.P.; Zhang, X.M. *J. Org. Chem.* **1998**, *63*, 7574.
- 14) Murray, C.J.; Jenks, W.P. *J. Am. Chem. Soc.* **1990**, *112*, 1880.
- 15) Rios, A.; O'Donoghue, A.C.; Amyes, T.L.; Richard, J.P. *Can. J. Chem.* **2005**, *83*, 1536.

- 16) a) Forbes, D.C.; Standen, M.C.; Lewis, D.L. *Org. Lett.* **2003**, *5*, 2283.; b) Forbes, D.C.; Amin, S.R.; Bean, C.J.; Standen, M.C. *J. Org. Chem.* **2006**, *71*, 8287.
- 17) Aggarwal, V.K.; Ford, J.G.; Fonquerna, S.; Adams, H.; Jones, R.V.H.; Fieldhouse, R. *J. Am. Chem. Soc.* **1998**, *120*, 8328.
- 18) Aggarwal, V.K.; Alonso, E.; Bae, I.; Hynd, G.; Lydon, K.M.; Palmer, M.J.; Patel, M.; Porcelloni, M.; Richardson, J.; Stenson, R.A.; Studley, J.R.; Vasse, J.L.; Winn, C.L. *J. Am. Chem. Soc.* **2003**, *125*, 10926.
- 19) Swain, C.G.; Burrows, W.D.; Schowen, B.J. *J. Org. Chem.* **1968**, *33*, 2534.
- 20) Swain, C.G.; Kaiser, L.E. *J. Am. Chem. Soc.* **1958**, *80*, 4089.
- 21) Wu, S.L.; Hargreaves, R.T.; Saunders Jr., W.H. *J. Org. Chem.* **1985**, *50*, 2392.
- 22) a) Hauser, C.R.; van Eenam, D.N.; *J. Am. Chem. Soc.* **1956**, *78*, 5698.
- 23) The driving force for dearomatization might be viewed as the simultaneous neutralization of both a positive and negative charge present within the sulfur ylide.
- 24) Barbella, G.; Garbesi, A.; Fava, A. *Helv. Chim. Acta* **1971**, *54*, 2297.
- 25) a) Aggrawal, V. K.; Charmant, J.P.H.; Fuentes, D.; Harvey, J.N.; Hynd, G.; Ohara, D.; Robiette, R.; Smith, C.; Vasse, J.L.; Winn, C.L. *J. Am. Chem. Soc.* **2006**, *128*, 2105; b) Aggrawal, V. K.; Hebach, C. *Org. Biomol. Chem.* **2005**, *3*, 1419.; c) Aggrawal, V. K.; Calamai, S.; Ford, J. G. *J. Chem. Soc. Perk. Trans. 1* **1997**, 593; d) Aggrawal, V. K.; Charmant, J.P.H.; Ciampi, C.; Hornby, J.M.; O'Brien, C.J.; Hynd, G.; Parsons, R. *J. Chem. Soc. Perk. Trans. 1* **2001**, 3159; e) Yoshimine, M.; Hatch, M.J. *J. Am. Chem. Soc.* **1967**, *89*, 5831.
- 26) Aggrawal, V. K.; Harvey, J. N.; Richardson, J. *J. Am. Chem. Soc.* **2002**, *124*, 5747.
- 27) a) Ohno, F.; Kawashima, T.; Okazaki, R. *J. Am. Chem. Soc.* **1996**, *118*, 697.; b) Kawashima, T.; Ohno, F.; Okazaki, R. *J. Am. Chem. Soc.* **1996**, *118*, 12455.; c) Kano, N.; Daicho, Y.; Kawashima, T. *Org. Lett.* **2006**, *8*, 4625.
- 28) Vedejs, E.; Peterson, M. J. *Top. Stereochem.* **1994**, *21*, 1.
- 29) Shi, Y. *Acc. Chem. Res.* **2004**, *37*, 488.
- 30) Darwish, D.; Hui, S.H.; Tomilson, R. *J. Am. Chem. Soc.* **1968**, *90*, 5631.
- 31) Darwish, D.; Tomilson, R. *J. Am. Chem. Soc.* **1968**, *90*, 5938.
- 32) Trost, B.M.; Hammen, R.F. *J. Am. Chem. Soc.* **1973**, *95*, 962.

- 33) Furukawa, N.; Sugihara, Y.; Fujihara, H. *J. Org. Chem.* **1989**, *54*, 4222.
- 34) Breau, L.; Ogilvie, W.W.; Durst, T. *Tetrahedron Lett.*, **1990**, *31*, 35.
- 35) Winn, C.L.; Bellenie, B.R.; Goodman, J.M. *Tetrahedron Lett.*, **2002**, *43*, 5427.
- 36) Julienne, K.; Metzner, P. *J. Org. Chem.* **1998**, *63*, 4532.
- 37) Breau, L.; Durst, T. *Tetrahedron: Asymmetry* **1991**, *2*, 367.
- 38) Solladie-Cavallo, A.; Diep-Vohuule, A. *J. Org. Chem.* **1995**, *60*, 3494.
- 39) Li, A.H.; Dai, L.X.; Hou, X.L.; Huang, Y.Z.; Li, F.W. *J. Org. Chem.* **1996**, *61*, 489.
- 40) Aggarwal, V. K.; *et al.* *J. Am. Chem. Soc.* **2003**, *125*, 10926.
- 41) a) Zheng, J.-C.; Liao, W.-W.; Tang, Y.; Sun, X.-L.; Dai, L.-X.; (b) Aggarwal, V.K.; Alonso, E.; Hynd, G.; Lydon, K.M.; Palmer, M.J.; Porcelloni, M.; Studley, J.R. *Angew. Chem. Int. Ed.* **2001**, *40*, 1430.; (c) Aggarwal, V.K.; Smith, H.W.; Hynd, G.; Jones, R.V.H.; Fieldhouse, R.; Spey, S.E. *J. Chem. Soc. Perkin Trans. 1* **2000**, 3267.
- 42) a) Vedejs E.; Fleck, T.; Hara, S. *J. Org. Chem.* **1987**, *52*, 4637.; b) Vedejs E.; Fleck, T.; *J. Am. Chem. Soc.* **1989**, *111*, 5861.

Chapter 5: Epoxidation Mechanism Explored

5.1: Research Objectives

The reaction between dimethylsulfonium benzylide and benzaldehyde in CH_3CN has been subjected to DFT calculations.¹ The focus of the study involved both the steps of ylide addition to benzaldehyde and the collapse of the resulting betaine intermediate to the corresponding epoxide. The key conclusions drawn from the study were that the ylide addition step was indeed rate determining and that this step involves a cisoid geometry between reacting partners. The results of this study are of particular relevance to epoxidations performed using the catalytic protocol of Aggarwal, in which the sulfur ylide is generated in the absence of base.

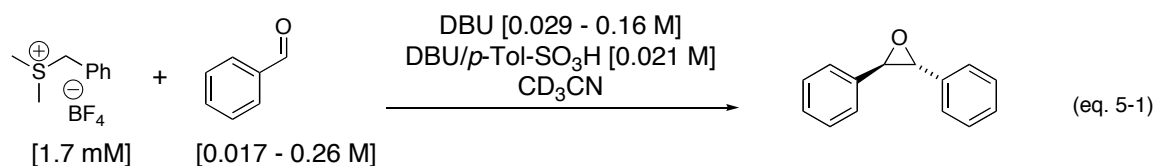
We sought to carry out a kinetic analysis of the epoxidation reaction under similar reaction conditions. As such the solvent of choice was accordingly CH_3CN and in order to generate the active sulfur ylide DBU was employed as base. This base was chosen because it is soluble in the purely organic solvent system of the study and demonstrated the highest reaction efficiency among a large number of amine bases explored. Naturally the ideal comparison of the aforementioned theoretical study would be to employ the actual reaction conditions of Aggarwal, however, to simplify kinetic analysis in this preliminary investigation base catalyzed generation of ylide was chosen.

The stated goals of this study were to experimentally determine a rate equation and to obtain activation parameters for the sulfur ylide epoxidation of benzaldehyde. In order to accomplish this, the reaction order with respect to the various reactants would

first need to be determined. This may initially seem a trivial matter in light of the obvious 1:1:1 stoichiometry of the reaction. Nonetheless two recent reports concerning the Baylis-Hillman² and Wittig-Horner³ reactions have proposed greater than first order dependence on benzaldehyde despite otherwise obvious 1:1 stoichiometries. Lastly it was deemed that transition state characteristics could be obtained by a series of mechanistic probes such as isotope and substituent effects. In doing so, the sulfur ylide epoxidation of benzaldehyde could be placed into context with other similar reactions involving additions to arylaldehydes such as the related Wittig olefination. Ultimately, this part of the study proved invaluable in unambiguously identifying the rate-determining step of the reaction.

5.2: Rate Studies

Epoxidations were carried out in CD₃CN under pseudo first order conditions of excess benzaldehyde and limiting sulfonium salt, equation 5-1. Both the pH and ionic strength of the solution were maintained at a constant value throughout the reaction by virtue of the DBU/DBUH⁺ buffer employed. Progress of the reaction could be effectively monitored by high field ¹H-NMR (600 MHz) for loss of sulfonium salt integrated relative to an internal standard *p*-Cl-styrene. Under the conditions used in the present study, the selectivity in favor of the *trans*-epoxide isomer is nearly complete (*circa* 98:2).



The kinetic traces obtained by plotting the natural logarithm of [sulfonium salt] versus time displayed clean pseudo first order behavior in excess of three half lives. Monitoring the reaction under increasing concentrations of DBU [0.029-0.16 M] and plotting k_{obs} versus [DBU] reveals a straight line passing through the origin within experimental error, Figure 5-1. This indicates that the reaction is first order with respect to base. The reaction was also monitored under increasing concentrations of benzaldehyde [0.017 – 0.26 M] and in this instance plotting k_{obs} versus [benzaldehyde] revealed saturation behavior, Figure 5-2.

Figure 5-1: Plot of k_{obs} Versus [DBU]

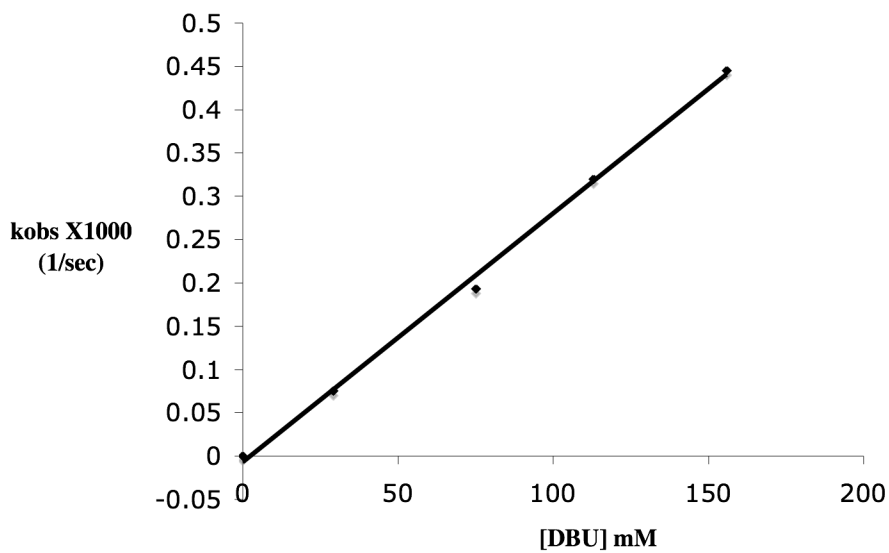
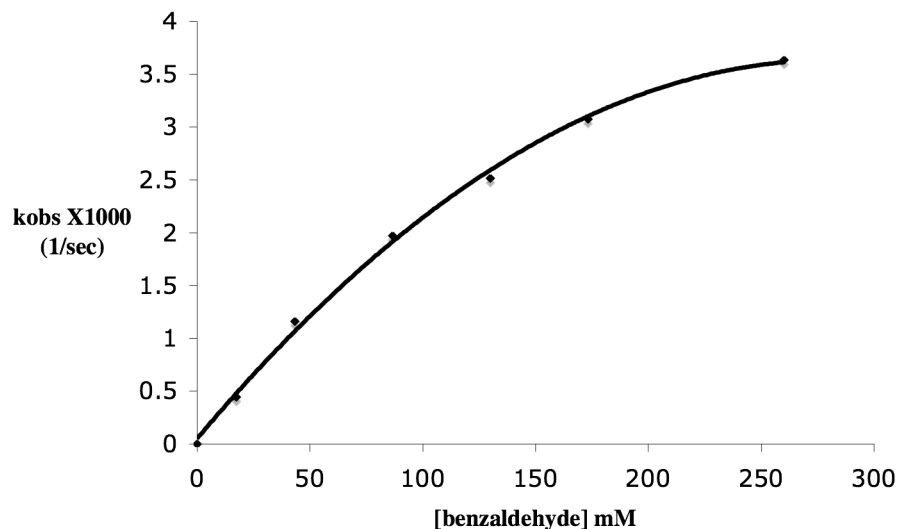
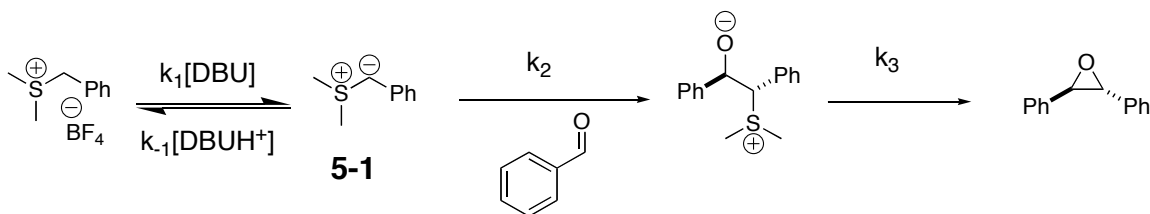


Figure 5-2: Plot of k_{obs} Versus [benzaldehyde]



Applying the steady state approximation at ylide **5-1** of Scheme 5-1 leads to the rate expression shown in equation 5-2.

Scheme 5-1: Epoxidation Mechanism



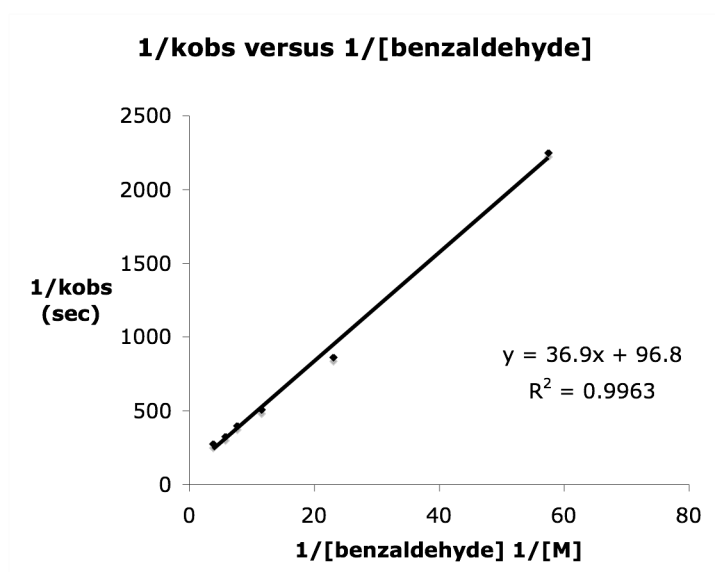
$$-\frac{d[\text{sulfonium salt}]}{dt} = \frac{k_1 k_2 [\text{benzaldehyde}][\text{DBU}][\text{sulfonium salt}]}{k_{-1}[\text{DBUH}^+] + k_2[\text{benzaldehyde}]} \quad (\text{eq. 5-2})$$

$$\text{where; } k_{\text{obs}} = \frac{k_1 k_2 [\text{benzaldehyde}][\text{DBU}]}{k_{-1}[\text{DBUH}^+] + k_2[\text{benzaldehyde}]} \quad (\text{eq. 5-3})$$

$$\text{and; } \frac{1}{k_{\text{obs}}} = \frac{k_{-1}[\text{DBUH}^+]}{k_1 k_2 [\text{DBU}][\text{benzaldehyde}]} + \frac{1}{k_1 [\text{DBU}]} \quad (\text{eq. 5-4})$$

The reciprocal plot of $1/k_{\text{obs}}$ versus $1/[\text{benzaldehyde}]$ is shown in Figure 5-3 from which k_1 is determined to be $6.6 \times 10^{-2} \text{ M}^{-1}\text{sec}^{-1}$. The ratio of the slope to the y-intercept can be used to determine the ratio k_{-1}/k_2 , which is found to be 18.4. This ratio may be used to gauge the commitment of the sulfur ylide (**5-1**) to product formation. Evidently, reversion of **5-1** to starting material by reprotonation is fast relative to electrophilic capture by benzaldehyde.

Figure 5-3: Reciprocal Plot of $1/k_{\text{obs}}$ Versus $1/[\text{benzaldehyde}]$



5.3: Activation Parameters

The rate expression of equation 5-2 contains three microscopic rate constants that cannot easily be solved simultaneously. Therefore in order to determine the rate dependence of the reaction on temperature and, hence the activation parameters for epoxidation, the rate expression of equation 5-2 needs to be converted into a form more amenable to our purposes. Equation (5-2) can be simplified to equation 5-5 under

reaction conditions in which, $k_1[\text{DBUH}^+] \gg k_2[\text{benzaldehyde}]$. The ratio k_1/k_2 was previously determined by means of reciprocal plot 5-3 and as such the pre-stated condition is easily obtained simply by adjusting the concentrations of $[\text{DBUH}^+]$ and $[\text{benzaldehyde}]$. The ratio of $k_1[\text{DBUH}^+] : k_2[\text{benzaldehyde}]$ was set to a constant value of 22:1 throughout the following set of experiments.

$$-\frac{d[\text{SM}]}{dt} = K_{\text{eq}} k_2 \frac{[\text{DBU}]}{[\text{DBUH}]} [\text{benzaldehyde}][\text{sulfonium salt}] \quad (\text{eq. 5-5})$$

Prior to constructing an Eyring plot and obtaining the activation parameters for this reaction the apparent second order rate constant (k_{app}) needed to be extracted from the experimentally determined k_{obs} at each temperature. From equation 5-5 we can define k_{obs} as:

$$k_{\text{obs}} = K_{\text{eq}} k_2 \frac{[\text{DBU}]}{[\text{DBUH}]} [\text{benzaldehyde}] \quad (\text{eq. 5-6})$$

where $k_{\text{app}} = K_{\text{eq}} k_2,$ (eq. 5-7)

and

$$k_{\text{app}} = \frac{k_{\text{obs}} [\text{DBUH}]}{[\text{benzaldehyde}][\text{DBU}]} \quad (\text{eq. 5-8})$$

Reactions were run in duplicate over a temperature range spanning 298 to 328 K and values of k_{obs} were determined in the usual manner. The observed pseudo first order rate constants and apparent second order rate constants obtained from equation 5-8 are shown in Table 5-1 and the plot of $\ln(k_{\text{app}}/T)$ versus $1/T$ is shown in Figure 5-4. From the

Eyring plot it was determined that $\Delta H^\ddagger = 11.8$ kcal/mol and $\Delta S^\ddagger = -35$ cal/mol. This corresponds to a free energy of activation, ΔG^\ddagger , of 22.2 kcal/mol at 298K. It should be noted that these activation parameters represent composite values derived from the apparent second order rate constant k_{app} , which in turn is related to K_{eq} and k_2 by equation 5-7. However, the activation free energy is likely to be dominated by the k_2 term. In particular, the large negative ΔS^\ddagger is consistent with a bimolecular addition resulting in the conversion of two molecules into a single activated complex. The analogous Arrhenius treatment of the temperature dependent rate data results in the calculation of E_a equal to 12.3 kcal.

Figure 5-4: Eyring Plot

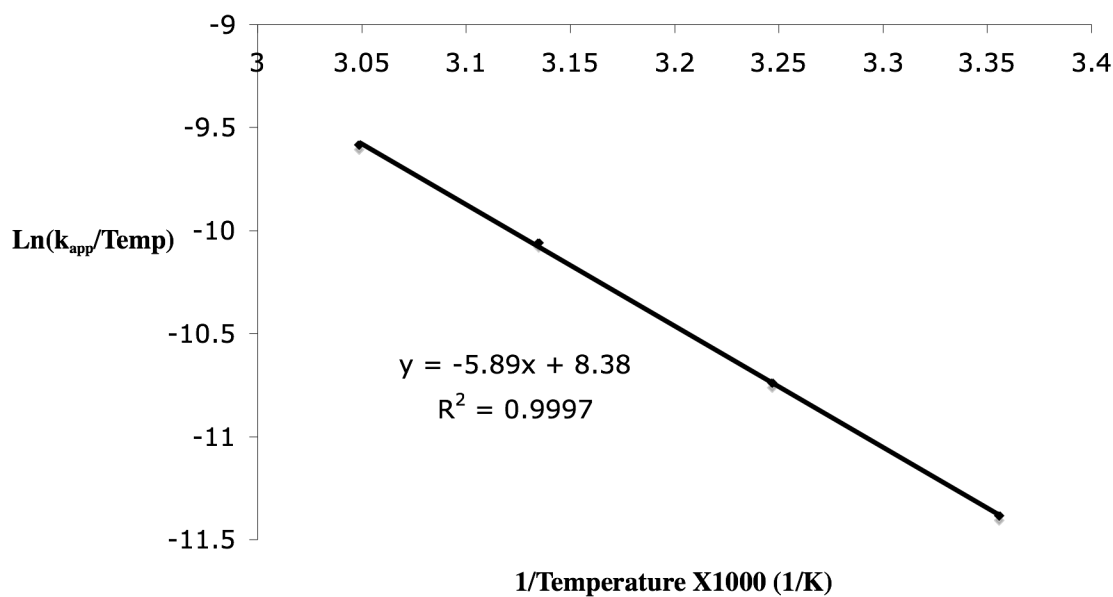
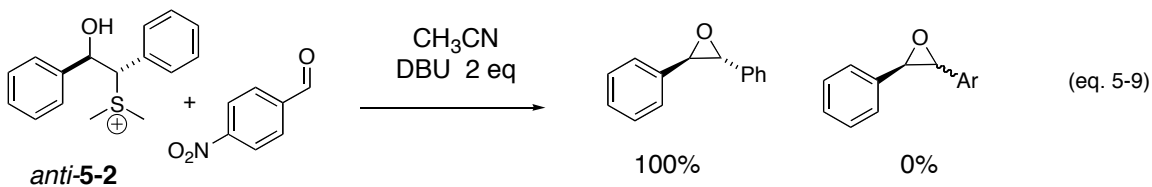


Table 5-1: Rate Constants k_{obs} and k_{app} as a Function of Temperature

Entry	Temperature (K)	k_{obs} ($\times 10^3 \text{ s}^{-1}$)	k_{app} ($\times 10^3 \text{ M}^{-1} \text{ s}^{-1}$)
1	298	0.45	3.4
2	308	0.88	6.7
3	319	1.8	13.6
4	328	3.0	22.6

5.4: Cross-Over Experiments

The irreversibility of sulfur ylide addition to benzaldehyde (k_2) has previously been demonstrated in the solvents DMSO and DCM by cross-over experiments.⁴ The results of these previous studies have been confirmed under the current reaction conditions, equation 5-9. Betaine precursor *anti*-5-2 underwent quantitative conversion to *trans*-stilbene oxide upon treatment with the base DBU. Cross-over products were not observed and accordingly the addition of sulfur ylide to benzaldehyde is interpreted as being an irreversible process.



5.5: ¹³C Carbon Isotope Effects

Kinetic isotope effects (KIEs) have the potential to broaden the understanding of mechanism by identifying atoms involved in bond change during the rate determining step of the reaction. For this reason, a ¹³C-KIE was sought for the carbonyl carbon of benzaldehyde. A primary isotope effect at this carbon would lend further support for the treatment of sulfur ylide addition to benzaldehyde as rate limiting.

¹³C-KIEs were determined by the Singleton protocol⁵ in which unlabelled, natural abundance ¹³C-containing benzaldehyde is subjected to a large-scale epoxidation and taken to high conversion. Following reaction, the unreacted starting material is recovered and the enrichment of the slower reacting isotope is determined via quantitative ¹³C-NMR. The *para*-carbon of benzaldehyde is assumed to undergo a negligible KIE during the reaction, and as such serves as a reference for the enrichment of ¹³C at the carbonyl center. From this data, a ¹³C-KIE can be calculated in accordance with standard theory utilizing Equation 5-10.⁶

$$\text{KIE} = \frac{\ln(1-F)}{\ln[(1-F)(R/R_0)]} \quad (\text{eq. 5-10})$$

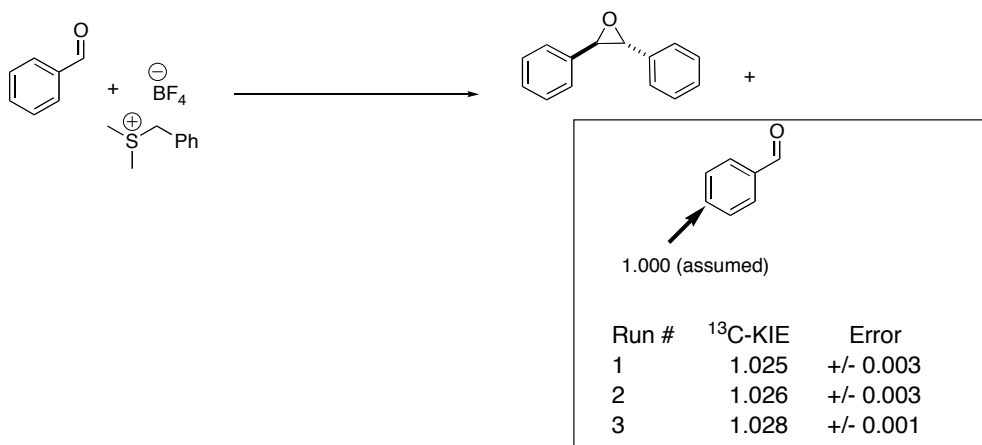
where; F = fractional conversion and R/R₀ = ratio ¹³C in benzaldehyde prior to and after reaction as determined by quantitative ¹³C-NMR.

The reactions were carried out on large scale and a deficiency of the sulfonium reagent was employed to ensure high but not quantitative conversion of the benzaldehyde

starting material. The unreacted benzaldehyde was isolated following a standard aqueous work-up, distilled at reduced pressure and subsequently subjected to quantitative ^{13}C -NMR analysis.⁷ In preparing the samples for NMR analysis, the NMR tube was charged with benzaldehyde (75% by volume) and for the purposes of obtaining a lock and preventing field drift, CDCl_3 (25% by volume) was also added. A T_1 determination was carried out and delays between successive pulses were set greater than ten times T_1 (144 seconds). In order to prevent truncation of the FID the acquisition time was set manually to acquire 256k points. Multiple spectra (at least five) were obtained following each experiment and the average integrations from these were then used to calculate the isotope effect using equation 5-10.

Initially the spectra were Fourier transformed and processed using standard parameters including an exponential decay resulting in line broadening of up to 1 Hz. Examination of the integration values revealed a significant amount of scatter with standard deviations of up to 0.6%. Adjusting the extent of zero filling performed on the FID led to no improvements. On the other hand removal of the line broadening function significantly improved the precision of the measurements despite the expected reduction in signal to noise ratio. Ultimately, the spectra were processed without applying a line broadening function and the integral regions were set so as to encompass the entire peak region spanning 0.12 ppm or greater than 10 times the half height peak width. The ^{13}C -KIE of the carbonyl carbon of benzaldehyde was determined to be 1.026 (average of three experiments) as is shown in Figure 5-5 along with the standard deviations calculated by propagation of errors.

Figure 5.5: ^{13}C Carbon Kinetic Isotope Effect (^{13}C -KIE)

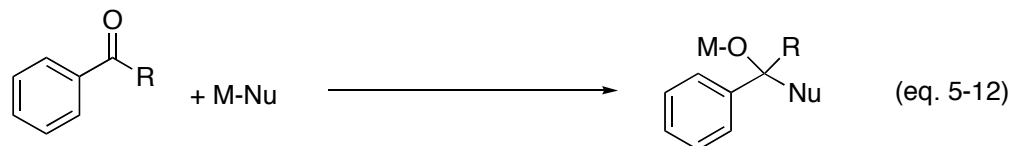


The observed large normal ^{13}C -KIE of 1.026 is indicative of significant bond change at the carbonyl carbon of benzaldehyde during the rate-determining step of the reaction. An isotope effect of this magnitude is consistent with the proposal that sulfur ylide addition to benzaldehyde (k_2) is rate limiting. A comparison can be made between ^{14}C - and ^{13}C -KIEs by converting between the two using equation 5-11 and the recommended value of $r = 1.9$ for carbon isotope effects.⁸ Accordingly the experimentally determined ^{13}C -KIE of 1.026 corresponds to a ^{14}C -KIE of 1.050. The carbonyl carbon isotope effects reported for the addition of various nucleophiles to benzophenone and benzaldehyde are shown in Table 5-2. The observed isotope effect of the present study is intermediate in magnitude between the values reported for the additions of lithium pinacolone enolate and $\text{Ph}_3\text{PCHPhNa}$ to benzaldehyde. Each of the reactions included in Table 5-2 have been interpreted in terms of a rate limiting polar addition mechanism.

$$r = \ln(^{14}\text{C KIE}) \quad (\text{eq. 5-11})$$

$\ln(^{13}\text{C KIE})$

Table 5-2: Various Carbon Isotope Effects for Arylcarbonyl Additions



R = H or Ph

Entry	Electrophile	Nucleophile	$^{13}\text{C-KIE}$	$^{14}\text{C-KIE}$
1	Ph ₂ CO	LiAlH ₄ /Et ₂ O ⁹		1.024
2	PhCHO	Li pinacolate ¹⁰	1.019	1.036 ^a
3	PhCHO	PhCHSMe₂	1.026	1.050^a
4	PhCHO	Ph ₃ PCHPhNa ¹¹		1.060
5	Ph ₂ CO	NaBH ₄ ⁹		1.066

^a) Calculated from equation 5-11.

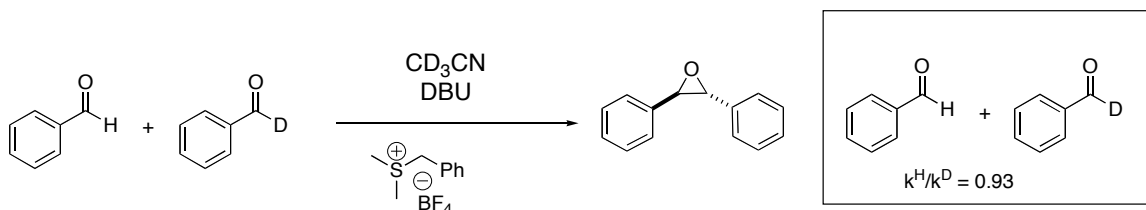
5.6: ^2H -Isotope Effects

Isotope effects derived from labeled atoms not directly undergoing bond change, so-called secondary isotope effects, are effective means of deducing transition state geometry. In particular, secondary deuterium kinetic isotope effects (SDKIEs) have been used as a probe for rehybridization at the attached carbon undergoing direct bond change during the reaction. Rate limiting addition of a nucleophilic species to an aldehyde is generally associated with an inverse SDKIE at the aldehydic proton. In other words, the

deuterated substrate reacts faster than protiated substrate. The inverse nature of the KIE, where $k^H/k^D < 1$, is interpreted as arising from an increase in the aldehydic C-H(D) vibrational force constant for out-of-plane bending on going from the ground state (sp^2) to the transition state (sp^3 -like).¹²

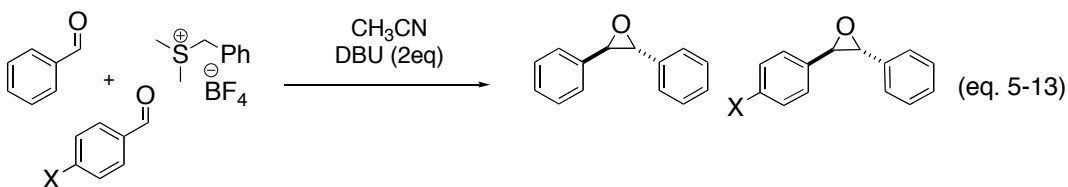
The SDKIE has been determined for the epoxidation of benzaldehyde with dimethylbenzylsulfonium tetrafluoroborate. A 55:45 mixture of benzaldehyde and d_1 -benzaldehyde were subjected to epoxidation under typical reaction conditions in CD_3CN , Figure 5-6.¹³ Prior to the addition of DBU to start the reaction, an aliquot was removed and the integration ratio of aldehydic:ortho protons was determined by 600 MHz 1H -NMR. A 20 second delay was employed between pulses to avoid any saturation effects. This value is used as a standard from which isotopic enrichment occurring during the reaction can be evaluated. Similarly, an aliquot was removed and analyzed following reaction for 3 hours. From this, the SDKIE was calculated using equation 5-10. An inverse SDKIE of 0.93 was determined for the addition of dimethylsulfonium benzylide to benzaldehyde. The inverse nature of the SDKIE is typical of processes involving sp^2 to sp^3 rehybridization in the transition state and is consistent with rate limiting addition of the sulfur ylide to benzaldehyde.

Figure 5-6: Secondary Deuterium Kinetic Isotope Effect (SDKIE)



5.7: Hammett Study

A Hammett study was conducted in order to assess the nature of charge development in the transition state of the reaction. The relative reactivity of substituted benzaldehydes was determined by a series of competition experiments, equation 5-13. At least a ten fold excess of benzaldehyde and *p*-X-benzaldehyde were allowed to compete for a limiting amount of sulfonium salt.¹⁴ The use of a large excess of the aldehyde reagents ensured that decreases in reactant concentration over the course of the reaction did not factor into the relative rates of the competing processes and that the product distribution was an accurate reflection of k_{rel} . Under these conditions k_{rel} can be calculated from equation 5-14.¹⁵ Following reaction, the competition runs were subjected to a crude aqueous work-up and the product distribution was determined by high field ¹H-NMR by integrating the benzylic proton peaks of the respective epoxide products.¹⁶ The resulting Hammett plot is shown in Figure 5-7 and the k_{rel} data are included in Table 5-3.

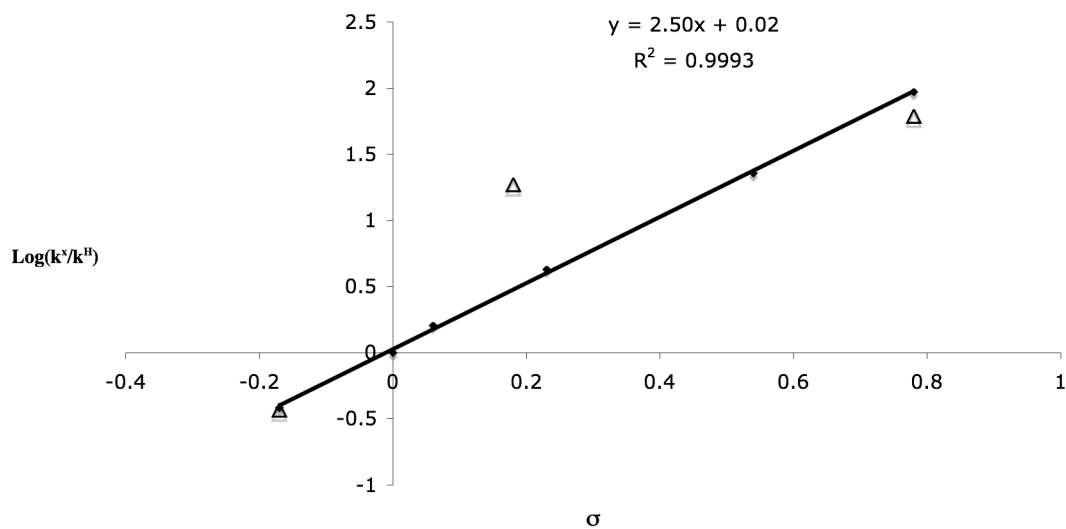


$$k^X/k^H = \frac{[\text{Product}^X]/[\text{Product}^H]}{[\text{Aldehyde}^X]/[\text{Aldehyde}^H]} \quad (\text{eq. 5-14})$$

The Hammett slope, ρ , is determined to be +2.50 for the reaction of dimethylsulfonium benzylidene with substituted benzaldehydes in CH₃CN. The positive sign of ρ reflects the fact that electron-withdrawing substituents on the aromatic ring accelerate the reaction. This finding is consistent with the observation that highly electron rich substrates, such as *para*-Me₂N-benzaldehyde, are not seen to undergo appreciable levels of conversion even at prolonged reaction times. These results confirm the

nucleophilic nature of the sulfur ylide reagent and furthermore indicate a substantial build-up of negative charge in the activated complex as it proceeds through to the transition state. The magnitude of ρ determined for the reaction is a relatively large value when compared to other nucleophilic additions to carbonyl substrates.

Figure 5-7: Hammett Plot^a



^a) Data points with triangle labels(Δ) are for *ortho*-substituted benzaldehydes

Table 5-3: Relative Rate Data for Benzaldehyde Competition Experiments

entry	X	σ	k^X/k^H	$\text{Log}(k^X/k^H)$
1	Me	-0.17	0.38	-0.42
2	F	0.06	1.6	0.20
3	Cl	0.23	4.3	0.63
4	CF ₃	0.54	22.6	1.35
5	NO ₂	0.78	93.6	2.00

5.8: *ortho*-Substituted Benzaldehydes

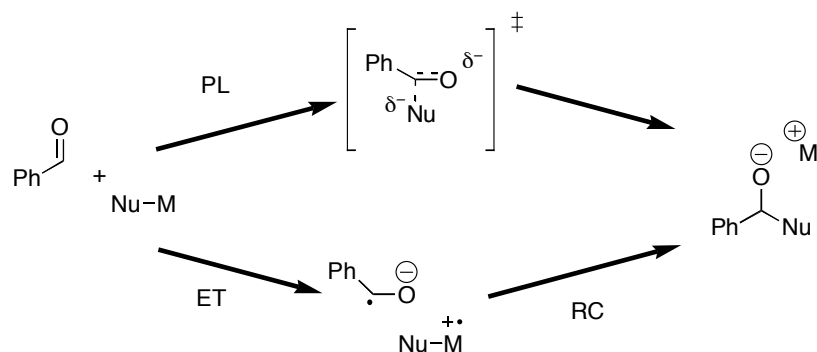
Typically *ortho*-substituted substrates are omitted from a Hammett study. This is because the proximity of the substituent to the reaction center often negates the isolation of electronic effects from steric interactions occurring during the reaction. Nonetheless, the relative reactivity of *ortho*-iodo-benzaldehyde with respect to benzaldehyde can be assessed via a competition experiment as described in Section 5.6. In this instance k_{rel} ($k^{\text{I}}/k^{\text{H}}$) is determined to be on the order of 19. A significant upward deviation can be seen when this value is plotted in Figure 5-9 using the σ_{para} value for an iodo-substituent.

Such an effect is generally unexpected in a reaction involving a nucleophilic addition. It might be predicted based on steric interactions between the reaction center and the *ortho*-substituent that the rate would decrease resulting in a downward deviation in the Hammett plot. In fact, the expected rate retardation is observed for both *ortho*-methyl and *ortho*-nitro substituents. Upward deviations in Hammett plots have been noted for phosphonium ylides reacting with substrates containing *ortho*-substituents bearing heteroatoms.¹⁷ In this case, the increased reactivity of these substrates is predicted to result from coordination of the heteroatom of the electrophile with the positively charged phosphorus atom of the nucleophilic Wittig reagent. It is unclear whether a similar effect is present in sulfur ylide epoxidations and indeed the present evidence for such an interaction is tenuous. Nonetheless, the result is intriguing in that it may signal the potential for the development of directed epoxidation strategies.

5.9: SET Versus PL Mechanisms

Nucleophilic additions to aryl substituted aldehydes and ketones have been shown to occur via either the classical two-electron polar addition (PL) mechanism or via an alternate SET process consisting of an electron transfer (ET) step followed by radical coupling (RC), Scheme 5-2. Examples of the SET mechanism are found in the addition of organolithium¹⁸ and Grignard reagents¹⁹ to arylsubstituted carbonyls as well as Wittig olefinations employing non-stabilized-phosphorus ylides.²⁰ Selectivity between the two competing mechanisms appears to be highly nucleophile dependent.

Scheme 5-2: Polar Addition and Single Electron Transfer Processes



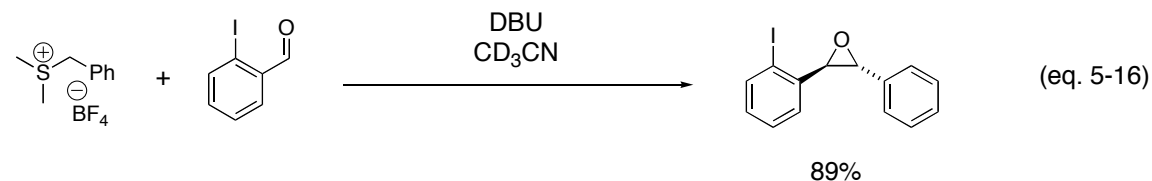
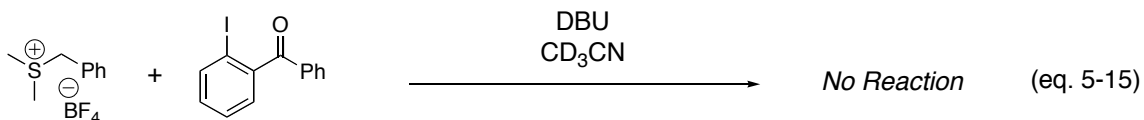
Distinguishing between a rate limiting PL and ET can be accomplished by a combination of heavy atom isotope effects and substituent effects on the reaction rate in other words, a Hammett study.¹⁰ Reactions proceeding through a PL type process generally lead to large normal carbon isotope effects and a significantly positive slope (>1) in a Hammett plot. A rate determining ET on the other hand may demonstrate

carbon isotope effects near unity and variable slopes in a Hammett plot, although these are generally found to be less than one. Gajewski has further demonstrated the use of SDKIEs in differentiating between rate limiting ET and PL processes.²¹ The utility of this test resides in the fact that a rate limiting PL addition leads to an increase in C-H bending frequency as the carbon goes from sp^2 to sp^3 hybridization and hence an inverse SDKIE is expected. While the benzyl ketyl radical formed in the ET process should lead to a normal SDKIE as a result of bond loosening of the aldehydic C-H. The observed ^{13}C -KIE (1.026), inverse SDKIE (0.93) and large ρ (+2.50) for the sulfur ylide epoxidation of benzaldehyde definitively rules out a rate-limiting electron transfer process.

Another possibility that ought to be considered is that the rate-determining step is actually radical coupling (RC). In fact there are examples of phosphonium ylides that are proposed to react with carbonyl substrates via an SET mechanism and where the second step (RC) is thought to be rate limiting.^{20b} Distinguishing between rate limiting PL and RC mechanistic scenarios is not trivial. Both processes can be expected to show similarly large heavy atom isotope effects and Hammett ρ 's. For this reason Yamataka has pioneered a probe to test for SET mechanisms proceeding through rate determining radical coupling.²² *o*-Iodo-benzophenone is subjected to reaction with the nucleophile in question. If RC is rate limiting, then persistence of the resulting benzyl ketyl radical can result in reduction of the iodo functionality.

Subjecting 2-iodobenzophenone to typical epoxidation conditions led to the complete recovery of starting material, equation 5-15. No reduction of 2-iodobenzophenone to benzophenone was observed. A modification to Yamataka's protocol was therefore implemented consisting of substituting *ortho*-iodobenzophenone

with *ortho*-iodo-benzaldehyde. The resulting *ortho*-iodostilbene oxide was isolated in 89% yield, equation 5-16. No reduced benzaldehyde or reduced stilbene oxide was detected in the crude reaction mixture by $^1\text{H-NMR}$. The total absence of any reduced species argues against an SET mechanism with rate limiting RC.



5.10: Discussion

The results of the current kinetic study reveal that the epoxidation reaction is first order with respect to DBU and sulfonium salt, while saturation behavior is observed with benzaldehyde. These results are consistent with the mechanistic proposal depicted in Scheme 5-1 with addition of sulfur ylide to benzaldehyde being rate limiting. The reaction is shown to proceed with a ΔG^\ddagger of 22.2 kcal/mol at 298 K. The analogous Arrhenius treatment of the temperature dependent rate data results in the calculation of $E_a = 12.3$ kcal. This value is larger than the E_a of 4.5 kcal calculated by Aggarwal using DFT calculations for the title reaction in CH_3CN .¹ The discrepancy between the two values is probably a result of the means in which each was determined. The DFT

calculations of Aggarwal calculated the energies of the various intermediates and transition states for the reaction between pre-formed dimethylsulfonium benzylide and benzaldehyde. On the other hand, the results presented here were obtained from a kinetic analysis of the reaction and necessarily include the acid base reaction between DBU and the sulfonium salt to generate the ylide species.

The observed carbonyl ^{13}C -KIE is most consistent with a reaction step in which this atom is heavily involved in reaction coordinate motion as in addition (k_2) of sulfur ylide to benzaldehyde. The large Hammett ρ of +2.50 is another indication of bond change at the carbonyl carbon during the RDS of the epoxidation. Specifically, it indicates that a build up of negative charge is occurring at the carbonyl carbon. A nucleophilic addition such as that depicted by k_2 might be expected to involve this magnitude of charge development. For example the Hammett ρ for hydrocyanation of benzaldehyde is reported to be +2.33,²³ reduction of acetophenone with sodium borohydride +3.06,²⁴ and addition of the phosphonium ylide $\text{Ph}_3\text{P}^+\text{C}^-\text{HPh}$ to benzaldehyde +2.77.¹⁷

Lastly, the inverse SDKIE (0.93) for the aldehydic proton of benzaldehyde is indicative of an sp^2 to sp^3 rehybridization occurring during the RDS of the multi-step epoxidation. This interpretation is in line with standard theory, which predicts this outcome based on changes in out-of-plane bending frequencies for sp^2 and sp^3 hybridized CH bonds. It would therefore appear that based on the results of heavy atom and secondary deuterium isotope effects as well as substituent effects on the reaction that treating k_2 of Scheme 1 as rate determining is fully justified.

A useful technique to experimentally probe transition state structure is to compare observed SDKIEs with the predicted equilibrium isotope effect for complete bond formation by means of equation 5-17.²¹ The parameter i is taken as an indication of progress along the reaction coordinate assuming that the observed SDKIE varies monotonically from reactant to product.

$$\text{KIE} = \text{EIE}^i \quad (\text{eq. 5-17})$$

The experimentally determined EIE for hydrocyanation of *p*-methoxybenzaldehyde is reported to be 0.78.²⁵ Hill has used a similar value to estimate the EIE for borohydride reductions of benzaldehyde.²⁶ Similarly an EIE of 0.78 has also been used in a study of organolithium and Grignard additions to benzaldehyde.²¹ Employing an EIE of 0.78 and equation 5-16 leads to the calculation of $i = 0.29$ for the sulfur ylide epoxidation of benzaldehyde. This would indicate moderate product character in the activated complex. However, it is not completely clear whether the EIE of 0.78 is a good model for the current reaction. In fact, Gajewski has demonstrated that the identity of the counter cation in the reaction strongly affects the magnitude of the predicted EIE.^{21a} Considering the large Hammett ρ (2.50) and ¹³C-KIE (1.026), it appears as though i may be an underestimation of the position of the transition state for sulfur ylide addition to benzaldehyde.

The use of isotope and substituent effects, in combination with Yamataka's radical-probe, have been used to definitively rule out any type of SET addition of dimethylsulfonium benzylyde to benzaldehyde. Certain unstabilized phosphonium ylides

have been proposed to undergo an SET type addition to arylcarbonyl compounds. However the semi-stabilized triphenylphosphonium benzylide analogue was shown to undergo PL type addition to benzaldehyde similar to the sulfonium benzylide studied here.²⁰

5.11: Conclusion

The Corey-Chaykovsky reaction between dimethylbenzyl sulfonium tetrafluoroborate and benzaldehyde has been studied by kinetic means. The results of this study confirm the rate determining nature of ylide addition to benzaldehyde as determined by cross over experiments⁴ and DFT calculations.^{1,4} The experimental activation parameters have been measured and found to agree remarkably well with those determined by DFT calculations provided that base catalyzed ylide generation is accounted for in the current study. For the first time, transition state characteristics have been probed for this reaction by a combination of isotopic and substituent effects. These results lend support for the conclusions drawn from kinetic analysis of the epoxidation reaction. Although the results of the current study fall short of positioning the TS along the reaction coordinate, they do shed light on charge development in the activated complex and provide a basis for future study of TS characteristics. Lastly, and by a combination of means, the addition of dimethylsulfonium benzylide to benzaldehyde has been shown to proceed by the classic two electron polar addition mechanism (PL).

5.12: Experimental Section

General Experimental: Dimethylbenzylsulfonium tetrafluoroborate²⁷ and **5-2**⁴ were prepared as previously described. Benzaldehyde, DBU and acetonitrile were all distilled prior to use. All other reagents were purchased in the highest grade available. NMR kinetic studies were performed on a Bruker 600 MHz spectrometer with temperature control capabilities. Detailed procedures for the cross-over experiments can be found in Section 6.8 and in reference 28.

General experimental procedure for determination of pseudo-first order rate constants (k_{obs}): New stock solutions of all reagents were prepared daily by weighing out a predetermined amount of reagent and diluting to a desired concentration in CD₃CN. Into a standard 5 mm NMR tube was added benzaldehyde [0.017 – 0.26 M], DBU [0.029 – 0.156 M], *p*-chlorostyrene [3.5 mM], DBU/*p*-toluenesulfonic acid [0.021 M] and CD₃CN. The NMR tube was then placed into a 600 MHz NMR spectrometer and equilibrated to the desired temperature for ten minutes during which time a lock was obtained and preliminary shimming and tuning of the probe was performed. The sample was ejected and dimethylbenzylsulfonium tetrafluoroborate [1.7 mM] was added via syringe to the NMR tube. The sample was shaken vigorously and then injected into the spectrometer. A new lock signal was obtained and shimming of the magnet was once again performed. Spectra were recorded in a multi-acquisition mode for a pre-determined amount of time

generally consisting of greater than three half lives. The kinetic traces obtained by plotting the natural log of dimethylbenzylsulfonium tetrafluoroborate concentration versus time are reproduced here. In certain instances it will be noticed that the slopes of these traces differ slightly from the values used to generate Figures 5-1 through to 5-4 in the main text. This is because each kinetic experiment was performed in duplicate and average values of k_{obs} used. However, only one trace per kinetic experiment under each set of conditions is reproduced here. The standard deviation between experiments under identical conditions is generally less than 10%.

Figure 5-8: Determination of k_{obs} dependence on [benzaldehyde], (expt #1)

Benzaldehyde [0.0174 M]

DBU [.156 M]

Temperature: 298 K

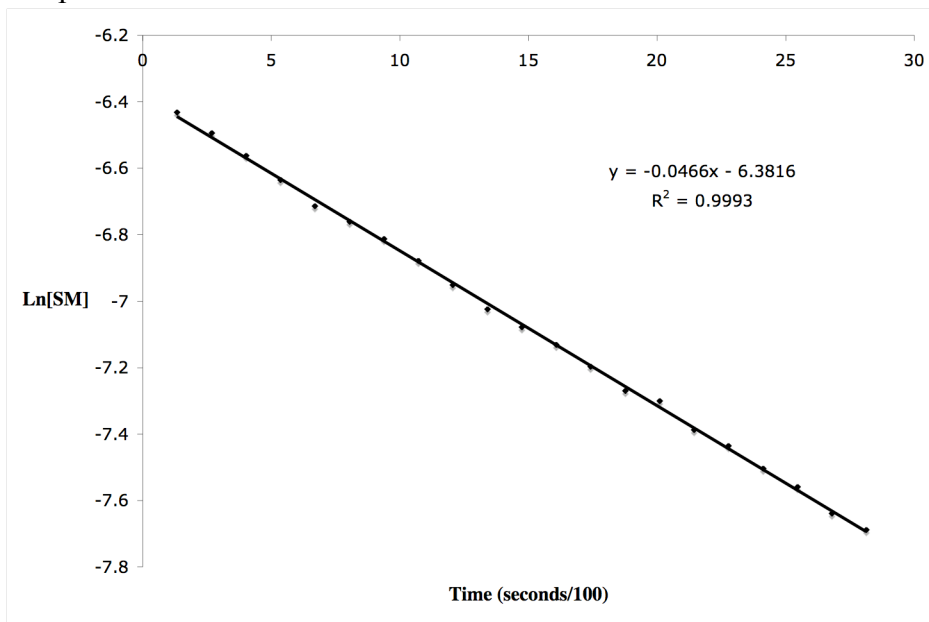


Figure 5-9: Determination of k_{obs} dependence on [benzaldehyde], (expt #2)

Benzaldehyde [0.0433 M]

DBU [.156 M]

Temperature: 298 K

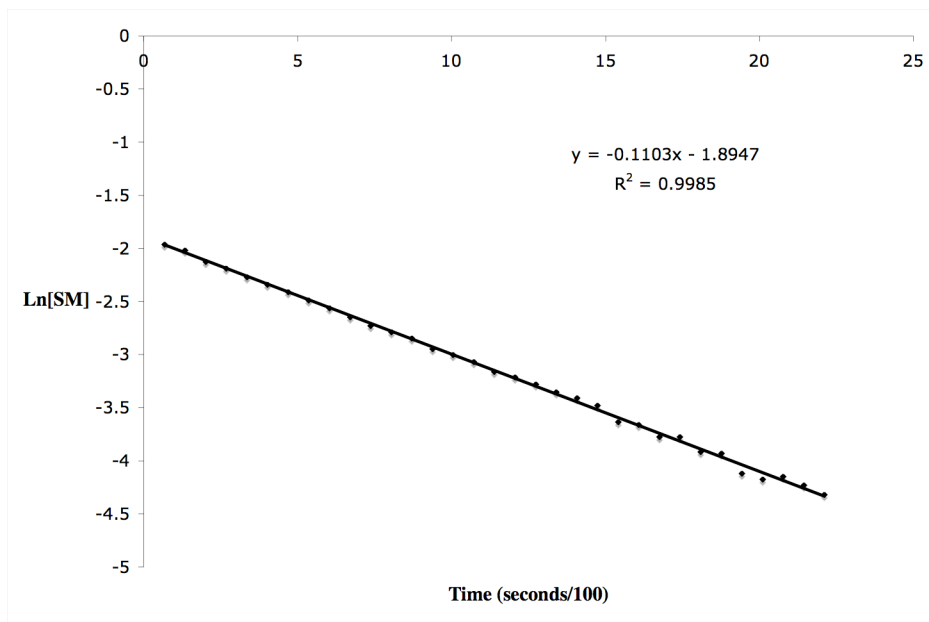


Figure 5-10: Determination of k_{obs} dependence on [benzaldehyde], (expt #3)

Benzaldehyde [0.0866 M]

DBU [.156 M]

Temperature: 298 K

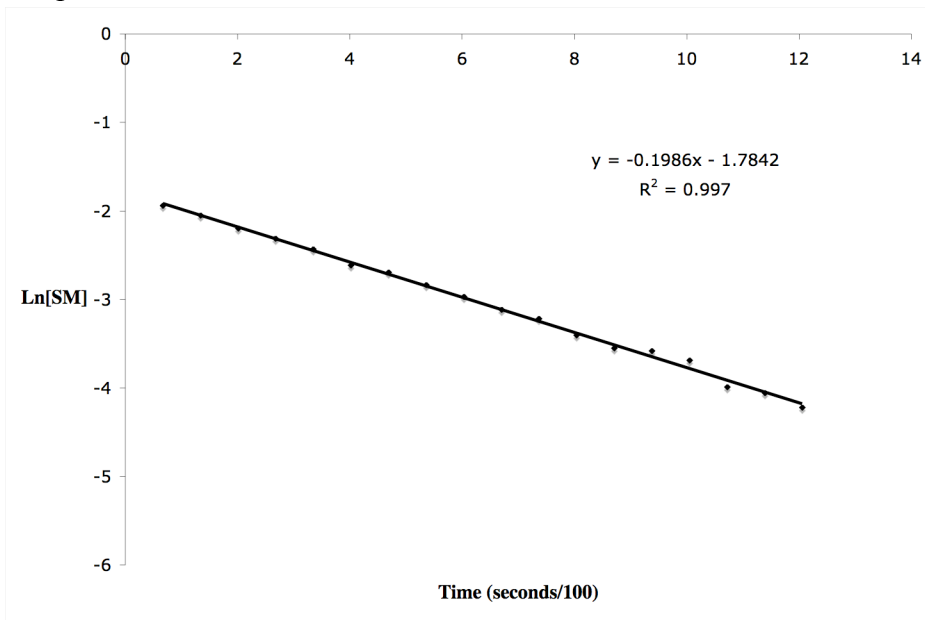


Figure 5-11: Determination of k_{obs} dependence on [benzaldehyde], (expt #4)

Benzaldehyde [0.130 M]

DBU [.156 M]

Temperature: 298 K

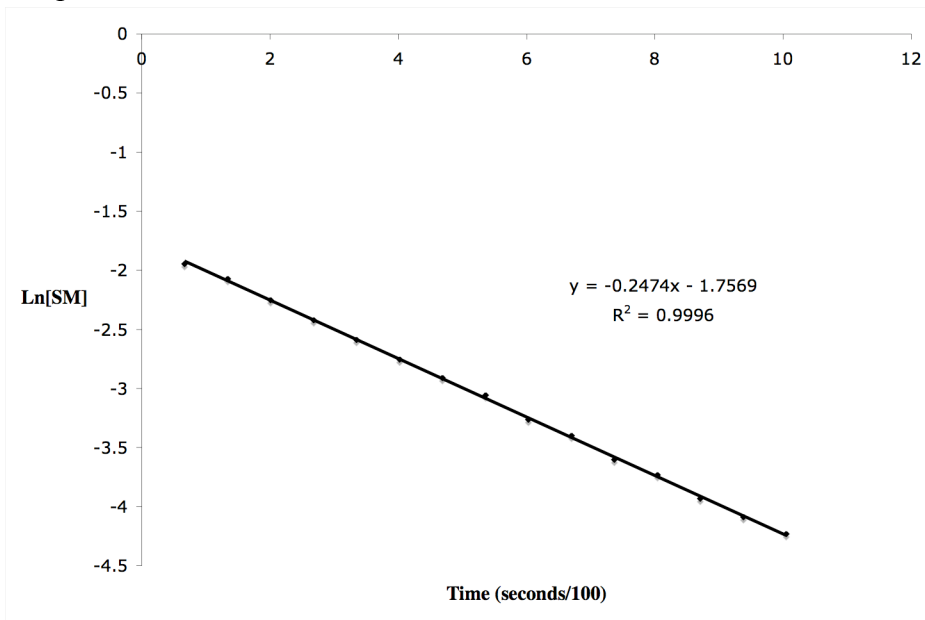


Figure 5-12: Determination of k_{obs} dependence on [benzaldehyde], (expt #5)

Benzaldehyde [0.173 M]

DBU [.156 M]

Temperature: 298 K

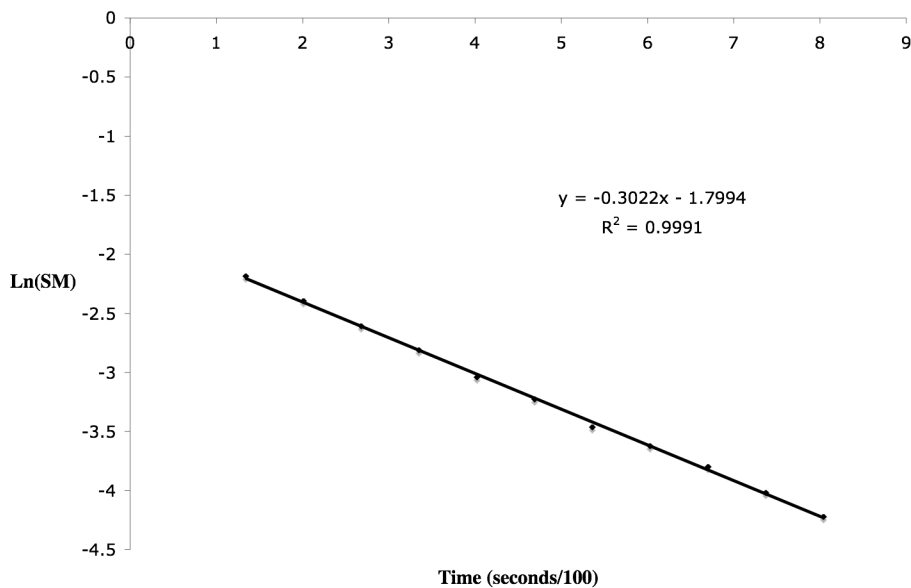


Figure 5-13: Determination of k_{obs} dependence on [benzaldehyde], (expt #6)

Benzaldehyde [0.260 M]

DBU [.156 M]

Temperature: 298 K

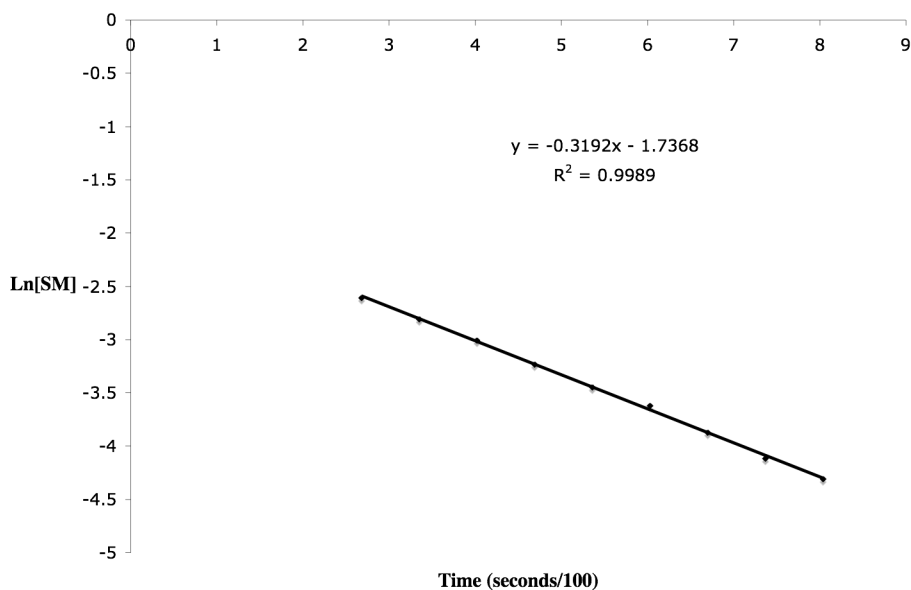


Figure 5-14: Determination of k_{obs} dependence on [DBU], experiment #1

Benzaldehyde [0.0174 M]

DBU [.0291 M]

Temperature: 298 K

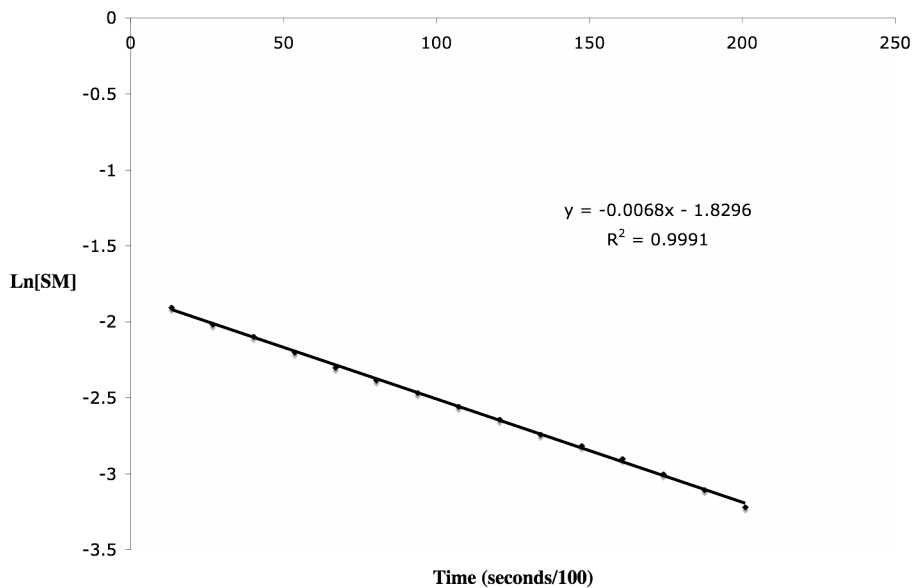


Figure 5-15: Determination of k_{obs} dependence on [DBU], experiment #2

Benzaldehyde [0.0174 M]

DBU [.0751 M]

Temperature: 298 K

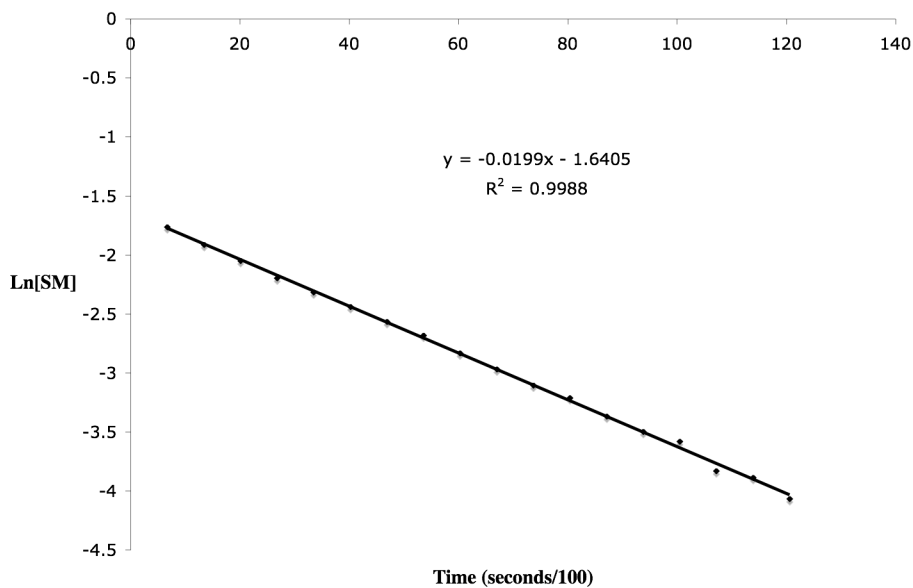


Figure 5-16: Determination of k_{obs} dependence on [DBU], experiment #3

Benzaldehyde [0.0174 M]

DBU [.113 M]

Temperature: 298 K

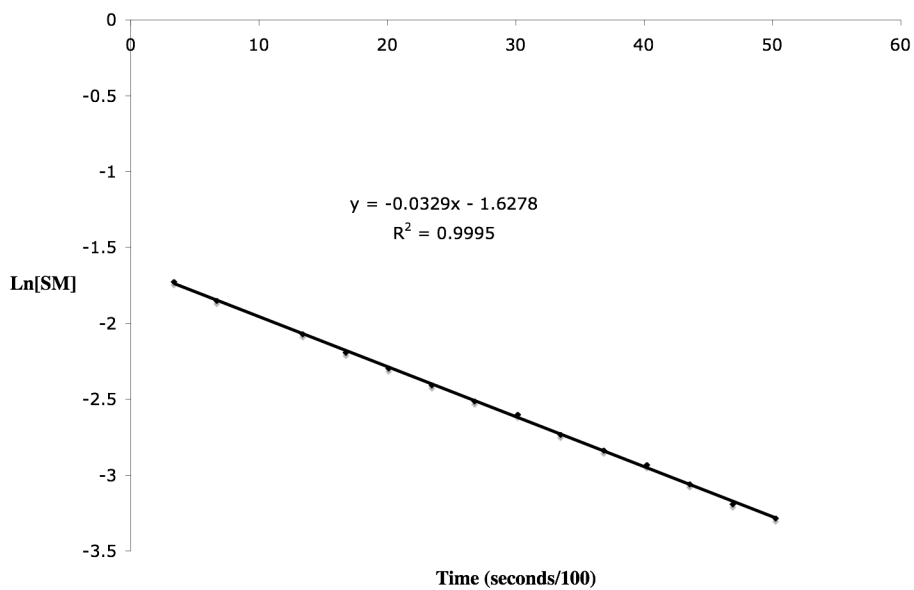


Figure 5-17: Plot of $\text{Ln}[k_{\text{obs}}]$ versus $\text{Ln}[\text{DBU}]$

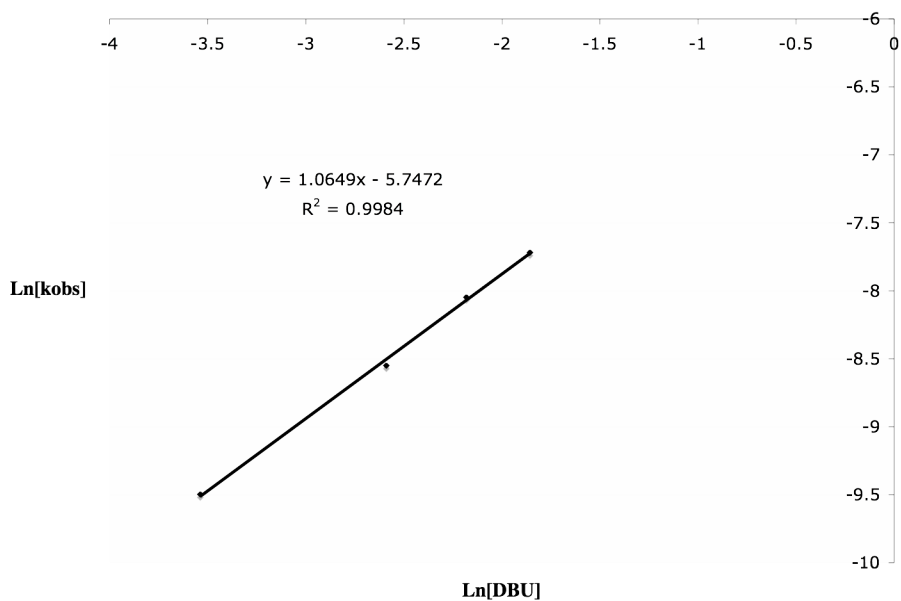


Figure 5-18: Temperature Studies, experiment #1

Benzaldehyde [0.0174 M]

DBU [.156 M]

Temperature: 308 K

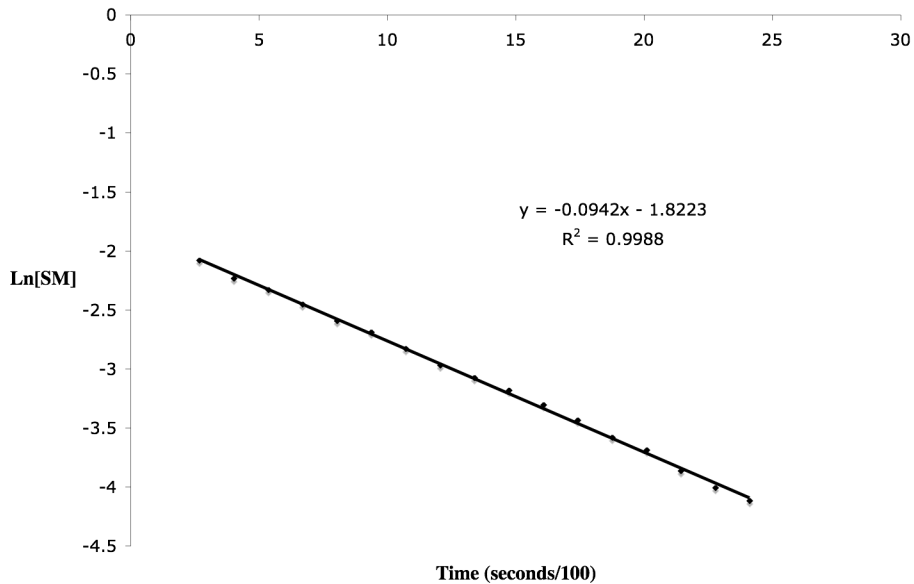


Figure 5-19: Temperature Studies, experiment #2

Benzaldehyde [0.0174 M]

DBU [.156 M]

Temperature: 319 K

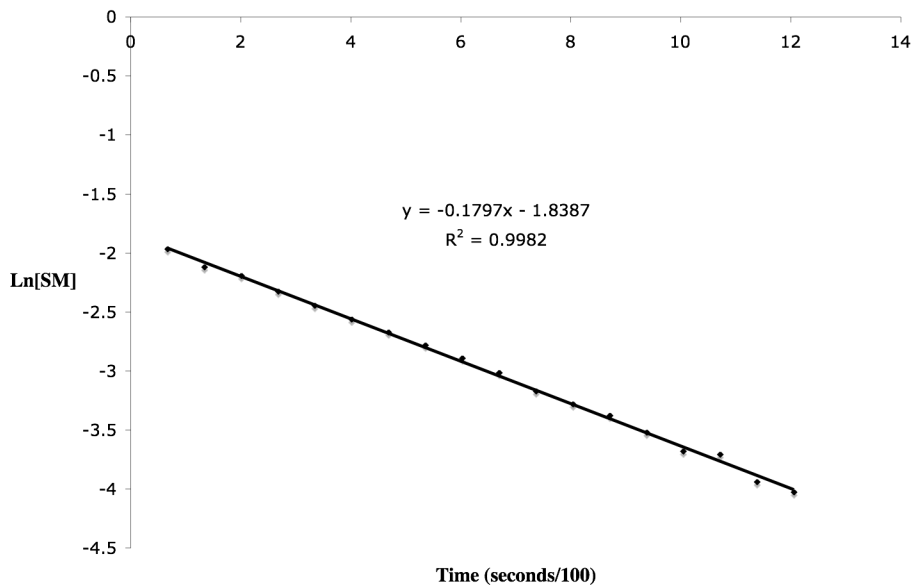
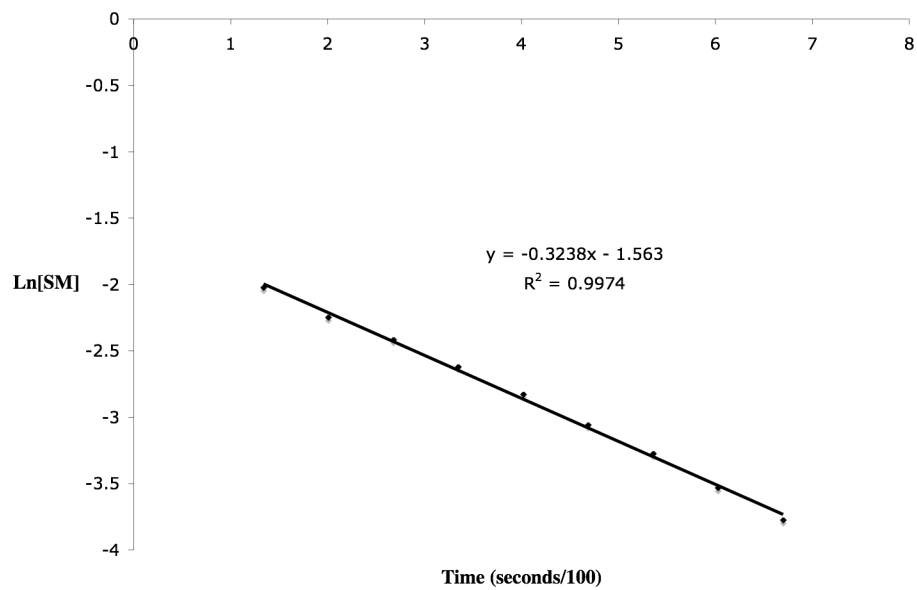


Figure 5-20: Temperature Studies, experiment #3

Benzaldehyde [0.0174 M]

DBU [.156 M]

Temperature: 328 K



Determination of ¹³C-KIE: Into a 1000 ml RBF equipped with stir bar was added successively benzaldehyde (8.52 g, 80.3 mmol), dimethylbenzylsulfonium tetrafluoroborate (18.32 g, 76.3 mmol), CH₃CN (500 ml) and finally DBU (17.95 g, 117.9 mmol). The reaction was left to stir at room temperature overnight at which time an aliquot was removed, concentrated at reduced pressure and an ¹H-NMR spectrum obtained from which conversion to product was determined to be 87.5%. The reaction was then quenched by the addition of saturated NH₄Cl, the aqueous layer was extracted with diethyl ether, dried with MgSO₄, filtered and the organic fraction concentrated on rotary evaporator. The crude material was next subjected to bulb-to-bulb distillation at full vacuum and at a temperature of 112 °C to recover 768 mg of unreacted benzaldehyde. The material so obtained was determined to be greater than 95% pure by ¹H-NMR and was directly subjected to quantitative ¹³C-NMR analysis. In preparing the sample for NMR analysis, the NMR tube was charged with 75% by volume benzaldehyde and 25% by volume CDCl₃. Quantitative ¹³C-NMR spectra were taken at 150.93 MHz using a 600 MHz Bruker spectrometer with inverse gated decoupling. All spectra were recorded at 298 K. The T₁ values were determined by the inversion recovery method and delays greater than 10 times T₁ were used in between successive pulses (144 seconds). The acquisition time was set manually to 3.999 seconds to collect 287764 points. The spectra were processed manually without applying an exponential decay (line broadening function) or performing any zero filling. A zero order base line correction was applied to all spectra. Integration ranges for all peaks of interest were set to a constant value of 0.120 ppm and this value was kept constant from one experiment to the next. The integral for the peak corresponding to the *para*-carbon was manually set to

1000 and acted as internal reference. Three KIE determinations were performed.

Isotopic enrichment in each KIE determination was performed by comparison to a benzaldehyde standard not subjected to epoxidation.

Table 5-4: ¹³C-NMR Data for KIE Determination

	C1 Integration	C1 Integration	C1 Integration	C1 Integration	C1 Integration
Experiment	Standard Expt. #1 and #2	KIE determination #1	KIE determination #2	Standard Expt. #3 ^a	KIE determination ^a #3
Spectra #1	930.347	964.866	957.074	973.780	1028.399
Spectra #2	923.603	955.080	956.186	969.456	1029.728
Spectra #3	927.648	962.471	965.189	970.837	1030.314
Spectra #4	928.796	959.223	959.374	976.064	1029.601
Spectra #5	926.809	962.250	965.057	971.629	1032.362
Spectra #6	927.734	-	957.674	975.586	1032.111
Spectra #7	-	-	-	975.082	1030.383
Spectra #8	-	-	-	976.622	-
Ave. Int.	927.489	960.778	960.092	973.632	1030.414
Std. dev. (ΔInt)	2.063	3.37	3.68	2.50	1.30

^{a)} Values obtained using 500 MHz spectrometer.

$$\text{KIE} = \frac{\ln(1-F)}{\ln(R/R_0(1-F))} \quad (\text{eq. 5-10})$$

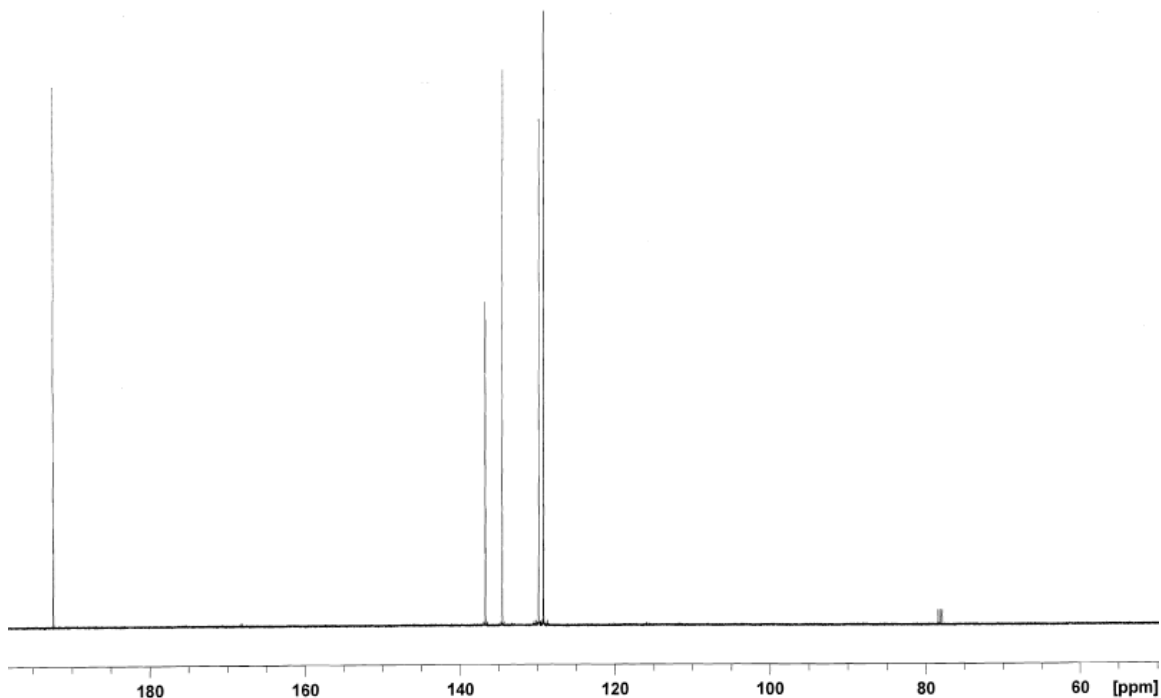
$$\Delta R/R_0 = R/R_0 \sqrt{(\Delta \text{Int}_{\text{std}}^2 / (\text{Ave. Int.})_{\text{std}}^2 + \Delta \text{Int}_{\text{expt}}^2 / (\text{Ave. Int.})_{\text{expt}}^2)} \quad (\text{eq. 5-18})$$

$$\Delta \text{KIE} = \frac{-\Delta R/R_0 \ln(1-F)}{R/R_0 \ln^2(R/R_0(1-F))} \quad (\text{eq. 5-19})$$

Table 5-5: Calculated ¹³C-KIE Data and Errors

KIE Determination	Conversion (%)	R/R ₀	ΔR/R ₀	KIE	ΔKIE
#1	76.0	1.0359	0.004	1.025	0.003
#2	75.1	1.0352	0.004	1.026	0.003
#3	87.5	1.0583	0.003	1.028	0.001

Figure 5-21: ^{13}C -NMR spectra of benzaldehyde



Determination of the secondary deuterium isotope effect (SDKIE) for benzaldehyde: Into a 50 ml flask equipped with a stir bar was added successively benzaldehyde (69.3 mg, 0.65 mmol), d₁-benzaldehyde (57.5 mg, 0.54 mmol), dimethylbenzylsulfonium tetrafluoroborate (239 mg, .99 mmol), *p*-chlorostyrene (32.6 mg, 0.26 mmol) as internal standard and CD₃CN (10 ml). An aliquot (200 uL) was removed from the stock solution, diluted with another 1 ml CD₃CN and stored under nitrogen and protected from light until ^1H -NMR was run to determine isotopic ratio prior to reaction. The stock solution was then split into two separate reaction vessels wrapped in aluminum foil and DBU (150 uL, 1.0 mmol) added via syringe to commence the reaction. The reaction was left to stir for 3 hrs at room temperature (295 K) at which time a 1 ml aliquot was removed and ^1H -NMR taken. A 600 MHz spectrometer was used to record ^1H -NMR spectra using a 20 second

delay between pulses. Multiple spectra were taken in all cases and average integration values used to determine R/R_o by comparison of integral sizes for the aldehydic proton (partially deuterated) to the *ortho* aromatic protons. The standard deviation for the NMR integrals and the errors associated with them in the DKIE determination are shown in Table 5-6.

Table 5-6: ¹H-NMR Data for SDKIE Determination

Expt #	$\frac{[SM^H]}{[SM^H]_0}$	Aldehyde-H Integration	Standard Deviation	Ortho-H Integration (assumed)	R/R _o	DR/R _o	k ^H /k ^D	DKIE
standard		273.784	0.35	1000	-	-	-	-
1	0.32	292.418	0.57	1000	0.918	0.002	0.9298	0.002
2	0.31	291.91	0.35	1000	0.920	0.002	0.9339	0.001

Determination of k_{rel} for Hammett Plot: The procedure to determine k^F/k^H is general to the procedure used to determine all k_{rel} values used to construct the Hammett plot. Into a flask equipped with a stir bar were added benzaldehyde (137 mg, 1.29 mmol), *p*-fluorobenzaldehyde (139 mg, 1.12 mmol), CH₃CN 6 ml, dimethylbenzylsulfonium tetrafluoroborate (34 mg, 0.14 mmol) and DBU (100 uL, 0.67 mmol). The reaction was left to stir overnight at room temperature at which time it was quenched with NH₄Cl_(sat) and extracted with dichloromethane (50 ml X 3). The organic layer was dried with MgSO₄, subjected to filtration and the filtrate evaporated to dryness. The product ratio was determined by high field ¹H-NMR (600 MHz) of the crude reaction mixture in C₆D₆. Equation 5-20 was used to calculate k_{rel}.

$$k_{\text{rel}} = \frac{[\text{epoxide}^{\text{X}}]/[\text{epoxide}^{\text{H}}]}{[\text{aldehyde}^{\text{X}}]/[\text{aldehyde}^{\text{H}}]} \quad (\text{eq. 5-20})$$

Epoxidation of ortho-iodobenzaldehyde: Into an RBF equipped with a stir bar were added *ortho*-iodobenzaldehyde (245 mg, 1.06 mmol), dimethylbenzylsulfonium tetrafluoroborate (359 mg, 1.50 mmol), CH₃CN 10 ml and DBU (300 mg, 1.97 mmol). The reaction was left to stir overnight at room temperature at which time it was quenched with NH₄Cl_(sat) and extracted with dichloromethane (X3). The organic layer was dried with MgSO₄ and filtered. The crude reaction mixture was purified by column chromatography and eluted with 5% EtOAc in hexanes. *trans-ortho*-iodostilbene oxide (304 mg, 89% yield). ¹H-NMR(500 MHz, CD₃CN) 7.90 ppm (dd, 0.86 Hz, 7.89 Hz, 1H), 7.12-7.49 ppm (m, 8H), 4.05 ppm (d, 1.67 Hz, 1H), 3.81 ppm (d, 1.98 Hz, 1H) ¹³C-NMR (500 MHz, CD₃CN) 140.41, 139.19, 137.35, 1130.27, 129.07, 129.03, 128.96, 126.44, 126.17, 96.42, 66.47, 62.11 ppm. HRMS (TOF MS EI+) calcd. 321.9855, found 321.9853 (C₁₄H₁₁O).

5.13: References

- 1) Aggrawal, V. K.; Harvey, J. N.; Richardson, J. J. *Am. Chem. Soc.* **2002**, *124*, 5747.
- 2) Price, E.P.; Broadwater, S.J.; Jung, H.M.; McQuade, D.T. *Org. Lett.* **2005**, *1*, 147.
- 3) Grabarnick, M.; Zamir, S. *Org. Proc. Res. Dev.* **2003**, *7*, 237.
- 4) Aggrawal, V. K.; Calamai, S.; Ford, J. G. *J. Chem. Soc. Perkin. Trans. 1* **1997**, 593.
- 5) Singleton, D. A.; Thomas, A. A. *J. Am. Chem. Soc.* **1995**, *117*, 9357.

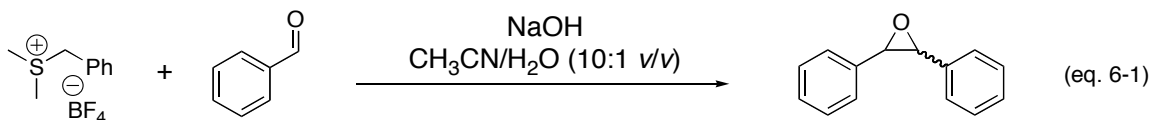
- 6) Melander, L.; Saunders, W.H. *Reaction Rates of Isotopic Molecules*, Wiley-Interscience Publication, New York, **1980**. Chapter 4, pages 95-102.
- 7) Crude reactions were checked by $^1\text{H-NMR}$ prior to isolation in order to determine percent conversion.
- 8) Melander, L.; Saunders, W.H. *Reaction Rates of Isotopic Molecules*, Wiley-Interscience Publication, New York, **1980**. Chapter 2, pages 52-54.
- 9) Yamataka, H.; Hanafusa, T. *J. Am. Chem. Soc.* **1986**, *108*, 6643.
- 10) Yamataka, H.; Nagareda, K.; Takatsuka, T.; Ando, K.; Hanafusa, T.; Nagase, S. *J. Am. Chem. Soc.* **1997**, *119*, 9975.
- 11) Yamataka, H.; Sasaki, D.; Kuwatani, Y.; Mishima, M.; Tsuno, Y. *J. Am. Chem. Soc.* **1993**, *115*, 8570.
- 12) Buncl, E.; Lee, C.C. *Secondary and Solvent Isotope Effects (Isotopes in Organic Chemistry)* **1997**, Elsevier Science Ltd.
- 13) All reagents were freshly prepared and/or purified just prior to use in order to prevent the Cannizzaro reaction. This transformation involves a primary deuterium isotope effect and therefore would be expected to alter isotopic fractionation in the experiment. For a full description of the experimental details see experimental section.
- 14) An excess of the slower reacting aldehyde was used in order to obtain a significant proportion of the product derived from this species and allow for accurate integrations to be made in the proton NMR spectrum.
- 15) Lansbury, P.T.; MacLeay, R.E. *J. Am. Chem. Soc.* **1965**, *87*, 831.
- 16) It often proved necessary to use different deuterated solvents in order to resolve the respective benzylic protons of the epoxide products.
- 17) Yamataka, H.; Nagareda, K.; Ando, K.; Hanafusa, T. *J. Org. Chem.* **1992**, *57*, 2865.
- 18) Yamataka, H.; Kawafuji, Y.; Nagareda, K.; Miyano, N.; Hanafusa, T. *J. Org. Chem.* **1989**, *54*, 4706.
- 19) a) Holm, T. *J. Am. Chem. Soc.* **1993**, *115*, 916.; b) Yamataka, H.; Matsuyama, T.; Hanafusa, T. *J. Am. Chem. Soc.* **1989**, *111*, 4912.
- 20) a) Yamataka, H.; Nagareda, K.; Takatsuka, T.; Ando, K.; Hanafusa, T.; Nagase, S. *J. Am. Chem. Soc.* **1993**, *115*, 8570.; b) Yamataka, H.; Takatsuka, T.; Hanafusa, T. *J. Org. Chem.*, **1996**, *61*, 722.

- 21) a) Gajewski, J.J.; Wojciech, B.; Harris, N.J.; Olson, L.P.; Gajewski, J.P. *J. Am. Chem. Soc.* **1999**, *121*, 326.; b) Gajewski, J.J.; Wojciech, B.; Brichford, N.; Henderson, J.L. *J. Org. Chem.* **2002**, *67*, 4236.
- 22) Yamataka, H.; Yamagushi, K.; Tsutomu, T. *Bull. Chem. Soc. Jpn.* **1992**, *65*, 1157.
- 23) Baker, J.W.; Hopkins, H.B. *J. Chem. Soc.* **1949**, 1089.
- 24) Bowden, K.; Hardy, M. *Tetrahedron*, **1966**, *22*, 1169.
- 25) Cordes, E.H.; Bull, H.G.; Amaral, L. *J. Am. Chem. Soc.* **1972**, 7579.
- 26) Hill, E.A.; Milosevich, S.A. *Tetrahedron Lett.*, **1976**, *35*, 3013.
- 27) Aggarwal, V.K.; Thompson, A.; Jones, R.V.H. *Tetrahedron. Lett.* **1994**, 8659.
- 28) Edwards, D.R.; Du, J.; Crudden, C.M. *Org. Lett.* **2007**, *9*, 2397.

Chapter 6: Epoxidations in an Aqueous System

6.1: Introduction

A second mechanistic study has been carried out in a mixed solvent system consisting of CH₃CN/H₂O (10:1 v/v), equation 6-1. The purpose of the investigation was to contrast the results of the last section concerning ylide epoxidations performed in purely organic solvent with a system better capable of supporting the various charges generated during conversion of aldehyde to epoxide. Indeed, it is seen that the reaction involves a proton transfer from a positively charged sulfonium salt to generate the zwitterionic sulfur ylide. This species then undergoes addition to benzaldehyde to generate yet another doubly charged species, the betaine intermediate. Lastly, a neutral epoxide is formed via ring closure and sulfide displacement, see Scheme 6-1. Given the various charged species generated along the reaction pathway and the ability of water as a co-solvent to stabilize these species, it was thought that mechanistic differences might in fact present themselves. Indeed, it was observed that the near complete regioselectivity in favor of *trans*-stilbene oxide for the reactions carried out in CH₃CN/DBU of Chapter 5, underwent significant erosion and that *cis*-stilbene oxide was produced in amounts of up to 15% under the aqueous conditions of the current study.

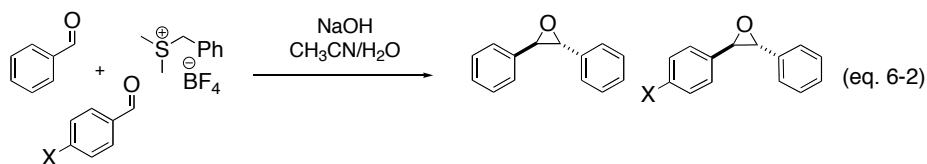


In the study reported in Chapter 5, absolute rate measurements were employed to deduce reaction order and activation parameters for the sulfur ylide epoxidation of

benzaldehyde. Under the current set of reaction conditions, the attainment of quality rate data proved elusive and as such a combination of relative rate and deuterium-labeling experiments were carried out.

6.2: Hammett Study

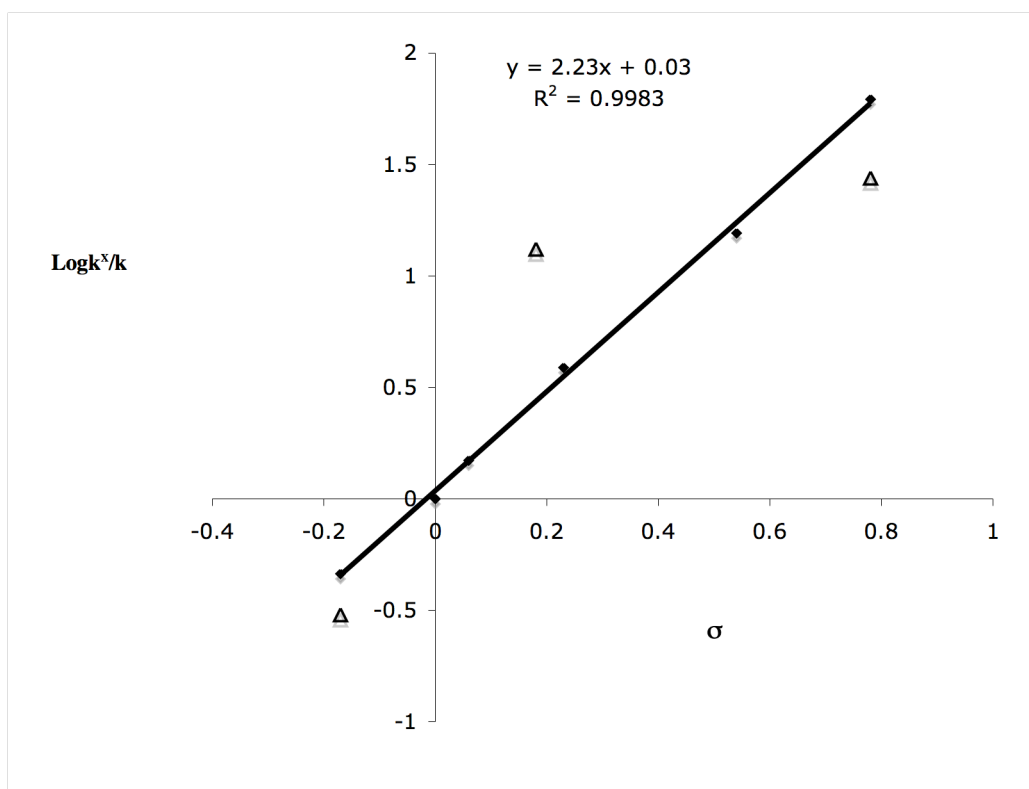
Substituent effects on the benzaldehyde reagent were studied in order to access the nature of charge development in the transition state for the reaction, equation 6-2. Relative rate constants were determined by competition experiments employing the previously described methodology. Significantly large ρ 's of 2.24 and 2.34 were obtained for *trans*-stilbene oxide and *cis*-stilbene oxide respectively, see Figures 6-1 and 6-2. On the whole, these values compare well with the previously determined value obtained in pure CH₃CN (2.50). The smaller magnitude of ρ determined for the current set of reaction conditions may result from the aqueous co-solvent employed, which, with its larger dielectric constant, is better able to dissipate charge.¹ From this study, it was determined that the k_{rel} for *p*-NO₂-benzaldehyde and benzaldehyde was 62.



Once again, *ortho*-substituted benzaldehydes were subjected to competition experiments and relative rate constants determined. Plotting the logarithm of k_{rel} versus the para-substituent constant, σ_p , revealed the expected downward deviation for *ortho*-Me and *ortho*-NO₂ substituents, while *ortho*-iodo-benzaldehyde displayed a significant upward deviation. These results are essentially identical to those reported in Chapter 5.

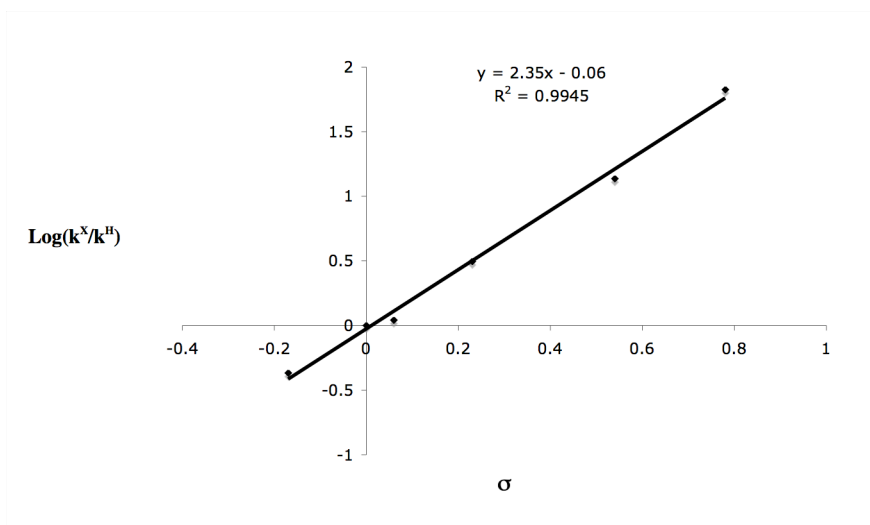
Interestingly, all *ortho* substituted benzaldehydes underwent epoxidation with increased levels of *trans* selectivity, for example *ortho*-iodostilbene oxide is obtained with 93% selectivity in favor of the *trans* isomer.

Figure 6-1: Hammett Plot (*trans*-stilbene oxide)^a



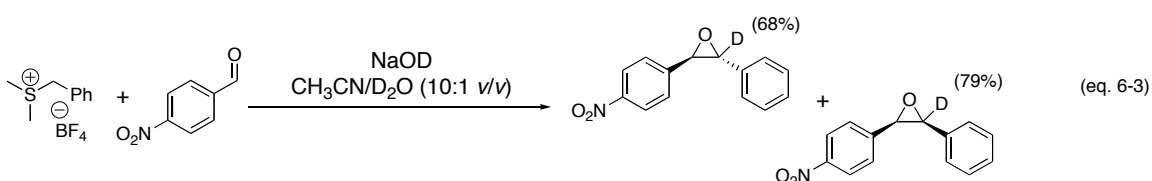
^a) Data points with triangle labels(Δ) are for *ortho*-substituted benzaldehydes

Figure 6-2: Hammett Plot (*cis*-stilbene oxide)



6.3: Deuterium Labeling Study

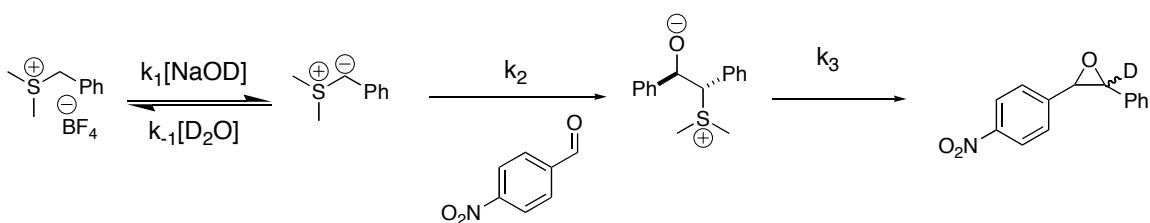
The next goal of the current mechanistic study was to verify that addition of sulfur ylide to benzaldehyde was in fact rate determining under aqueous reaction conditions. A rate limiting addition of ylide to benzaldehyde should be manifested in the form of a reversible proton transfer between sulfonium salt and hydroxide ion. To access the extent of reversibility in ylide generation a deuterium labeling study was carried out. The reactions were conducted in CH₃CN/D₂O (10:1, v/v) and 2 equivalents of NaOD were employed as base. The use of *p*-NO₂-benzaldehyde as substrate in the study permitted the direct determination of deuterium content in the epoxide products by simply integrating the relevant benzylic proton signals and comparing the size of the respective integrals. As a control, a ²H-NMR spectrum was also run to ensure that no deuterium had washed into the benzylic position corresponding to the aldehyde proton in the starting material and indeed no signal was observed.



Under typical reaction conditions employing a 1:1 ratio of *p*-NO₂-benzaldehyde and sulfonium salt, the deuterium content in *trans*-*para*-NO₂-stilbene oxide was determined to be 68% while the *cis*-isomer was determined to have undergone a slightly higher deuterium incorporation of 79%, equation 6-3. Efforts to monitor the epoxidation reaction under aqueous reaction conditions (CD₃CN/D₂O, 10:1 v/v) by ¹H-NMR

ultimately proved unsuccessful. However, it was repeatedly observed that upon addition of NaOD to the NMR tube, the sulfonium salt underwent quantitative deuteration prior to the recording of the first spectra. This fact further evidenced the fast nature of the proton transfer step. The high level of deuterium label incorporated into both epoxide isomers indicates that the sulfonium salt undergoes a reversible proton transfer (k_1/k_{-1}) prior to committing to product formation via k_2 or k_3 , Scheme 6-1.

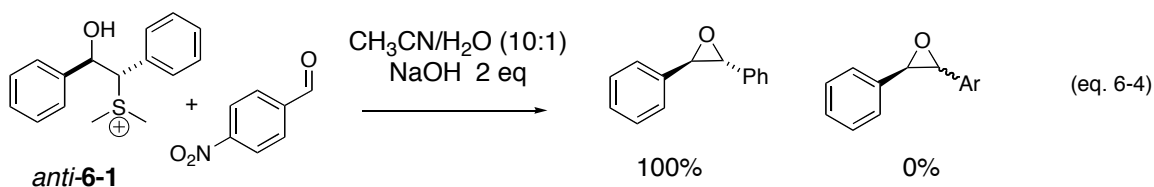
Scheme 6-1: Epoxidation Mechanism



6.4: Cross-Over Experiments with *anti*-1

Previous cross over experiments with *anti*-6-1 in DCM and DMSO have confirmed that addition of sulfur ylides to benzaldehyde is an irreversible process as was discussed in the Introduction.² In order to confirm like behavior under the current reaction conditions, a similar cross over experiment was undertaken. Treatment of *anti*-6-1 with NaOH in the mixed solvent system of CH₃CN/H₂O (10:1) was carried out using *p*-NO₂-benzaldehyde as the trapping agent (2 equivalents), equation 6-4. As stated, we have determined k_{rel} ($=k_{NO_2}/k_H$) for *p*-NO₂-benzaldehyde to be 62 in the epoxidation reaction with benzyldimethylsulfonium salts under these reaction conditions. Owing to the increased reactivity of this substrate and the fact that it is used in excess, the assumption that it will efficiently trap any free ylide that is generated is reasonable.

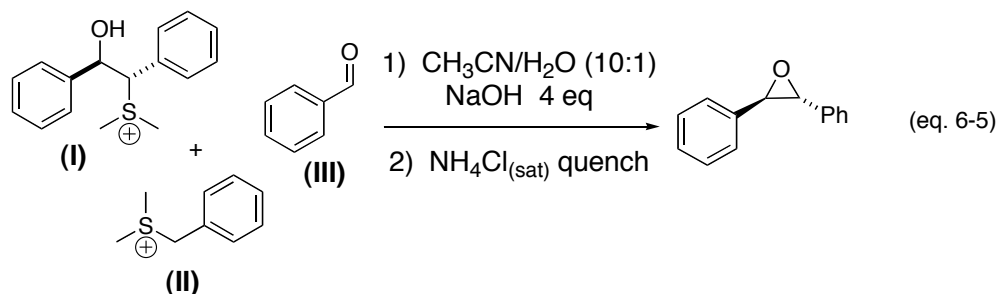
Under these reaction conditions, the only observable product obtained is *trans*-stilbene oxide, consistent with direct collapse of the anti-betaine to form the expected *trans*-epoxide product. The absence of any cross-over products indicates that the anti-betaine is formed irreversibly in the typical epoxidation reaction, in line with previous reports by Aggarwal.²



The relative rate at which *anti-1* collapses to product can be compared to the rate at which the typical epoxidation reaction proceeds by carrying out a competition experiment as outlined in equation 6-5.³ In the first part of the experiment, *anti-6-1* was treated with base and the reaction quenched with $\text{NH}_4\text{Cl}_{(\text{sat})}$ at ten minutes. The yield of *trans*-stilbene oxide under these conditions was determined to be 87% by $^1\text{H-NMR}$, Table 6-1, entry 1. This result indicated that *anti-6-1* had proceeded to high levels of conversion in this time frame. Next a 1:1:1 ratio of *anti-6-1*, benzaldehyde and benzyldimethylsulfonium tetrafluoroborate was subjected to the same reaction conditions and once again the reaction was quenched at 10 minutes. The yield of *trans*-stilbene oxide was determined to be 46%, Table 6-1, entry 2. Given that *anti-6-1* was already shown to proceed to high conversion in this time frame, it is reasonable to suggest the bulk of this 46% yield was derived from its collapse to epoxide product. As a control, benzyldimethylsulfonium tetrafluoroborate and benzaldehyde were reacted in the absence

of *anti*-**6-1** and once again the reaction quenched at ten minutes. The yield of *trans*-stilbene oxide was determined to be < 5%, Table 6-1, entry 3.

Table 6-1: Competition Experiments



Entry	I (equiv.)	II (equiv.)	III (equiv.)	Time (min)	Yield (%)
1	1	0	0	10	87
2	1	1	1	10	46
3	0	1	1	10	3

These results clearly indicate that the typical epoxidation reaction does not proceed to appreciable levels of conversion in this time frame (10 minutes). Furthermore the typical epoxidation reaction between benzyldimethylsulfonium tetrafluoroborate and benzaldehyde under aqueous conditions is always accompanied by production of *cis*-stilbene oxide. However, in all three of the competition experiments the integral corresponding to the benzylic protons of *cis*-stilbene oxide was either totally absent or too small to reliably integrate. This is further evidence that the production of *trans*-stilbene oxide in the competition experiment of entry 2 comes from collapse of the anti betaine rather than reversion of I to II and III and subsequent typical epoxidation is contributing only negligibly to the observed product.

A general picture of the relative rates of the various processes depicted in Scheme 6-1 may now be presented. The deuterium labeling results demonstrate that proton transfer (k_1/k_{-1}) is reversible as determined by label incorporation into the *p*-NO₂-stilbene oxide products. In all likelihood the extent of deuteration obtained for reaction of *p*-NO₂-benzaldehyde significantly underestimates the reversibility of this step for the reaction of benzaldehyde. As was previously stated, the k_{rel} for these two substrates is 62 and it might be supposed that near quantitative deuteration would be obtained if the labeling experiment were carried out on unsubstituted benzaldehyde.

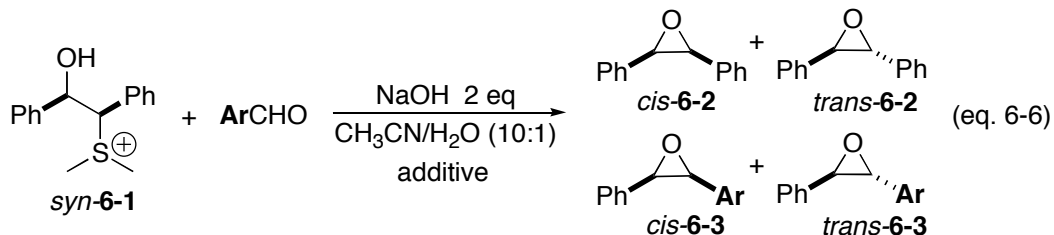
The results of the cross-over experiment demonstrate that *anti*-**6-1** does not revert to free benzaldehyde and sulfur ylide. It can then be stated that k_{-2} presents a significantly larger energy barrier to the betaine intermediate than does collapse to epoxide via k_3 . The competition experiments then give some indication of just how small a barrier there is to betaine collapse (k_3). It was seen that *anti*-**6-1** underwent high levels of conversion to epoxide while the typical epoxidation reaction underwent near negligible conversion in the same time frame. Ultimately, it is seen that the results of the current study in the solvent system of CH₃CN/H₂O (10:1 v/v) agree remarkably well the results of the last study in the purely organic solvent system and employing DBU as base. The sulfonium salt undergoes a fast and reversible proton transfer step prior to committing to product formation via addition to benzaldehyde (k_2). Sulfide displacement and generation of epoxide via ring closure does not appear to be a kinetically significant event.

6.5: Cross-Over Experiments with *syn-6-1*

Epoxidations conducted in the mixed solvent system of CH₃CN/H₂O (10:1 v/v) always led to the formation of *cis*-stilbene oxide as a minor by-product. It has previously been discussed that selectivity between *cis*- and *trans*-stilbene oxide formation in the epoxidation reaction has been proposed to result from a combined effect of irreversible sulfur ylide addition to form the *anti*-betaine while the *syn*-betaine is formed reversibly.^{2,4} The reversibility of *syn*-betaine formation under the current reaction conditions has been studied using *syn-6-1* in cross over experiments.

Carrying out a cross-over experiment on *syn-6-1* resulted in a vastly different outcome than with *anti-6-1*, equation 6-6. In this case, significant amounts of the cross-over products were obtained: *cis*-NO₂-stilbene oxide (*cis-6-3*) 10% and *trans*-NO₂-stilbene oxide (*trans-6-3*) 50%. *Trans*-stilbene oxide (*trans-6-2*) was also obtained in minor amounts, 9% with *cis*-stilbene oxide (*cis-6-2*) making up the mass balance at 31%; see Table 6-2, entry 1. The observation of cross-over products *cis* and *trans-6-3* indicates that the formation of the *syn*-betaine is reversible. However, the appearance of *trans*-stilbene oxide, albeit in minor amounts, was more difficult to explain.

Table 6-2. Cross-Over Studies with *syn*-**6-1**.^a



Entry	ArCHO	NaI	<i>cis</i> - 6-2	<i>trans</i> - 6-2	<i>cis</i> - 6-3	<i>trans</i> - 6-3
1	2 eq	–	31	9	10	50
2	10 eq	–	31	8	6	55
3	2 eq	1.5 eq	33	9	11	47

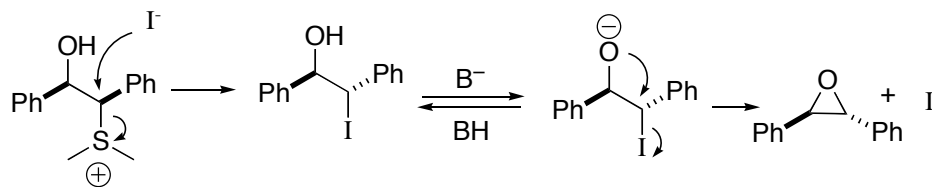
^aAr = *p*-nitrophenyl.

As noted, the k_{rel} for *para*-NO₂-benzaldehyde and benzaldehyde is 62:1 under the reaction conditions described. Despite this fact, the ratio of *trans*-**6-3** to *trans*-**6-2** obtained in the experiment is closer to 5:1. This is an order of magnitude lower than expected if both species are being produced via the free ylide, which then undergoes competitive trapping with the *para*-NO₂-benzaldehyde and benzaldehyde present in solution. Repeating the experiment with ten equivalents of *para*-NO₂-benzaldehyde to further bias formation of **6-3** remarkably gave the same result as with two equivalents (entry 2). This indicates that all the free ylide generated in the experiment is efficiently trapped by *para*-NO₂-benzaldehyde to form *para*-NO₂-stilbene oxide products.

In order to rule out the possibility that the *trans*-stilbene oxide is generated by a counterion promoted inversion of the betaine, the reaction was repeated in the presence of

excess iodide (entry 3). In this scenario, the iodide counter ion would first displace the sulfonium substituent with inversion at carbon in an S_N2-type process.⁵ The intermediate so generated would then undergo direct ring closure to provide stilbene oxide with *trans* geometry, and regenerate the iodide catalyst, Scheme 6-2.

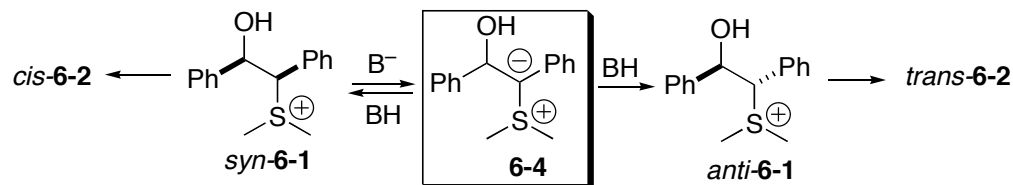
Scheme 6-2: Possible invertive process yielding *trans*-6-2 from *syn*-6-1.



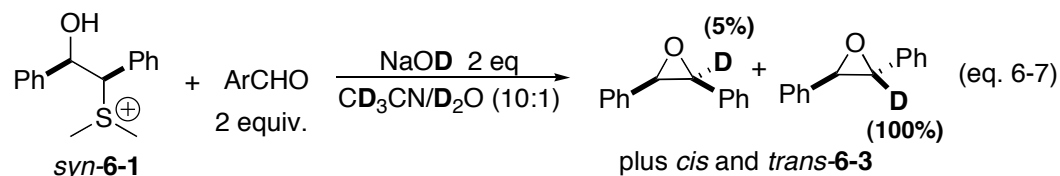
If this pathway were responsible for production of *trans*-stilbene oxide, the addition of exogenous iodide would be expected to alter the product distribution in the cross over experiment in favor of *trans*-stilbene oxide. As shown in Table 6-2, entry 3 the addition of 1.5 equivalents of NaI resulted in essentially no change in the product distribution. Consequently, a double inversion process such as that depicted in Scheme 6-2 can be discounted.

Having firmly ruled out (a) free ylide trapping with benzaldehyde and (b) counterion catalyzed isomerization of *syn*-betaine as sources of *trans*-stilbene oxide, we next turned to a third potential source of generating this product. Specifically, base catalyzed isomerization of *syn*-betaine-6-1 to *anti*-6-1; which could then undergo ring closure to afford *trans*-stilbene oxide. In this process, the *syn*-betaine would undergo deprotonation to furnish a new ylide species 6-4, Scheme 6-3. Betaines have previously been shown to be sp² hybridized⁶ and therefore reprotonation of 6-4 could occur from either face producing *anti*-6-1. Ring closure of *anti*-6-1 then produces *trans*-stilbene oxide.

Scheme 6-3: Base Catalyzed Isomerization



Evidence for the base catalyzed isomerization of betaines was obtained from a deuterium labeling study. The cross-over experiment was carried out with *syn*-6-1 as described in equation 6-6, but this time using $CH_3CN/D_2O/NaOD$. Under these reaction conditions, *trans*-stilbene oxide underwent quantitative deuteration at the expected site, equation 6-7. In contrast, only 5% deuteration was observed in the *cis* product.



These results indicated that once deprotonation of *syn*-6-1 occurs to generate 6-4, reprotonation or redeuteration occurs almost stereospecifically to yield *anti*-betaine 6-1, which collapses to yield *trans*-6-2. The reason for this specificity was illustrated by performing a similar cross-over experiment starting with *anti*-6-1. As expected, this substrate afforded no deuteration in the *trans*-stilbene oxide product, which was obtained quantitatively, i.e. without any cross over products. These two results indicate that only the *syn*-betaine and not the *anti*-betaine is sufficiently persistent to undergo the proton transfer/isomerization process. These findings further bolster Aggrawal's suggestion that the diastereoselectivity in typical epoxidations of this type results from a fast collapse of

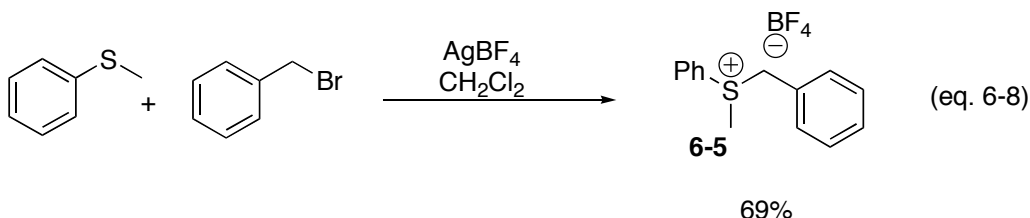
the *anti*-betaine to the corresponding *trans*-epoxide, compared with the slow collapse of *syn*-betaines.^{2,6}

It should be noted that the base catalyzed isomerization of betaines is not without precedent. Vedjes and co-workers elegantly demonstrated that phosphonium betaine analogues undergo similar deprotonations.⁷ Furthermore, Aggrawal has proposed that the near identical product distribution obtained in cross over experiments with *anti* and *syn*-betaines of ester and amide stabilized *N*-tosyl-protected imines may result from base catalyzed equilibration of betaines.⁸ However, since incomplete trapping of free ylide in these experiments could also account for the product distributions obtained, the definitive demonstration of interconversion of *syn* and *anti* betaines is important.⁹ Considering that ester and amide stabilized betaines represent even more activated substrates for base catalyzed isomerization, it is entirely likely that a similar process is operative with these substrates.

The present study on the reactivity of *syn*-**6-1** in cross over experiments convincingly demonstrates for the first time that betaine intermediates in the Corey-Chaykovsky reaction can indeed undergo a base catalyzed isomerization. This process is likely to increase diastereoselectivity in favor of the preferred *trans*-isomer. On the other hand if the *syn*- and *anti*-betaines result from addition to opposite faces of the aldehyde then deleterious consequences in terms of enantioselectivity can be envisioned.

6.6: Studies of other sulfonium reagents

Throughout the course of the study, a number of variations on the chosen reaction conditions were investigated, albeit often only briefly. Cross-over experiments were performed in both dichloromethane and DMSO. The results of these experiments essentially confirmed conclusions drawn from previous studies and this avenue of research was not pursued any further. A large number of amine bases other than DBU were tested in the reaction and other than the chiral base sparteine, little or no conversion to product was obtained employing these alternative reagents. The effects of substituents on sulfur were also investigated by substituting one and two of the methyl groups on dimethylbenzylsulfonium tetrafluoroborate with phenyl groups.



The synthesis of **6-5** is shown in equation 6-8. It is seen that an Ag^+ source is required to affect the desired benzylation of thioanisole. Employing **6-5** in the competition experiments with different benzaldehyde reagents permitted the determination of relative rate constants and the construction of yet another series of Hammett plots. These are shown in Figures 6-3 and 6-4 for the *trans* and *cis*-epoxides, respectively. Large positive slopes were obtained in each of these plots. Interestingly, the diastereoselectivity obtained employing **6-5** is significantly lower than that previously observed with dimethylbenzylsulfonium tetrafluoroborate. In the competition experiments, it was determined that *trans*:*cis*-epoxide ratios were generally in the range

of 1.6-1.7:1. Sulfonium salt **6-5** was also subjected to a deuterium labeling experiment, equation 6-9. Significant levels of deuterium were in fact observed in both the *cis* and *trans*-epoxide products although label incorporation employing **6-5** was decidedly lower than with the parent reagent dimethylbenzylsulfonium tetrafluoroborate.

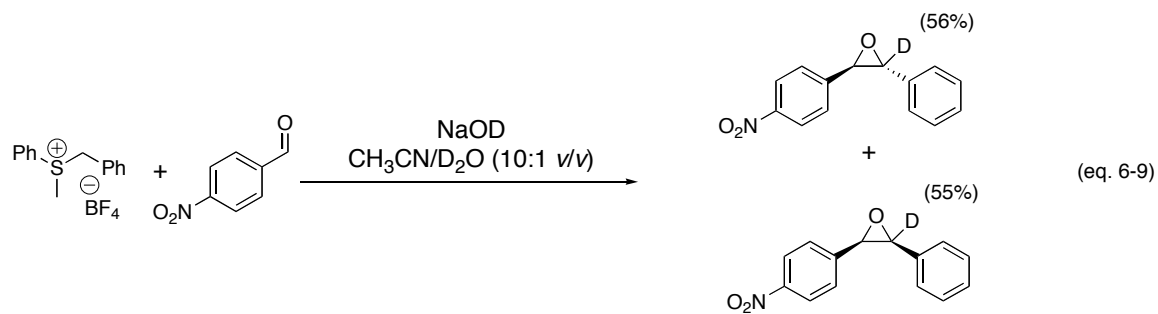


Figure 6-3: Hammett Plot for Sulfonium Salt **6-5** (*trans*-epoxide)

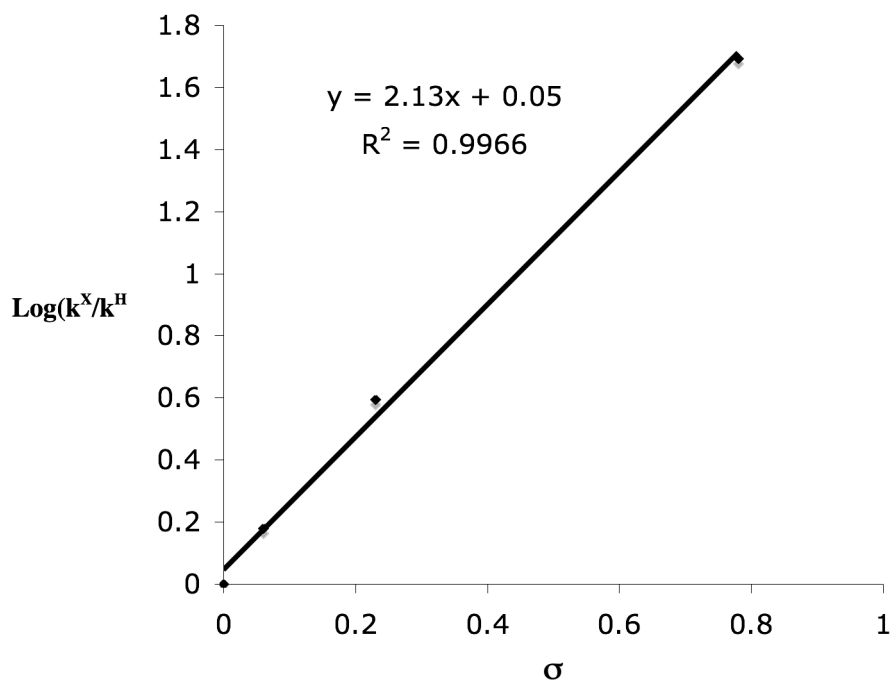
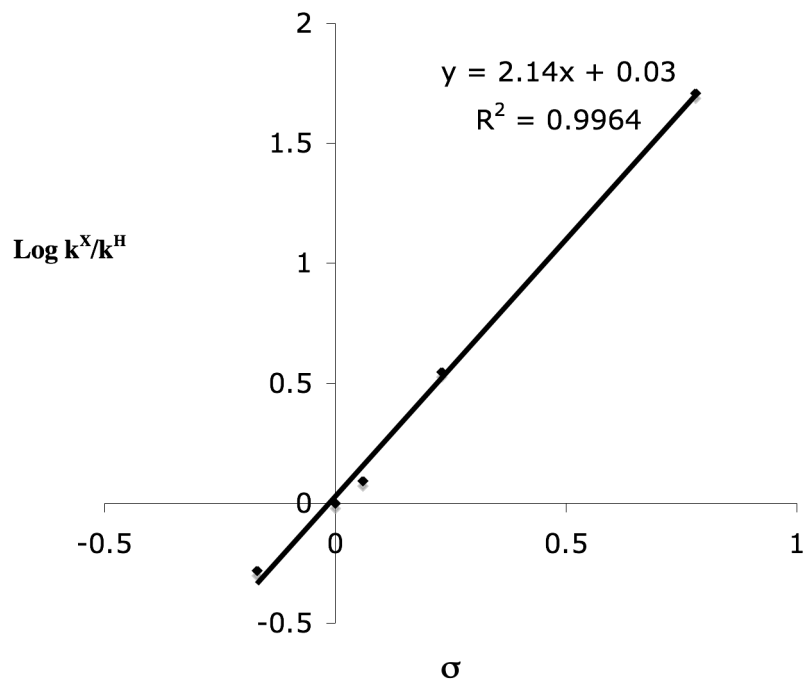
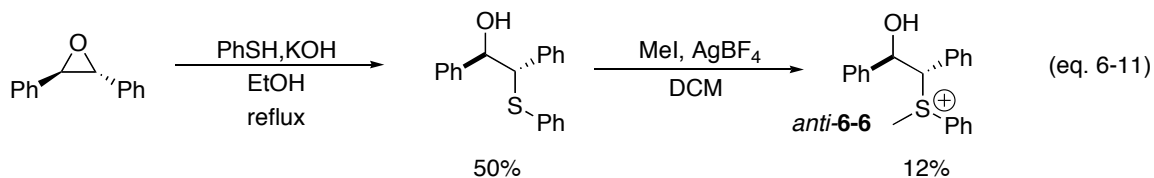
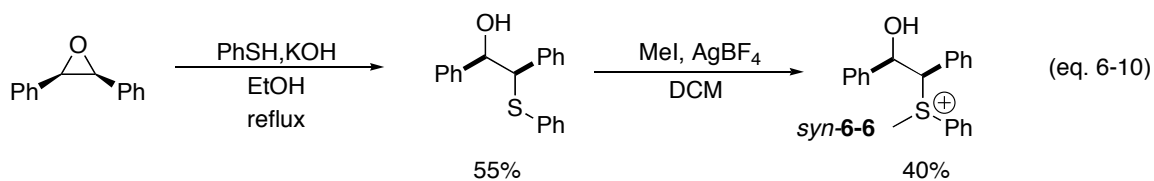


Figure 6-4: Hammett Plot for Sulfonium Salt **6-5** (*cis*-epoxide)



That lower *trans* selectivity is obtained in reactions employing **6-5**, as compared to the parent dimethylbenzyl sulfonium salt, provides a potential opportunity to confirm one of the currently held tenants in the field of ylide epoxidations. Namely that high *trans*-selectivity in sulfur ylide epoxidations results from a combination of irreversible formation of the *anti*-betaine, while the *syn*-betaine exists in equilibrium with free ylide and aldehyde.² If this statement is correct, then one can deduce that epoxidations mediated with **6-5** should display decreased reversibility of *syn*-betaine formation relative to that obtained with dimethylbenzylsulfonium tetrafluoroborate. This hypothesis can be verified simply by carrying out cross over experiments with betaines derived from **6-5** and comparing the results to those previously determined for *syn* and *anti*-**6-1**.



The synthesis of betaine precursors *syn* and *anti*-**6-6** are outlined in equations 6-10 and 6-11. It is seen that once again AgBF_4 was required to affect alkylation of the aryl-substituted sulfide. Subjecting *anti*-**6-6** to the cross over experiment and once again employing *para*- NO_2 -benzaldehyde as trapping agent led to the expected quantitative formation of *trans*-stilbene oxide, equation 6-12. Next *syn*-**6-6** was applied to the cross over experiment, the results of which are shown in Table 6-3. Direct closure to *cis*-stilbene oxide accounted for the vast majority of product formation in this case, 88%.

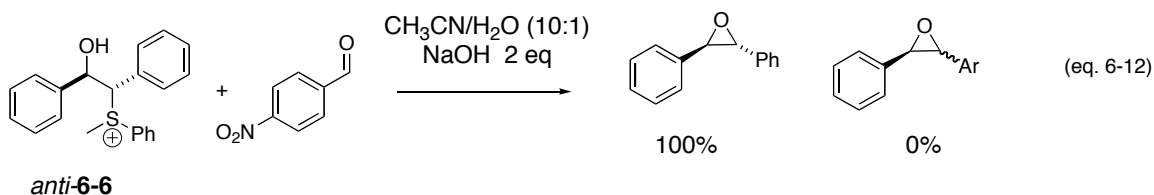
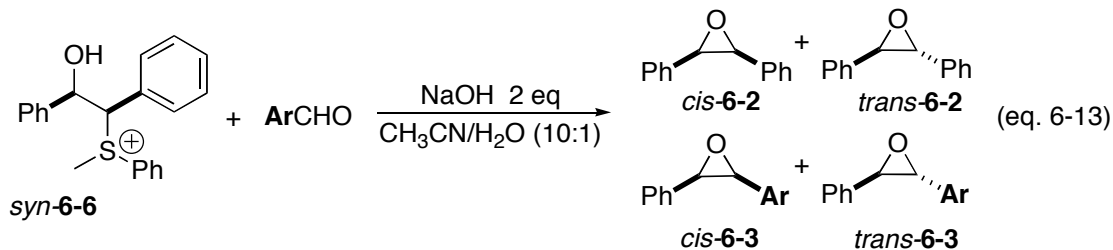


Table 6-3: Cross-Over Studies with *syn*-**6-6**.^a



<i>cis</i> - 2	<i>trans</i> - 2	<i>cis</i> - 3	<i>trans</i> - 3
88%	2%	4%	6%

^aAr = *p*-nitrophenyl.

Comparison of the results in Table 6-2 (*syn*-**6-1**) to those shown in Table 6-3 (*syn*-**6-6**) reveal that *syn*-**6-1** undergoes on the order of 60% total reversion to free ylide and aldehyde compared to the 10% reversion observed employing *syn*-**6-6**. These findings are in accord with the theory that increased selectivity for *trans*-epoxide production is correlated with increased reversibility in *syn*-betaine formation. It should be noted that once again *trans*-stilbene oxide formation was observed in the cross over experiment and its probable source is the base catalyzed isomerization process already discussed for *syn*-**6-1**. The low amount of this species formed in the reaction, however, precluded performing a deuterium labeling study to conclusively confirm the source of its formation.

Given that *syn*-betaine formation from sulfonium reagent **6-5** represents a nearly irreversible process, it only follows that selectivity in the reaction is largely a function of preferential addition of ylide to benzaldehyde to form either the *syn* or *anti*-betaine intermediate. Selectivity in the typical epoxidation reaction with **5** is on the order of 1.6-1.7:1 and therefore one may surmise that addition to form the isomeric betaines is

differentiated by as little as 0.30 kcal/mol at 25 °C.¹⁰ It is somewhat surprising that such a small energy difference is associated with the different addition geometries between ylide and benzaldehyde, although DFT calculations have previously predicted just such a phenomena.⁴

6.7: Conclusions

The epoxidation of benzaldehyde with dimethylbenzylsulfonium tetrafluoroborate has been studied in a mixed solvent system of CH₃CN/H₂O (10:1 v/v). At the outset of the study, it was anticipated that the inclusion of water as co-solvent might have an impact on the reaction. It does in fact alter the selectivity resulting in a greater production of the unwanted *cis*-stilbene oxide. Nonetheless, the general scheme for *trans*-stilbene oxide production remains largely intact. The generation of ylide from sulfonium salt is a fast and reversible proton transfer. The next step in the reaction is a rate determining addition of ylide to benzaldehyde. The effect of aqueous co-solvent is most clearly seen in the slope of the Hammett plot, which undergoes the expected decrease in magnitude from 2.5 to 2.3.

The base catalyzed isomerization of *syn*-**6-1** to *anti*-**6-1** has been demonstrated for the first time. It is likely that this process is specific to an aqueous solvent system as cross over experiments with *syn*-**6-1** in CH₃CN/DBU leads to near undetectable levels of *trans*-stilbene oxide. Comparison of the results obtained for **6-5** with the parent dimethylbenzylsulfonium tetrafluoroborate reagent revealed that increased reversibility in

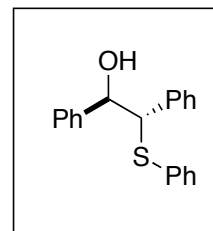
syn-betaine formation is correlated with higher levels of *trans*-epoxide formation in complete accord with theory.

6.8: Experimental Section

General Experimental: Dimethyl(benzyl)sulfonium tetrafluoroborate¹¹ and **6-5**¹² were prepared by the reported procedures. The betaine precursors *anti* and *syn*-**6-1** were prepared by the method of Aggarwal.¹³ NMR (¹H and ¹³C), mass spectra and melting points were all in accord with previously reported values. NaOD was prepared by the dropwise addition of D₂O to metallic sodium. Acetonitrile, diethyl ether and dichloromethane were purified by means of a solvent purification system consisting of alumina packed columns. Methyl iodide and sodium iodide were purchased from Aldrich and used without further purification. *p*-nitrobenzaldehyde and other solid aldehyde reagents were sublimed under reduced pressure and obtained as white needles. Benzaldehyde and other liquid aldehydes were distilled at reduced pressure prior to use.

Synthesis of alpha-Hydroxysulfonium Salt anti-6-6: *Trans*-stilbene oxide (1.27 g, 6.48 mmol) and thiophenol (2.0 ml, 19.5 mmol) were taken up in 10 ml anhydrous ethanol. To this was added KOH pellets (1.02 g, 18.2 mmol) and a reflux condenser was attached to the flask.

The reaction was refluxed under N₂ for three hours and then left



to stir at ambient temperature overnight. Ethanol was removed from the crude reaction mixture at reduced pressure and NaHCO_{3(sat)} added. The aqueous layer was extracted

with EtOAc. Concentration of the organic layer under reduced pressure furnished a brown oil that was taken up in diethyl ether and treated with hexanes to precipitate a gray solid, (988 mg, 50%).

$^1\text{H-NMR}$ (500 MHz, CD_3CN) 7.25 ppm (m, 15H), 5.10 ppm(app. t, 1H), 4.62 ppm (d, 6.13 Hz, 1H), 3.63 (d, 4.26 Hz, 1H).

$^{13}\text{C-NMR}$ (500 MHz, CD_3CN) 142.74, 139.45, 135.47, 131.61, 129.80, 129.20, 128.23, 128.15, 127.85, 127.54, 127.15 (2 peaks), 76.03, 60.12 ppm. HRMS (TOF MS EI+) calcd. 306.1065, found 306.1078 ($\text{C}_{20}\text{H}_{18}\text{OS}$).

A portion of the sulfide (453 mg, 1.44 mmol) obtained from the first reaction sequence was taken up in 6 mL of iodomethane. To the stirring solution was added AgBF_4 (280 mg, 1.44 mmol) in several batches over a thirty-minute period. The progress of the reaction was monitored by TLC for disappearance of starting material and at 3 hours the crude reaction mixture was filtered through a fritted funnel loaded with celite.

Concentration of the volatiles from the filtrate revealed a brownish-white semi-solid. This material was repeatedly recrystallized from dichloromethane and diethyl ether to yield 70 mg (12%) of the title compound.

$^1\text{H-NMR}$ (500 MHz, CD_3CN) 7.65 ppm (m, 3H), 7.51 ppm (app. t, 2H), 7.25 ppm (m, 10H), 5.74 ppm (app. t, 1H), 5.10 ppm (d, 4.03 Hz, 1H) 4.72 ppm (d, 3.84 Hz, 1H), 3.46 ppm (s, 3H).

$^{13}\text{C-NMR}$ (500 MHz, CD_3CN) 139.06, 134.79, 131.55, 130.94, 130.81, 130.16, 129.17, 128.86, 128.49, 128.44, 126.53, 123.35, 123.14, 71.10, 70.97, 24.72 ppm. HRMS (TOF MS) calcd. 321.13131, found 321.13023 ($\text{C}_{21}\text{H}_{21}\text{OS}$).

m. p. = 97-98 °C

Synthesis of alpha-Hydroxysulfonium Salt syn-6-6: *cis*-Stilbene oxide (1.60 g, 8.16 mmol) and thiophenol (2.5 ml, 24 mmol) were taken up in 15 mL of anhydrous ethanol. To this was added KOH (1.3 g, 24 mmol) and a reflux condenser was then attached to the flask. Reaction was refluxed under N₂ for six hours and then left to stir at ambient temperature overnight. Ethanol was removed from the crude reaction mixture at reduced pressure and NaHCO_{3(sat)} added. The aqueous layer was extracted with EtOAc.

Concentration of the organic layer under reduced pressure furnished a brown semi-solid, which was triturated with hexanes to reveal a yellow oil, (1.362 mg, 55%). This material was subjected to ¹H-NMR and determined to be sufficiently pure to be carried forward in the subsequent alkylation procedure. In the next reaction sequence, the sulfide (1.362 g, 4.45 mmol) was taken up in 20 ml of iodomethane. To this was added AgBF₄ (866 mg, 4.45 mmol) and the reaction diluted with 10 ml dichloromethane to increase fluidity. The reaction was left to stir for six hours upon which time the stirring suspension was filtered through a fritted funnel packed with celite. Concentration of the volatiles on a rotary evaporator revealed a colorless solid that could be repeatedly recrystallized from dichloromethane and diethyl ether to yield 567 mg (40%) of the title compound.

¹H-NMR(500 MHz, CD₃CN) 7.40 ppm (m, 15H), 5.46 ppm (dd, 2.74 Hz, 10.39 Hz, 1H), 5.33 ppm (d, 10.53 Hz, 1H), 4.89 ppm (d, 3.30 Hz, 1H), 3.40 ppm (s, 3H).

¹³C-NMR (500 MHz, CD₃CN) 140.07, 134.60, 132.12, 131.35, 130.75, 130.56, 130.14, 129.34, 129.21, 128.93, 127.58, 122.75, 75.16, 73.32, 27.86 ppm.

HRMS (TOF MS) calcd. 321.13131, found 321.13024 (C₂₁H₂₁OS).

Deuterium labeling experiment: Into a 25 ml flask equipped with a stirring bar was added *p*-nitrobenzaldehyde (70.5 mg, 0.47 mmol) and dimethyl(benzyl)sulfonium tetrafluoroborate (120 mg, 0.50 mmol). This was taken up in acetonitrile (5 ml) and D₂O (250 uL). The reaction was stirred for five minutes until dissolution occurred. To this was added 4M NaOD (250 uL, 1.0 mmol). The reaction was left to stir overnight at ambient temperature. The reaction was quenched by the addition of saturated NH₄Cl and extracted with dichloromethane (X3). The organic layer was dried with MgSO₄, subjected to filtration and evaporated to dryness. ¹H-NMR of crude material showed that the ratio of *trans*-stilbene oxide to *cis*--stilbene oxide was 5:1 as determined by comparison of aryl substituted benzyl peaks. Deuterium content in each isomer was determined by comparing the peak sizes for the respective aryl-substituted benzyl proton to the phenyl-substituted benzyl proton. From this it was determined that the deuterium content in the *trans*-isomer was 68% while that of the *cis*-isomer was 79%. (The deuterium labeling experiment, employing sulfonium salt **6-5**, was performed in an analogous manner.)

Competitions Experiment 1: Into a 25 ml flask equipped with a stirring bar was added *anti*-**6-1** (38.6 mg, 0.10 mmol). This was taken up in acetonitrile (2 ml) and H₂O (167 uL). The reaction was stirred for five minutes until dissolution occurred. To this was added 6M NaOH (33 uL, 0.20 mmol). The reaction was left to stir at ambient temperature for ten minutes. The reaction was quenched by the addition of saturated NH₄Cl and the crude mixture extracted with dichloromethane (three times). The organic layer was dried with MgSO₄, subjected to filtration and evaporated to dryness. To the

concentrated crude material was added *p*-chlorostyrene (18.1 mg, 0.131 mmol) as internal standard. Yield of *trans*-stilbene oxide as determined by ¹H-NMR integrated relative to *p*-chlorostyrene was 87%.

Competitions Experiment 2: Into a 25 ml flask equipped with a stirring bar was added *anti*-**6-1** (36.7 mg, 0.095 mmol), benzaldehyde (10 uL, .099 mmol) and dimethyl(benzyl)sulfonium tetrafluoroborate (24 mg, 0.10 mmol). This was taken up in acetonitrile (2 ml). The reaction was stirred for five minutes until dissolution occurred. To this was added 2M NaOH (200 uL, 0.40 mmol). The reaction was left to stir at ambient temperature for ten minutes. The reaction was quenched by the addition of saturated NH₄Cl and extracted with dichloromethane (three times). Organic layer was dried with MgSO₄, subjected to filtration and evaporated to dryness. To the concentrated crude material was added *p*-chlorostyrene (19.8 mg, 0.143 mmol) as internal standard. Yield of *trans*-stilbene oxide as determined by ¹H-NMR integrated relative to *p*-chlorostyrene was 47%.

Competitions Experiment 3: Into a 25 ml flask equipped with a stirring bar was added benzaldehyde (10.6 mg, 0.10 mmol) and dimethyl(benzyl)sulfonium tetrafluoroborate (30 mg, 0.12 mmol). This was taken up in acetonitrile (2 ml) and H₂O (30 uL). The reaction was stirred for five minutes until dissolution occurred. To this was added 2M NaOH (170 uL, 0.34 mmol). The reaction was left to stir at ambient temperature for ten minutes. Reaction was quenched by the addition of saturated NH₄Cl and extracted with dichloromethane (three times). Organic layer was dried with MgSO₄, subjected to

filtration and evaporated to dryness. To the concentrated crude material was added *p*-chlorostyrene (18.9 mg, 0.136 mmol) as internal standard. Yield of *trans*-stilbene oxide as determined by ¹H-NMR integrated relative to *p*-chlorostyrene was 3%.

Typical cross over experiment with syn-6-1: Into a 25 ml flask equipped with a stirring bar was added *alpha*-hydroxysulfonium salt *syn-6-1* (34.8 mg, 0.09 mmol) and *p*-nitrobenzaldehyde (32.3 mg, 0.21 mmol). This was taken up in 2 ml CH₃CN and 170 μ L distilled water. After the material completely dissolved, 6 M NaOH (30 μ L, 0.18 mmol) was added. The reaction was left to stir overnight at room temperature at which time it was quenched with NH₄Cl_(sat) and extracted with dichloromethane (three times). The organic layer was dried with MgSO₄, subjected to filtration and evaporated to dryness. The product ratio was determined by high field ¹H-NMR (600 MHz) in CDCl₃.

Deuterium labeling experiment with syn-6-1: Into a 25 ml flask equipped with a stirring bar was added *alpha*-hydroxysulfonium salt *syn-6-1* (400 mg, 1.04 mmol) and *p*-nitrobenzaldehyde (300 mg, 1.99 mmol). This was taken up in 13 ml CH₃CN and 870 μ L D₂O. After the material was completely dissolved, 4.65 M NaOD (430 μ L, 2 mmol) was added to the reaction vessel. The reaction was left to stir overnight at room temperature at which time it was quenched with NH₄Cl_(sat) and extracted with dichloromethane (three times). The organic layer was dried with MgSO₄, subjected to filtration and evaporated to dryness. The crude material was purified by column chromatography (gradient elution 1–10% EtOAc in hexanes). The products of the reaction were identified by ¹H-NMR (600 MHz) in CDCl₃ and compared to authentic samples. The first fraction contained a

mixture of *cis*- and *trans*-stilbene oxides (**6-2**) in a ratio of 3:1 (*cis:trans*), (68 mg, 0.35 mmol, 34%yield). Integrating the size of the benzylic epoxide peaks and comparing these to the integrals obtained for the resolved aromatic peaks allowed for the determination of the deuterium content in the isomers. These values are reported in the main text. Deuterium NMR was also run on this fraction. The only peaks observed in the spectrum corresponded to the benzylic protons (deuterium atoms) of *cis*- and *trans*-stilbene oxides. These were integrated in a ratio of 4:1 (*trans:cis*). The second fraction contained a mixture of *cis*- and *trans*-*p*-nitrostilbene oxides (**6-3**) in a ratio of 1:3 (*cis:trans*), (134 mg, 0.56 mmol, 54%yield). Mass balance 88%.

Determination of k_{rel} between benzaldehyde and p-nitrobenzaldehyde: The following procedure is typical of all k_{rel} determinations performed in the study. Into a flask equipped with a stirring bar were added benzaldehyde (701 mg, 6.61 mmol), *p*-nitrobenzaldehyde (119 mg, 0.79 mmol), CH₃CN 10 ml, distilled water 800 uL, dimethyl(benzyl)sulfonium tetrafluoroborate (24 mg, 0.1 mmol) and 6 M NaOH (200 uL, 1.20 mmol). The reaction was left to stir overnight at room temperature after which time it was quenched with NH₄Cl_(sat) and extracted with dichloromethane (three times). The organic layer was dried with MgSO₄, subjected to filtration and evaporated to dryness. The product ratio was determined by high field ¹H-NMR (600 MHz) of the crude reaction mixture. Equation 1 was used to calculate k_{rel} .

$$k_{rel} = \frac{(\text{Product})_X / (\text{Product})_H}{(\text{Reactant})_X / (\text{Reactant})_H} \quad (\text{eq. 6-14})$$

6.9: References

- 1) Dielectric constant of water is 80 (300K) compared to 37.5 (294K) for CH₃CN. Isaacs, N. *Physical Organic Chemistry*, Longman Group, London, **1998**.
- 2) Aggrawal, V. K.; Calamai, S.; Ford, J. G. *J. Chem. Soc. Perkin. Trans. I* **1997**, 593.
- 3) For an example of a similar competition experiment see: Yoshimine, M.; Hatch, M.J. *J. Am. Chem. Soc.* **1967**, *89*, 5831.
- 4) Aggrawal, V. K.; Harvey, J. N.; Richardson, J. *J. Am. Chem. Soc.* **2002**, *124*, 5747.
- 5) Ratts, K. W.; Yao, A. N. *J. Org. Chem.* **1966**, *31(6)*, 1689.
- 6) Aggrawal, V. K.; Schade, S.; Taylor, B. *J. Chem. Soc. Perk. Trans. I* **1997**, 2811.
- 7) a) Vedejs E.; Fleck, T.; Hara, S. *J. Org. Chem.* **1987**, *52*, 4637.; b) Vedejs E.; Fleck, T.; *J. Am. Chem. Soc.* **1989**, *111*, 5861.
- 8) Aggrawal, V. K.; Charmant, J.P.H.; Ciampi, C.; Hornby, J.M.; O'Brien, C.J.; Hynd, G.; Parsons, R. *J. Chem. Soc. Perkin. Trans. I* **2001**, 3159.
- 9) Indeed no relative rate data for the two competing substrates was provided in the report.
- 10) The difference in activation energy (E_a) for *syn* and *anti*-betaine formation was calculated using the Arrhenius equation where $\ln(k) = -E_a/RT + \ln(A)$ and substituting product ratios for the ratio of k^{trans}/k^{cis} .
- 11) Aggrawal, V. K.; Thompson, A.; Jones, R. V. H. *Tetrahedron Lett.* **1994**, 8659.
- 12) Saeva, F.D.; Morgan, B.P. *J. Am. Chem. Soc.* **1984**, *106*, 4121.
- 13) Aggrawal, V. K.; Calamai, S.; Ford, J. G. *J. Chem. Soc. Perkin. Trans. I* **1997**, 593.

Chapter 7: Conclusions and Future Work

In Part A of this thesis were presented the results and conclusions pertaining to our studies in the area of rhodium catalyzed hydroborations. A strategy was disclosed in Chapter 2 for the conversion of olefinic substrates into linear aldehydes. The methodology provides a viable alternative to hydroformylation strategies and does so in one-pot and without the need for carbon monoxide. In Chapter 3 were described the results of a study into the controlling elements of rhodium catalyzed hydroboration regioselectivity, the key step in the previous sequence. The reaction mechanism was characterized by a combination of substituent effects, labeling studies and kinetic isotope effects. These mechanistic probes illustrated differences in reactivity between the hydroborations of electron rich and electron poor substrates. Future work in this area should focus on isolating the individual steps of the hydroboration reaction mechanism and obtaining physical data for the individual step. The physical data, whether it is in the form of a Hammett ρ or an isotope effect, might then be used to better understand the precise nature of the transformation, as well as identify similar steps as rate determining in more complex systems.

Part B of the thesis discloses the results and conclusions of the first comprehensive experimental study of the Corey-Chaykovsky epoxidation. Rate data was obtained by monitoring the reaction progress under pseudo first order conditions. The first rate equation for the reaction between sulfur ylides and arylaldehydes was proposed and the activation parameters were determined by experimental means for the first time. The structure of the activated complex was probed by a combination of primary and secondary isotope effects, as well as with substituent effects in the form of a Hammett

study. The physical data obtained in the experimental portion of this study should in the future be combined with modern theoretical means and the transition state structure calculated.
